Advances in High Energy Physics

Implications of Gravitational Particle Creation

Lead Guest Editor: Subhajit Saha
Guest Editors: Kazuharu Bamba and Martiros Khurshudyan

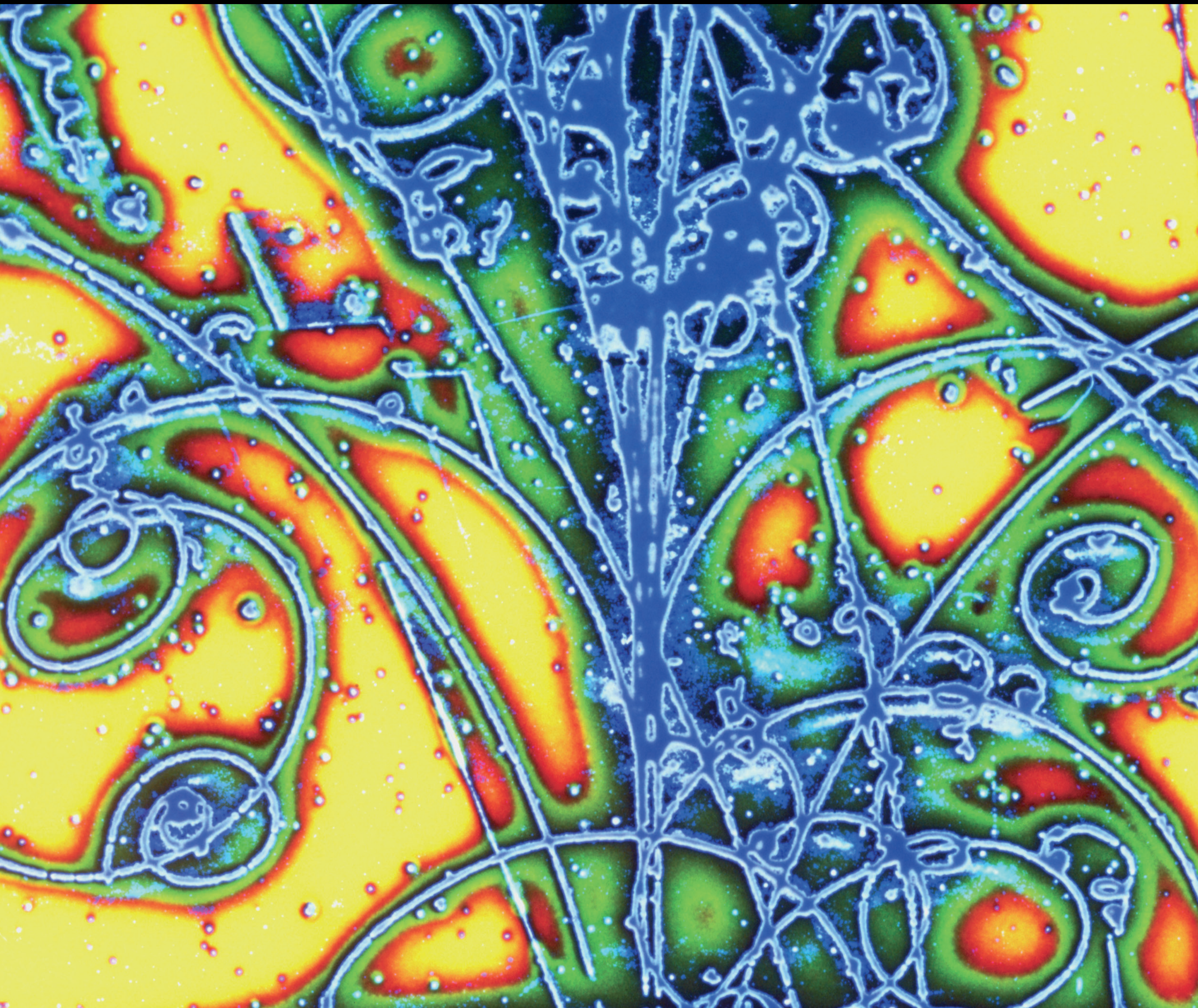

Implications of Gravitational Particle Creation

Advances in High Energy Physics

Implications of Gravitational Particle Creation

Lead Guest Editor: Subhajit Saha
Guest Editors: Kazuharu Bamba and Martiros Khurshudyan

Copyright © 2019 Hindawi. All rights reserved.

This is a special issue published in "Advances in High Energy Physics." All articles are open access articles distributed under the Creative Commons Attribution License, which permits unrestricted use, distribution, and reproduction in any medium, provided the original work is properly cited.

Editorial Board

Antonio J. Accioly, Brazil
Giovanni Amelino-Camelia, Italy
Luis A. Anchordoqui, USA
Michele Arzano, Italy
T. Asselmeyer-Maluga, Germany
Alessandro Baldini, Italy
Marco Battaglia, Switzerland
Lorenzo Bianchini, Switzerland
Roelof Bijker, Mexico
Burak Bilki, USA
Rong-Gen Cai, China
Anna Cimmino, France
Osvaldo Civitarese, Argentina
Andrea Coccaro, Italy
Shi-Hai Dong, Mexico
Mariana Frank, Canada
Ricardo G. Felipe, Portugal
Chao-Qiang Geng, Taiwan
Philippe Gras, France
Xiaochun He, USA
Luis Herrera, Spain
Filipe R. Joaquim, Portugal
Aurelio Juste, Spain
Theocharis Kosmas, Greece
Ming Liu, USA
Enrico Lunghi, USA
Salvatore Mignemi, Italy
Omar G. Miranda, Mexico
Grégory Moreau, France
Piero Nicolini, Germany
Carlos Pajares, Spain
Sergio Palomares-Ruiz, Spain
Giovanni Pauletta, Italy
Yvonne Peters, UK
Anastasios Petkou, Greece
Alexey A. Petrov, USA
Thomas Rössler, Sweden
Diego Saez-Chillon Gomez, Spain
Takao Sakaguchi, USA
Juan José Sanz-Cillero, Spain
Edward Sarkisyan-Grinbaum, USA
Sally Seidel, USA
George Siopsis, USA
Luca Stanco, Italy
Jouni Suhonen, Finland
Mariam Tórtola, Spain
Smarajit Triambak, South Africa
Jose M. Udías, Spain
Elias C. Vagenas, Kuwait
Sunny Vagnozzi, UK
Yau W. Wah, USA

Contents

Hindawi
Advances in High Energy Physics
Volume 2019, Article ID 1307167, 2 pages
https://doi.org/10.1155/2019/1307167

Editorial

Implications of Gravitational Particle Creation

Subhajit Saha,[1] **Kazuharu Bamba**,[2] **and Martiros Khurshudyan**[3]

[1]*Department of Mathematics, Panihati Mahavidyalaya, Kolkata 700110, India*
[2]*Division of Human Support System, Faculty of Symbiotic Systems Science, Fukushima University, Fukushima 960-1296, Japan*
[3]*CAS Key Laboratory for Research in Galaxies and Cosmology, Department of Astronomy, University of Science and Technology of China, Hefei 230026, China*

Correspondence should be addressed to Subhajit Saha; subhajit1729@gmail.com

Received 25 July 2019; Accepted 25 July 2019; Published 5 August 2019

Copyright © 2019 Subhajit Saha et al. This is an open access article distributed under the Creative Commons Attribution License, which permits unrestricted use, distribution, and reproduction in any medium, provided the original work is properly cited.

L. Parker discovered in the early sixties that the expansion of the Universe can lead to creation of particles out of the vacuum. He pulled together quantum mechanics and general relativity and found that the expansion of the Universe, or, in general, a time-variant gravitational field can lead to an impromptus production of (quantum) particles. The Cosmic Microwave Background (CMB) was discovered by Penzias and Wilson around the same time, which brought new insights into Cosmology and which provided the strongest support to the Big-Bang Theory. In 1992, the COBE (Cosmic Background Explorer) satellite detected small fluctuations in the average temperature of the CMB for the first time. This has later been confirmed by many other experiments, including the Planck satellite. Quantum field theory in curved spacetime and, in particular, gravitational particle creation provides the mechanism driving primitive fluctuations which created the tiny perturbations in the CMB temperature. The creation of galaxies and galactic clusters by clumping of matter can also be explained by this mechanism. Parker's formalism led Hawking to realize that black holes also create particles, in a way consistent with the laws of thermodynamics. Hawking's beautiful result was very influential. It revealed that the second law of thermodynamics was valid for systems that included black holes. This established a deep connection between thermodynamics and general relativity.

In recent years, gravitational particle creation is being considered as a viable alternative to Dark Energy (DE) models due to difficulties in identifying the true nature as well as the origin of DE which is considered to have exotic properties such as a huge negative pressure. The Cosmological Constant, which is supported by most observations as the driving force behind the late time cosmic acceleration, is also plagued by serious problems such as the Cosmological Constant problem and coincidence problem. At this juncture, the natural process of gravitational particle creation is speculated to explain not only the presently observed accelerated epoch of the Universe but also the inflationary phase in the early Universe as prophesied by Alan Guth in 1981. In fact, there have been several studies which have confirmed that this process is well equipped to explain the evolutionary stages of the Universe and is also thermodynamically stable. However, there are several drawbacks too, the most important one among them is that the exact rate of particle creation has still not been determined. Consequently, researchers mostly resort to phenomenological considerations to tackle this problem. Moreover, there have been a very few observational studies in this direction and more such studies are needed to understand this mechanism at a deeper level.

In this special issue, we have devoted our attention to understanding the significance of the gravitationally induced particle creation mechanism in the context of Cosmology. Several authors have made their contributions to this Special Issue. We hope that the readers find these articles useful for furthering their research and also gain insights into this very important and rapidly emerging research field.

Conflicts of Interest

All the Guest Editors declare that there is no conflict of interests regarding the publication of this paper.

Subhajit Saha
Kazuharu Bamba
Martiros Khurshudyan

Hindawi
Advances in High Energy Physics
Volume 2019, Article ID 5208712, 7 pages
https://doi.org/10.1155/2019/5208712

Research Article

Particle Production via Dirac Dipole Moments in the Magnetized and Nonmagnetized Exponentially Expanding Universe

Semra Gurtas Dogan,[1] Ganim Gecim,[2] and Yusuf Sucu[1]

[1] *Department of Physics, Faculty of Science, Akdeniz University, 07058 Antalya, Turkey*
[2] *Department of Astronomy and Astrophysics, Faculty of Science, Atatürk Univ., 25240 Erzurum, Turkey*

Correspondence should be addressed to Yusuf Sucu; ysucu@akdeniz.edu.tr

Received 5 April 2019; Revised 25 June 2019; Accepted 7 July 2019; Published 22 July 2019

Academic Editor: Kazuharu Bamba

Copyright © 2019 Semra Gurtas Dogan et al. This is an open access article distributed under the Creative Commons Attribution License, which permits unrestricted use, distribution, and reproduction in any medium, provided the original work is properly cited. The publication of this article was funded by SCOAP[3].

In the present paper, we solve the Dirac equation in the 2+1 dimensional exponentially expanding magnetized by uniform magnetic field and nonmagnetized universes, separately. Asymptotic behaviors of the solutions are determined. Using these results we discuss the current of a Dirac particle to discuss the polarization densities and the magnetization density in the context of Gordon decomposition method. In this work we also calculate the total polarization and magnetization, to investigate how the magnetic field affects the particle production. Furthermore, the electric and the magnetic dipole moments are calculated, and based on these, we have discussed the effects of the dipole moments on the charge distribution of the universe and its conductivity for both the early and the future time epoch in the presence/absence of a constant magnetic field and exponentially expanding spacetime.

1. Introduction

One of the most interesting and important results of the formulation of the relativistic quantum mechanics in curved spacetime is the particle creation event in the expanding universe which was firstly discussed by Parker for the scalar particles and Dirac particles [1–3]. So, he computed the number density of the created particles by means of the Bogolibov transformation by using the out vacuum states constructed from the solutions of the relativistic particles wave equations. After these important works of Parker, the solutions of the relativistic particle wave equations have extensively been studied in various 3+1 dimensional spacetime backgrounds [4–19]. Using the WKB approach, the number density and renormalized energy-momentum tensor of the created spin-1/2 particle in the spatially flat (3+1)-dimensional Friedmann-Robertson-Walker (FRW) spacetime have been calculated [20]. The effect of the scalar particle creation on the collapse of a spherically symmetric massive star was investigated and it was demonstrated that the collapsing process was not independent from the particle creation rate [21]. Moreover, in [22] thermodynamics laws and equilibrium conditions are discussed in the presence of particle creation in the context of the (3+1)-dimensional Chern-Simons gravity theory. Recently, creation of the massless fermion in the Bianchi type-I spacetime investigated and showed that the massless particles can be created during the early anisotropic expansion epoch [23].

The Gordon decomposition of the Dirac currents is another useful tool for discussing the particle creation phenomena [4, 9, 10, 24]. In the decomposition method, the Dirac currents constructed from the solutions of the Dirac equations are separated into three parts, the convective, polarization with three components, and magnetization with three components, in the 3+1 dimensional spacetime. This method includes some complexities stemming from the 3+1 dimensional spacetime. Using this method in a 2+1 dimensional curved spacetime, the densities of the particle currents are separated into three parts, as in the 3+1 dimensional spacetime, but polarization density has two components and the magnetization density has only one component [24], and, moreover, as the Dirac spinor can be defined by only two components, the computations in the 2+1 dimensional spacetime become more simple than that of 3+1 dimensional spacetime. Because of the simplicity stemming from the dimensions, the dipole moments that are computed from the polarization and magnetization densities of the Dirac electron under influence in a constant magnetic field are easily computed and their result are, furthermore, compatible with the current experimental results [25]. With these motivations, in this study, we solve the Dirac equation in the 2+1 dimensional exponentially expanding magnetized by uniform magnetic field and nonmagnetized universes, separately, and discuss the particle creation event by means of the Dirac currents written in terms of these solutions. As a result, we observe that the polarization and magnetization parts of the currents are affected differently whether the exponentially expanding universe is magnetized or not and find expressions for the electric and magnetic dipole moments by integrating the polarization and magnetization densities on hypersurface.

The outline of the work is as follows; in Section 2, we, at first, discuss the Dirac equation solutions in the 2+1 dimensional exponentially expanding universe. In Section 3, the Dirac equation is solved in the 2+1 dimensional exponentially expanding universe with a constant magnetic field. In Section 4, we derive the components of Dirac currents for the solutions obtained in Sections 2 and 3 and also compute the polarization density, the magnetization density, total polarization (electric dipole moment), and the total magnetization (magnetic dipole moment). Finally, the last section, conclusion, includes a discussion about the results of this work.

2. Dirac Particle in the 2+1 Dimensional Exponentially Expanding Universe

The behavior of the electron in 2+1 dimensional curved space is represented by the covariant form of the Dirac equation [24], which is important application in curved spacetime [26–33]

$$\left\{i\overline{\sigma}^{\nu}(x)\left[\partial_{\nu}-\Gamma_{\nu}+ieA_{\nu}\right]\right\}\Psi(x)=m\Psi(x), \qquad (1)$$

where $\Psi(x)=\binom{\Psi_1}{\Psi_2}$ is the Dirac spinorial wave function with two components that are positive and negative energy eigenstates, m is the mass of Dirac particle, e is the charge of the Dirac particle, and A_ν are 3-vectors of electromagnetic potential. Using triads, $e^{\nu}_{(i)}(x)$, Dirac matrices that dependent on spacetime, $\overline{\sigma}^{\nu}(x)$, are written in terms of the constant Dirac matrices, $\overline{\sigma}^{i}$;

$$\overline{\sigma}^{\nu}(x)=e^{\nu}_{(i)}(x)\,\overline{\sigma}^{i}. \qquad (2)$$

So, we choose the constant Dirac matrices, $\overline{\sigma}^{i}$, in the flat spacetime as follows:

$$\overline{\sigma}^{i}=\left(\overline{\sigma}^{0},\overline{\sigma}^{1},\overline{\sigma}^{2}\right) \qquad (3)$$

with

$$\begin{aligned}\overline{\sigma}^{0}&=\sigma^{3},\\ \overline{\sigma}^{1}&=i\sigma^{1},\\ \overline{\sigma}^{2}&=i\sigma^{2},\end{aligned} \qquad (4)$$

where σ^1, σ^2, and σ^3 are Pauli matrices. The spin connection, $\Gamma_\nu(x)$, for the diagonal metrics is defined as

$$\Gamma_{\nu}(x)=-\frac{1}{4}g_{\tau\alpha}\Gamma^{\alpha}_{\nu\beta}\left[\overline{\sigma}^{\tau}(x),\overline{\sigma}^{\beta}(x)\right], \qquad (5)$$

where $\Gamma^{\alpha}_{\nu\beta}$ is the Christoffel symbol given as follows [34]:

$$\Gamma^{\alpha}_{\nu\beta}=\frac{1}{2}g^{\lambda\alpha}\left[\partial g_{\beta\lambda,\nu}+\partial g_{\nu\lambda,\beta}-\partial g_{\beta\nu,\lambda}\right]. \qquad (6)$$

Also, the metric tensor $g_{\beta\nu}(x)$ is written in terms of triads as follows:

$$g_{\beta\nu}(x)=e^{(i)}_{\beta}(x)\,e^{(j)}_{\nu}(x)\,\eta_{(i)(j)}, \qquad (7)$$

where β and ν are curved spacetime indices run from 0 to 2, i and j are flat spacetime indices run 0 to 2, and $\eta_{(i)(j)}$ is the signature with (1,-1,-1).

The (2+1) dimensional de Sitter spacetime metric can be written as [35]

$$ds^2=dt^2-e^{2Ht}\left[dr^2+r^2d\phi^2\right] \qquad (8)$$

where H is Hubble parameter. From (3)-(8), the spin connections for the metric read

$$\begin{aligned}\Gamma_0&=0,\\ \Gamma_1&=-\frac{H}{2}e^{Ht}\overline{\sigma}^{0}\overline{\sigma}^{1},\\ \Gamma_2&=-\frac{1}{2}\left[rHe^{Ht}\overline{\sigma}^{0}\overline{\sigma}^{2}+\overline{\sigma}^{1}\overline{\sigma}^{2}\right].\end{aligned} \qquad (9)$$

Using (2), (8), and (9), then the Dirac equation in the 2+1 dimensional exponentially expanding universe becomes

$$\begin{aligned}&\left\{\overline{\sigma}^{0}\left(\partial_t+H\right)+im+e^{-Ht}\left[\overline{\sigma}^{1}\left(\partial_r+\frac{1}{2r}\right)+\frac{\overline{\sigma}^{2}}{r}\partial_\phi\right]\right\}\\ &\quad\cdot\Psi(x)=0.\end{aligned} \qquad (10)$$

Letting (4) and (10) and the Dirac spinor, $\Psi(x)=\binom{\Psi_1}{\Psi_2}$, we write the Dirac equation in explicit form as follows:

$$\begin{aligned}&\left[\partial_t+im+H\right]\psi_1+ie^{-Ht}\left[\partial_r+\frac{1}{2r}-\frac{i}{r}\partial_\phi\right]\psi_2=0\\ &\left[\partial_t-im+H\right]\psi_2-ie^{-Ht}\left[\partial_r+\frac{1}{2r}+\frac{i}{r}\partial_\phi\right]\psi_1=0.\end{aligned} \qquad (11)$$

To find the solutions of (11), thanks to the separation of variables method, the wave function components can be defined as

$$\begin{pmatrix}\Psi_1\\ \Psi_2\end{pmatrix}=e^{ik\phi}\begin{pmatrix}T_1(t)R_1(r)\\ T_2(t)R_2(r)\end{pmatrix}. \qquad (12)$$

By these definitions, the Dirac equation is separated into the following two differential equation systems:

$$\begin{aligned}\left[\frac{d}{dr}+\frac{1}{2r}+\frac{k}{r}\right]R_2(r)&=-\lambda R_1(r)\\ \left[\frac{d}{dr}+\frac{1}{2r}-\frac{k}{r}\right]R_1(r)&=\lambda R_2(r)\end{aligned} \qquad (13)$$

and

$$\left[\frac{d}{dt}+im+H\right]T_1(t)=i\lambda e^{-Ht}T_2(t)$$
$$\left[\frac{d}{dt}-im+H\right]T_2(t)=i\lambda e^{-Ht}T_1(t),\tag{14}$$

where λ is a separation constant, and we find the solutions of (13) in terms of the Bessel and confluent hypergeometric functions as follows:

$$\begin{aligned}R_1(r)&=AJ_{k-1/2}(\lambda r)\\&=A\frac{e^{-i\lambda r}(\lambda r/2)^{k-1/2}}{\Gamma(k+1/2)}{}_1F_1[k,2k;i2r\lambda],\\R_2(r)&=BJ_{k+1/2}(\lambda r)\\&=B\frac{e^{-i\lambda r}(\lambda r/2)^{k+1/2}}{\Gamma(k+3/2)}{}_1F_1[k+1,2k+2;i2r\lambda].\end{aligned}\tag{15}$$

On the other hand, to solve (14), we must define a new variable such as $z=(\lambda/H)e^{-Ht}$. With the definition $n=-i(m/H)$, the solutions of (14) are obtained in terms of Bessel functions or confluent hypergeometric functions:

$$\begin{aligned}T_1(z)&=Cz^{3/2}J_{n+1/2}(z)\\&=Cz^{3/2}\frac{e^{-iz}(z/2)^{n+1/2}}{\Gamma(n+3/2)}{}_1F_1[n+1,2n+2;i2z]\\T_2(z)&=Dz^{3/2}J_{n-1/2}(z)\\&=Dz^{3/2}\frac{e^{-iz}(z/2)^{n-1/2}}{\Gamma(n+1/2)}{}_1F_1[n,2n;i2z]\end{aligned}\tag{16}$$

Then, the wave function, $\Psi(x)$, can be written as

$$\Psi=Nz^{3/2}e^{ik\phi}\begin{pmatrix}J_{n+1/2}(z)\,J_{k-1/2}(\lambda r)\\J_{n-1/2}(z)\,J_{k+1/2}(\lambda r)\end{pmatrix}\tag{17}$$

where N is normalization constant. To find the normalization constant, we use the Dirac-delta normalization condition [4, 36, 37]:

$$\int\sqrt{|g|}\overline{\Psi}\overline{\sigma}^0\Psi\,d\sigma=\delta\left(\lambda-\lambda'\right)\tag{18}$$

where g is determinant of the metric tensor and $\overline{\Psi}=\Psi^{\dagger}\overline{\sigma}^0$ and $d\sigma=drd\phi$ for the surface $t=constant$ [25]. Thus, the normalization constant is computed as

$$|N|^2=\frac{H^2}{4\pi z\lambda J_{n-1/2}(z)\,J_{n+1/2}(z)},\tag{19}$$

where we use the following relation [4, 36, 37]:

$$\int_0^\infty rJ_{k+1/2}(\lambda r)\,J_{k+1/2}\left(\lambda' r\right)dr=\frac{1}{\lambda}\delta\left(\lambda'-\lambda\right).\tag{20}$$

3. Dirac Particle in the 2+1 Dimensional Exponentially Expanding Magnetized Universe

It is interesting in discussing if the universe is under influence in an external constant magnetic field in the beginning time. Therefore, an electromagnetic potential can be chosen as $A_0=0$ and $\overrightarrow{A}(r,\phi)=(1/2)B_0r\,\hat{\phi}$ for a constant magnetic field in 2+1 dimensional spacetime. Then, the Dirac equation in the 2+1 dimensional exponential expanding universe with a constant magnetic field becomes

$$\begin{aligned}&\Big\{\overline{\sigma}^0(\partial_t+H)+im\\&\quad+e^{-Ht}\left[\overline{\sigma}^1\left(\partial_r+\frac{1}{2r}\right)+\overline{\sigma}^2\left(\frac{1}{2r}\partial_\phi+\frac{ieB_0}{2}\right)\right]\Big\}\Psi(x)\\&\quad=0\end{aligned}\tag{21}$$

and, thus, the explicit form of the equation is written as

$$\begin{aligned}&(\partial_t+im+H)\,\psi_1+ie^{-Ht}\left(\partial_r+\frac{1}{2r}-\frac{i}{r}\partial_\phi+\frac{eB_0}{2}\right)\psi_2\\&\quad=0\\&(\partial_t-im+H)\,\psi_2-ie^{-Ht}\left(\partial_r+\frac{1}{2r}+\frac{i}{r}\partial_\phi-\frac{eB_0}{2}\right)\psi_1\\&\quad=0\end{aligned}\tag{22}$$

To solve (22), we use the same procedure as the section before. The solutions of the equations are

$$\Psi=\frac{Nz^{3/2}e^{ik\phi}}{\sqrt{\rho}}\begin{pmatrix}J_{n+1/2}(z)\,W_{\kappa,\eta}(\rho)\\J_{n-1/2}(z)\left[\dfrac{(\rho-2\eta-1)\left(\sqrt{e^2B_0^2-4\lambda^2}-eB_0\right)}{2\lambda\rho}W_{\kappa,\eta}(\rho)-\dfrac{\sqrt{e^2B_0^2-4\lambda^2}}{\lambda\rho}W_{\kappa+1,\eta}(\rho)\right]\end{pmatrix}\tag{23}$$

where $\kappa=-ekB_0/\sqrt{e^2B_0^2-4\lambda^2}$, $\eta=k-1/2$, $\rho=\sqrt{e^2B_0^2-4\lambda^2}r$, and N is normalization constant. As all the contributions for particle creation and dipole moments are taking place from the boundaries, we can write the wave function in the following asymptotic form [36]:

$$\Psi \sim N z^{3/2} e^{ik\phi} \rho^{\kappa-1/2} e^{-\rho/2} \begin{pmatrix} \dfrac{1}{\Gamma(n+3/2)}\left(\dfrac{z}{2}\right)^{n+1/2} \\ \dfrac{1}{\Gamma(n+1/2)}\left(\dfrac{z}{2}\right)^{n-1/2} \dfrac{\left[(\rho-2\eta-1)\left(\sqrt{e^2B_0^2-4\lambda^2}-eB_0\right)-2\rho\sqrt{e^2B_0^2-4\lambda^2}-eB_0\right]}{2\lambda\rho} \end{pmatrix}. \quad (24)$$

Then, the normalization constant can be obtained from (18) as follows:

$$|N|^2 \sim \frac{H^2(\eta+1/2)^2(1-4n^2)}{\cos(n\pi)} \cdot \frac{1}{\left[z^2\left((\eta+1/2)^2-\kappa^2\right)\Gamma(2\kappa)+(1-4n^2)\Gamma(2\kappa-2)\right]}, \quad (25)$$

where we use $\Gamma(-n+3/2)\Gamma(n+3/2) = \pi(1-4n^2)/4\cos(n\pi)$ and $\Gamma(-n+1/2)\Gamma(n+1/2) = \pi/\cos(n\pi)$.

4. Dirac Currents

The 2+1 dimensional Dirac current is written as

$$J^{\nu} = \overline{\Psi}\overline{\sigma}^{\nu}(x)\Psi \quad (26)$$

where $\overline{\Psi}$ is Hermitian conjugate of the Dirac spinor Ψ and equal to $\overline{\Psi} = \Psi^{\dagger}\overline{\sigma}^0 = \Psi^{\dagger}\sigma^3$ [24]. As shown in [24], (26) is expressed in explicit form as follows:

$$\begin{aligned} J^{\tau} &= \frac{1}{2m}\left(\overline{\Psi}\overline{\sigma}^{\tau\upsilon}(t,r)\Psi\right)_{,\upsilon} \\ &- \frac{1}{2m}\overline{\Psi}\left(\frac{i}{2}g^{\tau\upsilon}\overleftrightarrow{\partial_{\upsilon}} - eA^{\tau}\right)\Psi \\ &- \frac{i}{4m}\overline{\Psi}\left[\overline{\sigma}^{\upsilon}(t,r),\overline{\sigma}^{\tau}_{,\upsilon}(t,r)\right]\Psi \\ &- \frac{i}{2m}\overline{\Psi}\left[\overline{\sigma}^{\upsilon}(t,r)\Gamma_{\upsilon},\overline{\sigma}^{\tau}(t,r)\right]\Psi \\ &- \frac{i}{4m}\overline{\Psi}\left[\overline{\sigma}^{\upsilon}_{,\upsilon}(t,r),\overline{\sigma}^{\tau}(t,r)\right]\Psi \end{aligned} \quad (27)$$

The components of the Dirac current in the 2+1 dimensional exponential expanding universe, J^0 and J^k, are

$$\begin{aligned} J^0 &= \frac{1}{2m}\partial_k\left[\overline{\Psi}\overline{\sigma}^{0k}(t,r)\Psi\right] - \frac{1}{2m}\overline{\Psi}\left(\frac{i}{2}\overleftrightarrow{\partial^0} - qA^0\right)\Psi \\ &- \frac{i}{2mr}\exp(-Ht)\overline{\Psi}\overline{\sigma}^1\overline{\sigma}^0\Psi \end{aligned} \quad (28)$$

and

$$\begin{aligned} J^k &= \frac{1}{2m}\partial_0\left(\overline{\Psi}\overline{\sigma}^{0k}(t,r)\Psi\right) + \frac{1}{2m}\partial_l\left(\overline{\Psi}\overline{\sigma}^{lk}(t,r)\Psi\right) \\ &- \frac{1}{2m}\overline{\Psi}\left(\frac{i}{2}\overleftrightarrow{\partial^k} - qA^k\right)\Psi \\ &+ i\frac{3H}{2mr}\exp(-Ht)\overline{\Psi}\overline{\sigma}^0\overline{\sigma}^k\Psi \\ &+ \delta_{k2}i\frac{3H}{2mr}\exp(-Ht)\overline{\Psi}\overline{\sigma}^1\overline{\sigma}^2\Psi \end{aligned} \quad (29)$$

where $k,l = 1,2$, $\overline{\sigma}^{0k} = i/2[\overline{\sigma}^0,\overline{\sigma}^k(t,r)]$, $\overline{\sigma}^{kl} = i/2[\overline{\sigma}^k(t,r),\overline{\sigma}^l(t,r)]$, and δ_{k2} is Dirac-delta function. Also these components can be rewritten in terms of the convective, the polarization, and magnetization parts as follows:

$$J_0 = \partial_k\mathbf{P}_k + \rho_{convective} - \frac{i}{2mr}\exp(-Ht)\overline{\Psi}\overline{\sigma}^1\overline{\sigma}^0\Psi \quad (30)$$

and

$$\begin{aligned} J_k &= \partial_0\mathbf{P}_k + \partial_l\mathbf{M}_{[lk]} + J_{k\ convective} \\ &+ i\frac{3H}{2mr}\exp(-Ht)\overline{\Psi}\overline{\sigma}^0\overline{\sigma}^k\Psi \\ &+ \delta_{k2}i\frac{3H}{2mr}\exp(-Ht)\overline{\Psi}\overline{\sigma}^1\overline{\sigma}^2\Psi \end{aligned} \quad (31)$$

where $\mathbf{P}_{0k}$ are polarization densities and $\mathbf{M}_{[lk]}$ is magnetization density, and their explicit forms are given by

$$P^{0k} = \frac{1}{2m}\overline{\Psi}\overline{\sigma}^{k0}(t,r)\Psi \quad (32)$$

and

$$M^{[lk]} = \frac{1}{2m}\overline{\Psi}\overline{\sigma}^{lk}(t,r)\Psi, \quad (33)$$

respectively. From these relations, the total polarizations, p_l^0, and magnetization, μ, are defined as

$$p_l^0 = \int P^{0k}\,d\Sigma_{kl} \quad (34)$$

and

$$\mu = \int M^{kl}\,d\Sigma_{kl}, \quad (35)$$

where $d\Sigma_{kl}$ is an hypersurface for t =constant and $d\Sigma_{kl} = \sqrt{|g|}d^2x = e^{2Ht}r\,dr\,d\phi$ [25].

Now, we are going to discuss the Dirac currents and the dipole moments expressions for the exponentially expending universe. So, inserting (17) and its conjugate into (26), we compute the components of the Dirac currents in asymptotic region as follows:

$$J^0 \approx \frac{H^2}{2\lambda^2\pi^2}\frac{z^2}{r},$$
$$J^1 \approx \frac{H^3 z^2\left[(2n+1)^2 - z^2\right]}{4\pi^2\lambda^3(2n+1)r}\sin\left(\lambda r - \frac{k\pi}{2}\right), \quad (36)$$
$$J^2 \approx i\frac{H^3 z^2\left[z^2 - (2n+1)^2\right]}{4\pi^2\lambda^3(2n+1)r}\sin\left(\lambda r - \frac{k\pi}{2}\right).$$

Similarly, substituting (17) and its conjugate in (32) and (33), the components of the polarization densities and the magnetization density are written as follows:

$$P^1 = A(z)\,J_{k+1/2}(\lambda r)\,J_{k-1/2}(\lambda r),$$
$$P^2 = B(z)\,\frac{1}{r}J_{k+1/2}(\lambda r)\,J_{k-1/2}(\lambda r), \quad (37)$$
$$M_{12} = \frac{\lambda^4 r}{8\pi m^3}\left[J_{k+1/2}(\lambda r)\,J_{k+1/2}(\lambda r) - J_{k-1/2}(\lambda r)\,J_{k-1/2}(\lambda r)\right],$$

respectively, where we use the following abbreviations:

$$A(z) = i\frac{H^3 z^3}{8\pi\lambda^2 m}\left[\frac{J_{n+1/2}(z)}{J_{n-1/2}(z)} - \frac{J_{n-1/2}(z)}{J_{n+1/2}(z)}\right], \quad (38)$$
$$B(z) = -iA(z).$$

Giving to the polarization densities and magnetization density depending spacetime coordinates, we can say that particle production event takes place. To calculate the total polarizations and magnetization, we insert (37), the polarization densities, and magnetization density, into (34) and (35), respectively, and later integrate them on the hypersurface. Then, we obtain the total polarization densities (electric dipole moments) and magnetization density (magnetic dipole moment) as follows:

$$p^1 = 0,$$
$$p^2 = \frac{\pi\lambda}{H^2}\frac{B(z)}{z^2}, \quad (39)$$
$$\mu = 0,$$

where we use the integral representation of Bessel function [36] and p^1 and p^2 are total polarizations, i.e., electric dipole moment components, and also μ is total magnetization, i.e., magnetic dipole moment. From these results, we see that the particle creation events are affected from only p^2 total polarization density, electric dipole moment. On the other hand, in the limit $t \longrightarrow -\infty$ $(z \longrightarrow \infty)$, p^2 vanishes by the following way:

$$p^2 \longrightarrow \frac{zH}{4\lambda m}\left[\frac{2\cos^2(z - n\pi/2) - 1}{\sin(2z - n\pi)}\right] \longrightarrow 0, \quad (40)$$

that is, there is not particle production in this limit or the universe has a symmetric charge distribution in the beginning time and, of course, the universe has not any dipole moments, but, in the limit $t \longrightarrow +\infty$ $(z \longrightarrow 0)$, p^2 becomes

$$p^2 \longrightarrow \frac{e\hbar H}{4\lambda mc^2}\left[\frac{z^2 - \left(1 - i\left(2mc^2/\hbar H\right)\right)^2}{1 - i\left(2mc^2/\hbar H\right)}\right] \longrightarrow -\frac{e}{2\lambda\delta}\exp(-i\delta), \quad (41)$$

where $\hbar$ is Planck constant, c is the speed of light, and $\delta = 2mc^2/\hbar H$, and, thus, the universe has a permanent complex dipole moment, which it oscillates with Zitterbewegung frequency, $2mc^2/\hbar$.

To calculate the Dirac current components for the Dirac particle in the 2+1 dimensional exponentially expanding magnetized universe, we insert (24) and its conjugate in (26). Thus, we find that the current components are

$$J^0 \approx \frac{H^2 k^2}{z^2(k^2-\kappa^2)\Gamma(2\kappa) + e^2B_0^2(1-4n^2)\Gamma(2\kappa-2)} \cdot z^3\rho^{2\kappa-1}e^{-\rho}\left[z + \frac{(1-4n^2)}{z(k^2-\kappa^2)\rho^2}\left[(2k-\rho)(k+\kappa) + 2k\rho\right]^2\right]$$
$$J^1 \approx i\frac{4nH^3eB_0k^2\kappa}{\pi(k^2-\kappa^2)}z^4\rho^{2\kappa-2}e^{-\rho}\left[(2k-\rho)(k+\kappa) + 2k\rho\right] \quad (42)$$
$$J^2 \approx \frac{4H^3k^3z^4}{\pi(k^2-\kappa^2)} \cdot \frac{(\rho-2k)(k+\kappa)+2k\rho}{z^2(k^2-\kappa^2)\Gamma(2\kappa) + (1-4n^2)\Gamma(2\kappa-2)} \cdot \rho^{2\kappa-3}e^{-\rho}.$$

Using (24) in (32) and in (33), the components of polarization and magnetization can be found as follows:

$$P^1 \approx \frac{2H^3eB_0k^2z^4\kappa}{(k^2-\kappa^2)\pi m}\frac{(2k-\rho)(k+\kappa)+2k\rho}{2z^2\lambda^2\kappa^2\Gamma(2\kappa) + e^2B_0^2(1-4n^2)\Gamma(2\kappa-2)} \cdot \rho^{2\kappa-2}e^{-\rho}$$
$$P^2 \approx i\frac{4nH^3k^3z^4}{\pi m(k^2-\kappa^2)}\frac{\left[(2k-\rho)(k+\kappa)+2k\rho\right]}{z^2(k^2-\kappa^2)\Gamma(2\kappa) + (1-4n^2)\Gamma(2\kappa-2)} \cdot \rho^{2\kappa-3}e^{-\rho}$$
$$M_{12} \approx \frac{2H^4eB_0k^3z^5\left(4n^2-1\right)\kappa}{\pi m(k^2-\kappa^2)\left[4z^2\lambda^2\kappa^2\Gamma(2\kappa) + eB_0(1-4n^2)\Gamma(2\kappa-2)\right]}$$

$$\cdot \rho^{2\kappa-2}e^{-\rho} \times \left[\frac{z}{(1-4n^2)} + \frac{1}{z(k^2-\kappa^2)\rho^2}\left[(2k-\rho)(k+\kappa)+2k\rho\right]^2\right] \quad (43)$$

To calculate the total polarizations and total magnetization, we insert (43) into (34) and (35). Then, using the integral representation of Bessel function [36], we find the following dipole moments expressions:

$$\begin{aligned} p^1 &\approx \frac{He^3B_0^3k^4z^2}{\kappa^3 m} \cdot \frac{2(k-\kappa)^2\Gamma(2\kappa)}{z^2(k^2-\kappa^2)\Gamma(2\kappa)+(1-4n^2)\Gamma(2\kappa-2)}, \\ p^2 &\approx i\frac{2nHe^4B_0^4k^5z^2}{\kappa^4 m} \cdot \frac{\left(2k^2-2\kappa^2+4k\kappa+\kappa-k\right)\Gamma(2\kappa-1)}{z^2(k^2-\kappa^2)\Gamma(2\kappa)+(1-4n^2)\Gamma(2\kappa-2)}, \\ \mu &\approx \frac{H^2e^3B_0^3k^5}{(k^2-\kappa^2)\kappa^3 m}z^3. \end{aligned} \quad (44)$$

From these expressions, we see that, in finite time intervals, the particle creation is influenced by both polarization and magnetization components. On the other hand, in the limit $t \longrightarrow \infty$ ($z \longrightarrow 0$) the magnetic dipole moment, μ, goes to zero faster than the electric dipole moment components, p^1 and p^2. Therefore, the electric dipole moments in the particle creation events become more dominant than the magnetic dipole moment in finite time intervals if there exists in an external constant magnetic field.

5. Summary and Conclusion

We exactly solve the Dirac equation in existence of the exponentially expanding magnetized and nonmagnetized universe and, from these solutions, derive some expressions for the Dirac current components and dipole moments. The particle creation in the exponentially expanding universe is only affected by the p^2 polarization in the finite time interval. However, this component goes to zero in the limit $t \longrightarrow -\infty$, i.e., in the beginning of the universe, but, in the limit $t \longrightarrow +\infty$, the universe has a permanent complex dipole moment oscillating with Zitterbewegung frequency, $2mc^2/\hbar$: $p^2 \simeq -(e/2\lambda\delta)\exp(-i\delta)$. The complexity of the dipole moment points out the conductivity of the exponentially expanding universe. Also, the universe has the electric and magnetic dipole moments which are dependent on time in existence of an external constant magnetic field with the expansion such that, in the limit $t \longrightarrow -\infty$, the dipole moment expressions become infinite, but, in the limit $t \longrightarrow \infty$, they go to zero. The dependence on time of the polarization and magnetization shows that the particle creation happens. Furthermore, in the limit $t \longrightarrow \infty$ ($z \longrightarrow 0$), the particle creation events are affected only via the polarization because the magnetization, m, goes to zero faster than p^1 and p^2. From the point of view, we point out that the exponential expansion of the universe causes a particle creation, a permanent complex electric dipole moment and asymmetric charge distribution, but, in existence of an external constant magnetic field with exponential expansion in time, the universe charge distribution is get and getting symmetric and thus all the dipole moments become zero as $t \longrightarrow \infty$.

Data Availability

No data were used to support this study.

Conflicts of Interest

The authors declare that there is no conflict of interests regarding the publication of this paper.

References

[1] L. Parker, "Particle creation in expanding universes," *Physical Review Letters*, vol. 21, no. 8, article no. 562, 1968.

[2] L. Parker, "Quantized fields and particle creation in expanding universes. I," *Physical Review*, vol. 183, no. 5, article no. 1057, 1969.

[3] L. Parker, "Quantized fields and particle creation in expanding universes. II," *Physical Review D*, vol. 3, no. 2, article no. 346, 1971.

[4] A. O. Barut and I. H. Duru, "Exact solutions of the Dirac equation in spatially flat Robertson-Walker space-times," *Physical Review D*, vol. 36, no. 12, article no. 3705, 1987.

[5] I. Sakalli and M. Halilsoy, "Solution of the Dirac equation in the near horizon geometry of an extreme Kerr black hole," *Physical Review D: Particles, Fields, Gravitation and Cosmology*, vol. 69, no. 12, article no. 124012, 2004.

[6] A. Zecca, "Comoving self-gravitating scalar field in the Newman Penrose formalism," *International Journal of Theoretical Physics*, vol. 45, no. 2, pp. 385–393, 2006.

[7] S. Moradi, "Exact solutions of dirac equation and particle creation in (1+3)-dimensional robertson-walker spacetime," *International Journal of Theoretical Physics*, vol. 48, no. 4, pp. 969–980, 2009.

[8] S. Moradi, "Particle creation in asymptotically Minkowskian spacetimes," *Journal of Geometry and Physics*, vol. 59, no. 2, pp. 173–184, 2009.

[9] N. G. Sarkar and S. Biswas, "Particle production in curved spacetime," *Pramana*, vol. 50, no. 2, pp. 109–131, 1998.

[10] N. G. Sarkar and S. Biswas, "Particle production in de Sitter space-time," *International Journal of Modern Physics A*, vol. 15, no. 4, pp. 497–508, 2000.

[11] Y. Sucu and N. Unal, "Vector bosons in the expanding universe," *European Physical Journal C*, vol. 44, no. 2, pp. 287–291, 2005.

[12] Y. Sucu and N. Ünal, "Dirac equation in Euclidean Newman-Penrose formalism with applications to instanton metrics," *Classical and Quantum Gravity*, vol. 21, no. 6, pp. 1443–1451, 2004.

[13] M. Dernek, S. Gurtas Dogan, Y. Sucu, N. Unal, and J. Phys, "Relativistic quantum mechanical spin-1 wave equation in 2 + 1 dimensional spacetime," *Turkish Journal of Physics*, vol. 42, pp. 509–526, 2018.

[14] C. Tekincay, Y. Sucu, and J. Phys, "Photon in a cylindrical resonant cavity," *Turkish Journal of Physics*, vol. 42, pp. 175–182, 2018.

[15] H. Hassanabadi, E. Maghsoodi, and S. Zarrinkamar, "Dirac equation with vector and scalar cornell potentials and an external magnetic field," *Annals of Physics*, vol. 525, no. 12, pp. 944–950, 2013.

[16] H. Hassanabadi, H. Sobhani, and W. S. Chung, "Scattering study of fermions due to double Dirac delta potential in quaternionic relativistic quantum mechanics," *Advances in High Energy Physics*, vol. 2018, Article ID 8124073, 7 pages, 2018.

[17] M. Hosseinpour, H. Hassanabadi, and M. de Montigny, "The Dirac oscillator in a spinning cosmic string spacetime," *The European Physical Journal C*, vol. 79, article 311, 2019.

[18] A. N. Ikot, H. Hassanabadi, N. Salehl, H. P. Obong, and M. C. Onyeaju, "Scattering states of Cusp potential in minimal length Dirac equation," *Indian Journal of Physics*, vol. 89, no. 11, pp. 1221–1226, 2015.

[19] M. Hamzavi, A. A. Rajabi, and H. Hassanabadi, "Exactly complete solutions of the Dirac equation with pseudoharmonic potential including linear plus Coulomb-like tensor potential," *International Journal of Modern Physics A*, vol. 26, no. 7-8, pp. 1363–1374, 2011.

[20] S. Ghosh, "Creation of spin 1/2 particles and renormalization in FLRW spacetime," *Physical Review D: Particles, Fields, Gravitation and Cosmology*, vol. 91, no. 12, article no. 124075, 2015.

[21] S. Bhattacharjee, S. Saha, and S. Chakraborty, "Does particle creation mechanism favour formation of black hole or naked singularity?" *The European Physical Journal C*, vol. 78, article 488, 2018.

[22] A. Jawad, S. Sami, and S. Rafique, "Thermodynamics of various entropies in specific modified gravity with particle creation," *Advances in High Energy Physics*, vol. 2018, Article ID 9471346, 17 pages, 2018.

[23] A. Bhoonah, "Gravitational fermion creation during an anisotropic phase of cosmological expansion," *Physical Review D: Particles, Fields, Gravitation and Cosmology*, vol. 99, article 105003, Article ID 105003, 2019.

[24] Y. Sucu and N. Ünal, "Exact solution of Dirac equation in 2+1 dimensional gravity," *Journal of Mathematical Physics*, vol. 48, no. 5, article no. 052503, 2007.

[25] S. Gurtas Dogan, G. Gecim, and Y. Sucu, "A new approach to compute the dipole moments of a Dirac electron," 2019, https://arxiv.org/abs/1907.02393.

[26] O. Gurtug, S. Mazharimousavi, and M. HHalilsoy, "Classical and quantum analysis of an Einstein-Scalar solution in 2 + 1 dimensions," *The European Physical Journal plus*, vol. 132, no. 4, article no. 161, 2017.

[27] O. Gurtug, M. Halilsoy, and S. Habib Mazharimousavi, "Quantum probes of timelike naked singularities in 2 + 1-dimensional power-law spacetimes," *Advances in High Energy Physics*, vol. 2015, Article ID 684731, 10 pages, 2015.

[28] G. Gecim, Y. Kucukakca, and Y. Sucu, "Noether gauge symmetry of dirac field in (2 + 1)-dimensional gravity," *Advances in High Energy Physics*, vol. 2015, Article ID 567395, 7 pages, 2015.

[29] G. Gecim and Y. Sucu, "Dirac field as a source of the inflation in 2 +1 dimensional teleparallel gravity," *Advances in High Energy Physics*, vol. 2017, Article ID 2056131, 9 pages, 2017.

[30] G. Gecim and Y. Sucu, "Cosmological Solutions in 2 + 1-Dimensional New Massive Gravity in the Presence of the DIRac Field," *Gravitation & Cosmology*, vol. 25, no. 2, pp. 179–183, 2019.

[31] G. Gecim and Y. Sucu, "Quantum gravity effect on the tunneling particles from Warped-AdS$_3$ black hole," *Modern Physics Letters A*, vol. 33, no. 28, article no. 1850164, 2018.

[32] G. Gecim and Y. Sucu, "The GUP effect on Hawking radiation of the 2 + 1 dimensional black hole," *Physics Letters B*, vol. 773, pp. 391–394, 2017.

[33] G. Gecim, Y. Sucu, and Adv., "Quantum gravity effect on the tunneling particles from 2 + 1-dimensional new-type black hole," *Advances in High Energy Physics*, vol. 2018, Article ID 8728564, 7 pages, 2018.

[34] S. Weinberg, *Gravitation and Cosmology: Principles and Applications of the General Theory of Relativity*, John Wiley and Sons, New York, NY, USA, 1972.

[35] M. Kenmoku, S. Uchida, and T. Matsuyama, "Conical singular solutions in (2+1)-dimensional gravity employing the ADM canonical formalism," *International Journal of Modern Physics D*, vol. 12, no. 4, pp. 677–687, 2003.

[36] I. S. Gradshteyn and I. M. Ryzhik, *Table of Integrals, Series, and Products*, Elsevier Press, New York, NY, USA, 7th edition, 2007.

[37] J. D. Jackson, *Classical Electrodynamics*, John Wiley and Sons, New York, NY, USA, 1999.

Hindawi
Advances in High Energy Physics
Volume 2019, Article ID 5356121, 12 pages
https://doi.org/10.1155/2019/5356121

Research Article

Broken Lifshitz Invariance, Spin Waves, and Hydrodynamics

Dibakar Roychowdhury

Department of Physics, Indian Institute of Technology Roorkee, Roorkee 247667, Uttarakhand, India

Correspondence should be addressed to Dibakar Roychowdhury; dibakarphys@gmail.com

Received 3 December 2018; Accepted 30 April 2019; Published 2 June 2019

Guest Editor: Martiros Khurshudyan

Copyright © 2019 Dibakar Roychowdhury. This is an open access article distributed under the Creative Commons Attribution License, which permits unrestricted use, distribution, and reproduction in any medium, provided the original work is properly cited. The publication of this article was funded by SCOAP^3.

In this paper, based on the basic principles of thermodynamics, we explore the hydrodynamic regime of interacting Lifshitz field theories in the presence of broken rotational invariance. We compute the entropy current and discover new dissipative effects which are consistent with the principle of local entropy production in the fluid. In our analysis, we consider both the parity even and the parity odd sector upto first order in the derivative expansion. Finally, we argue that the present construction of the paper could be systematically identified as that of the hydrodynamic description associated with *spin waves* (away from the domain of quantum criticality) under certain limiting conditions.

1. Overview and Motivation

Low temperature phases of various *strange metal* systems have been a mysterious issue since their discovery. One of the key reasons for this lies behind the fact that unlike the ordinary metallic systems, strange metals do not possess any *quasiparticle* description close to its Fermi surface. These systems are therefore known as *Non-Fermi liquids*(the enthusiastic reader is also referred to the review [1] and references therein) [2–5].

Matter in this quantum critical domain (so called *quantum liquids*) exhibits certain fascinating features as the temperature is lowered substantially as follows.

(1) The ratio between the specific heat and the temperature turns out to be very large indicating the fact that the effective mass for electrons could be many orders larger in magnitude than the free electron mass near its Fermi surface.

(2) The resistivity grows linearly with temperature, namely, $\rho \sim T$, which is also strange from the point of view of a Fermi liquid theory.

All the above features therefore strongly suggest the breakdown of the usual Fermi liquid theory in the domain of quantum criticality and as a result the low temperature physics of strongly correlated many body systems has remained as a puzzle for the past couple of decades.

However, for various reasons, it is widely believed that the physics within this quantum critical domain is mostly governed by the obvious scaling symmetries of the underlying Quantum Critical Point (QCP). It is by now quite evident that the isometry group associated with QCPs is that of Lifshitz type; namely, the scaling symmetries are anisotropic at the fixed point [6]:

$$\begin{aligned} \mathbf{x} &\longrightarrow \lambda \mathbf{x}, \\ t &\longrightarrow \lambda^{z} t \end{aligned} \tag{1}$$

where z is the dynamic critical exponent [7, 8].

The purpose of the present paper is however not to explore physics within this domain of quantum criticality; it is rather slightly away from it by explicitly breaking symmetries associated with the fixed point. In the following, we illustrate this in a bit detail.

It turns out that QCPs with Lifshitz isometry group explicitly break Lorentz boost invariance and on the other hand preserve rotational symmetry as well as the translational invariance. The long wavelength dynamics associated with these fixed points has been explored extensively from both the perspective of a fluid description and the AdS/CFT duality [9–18]. Keeping this literature in mind, in the present paper, we are however interested in the question whether there exists any notion of hydrodynamics beyond the domain of quantum criticality and a possible systematic formulation of it based on the fundamental principles of Thermodynamics. In the following, we systematically quote the purpose of the present analysis:

(1) We would like to explore the validity of the hydrodynamic description in a situation when the full Lifshitz algebra is broken down to some reduced symmetry group of it. It would be indeed quite interesting to explore what happens if we relax the condition of rotational symmetry and in particular how does it affect the parity odd transports of the theory. Naturally, it relaxes many of the previous constraints of the theory and allows additional tensor structures in the constitutive relations which were previously incompatible with the underlying symmetry of the system.

(2) The ultimate goal of our analysis is to write down an *entropy current* [19–24] in the presence of broken symmetry generators and explore how does it constraint the additional transports of the system which have emerged due to the symmetry breaking effect. In other words, we would like to explore whether there exist new dissipative effects (which are consistent with the principle of local entropy production) away from the domain of quantum criticality. In this regard, we consider both the parity even and the parity odd sector of the hydrodynamic constitutive relations and in particular explore how the parity odd transports are affected due to the presence of anisotropy in the system. In this sense, the present analysis is valid for all of those fluid systems whose underlying isometry group comprises that of the broken generators of the Lifshitz algebra.

Two questions are quite obvious at this stage: (1) How do we introduce anisotropy in our system and (2) What are the low lying physical d.o.f. of the system that one would like to interpret in spite of the fact that hydrodynamics is an *effective* description and does not rely on the microscopic details of the system.

The anisotropy that we introduce in our analysis is in fact quite similar in spirit to that with the earlier analysis [25, 26]. However, as we shall see shortly, the interpretation as well as the motivation for introducing such anisotropy is completely different in spirit from that of the relativistic scenario.

In our analysis, we introduce anisotropy by means of four vectors, $\mathfrak{v}^{\mu}$ pointing along a specific direction. We associate a term $\Delta(= P_{\perp} - P_{\parallel})$ with those four vectors which corresponds to the fact that the pressure along two different directions is different even in the rest frame of the fluid. With the introduction of this anisotropy, our next task turns out to be to write down all possible tensor structures which are possible to construct out of the basic variables of the fluid system under consideration, namely, the fluid velocity ($\mathfrak{u}^{\mu}$), temperature (T), chemical potential (μ_c), and the anisotropy ($\mathfrak{v}^{\mu}$). More specifically, one should be able to write down a number of tensor structures within the constitutive relations with arbitrary transports which could be fixed later by demanding the positivity of the so called entropy current. Moreover, it is to be noted that as the present theory is considered to be a *slow* deformation ($|\Delta| \ll 1$) of the original Lifshitz hydrodynamics, therefore one must recover the known results of the Lifshitz theory as the fixed point is approached ($\Delta \longrightarrow 0$).

As far as the d.o.f. are concerned, the answer is rather tricky. However, we claim that the present analysis could be used to model the hydrodynamic description associated with *spin waves* [27–30] in certain appropriate limit. The reason for this claim is the following. First of all, one should note that *spin waves* could be thought of as being low lying excitation of certain material like dimer *antiferromagnet* above its ground state. In other words, spin waves could be thought of as being the *gapless*(this renders that the underlying theory is scale invariant) excitation (*Goldstone modes*) associated with the broken $O(3)$ symmetry (at the level of hydrodynamics such symmetry breaking effects should be manifested in terms of the emergence of the pressure anisotropy in the constitutive relations of the conserved quantities). These excitations therefore clearly break the underlying rotational invariance of the system and they vanish as one approaches the domain of quantum crticality [27–30]. In the following, we illustrate these points in detail. In particular, we try to explain what do we exactly mean by spin wave hydrodynamics.

It turns out that the classical hydrodynamic description of spin waves is valid as long as spin wave fluctuations are smaller than the correlation length [27, 28]:

$$\xi \sim \frac{c}{T} \log \left(\frac{T}{\left|\mu_c - \mu_{QCP}\right|^{z\nu}} \right) \tag{2}$$

where μ_{QCP} is the value of the chemical potetial exactly at the critical point and the energy of the spin wave excitation could be thought of $\leq c\xi^{-1}$. In other words, we are still in the region where the effective correlation is still much greater than the low temperature thermal fluctuations of the system. Therefore the hydrodynamic description is still valid. Our ultimate goal would be to investigate whether it is at all possible to write down an entropy current under such circumstances.

The organization of the rest of the paper is the following. In Section 2, we provide the basic anisotropic construction for the most general charged dissipative fluids in the presence of a global $U(1)$ anomaly. In Section 3, we compute the entropy current for both the parity even and the parity odd sector of the theory. Finally, we conclude in Section 4.

Note Added. The entropy production in Lifshitz fluids might have direct or indirect consequences on gravitational particle production through the remarkable identification of gravitational dynamics as an entropic force [31] whose relativistic generalization leads to Einstein's general theory of relativity.

2. Basics

The purpose of the present calculation is to explore the consequences of *broken* rotational invariance on chiral Lifshitz hydrodynamics [14]. However, to start with we first introduce the notion of chiral anomaly in the context of Lifshitz hydrodynamics as (the reader should not get confused with the index $a(= 1, .., N)$ as the index associated with internal symmetry (non-abelian) generators. This index simply corresponds to the fact that to start with we have N number of anomalous $U(1)$ charges in our system. However, in the subsequent analysis we would perform our computation for the simplest case with $a = 1$. The corresponding result for multiple abelian charges could be generalized easily) [14]

$$\partial_\mu \mathfrak{T}^{\mu\nu} = \mathfrak{F}^{a\nu\sigma} \mathfrak{j}^a_\sigma$$
$$\partial_\mu \mathfrak{j}^{a\mu} = \mathfrak{c}^{abc} \mathfrak{E}^b . \mathfrak{B}^c \tag{3}$$

where the anomaly coefficients are given by the rank 3 tensor $\mathfrak{c}^{abc}$. Here, $\mathfrak{j}^a_\mu$s are the N anomalous $U(1)$ currents and $\mathfrak{F}^a_{\nu\sigma}(= \partial_\nu \mathfrak{A}^a_\sigma - \partial_\sigma \mathfrak{A}^a_\nu)$ are the N abelian field strength tensors of the theory. The electric and the magnetic field strengths are, respectively, given by

$$\mathfrak{E}^{a\mu} = \mathfrak{F}^{a\mu\sigma} \mathfrak{u}_\sigma$$
$$\mathfrak{B}^{a\mu} = \frac{1}{2} \varepsilon^{\mu\nu\lambda\sigma} \mathfrak{u}_\nu \mathfrak{F}^a_{\lambda\sigma}. \tag{4}$$

We start our analysis by writing down the constitutive relations (compatible with the reduced symmetries of the system) for both the stress tensor and the charge currents associated with the underlying hydrodynamic description. We choose to work in the so called Landau frame [14].

We first focus on the stress tensor part. It typically consists of the following two pieces (the reader should be aware of the fact that to start with Lifshitz field theories are QFTs for which $z > 1$. As a result such theories by no means could be connected to relativistic QFTs with Lorentz invariance (for which, $z = 1$). In other words, Lifshitz QFTs do not possess a smooth Lorentzian limit and therefore it is not correct to interpret Lifshitz QFTs as nonrelativistic QFTs simply because they lack Lorentz boost generators. On the other hand, because of the presence of the gapless excitation in the theory, one might still hope to find some upper bound for the speed of particles in the theory which could be identified as the speed of light (c) as well. However, one could switch over to the corresponding nonrelativistic regime by taking appropriate (v^i/c) limit which would render nonrelativistic QFTs with broken Galilean boost invariance [9]):

$$\mathfrak{T}^{\mu\nu} = \mathfrak{T}^{\mu\nu}_{(ideal)} + \mathfrak{T}^{\mu\nu}_{(D)} \tag{5}$$

where $\mathfrak{T}^{\mu\nu}_{(ideal)}$ is the nondissipative (ideal) part of the stess tensor. On the other hand, $\mathfrak{T}^{\mu\nu}_{(D)}$ is the dissipative piece of the stress tensor that includes all the *first* order derivative expansions such as that in the Landau frame [9]:

$$\mathfrak{u}_\mu \mathfrak{T}^{\mu\nu}_{(D)} = 0. \tag{6}$$

Since the full Lifshitz isometry group is now broken down to some reduced subset of it, therefore, to start with and in principle we are allowed to incorporate more generic tensor structures in the constitutive relation which were previously disallowed due to the presence of the underlying rotational invariance. Therefore in some sense the analysis of the present paper generalizes all the previous studies in the literature [9–14]. On top of it, due to the presence of additional transports in the theory, the present analysis also turns out to be a bit more intricate compared to its relativistic counterpart. In the following we elaborate these issues into much more detail.

The starting point of our analysis is quite straightforward. We write all possible distinct tensor structures which are allowed by the (reduced) symmetry of the system (consistent with the Landau frame criterion) and we express our constitutive relations as a linear combination of each of these structures. The coefficients associated with these tensor structures are finally constrained by the principle of positivity of entropy production. Those transports which do not seem to be consistent with this physical constraint are set to be zero although they are allowed by the symmetry of the system. Keeping these facts in mind, the ideal part of the stress tensor could be formally expressed as (this form of the stress tensor is unique and is indeed consistent with the Landau frame criterion, namely, $\mathfrak{T}^{\mu\nu}\mathfrak{u}_\nu = -\epsilon \mathfrak{u}^\mu$ [9]. Moreover, here $\mathfrak{g}_{\mu\nu}$ is the background metric with signature $(-,+,+,+)$)

$$\mathfrak{T}^{\mu\nu}_{(ideal)} = (\epsilon + P_\perp) \mathfrak{u}^\mu \mathfrak{u}^\nu + P_\perp \mathfrak{g}^{\mu\nu} - \Delta \mathfrak{v}^\mu \mathfrak{v}^\nu \tag{7}$$

where $\Delta = P_\perp - P_\parallel$ is the difference between the transverse and the longitudinal pressures (note that the above choice (7) also stems from the fact that at the ideal level the fluid stress tensor must be diagonal) [25, 26]. Here, $\mathfrak{u}^\mu$ is the usual fluid velocity and $\mathfrak{v}^\mu$ is the spacelike vector that defines the anisotropy in the system and is pointing along the longitudinal axis (the longitudinal axis defines the anisotropy in the system along the direction perpendicular to the reaction plane. $P_\parallel$ is the pressure along this longitudinal axis, whereas on the other hand $P_\perp$ is the pressure along the direction perpendicular to this axis) such that they are mutually orthogonal to each other; namely (it turns out that the Landau frame criterion (6) and the velocity normalization (8) are intimately related to each other. Note that the Landau frame criterion (6) looks quite natural in the sense that it simply implies the fact that in the rest frame of the fluid the zeroth component of the stress tensor must be equal to the rest energy (density) of the fluid and this is the universal claim that should be valid for all classes of QFTs irrespective of their underlying symmetry group. Now it turns out that, given the stress tensor (5), the above criterion could be satisfied if we choose the specific normalization (8) for the velocity field ($\mathfrak{u}^\mu$) which therefore turns out to be a natural choice even for Lifshitz systems) [25, 26],

$$\mathfrak{u}^\mu \mathfrak{u}_\mu = -1,$$
$$\mathfrak{v}^\mu \mathfrak{v}_\mu = 1, \tag{8}$$
$$\mathfrak{u}^\mu \mathfrak{v}_\mu = 0.$$

Considering the *local* rest frame of the fluid,

$$\mathfrak{u}^\mu = (1,0,0,0),$$
$$\mathfrak{v}^\mu = (0,0,0,1) \tag{9}$$

It is indeed quite straightforward to show

$$\mathfrak{T}^{\mu\nu}_{(ideal)} = \mathrm{diag}(\epsilon, P_\perp, P_\perp, P_\parallel) \tag{10}$$

which is clearly consistent with the fact that the momentum density vanishes in the local rest frame of the ideal fluid.

Before we proceed further, one nontrivial yet simple check is inevitable. We consider the Lifshitz Ward identity (note that the Ward identity is always satisfied if the underlying scaling symmetry is preserved which is precisely the case for our analysis as the spin wave excitation is gapless [27, 28]) [9]:

$$zT^{0}{}_{0} + \delta^{i}_{j}T^{j}{}_{i} = 0 \tag{11}$$

which for the present case yields

$$z\epsilon = dP_{\perp} + \Delta \tag{12}$$

where d is the number of spatial dimensions. This clearly suggests that the corresponding equation of state is modified due to the presence of anisotropy (spin wave excitations) in the system. Suppose for the time being that we are dealing with an uncharged fluid where the temperature (T) is the only scale in our theory. Therefore, it turns out that the above equation of state (12) could be obtained from the Euler relation

$$\epsilon + P_{\perp} = T\mathfrak{s} \tag{13}$$

if we demand the following nontrivial scaling relations:

$$\epsilon \sim P_{\perp,\parallel} \sim T^{(z+d)/z+\theta} \tag{14}$$

where the exponent $\theta(= \Delta/zP_{\perp})$ clearly vanishes near the fixed point of the theory and as a result one recovers the standard scaling relations [9].

We now focus on the dissipative part of the stress tensor (5). After a straightforward computation, one could in fact express the dissipative contributions to the stress tensor (5) into the following two pieces; namely (note that here we have assumed $\partial.\mathfrak{v} = 0$ as there do not exist any sources for anisotropy [25, 26]),

$$\mathfrak{T}^{\mu\nu}_{(D)} = \mathfrak{T}^{(0)\mu\nu}_{(D)} + \Delta\mathfrak{T}^{(\Delta)\mu\nu}_{(D)} \tag{15}$$

where the first piece (here, $\omega^{\mu} = (1/2)\varepsilon^{\mu\nu\rho\sigma}\mathfrak{u}_{\nu}\partial_{\rho}\mathfrak{u}_{\sigma}$ is the so called *vorticity* factor [32, 33])

$$\begin{aligned}
\mathfrak{T}^{(0)\mu\nu}_{(D)} &= \mathfrak{S}^{(0)\mu\nu} + \mathfrak{u}^{\mu}\mathfrak{G}^{(0)\nu} + \mathcal{O}\left(\partial^{2}\right) \\
\mathfrak{S}^{(0)\mu\nu} &= -\eta\sigma^{\mu\nu}_{(\mathfrak{u})} - \zeta\mathfrak{P}^{\mu\nu}\left(\partial.\mathfrak{u}\right) \\
\mathfrak{G}^{(0)\mu} &= -\alpha_{1}\mathfrak{u}^{\sigma}\partial_{\sigma}\mathfrak{u}^{\mu} - 2\alpha_{2}\left(\mathfrak{E}^{\mu} - T\mathfrak{P}^{\mu\sigma}\partial_{\sigma}\left(\frac{\mu_{c}}{T}\right)\right) \\
&\quad - \beta_{\omega}T\omega^{\mu} - \beta_{\mathfrak{B}}T\mathfrak{B}^{\mu}
\end{aligned} \tag{16}$$

contains the usual contributions to the stress tensor that do not include any effects of anisotropy [14]. On the other hand, the second piece (the transport associated with the Θ term should be considered in a more general sense. When we discuss the parity even sector it should be thought of as the parity even transport while for the parity odd sector we would replace it accordingly by parity odd transports)

$$\begin{aligned}
\mathfrak{T}^{(\Delta)\mu\nu}_{(D)} &= \mathfrak{S}^{(\Delta)\mu\nu} + \mathfrak{Q}^{(\Delta)\mu\nu} + \mathfrak{u}^{\mu}\mathfrak{G}^{(\Delta)\nu} + \mathcal{O}\left(\partial^{2}\right) \\
\mathfrak{S}^{(\Delta)\mu\nu} &= -\lambda\sigma^{\mu\nu}_{(\mathfrak{v})} - \mathfrak{P}^{\mu\nu}\left(\left(\mathfrak{v}.\mathfrak{G}\right) - \kappa_{2}\Delta\left(\left(\partial.\mathfrak{u}\right) + \Theta\right)\right) \\
&\quad + \mathfrak{v}^{\mu}\mathfrak{G}^{\nu} + \mathfrak{v}^{\nu}\mathfrak{G}^{\mu} \\
&\quad - \mathfrak{v}^{\mu}\mathfrak{v}^{\nu}\left(\left(\mathfrak{v}.\mathfrak{G}\right) - \kappa_{2}\Delta\Theta + \xi_{1}\mathfrak{u}.\partial\left(\frac{\mu_{c}}{T}\right) - \xi_{2}\mathfrak{u}^{\lambda}\mathfrak{u}^{\sigma}\partial_{\lambda}\mathfrak{v}_{\sigma}\right. \\
&\quad \left. + 2\kappa_{2}\Delta\left(\left(\partial.\mathfrak{u}\right) + \Theta\right)\right) \\
\mathfrak{Q}^{(\Delta)\mu\nu} &= \mathfrak{u}^{\mu}\mathfrak{v}^{\nu}\left(\left(\mathfrak{v}.\mathfrak{G}\right) - \kappa_{2}\Delta\Theta + \kappa_{3}\mathfrak{u}.\partial\left(\frac{\mu_{c}}{T}\right)\right) \\
\mathfrak{G}^{(\Delta)\mu} &= \kappa_{1}\mathfrak{v}^{\sigma}\partial_{\sigma}\mathfrak{u}^{\mu} + \kappa_{2}\mathfrak{v}^{\mu}\left(\left(\partial.\mathfrak{u}\right) + \Theta\right)
\end{aligned} \tag{17}$$

contains all the first order dissipative corrections to the stress tensor (5) that explicitly include the effects of anisotropy. At this stage it is customary to note that in order to arrive at the above relations (16), (17), we have used the following definitions and/or the identifications; namely,

$$\begin{aligned}
\mathfrak{S}^{\mu\nu} &= \mathfrak{S}^{(0)\mu\nu} + \Delta\mathfrak{S}^{(\Delta)\mu\nu} \\
\mathfrak{G}^{\mu} &= \mathfrak{G}^{(0)\mu} + \Delta\mathfrak{G}^{(\Delta)\mu} \\
\sigma^{\mu\nu}_{(\mathfrak{x})} &= \mathfrak{P}^{\mu\sigma}\mathfrak{P}^{\nu\lambda}\left(\partial_{\sigma}\mathfrak{x}_{\lambda} + \partial_{\lambda}\mathfrak{x}_{\sigma} - \delta_{\mathfrak{x},\mathfrak{u}}\frac{2}{3}\mathfrak{P}_{\sigma\lambda}\left(\partial.\mathfrak{x}\right)\right), \\
&\qquad (\mathfrak{x} = \mathfrak{u}, \mathfrak{v}) \\
\Theta &= \mathfrak{v}^{\sigma}\left(-\mathfrak{E}_{\sigma} - \mathfrak{B}_{\sigma} + T\partial_{\sigma}\left(\frac{\mu_{c}}{T}\right) - \omega_{\sigma}\right)
\end{aligned} \tag{18}$$

with $\mathfrak{P}^{\mu\nu} = \mathfrak{u}^{\mu}\mathfrak{u}^{\nu} + \mathfrak{g}^{\mu\nu}$ as the projection operator. At this stage it is also noteworthy to mention that the entity $\mathfrak{G}^{\mu}$ contains all the first order dissipative corrections in the basic hydrodynamic variables, namely, the fluid velocity ($\mathfrak{u}^{\mu}$), chemical potential (μ), and the temperature (T). Moreover, here the entity $\mathfrak{u}_{\mu}\mathfrak{G}^{\mu} = 0$ in the Landau frame [14].

Finally, the $U(1)$ charged current could be formally expressed as (in principle one could have added a term proportional to $\mathfrak{v}^{\mu}$ at the zeroth order level in the derivative expansion. However, as far as the present analysis is concerned we switch off all the components of the electric current along the direction of the anisotropic vector field [25, 26])

$$\mathfrak{j}^{a\mu} = \varrho^{a}\mathfrak{u}^{\mu} + \mathfrak{D}^{a\mu} + \mathcal{O}\left(\partial^{2}\right) \tag{19}$$

where the function $\mathfrak{D}^{a\mu}$ contains all possible dissipative corrections in the first order derivative expansion; namely (one could formally express $\mathfrak{D}^{a\mu} \equiv \mathfrak{D}^{(0)a\mu} + \Delta\mathfrak{D}^{(\Delta)a\mu}$),

$$\mathfrak{D}^{a\mu} = 2\alpha_3^a \mathfrak{u}^\sigma \partial_\sigma \mathfrak{u}^\mu + (\sigma_D)^a{}_b \left(\mathfrak{E}^{b\mu} - T\mathfrak{P}^{\mu\sigma}\partial_\sigma \left(\frac{\mu_c^b}{T}\right)\right) + \varsigma_\omega^a \omega^\mu + (\varsigma_{\mathfrak{B}})^a{}_b \mathfrak{B}^{b\mu} + \Delta\mathfrak{D}^{(\Delta)a\mu} \tag{20}$$

$$\mathfrak{D}^{(\Delta)a\mu} = \kappa_1^a \mathfrak{v}^\sigma \partial_\sigma \mathfrak{u}^\mu - \mathfrak{v}^\mu \left((\mathfrak{v}.\mathfrak{G}^a) - \Delta(\kappa_2)^a{}_b \Theta^b + \gamma_1^a \mathfrak{v}^\lambda \mathfrak{u}^\sigma \partial_\sigma \mathfrak{u}_\lambda + (\gamma_2)^a{}_b \mathfrak{u}.\partial\left(\frac{\mu_c^b}{T}\right)\right)$$

such that in the Landau frame, $\mathfrak{u}_\mu \mathfrak{j}^{a\mu} = -\varrho^a$.

3. Entropy Current

The purpose of this section is to construct a systematic hydrodynamic description away from the quantum critical region with Lifshitz isometry group. In order to do that, in this paper we illustrate the simplest case with $N = 1$.

3.1. Thermodynamic Identities. As a first step of our analysis, we first construct some basic thermodynamic identities which will be required in the subsequent analysis. Considering the following identity (in order to avoid confusion, we denote chemical potential as μ_c),

$$\mathbb{I} = \mathfrak{u}_\nu \partial_\mu \mathfrak{T}^{\mu\nu} + \mu_c \partial_\mu \mathfrak{j}^\mu \tag{21}$$

and using (3), it is indeed quite trivial to note that $\mathbb{I} \sim \mathcal{O}(\partial^2)$ which therefore clearly suggests that at the zeroth order level in the derivative expansion of $\mathfrak{T}^{\mu\nu}$ and $\mathfrak{j}^\mu$ one must have $\mathbb{I} = 0$ which naturally yields

$$-\mathfrak{u}^\mu \partial_\mu \epsilon + \frac{(\epsilon + P_\perp)}{\mathfrak{s}} \mathfrak{u}^\mu \partial_\mu \mathfrak{s} - \Delta \mathfrak{u}_\nu \mathfrak{v}^\mu \partial_\mu \mathfrak{v}^\nu + \mu_c \partial_\mu \varrho \mathfrak{u}^\mu - \frac{\mu_c \varrho}{\mathfrak{s}} \mathfrak{u}^\mu \partial_\mu \mathfrak{s} = 0 \tag{22}$$

where $\mathfrak{s}$ is the so called entropy density such that $\partial_\mu(\mathfrak{s}\mathfrak{u}^\mu) = 0$.

We would now like to interpret the entity $\mathfrak{v}^\mu \partial_\mu \mathfrak{v}^\nu$ above in (22). To do that, let us first note that in the so called *boosted* frame one could formally express the four velocities as

$$\mathfrak{u}^\mu = \left(\frac{1}{\sqrt{1-\beta^2}}, \frac{\beta^i}{\sqrt{1-\beta^2}} \right), \quad (i = x, y, z)$$
$$\mathfrak{v}^\mu = \left(\frac{\beta_z}{\sqrt{1-\beta^2-\beta_z^2}}, 0, 0, \frac{\sqrt{1-\beta^2}}{\sqrt{1-\beta^2-\beta_z^2}} \right) \tag{23}$$

which clearly satisfy the above constraint in (8). Here, $\beta^i (= v^i/c)$ are the arbitrary boosts along three different spatial directions. Using (23), it is indeed quite straight forward to show

$$\mathfrak{v}^\mu \partial_\mu \mathfrak{v}^\nu = \partial^\nu \log \vartheta(\beta) \tag{24}$$

where the function $\vartheta(\beta)$ could be formally expressed as

$$\vartheta(\beta) = \frac{\beta_z}{\sqrt{1-\beta^2-\beta_z^2}} \delta_{\nu,0} + \frac{\sqrt{1-\beta^2}}{\sqrt{1-\beta^2-\beta_z^2}} \delta_{\nu,z}. \tag{25}$$

Using (25), one could now formally express (20) as

$$-\mathfrak{u}^\mu \partial_\mu \epsilon + \frac{(\epsilon + P_\perp)}{\mathfrak{s}} \mathfrak{u}^\mu \partial_\mu \mathfrak{s} - \frac{\Delta}{\vartheta} \mathfrak{u}^\nu \partial_\nu \vartheta + \mu_c (\partial_\mu \varrho) \mathfrak{u}^\mu - \frac{\mu_c \varrho}{\mathfrak{s}} \mathfrak{u}^\mu \partial_\mu \mathfrak{s} = 0. \tag{26}$$

Following the arguments of [25, 26], next we introduce the so called *generalized* energy density function

$$\epsilon = \epsilon(\varrho, \mathfrak{s}, \vartheta) \tag{27}$$

which naturally yields

$$d\epsilon = \left(\frac{\partial \epsilon}{\partial \mathfrak{s}}\right)_{\varrho,\vartheta} d\mathfrak{s} + \left(\frac{\partial \epsilon}{\partial \varrho}\right)_{\mathfrak{s},\vartheta} d\varrho + \left(\frac{\partial \epsilon}{\partial \vartheta}\right)_{\mathfrak{s},\varrho} d\vartheta = T d\mathfrak{s} + \mu_c d\varrho - \frac{\Delta}{\vartheta} d\vartheta. \tag{28}$$

The above equation (28) could be thought of as the modified first law of thermodynamics in the presence of anisotropies. The first two terms are precisely the contributions arising from the entropy density as well as the charge density associated with the system whereas, on the other hand, the last term is precisely the anisotropic contribution to the energy density of the system.

Finally, using (26) and (28), it is quite useful to obtain the following set of identities:

$$\epsilon + P_\perp = T\mathfrak{s} + \mu_c \varrho$$
$$dP_\perp = \mathfrak{s} dT + \varrho d\mu_c + \frac{\Delta}{\vartheta} d\vartheta \tag{29}$$

which we use in the subsequent discussions.

Before we conclude this section, it is now customary to derive the so called equation for the entropy current [34] in the presence of the pressure anisotropy. Using (3), it is indeed quite trivial to note down the following conservation equation:

$$\mathfrak{u}_\nu \partial_\mu \mathfrak{T}^{\mu\nu} + \mu_c \partial_\mu \mathfrak{j}^\mu = -\mathfrak{E}^\mu \mathfrak{j}_\mu + \mu_c \mathfrak{c} \mathfrak{E}^\mu \mathfrak{B}_\mu \tag{30}$$

which by virtue of the arguments as mentioned above in (21) gives rise to nontrivial contributions at the quadratic order in the derivative expansion; namely,

$$\partial_\mu \mathbb{J}_{\mathfrak{s}}^\mu = -\frac{1}{T} \partial_\mu \mathfrak{u}_\nu \mathfrak{S}^{(0)\mu\nu} - \mathfrak{D}^{(0)\mu} \left(\mathfrak{P}_{\mu\nu} \partial^\nu \left(\frac{\mu_c}{T}\right) - \frac{\mathfrak{E}_\mu}{T} \right) - \frac{\mu_c}{T} \mathfrak{c} \mathfrak{E}.\mathfrak{B} - \frac{1}{T} \mathfrak{G}^{(0)\nu} \mathfrak{u}^\mu \partial_\mu \mathfrak{u}_\nu + \Delta \mathbb{M}^{(\Delta)} \tag{31}$$

where

$$\mathbb{J}^{\mu}_{\mathfrak{s}} = \mathfrak{s}\mathfrak{u}^{\mu} - \frac{\mu_c}{T}\mathfrak{D}^{\mu} = \mathbb{J}^{(0)\mu}_{\mathfrak{s}} + \Delta\mathbb{J}^{(\Delta)\mu}_{\mathfrak{s}} \tag{32}$$

is the so called entropy current of the system. Clearly, from (32), it is quite evident that in the presence of pressure anisotropies, the so called entropy current of the system receives nontrivial corrections which is naturally reflected in its divergence equation (31). The first part on the R.H.S. of (31) is the usual contribution to the entropy current in the absence of pressure anisotropy [14]. The entity $\mathbb{M}^{(\Delta)}$, on the other hand, summaries all the anisotropic contributions to the divergence equation; namely,

$$\begin{aligned}\mathbb{M}^{(\Delta)} &= -\frac{1}{T}\partial_{\mu}\mathfrak{u}_{\nu}\mathfrak{S}^{(\Delta)\mu\nu} \\ &\quad - \mathfrak{D}^{(\Delta)\mu}\left(\mathfrak{P}_{\mu\nu}\partial^{\nu}\left(\frac{\mu_c}{T}\right) - \frac{\mathfrak{E}_{\mu}}{T}\right) \\ &\quad - \frac{1}{T}\mathfrak{G}^{(\Delta)\nu}\mathfrak{u}^{\mu}\partial_{\mu}\mathfrak{u}_{\nu} + \frac{1}{T}\mathfrak{u}_{\nu}\partial_{\mu}\mathfrak{Q}^{(\Delta)\mu\nu}.\end{aligned} \tag{33}$$

3.2. A Note on the Parity Even Sector. Before we proceed further, at this stage it is noteworthy to mention that the parity breaking terms would definitely modify the entropy current as expected from the earlier analysis [34]. However, before moving to the parity *odd* sector, it is customary to check the parity even sector in the presence of pressure anisotropy (in the subsequent discussion of this subsection we consider only the parity even part of (31). In principle, one could do this since the two sectors do not get mixed up even in the presence of anisotropy [14]. A careful investigation would reveal the fact that this is the unique feature of first order dissipative hydrodynamics which essentially truncates constitutive relations upto leading order in $\mathfrak{G}^{\mu}$). As the reader might have noticed so far that due to the presence of the pressure anisotropy in the system even in the parity even sector of the stress tensor (17) (as well as the charge current (22)) we encounter a number of additional transports which need to be fixed first. We expect to fix these coefficients purely from the condition of the positivity of the entropy current; namely, $\partial_{\mu}\mathbb{J}^{\mu}_{\mathfrak{s}} \geq 0$.

We would first consider the parity *even* sector in (31); namely,

$$\begin{aligned}\partial_{\mu}\mathbb{J}^{(P)\mu}_{\mathfrak{s}} &= -\frac{1}{T}\partial_{\mu}\mathfrak{u}_{\nu}\mathfrak{S}^{(0)\mu\nu} \\ &\quad - \mathfrak{D}^{(0,P)\mu}\left(\mathfrak{P}_{\mu\nu}\partial^{\nu}\left(\frac{\mu_c}{T}\right) - \frac{\mathfrak{E}_{\mu}}{T}\right) \\ &\quad - \frac{1}{T}\mathfrak{G}^{(0,P)\nu}\mathfrak{u}^{\mu}\partial_{\mu}\mathfrak{u}_{\nu} + \Delta\mathbb{M}^{(\Delta,P)}\end{aligned} \tag{34}$$

where each of the individual entities could be formally expressed as

$$\begin{aligned}\mathbb{M}^{(\Delta,P)} &= -\frac{1}{T}\partial_{\mu}\mathfrak{u}_{\nu}\mathfrak{S}^{(\Delta,P)\mu\nu} - \mathfrak{D}^{(\Delta,P)\mu}\left(\mathfrak{P}_{\mu\nu}\partial^{\nu}\left(\frac{\mu_c}{T}\right)\right. \\ &\quad \left. - \frac{\mathfrak{E}_{\mu}}{T}\right) - \frac{1}{T}\mathfrak{G}^{(\Delta,P)\nu}\mathfrak{u}^{\mu}\partial_{\mu}\mathfrak{u}_{\nu} + \frac{1}{T}\mathfrak{u}_{\nu}\partial_{\mu}\mathfrak{Q}^{(\Delta,P)\mu\nu} \\ \mathfrak{S}^{(\Delta,P)\mu\nu} &= -\lambda\sigma^{\mu\nu}_{(\mathfrak{v})} - \mathfrak{P}^{\mu\nu}\left(\left(\mathfrak{v}.\mathfrak{G}^{(P)}\right)\right. \\ &\quad \left. - \kappa_2\Delta\left((\partial.\mathfrak{u}) + \Theta^{(P)}\right)\right) + \mathfrak{v}^{\mu}\mathfrak{G}^{(P)\nu} + \mathfrak{v}^{\nu}\mathfrak{G}^{(P)\mu} \\ &\quad - \mathfrak{v}^{\mu}\mathfrak{v}^{\nu}\left(\left(\mathfrak{v}.\mathfrak{G}^{(P)}\right) - \kappa_2\Delta\Theta^{(P)} + \xi_1\mathfrak{u}.\partial\left(\frac{\mu_c}{T}\right)\right. \\ &\quad \left. - \xi_2\mathfrak{u}^{\lambda}\mathfrak{u}^{\sigma}\partial_{\lambda}\mathfrak{v}_{\sigma} + 2\kappa_2\Delta\left((\partial.\mathfrak{u}) + \Theta^{(P)}\right)\right) \\ \mathfrak{D}^{(0,P)\mu} &= 2\alpha_3\mathfrak{u}^{\sigma}\partial_{\sigma}\mathfrak{u}^{\mu} + \sigma_D\left(\mathfrak{E}^{\mu} - T\mathfrak{P}^{\mu\sigma}\partial_{\sigma}\left(\frac{\mu_c}{T}\right)\right) \\ \mathfrak{D}^{(\Delta,P)\mu} &= \kappa_1\mathfrak{v}^{\sigma}\partial_{\sigma}\mathfrak{u}^{\mu} - \mathfrak{v}^{\mu}\left(\left(\mathfrak{v}.\mathfrak{G}^{(P)}\right) - \kappa_2\Delta\Theta^{(P)}\right. \\ &\quad \left. + \gamma_1\mathfrak{v}^{\lambda}\mathfrak{u}^{\sigma}\partial_{\sigma}\mathfrak{u}_{\lambda} + \gamma_2\mathfrak{u}.\partial\left(\frac{\mu^b_c}{T}\right)\right) \\ \mathfrak{Q}^{(\Delta,P)\mu\nu} &= \mathfrak{u}^{\mu}\mathfrak{v}^{\nu}\left(\left(\mathfrak{v}.\mathfrak{G}^{(P)}\right) - \kappa_2\Delta\Theta^{(P)} + \kappa_3\mathfrak{u}.\partial\left(\frac{\mu_c}{T}\right)\right) \\ \mathfrak{G}^{(P)\mu} &= \mathfrak{G}^{(0,P)\mu} + \Delta\mathfrak{G}^{(\Delta,P)\mu} \\ \mathfrak{G}^{(0,P)\mu} &= -\alpha_1\mathfrak{u}^{\sigma}\partial_{\sigma}\mathfrak{u}^{\mu} - 2\alpha_2\left(\mathfrak{E}^{\mu} - T\mathfrak{P}^{\mu\sigma}\partial_{\sigma}\left(\frac{\mu_c}{T}\right)\right) \\ \mathfrak{G}^{(\Delta,P)\mu} &= \kappa_1\mathfrak{v}^{\sigma}\partial_{\sigma}\mathfrak{u}^{\mu} + \kappa_2\mathfrak{v}^{\mu}\left((\partial.\mathfrak{u}) + \Theta^{(P)}\right) \\ \Theta^{(P)} &= \mathfrak{v}^{\sigma}\left(-\mathfrak{E}_{\sigma} + T\partial_{\sigma}\left(\frac{\mu_c}{T}\right)\right).\end{aligned} \tag{35}$$

At this stage, it is also noteworthy to mention that some of the transports appearing in the isotropic part of the parity even sector also appear in its anisotropic counterpart. As a consequence of this, all the previously determined constraints [14] on the transport coefficients of the (isotropic) parity even sector (in the constitutive relations) might not hold good and one therefore needs to redo the calculations. In the following we enumerate each of the entities in (34) separately. A straightforward computation yields the following:

(I)

$$-\frac{1}{T}\partial_{\mu}\mathfrak{u}_{\nu}\mathfrak{S}^{(0)\mu\nu} = \frac{\eta}{T}\sigma^{\mu\nu}\sigma_{\mu\nu} + \frac{\zeta}{T}(\partial.\mathfrak{u})^2. \tag{36}$$

(II)

$$\begin{aligned}&- \mathfrak{D}^{(0,P)\mu}\left(\mathfrak{P}_{\mu\nu}\partial^{\nu}\left(\frac{\mu_c}{T}\right) - \frac{\mathfrak{E}_{\mu}}{T}\right) \\ &\quad = \frac{\sigma_D}{T}\left(\mathfrak{E}_{\mu} - T\mathfrak{P}_{\mu\nu}\partial^{\nu}\left(\frac{\mu_c}{T}\right)\right)^2 + \frac{\alpha_3}{T}\mathfrak{P}^{\mu\nu}\mathrm{K}_{\mu\nu}\Theta^{(P)}\end{aligned} \tag{37}$$

where

$$\mathrm{K}_{\alpha\beta} = \partial_{\alpha}\mathfrak{v}_{\beta} + \partial_{\beta}\mathfrak{v}_{\alpha}. \tag{38}$$

(III)

$$-\frac{1}{T}\mathfrak{G}^{(0,P)\nu}\mathfrak{u}^{\mu}\partial_{\mu}\mathfrak{u}_{\nu} = \frac{\alpha_1}{T}\left(\mathfrak{u}^{\sigma}\partial_{\sigma}\mathfrak{u}^{\mu}\right)^2 + \frac{\alpha_2}{T}\mathfrak{P}^{\mu\nu}\mathrm{K}_{\mu\nu}\Theta^{(P)}. \tag{39}$$

(IV)

$$\begin{aligned}-\frac{1}{T}\partial_{\mu}\mathfrak{u}_{\nu}\mathfrak{G}^{(\Delta,P)\mu\nu} = {} & \frac{\lambda\mathrm{K}^{\mu\nu}}{T}\left(\partial_{\sigma}\mathfrak{u}_{\nu}\mathfrak{u}_{\mu}u^{\sigma} + \frac{\mathrm{Q}_{\mu\nu}}{2}\right) \\ & + \frac{\alpha_1}{T}(\partial.\mathfrak{u})\mathfrak{P}^{\mu\nu}\mathrm{K}_{\mu\nu} \\ & + \frac{\xi_1}{2T}\left(\mathfrak{v}^{\mu}\mathfrak{v}^{\nu}\mathrm{Q}_{\mu\nu}\right)\left(\mathfrak{u}.\partial\left(\frac{\mu_c}{T}\right)\right) \\ & + \frac{\alpha_1}{T}\mathfrak{v}^{\mu}\mathfrak{u}^{\sigma}\mathrm{Q}_{\mu\nu}\partial_{\sigma}\mathfrak{u}^{\nu} \\ & + \frac{2\alpha_2}{T}(\partial.\mathfrak{u})\Theta^{(P)} \\ & + \frac{\Delta(\kappa_1-\kappa_2)}{2T}(\partial.\mathfrak{u})\mathfrak{v}^{\mu}\mathfrak{v}^{\nu}\mathrm{Q}_{\mu\nu} \\ & - \frac{\alpha_2}{T}\mathfrak{v}^{\mu}\mathfrak{v}^{\nu}\mathrm{Q}_{\mu\nu}\Theta^{(P)} \\ & - \frac{\Delta\kappa_1}{T}\mathfrak{v}^{\mu}\mathfrak{v}^{\sigma}\mathrm{Q}_{\mu\nu}\partial_{\sigma}\mathfrak{u}^{\nu} \\ & + \frac{(\alpha_1-\xi_2)}{4T}\mathfrak{P}^{\sigma\lambda}\mathrm{K}_{\sigma\lambda}\mathfrak{v}^{\mu}\mathfrak{v}^{\nu}\mathrm{Q}_{\mu\nu} \\ & + \frac{\Delta\kappa_1}{4T}\left(\mathfrak{v}^{\mu}\mathfrak{v}^{\nu}\mathrm{Q}_{\mu\nu}\right)^2\end{aligned} \tag{40}$$

where

$$\mathrm{Q}_{\alpha\beta} = \partial_{\alpha}\mathfrak{u}_{\beta} + \partial_{\beta}\mathfrak{u}_{\alpha}. \tag{41}$$

(V)

$$\begin{aligned}& -\mathfrak{D}^{(\Delta,P)\mu}\left(\mathfrak{P}_{\mu\nu}\partial^{\nu}\left(\frac{\mu_c}{T}\right) - \frac{\mathfrak{E}_{\mu}}{T}\right) \\ & \quad = -\frac{\kappa_1(1-\Delta)}{2T}\mathfrak{v}^{\mu}\mathfrak{v}^{\nu}\mathrm{Q}_{\mu\nu}\Theta^{(P)} + \frac{2\alpha_2}{T}\Theta^{2(P)} \\ & \quad + \frac{(\alpha_1-\gamma_1)}{2T}\mathfrak{P}^{\mu\nu}\mathrm{K}_{\mu\nu}\Theta^{(P)} + \frac{\Delta\kappa_2}{T}(\partial.\mathfrak{u})\Theta^{(P)} \\ & \quad + \frac{\gamma_2}{T}\Theta^{(P)}\mathfrak{u}.\partial\left(\frac{\mu_c}{T}\right).\end{aligned} \tag{42}$$

(VI)

$$\begin{aligned}-\frac{1}{T}\mathfrak{G}^{(\Delta,P)\nu}\mathfrak{u}^{\mu}\partial_{\mu}\mathfrak{u}_{\nu} = {} & -\frac{\kappa_1}{T}\mathfrak{v}^{\mu}\mathfrak{u}^{\sigma}\mathrm{Q}_{\mu\nu}\partial_{\sigma}\mathfrak{u}^{\nu} \\ & - \frac{\kappa_1}{T}\mathfrak{u}^{\mu}\mathfrak{u}^{\sigma}\mathrm{K}_{\mu\nu}\partial_{\sigma}\mathfrak{u}^{\nu} \\ & - \frac{(\kappa_1-\kappa_2)}{2T}(\partial.\mathfrak{u})\mathfrak{P}^{\mu\nu}\mathrm{K}_{\mu\nu} \\ & + \frac{\kappa_1}{T}\mathfrak{u}^{\mu}\partial_{\mu}\mathfrak{v}_{\nu}\partial_{\sigma}\left(\mathfrak{u}^{\sigma}\mathfrak{u}^{\nu}\right) \\ & + \frac{\kappa_2}{2T}\mathfrak{P}^{\mu\nu}\mathrm{K}_{\mu\nu}\Theta^{(P)}.\end{aligned} \tag{43}$$

(VII)

$$\begin{aligned}\frac{1}{T}\mathfrak{u}_{\nu}\partial_{\mu}\mathfrak{Q}^{(\Delta,P)\mu\nu} = {} & \frac{\alpha_1}{4T}\left(\mathfrak{P}^{\mu\nu}\mathrm{K}_{\mu\nu}\right)^2 + \frac{\alpha_2}{T}\mathfrak{P}^{\mu\nu}\mathrm{K}_{\mu\nu}\Theta^{(P)} \\ & + \frac{\Delta\kappa_1}{4T}\mathfrak{P}^{\lambda\sigma}\mathrm{K}_{\lambda\sigma}\mathfrak{v}^{\mu}\mathfrak{v}^{\nu}\mathrm{Q}_{\mu\nu} \\ & + \frac{\Delta\kappa_2}{2T}(\partial.\mathfrak{u})\mathfrak{P}^{\mu\nu}\mathrm{K}_{\mu\nu} \\ & + \frac{\kappa_3}{2T}\left(\mathfrak{P}^{\mu\nu}\mathrm{K}_{\mu\nu}\right)\left(\mathfrak{u}.\partial\left(\frac{\mu_c}{T}\right)\right).\end{aligned} \tag{44}$$

(i) Observations. In order for the entropy current (34) to be positive definite, from the above computations (36), (38), (39), (41), (42), (43), and (44) we observe the following (in the following discussion we assume, $\Delta > 0$).

(1) Three of the following transports need to be positive definite, namely,

$$\begin{aligned}\eta &\geq 0, \\ \zeta &\geq 0, \\ \sigma_D &\geq 0.\end{aligned} \tag{45}$$

(2) The rest of the transports satisfy nontrivial algebraic identities, part of which could be simplified further in order to obtain

$$\begin{aligned}&\lambda = \alpha_2 = \alpha_1, \\ &\kappa_2 = \kappa_1, \\ &\xi_2 = \kappa_1(2\Delta-1) - \alpha_1, \\ &\Delta\gamma_1 - 2\alpha_3 = (3\Delta+2)\alpha_1 + \Delta\kappa_1 \geq 0, \\ &\qquad \alpha_1, \alpha_2 \geq 0, \ \kappa_1 \geq 0.\end{aligned} \tag{46}$$

(3) The rest of the constraints could be formally expressed as

$$\begin{aligned}&\lambda\mathrm{K}^{\mu\nu}\mathrm{Q}_{\mu\nu} + 2\kappa_1\left(\mathfrak{P}^{\mu\nu}\mathrm{K}_{\mu\nu}(\partial.\mathfrak{u}) + \left(\mathfrak{u}^{\mu}\partial_{\mu}\mathfrak{v}_{\nu}\right)\left(\mathfrak{u}^{\sigma}\partial_{\sigma}\mathfrak{u}^{\nu}\right)\right. \\ &\quad \left. - \Delta\mathfrak{v}^{\mu}\left(\mathfrak{v}^{\sigma}\partial_{\sigma}\mathfrak{u}^{\nu}\right)\mathrm{Q}_{\mu\nu}\right) = 0 \\ &\xi_1\left(\mathfrak{v}^{\mu}\mathfrak{v}^{\nu}\mathrm{Q}_{\mu\nu}\right) + 2\gamma_2\Theta^{(P)} + \kappa_3\left(\mathfrak{P}^{\mu\nu}\mathrm{K}_{\mu\nu}\right) = 0.\end{aligned} \tag{47}$$

In other words, once we move away from the quantum criticality (by breaking symmetries associated with it) a number of additional transports appear which are found to obey nontrivial constraints among themselves. However, all of these new transports cannot be determined uniquely as we have lesser number of constraints available. It turns out that once we determine a few of them, the rest is trivially fixed due to constraints (46)-(47) present in the system.

3.3. Some Useful Relations. We now focus solely on the parity *odd* sector of (31). Before we proceed further, it is now customary to derive certain useful identities that would be required in the subsequent analysis of the entropy current.

(i) Derivation of $\partial_\mu \omega^\mu$. We start our analysis by noting down the following identity [14]:

$$\mathfrak{u}^\mu \mathfrak{u}^\nu \partial_\mu \omega_\nu = -\frac{1}{2}\partial_\mu \omega^\mu. \tag{48}$$

Next, using conservation equation (3) we find

$$\omega_\nu \partial_\mu \mathfrak{T}^{\mu\nu} = \varrho \omega_\mu \mathfrak{E}^\mu + \mathcal{O}\left(\partial^3\right). \tag{49}$$

Finally, using (7), (24), and (49) we obtain

$$\partial_\mu \omega^\mu = -\frac{2}{(\epsilon + P_\perp)}\omega^\mu \mathbb{W}_\mu + \mathcal{O}\left(\partial^3\right) \tag{50}$$

where the vector $\mathbb{W}^\mu$ could be formally expressed as

$$\mathbb{W}^\mu = g^{\mu\nu}\left(\partial_\nu P_\perp - \Delta\partial_\nu \log \vartheta\right) - \varrho \mathfrak{E}^\mu - \mathfrak{v}^\mu \mathfrak{v}^\nu \partial_\nu \Delta. \tag{51}$$

(ii) Derivation of $\partial_\mu \mathfrak{B}^\mu$. We start our analysis with the following identity [14]:

$$\partial_\mu \mathfrak{B}^\mu = \mathfrak{u}^\nu \partial_\nu \mathfrak{u}_\mu \mathfrak{B}^\mu - 2\omega_\mu \mathfrak{E}^\mu = -\mathfrak{u}^\mu \mathfrak{u}^\nu \partial_\mu \mathfrak{B}_\nu - 2\omega_\mu \mathfrak{E}^\mu \tag{52}$$

Following the same steps as above we note that

$$\mathfrak{B}_\nu \partial_\mu \mathfrak{T}^{\mu\nu} = \varrho \mathfrak{B}_\mu \mathfrak{E}^\mu + \mathcal{O}\left(\partial^3\right). \tag{53}$$

Finally, using (7), (24), and (52) we find

$$\partial_\mu \mathfrak{B}^\mu = -2\omega_\mu \mathfrak{E}^\mu - \frac{1}{(\epsilon + P_\perp)}\mathfrak{B}^\mu \mathbb{W}_\mu + \mathcal{O}\left(\partial^3\right). \tag{54}$$

3.4. Parity Odd Sector. Following the prescription of [34], we modify our entropy current as

$$\mathbb{J}^\mu_{\mathfrak{s}} \longrightarrow \mathbb{J}^\mu_{\mathfrak{s}} + \mathbb{D}_\omega \omega^\mu + \mathbb{D}_{\mathfrak{B}} \mathfrak{B}^\mu = \mathbb{J}^\mu_{\mathfrak{s}} + \widetilde{\mathbb{J}}^\mu_{\mathfrak{s}} \tag{55}$$

which yields the divergence equation as (at this stage it is noteworthy to mention that here by $\not{P}$ we explicitly mean all the parity *odd* terms of the entropy current (31))

$$\begin{aligned}\partial_\mu \mathbb{J}^{(\not{P})\mu}_{\mathfrak{s}} &= -\mathfrak{D}^{(0,\not{P})\mu}\left(\mathfrak{P}_{\mu\nu}\partial^\nu\left(\frac{\mu_c}{T}\right) - \frac{\mathfrak{E}_\mu}{T}\right) \\ &\quad - \frac{\mu_c}{T}\mathfrak{c}\mathfrak{E}_\mu \mathfrak{B}^\mu - \frac{1}{T}\mathfrak{G}^{(0,\not{P})\nu}\mathfrak{u}^\mu \partial_\mu \mathfrak{u}_\nu + \Delta \mathbb{M}^{(\Delta,\not{P})} \\ &\quad + \partial_\mu \widetilde{\mathbb{J}}^\mu_{\mathfrak{s}}\end{aligned} \tag{56}$$

where the function $\mathbb{M}^{(\Delta,\not{P})}$ could be formally expressed as

$$\begin{aligned}\mathbb{M}^{(\Delta,\not{P})} &= -\frac{1}{T}\partial_\mu \mathfrak{u}_\nu \mathfrak{S}^{(\Delta,\not{P})\mu\nu} \\ &\quad - \mathfrak{D}^{(\Delta,\not{P})\mu}\left(\mathfrak{P}_{\mu\nu}\partial^\nu\left(\frac{\mu_c}{T}\right) - \frac{\mathfrak{E}_\mu}{T}\right) \\ &\quad - \frac{1}{T}\mathfrak{G}^{(\Delta,\not{P})\nu}\mathfrak{u}^\mu \partial_\mu \mathfrak{u}_\nu + \frac{1}{T}\mathfrak{u}_\nu \partial_\mu \mathfrak{Q}^{(\Delta,\not{P})\mu\nu}.\end{aligned} \tag{57}$$

In the following, we enumerate each of the individual terms one by one.

(I)

$$\begin{aligned}&-\mathfrak{D}^{(0,\not{P})\mu}\left(\mathfrak{P}_{\mu\nu}\partial^\nu\left(\frac{\mu_c}{T}\right) - \frac{\mathfrak{E}_\mu}{T}\right) \\ &\quad = \frac{\varsigma_\omega}{T}\omega^\mu \mathfrak{E}_\mu - \varsigma_\omega \omega^\mu \partial_\mu\left(\frac{\mu_c}{T}\right) + \frac{\varsigma_{\mathfrak{B}}}{T}\mathfrak{E}_\mu \mathfrak{B}^\mu \\ &\quad - \varsigma_{\mathfrak{B}} \mathfrak{B}^\mu \partial_\mu\left(\frac{\mu_c}{T}\right).\end{aligned} \tag{58}$$

(II)

$$\begin{aligned}&-\frac{1}{T}\mathfrak{G}^{(0,\not{P})\nu}\mathfrak{u}^\mu \partial_\mu \mathfrak{u}_\nu \\ &\quad = \frac{\left(\beta_\omega \omega^\mu + \beta_{\mathfrak{B}} \mathfrak{B}^\mu\right)}{(\epsilon + P_\perp)}\left(\varrho \mathfrak{E}_\mu - \partial_\mu P_\perp + \Delta \partial_\mu \log \vartheta\right).\end{aligned} \tag{59}$$

At this stage it is noteworthy to mention that in deriving the above relation we have used the conservation equation (3) in order to obtain (in our derivation we have assumed that $\mathfrak{v}^\mu \partial_\mu \Delta = 0$ which corresponds to the fact that the gradient of the pressure difference is orthogonal to the anisotropy vector $\mathfrak{v}^\mu$ [25, 26])

$$\begin{aligned}\mathfrak{a}^\mu &= \mathfrak{u}^\nu \partial_\nu \mathfrak{u}^\mu \\ &= \frac{1}{(\epsilon + P_\perp)}\left(\varrho \mathfrak{E}^\mu - \mathfrak{P}^{\mu\nu}\left(\partial_\nu P_\perp - \Delta \partial_\nu \log \vartheta\right)\right).\end{aligned} \tag{60}$$

Therefore, to be precise, we are looking for an *on shell* cancellation in the parity odd sector of the entropy current where the last term corresponds to the anisotropic contribution to the acceleration of the fluid particles [14].

(III)

$$-\frac{1}{T}\partial_\mu \mathfrak{u}_\nu \mathfrak{S}^{(\Delta,\not{P})\mu\nu} = \left(\beta_\omega \omega^\mu + \beta_{\mathfrak{B}} \mathfrak{B}^\mu\right)\left(\mathfrak{v}^\nu \mathrm{Q}_{\mu\nu} - \mathfrak{v}_\mu \mathbb{N}\right) \tag{61}$$

where $\mathbb{N} = \partial.\mathfrak{u} - 2\mathfrak{u}^\mu \partial_\mu \log \vartheta$.

(IV)

$$\begin{aligned}&-\mathfrak{D}^{(\Delta,\not{P})\mu}\left(\mathfrak{P}_{\mu\nu}\partial^\nu\left(\frac{\mu_c}{T}\right) - \frac{\mathfrak{E}_\mu}{T}\right) \\ &\quad = -\left(\beta_\omega \omega^\mu + \beta_{\mathfrak{B}} \mathfrak{B}^\mu\right)\mathfrak{v}_\mu \Theta^{(P)}.\end{aligned} \tag{62}$$

(V)

$$-\frac{1}{T}\mathfrak{G}^{(\Delta,\not{P})\nu}\mathfrak{u}^\mu \partial_\mu \mathfrak{u}_\nu = \left(\beta_\omega \omega^\mu + \beta_{\mathfrak{B}} \mathfrak{B}^\mu\right)\mathfrak{v}_\mu\left(\mathfrak{v}.\mathfrak{a}\right). \tag{63}$$

(VI)

$$\frac{1}{T}\mathfrak{u}_{\nu}\partial_{\mu}\mathfrak{Q}^{(\Delta,\not{P})\mu\nu} = \left(\beta_{\omega}\omega^{\mu} + \beta_{\mathfrak{B}}\mathfrak{B}^{\mu}\right)\mathfrak{v}_{\mu}\left(\mathfrak{v}.\mathfrak{a}\right). \tag{64}$$

Finally, collecting all the individual pieces in (56) we arrive at the following set of constraint equations, namely,

$$\begin{aligned}
&\partial_{\mu}\mathbb{D}_{\omega} - \frac{\left(2\mathbb{D}_{\omega} + \beta_{\omega}\right)}{\left(\epsilon + P_{\perp}\right)}\left(\partial_{\mu}P_{\perp} - \Delta\partial_{\mu}\log\vartheta\right) - \varsigma_{\omega}\partial_{\mu}\left(\frac{\mu_c}{T}\right) \\
&\quad + \Delta\beta_{\omega}\mathfrak{v}^{\nu}\left(\mathrm{Q}_{\mu\nu} - g_{\mu\nu}\mathbb{Z}\right) = 0 \\
&\frac{\left(2\mathbb{D}_{\omega} + \beta_{\omega}\right)\varrho}{\left(\epsilon + P_{\perp}\right)} - 2\mathbb{D}_{\mathfrak{B}} + \frac{\varsigma_{\omega}}{T} = 0 \\
&\partial_{\mu}\mathbb{D}_{\mathfrak{B}} - \frac{\left(\mathbb{D}_{\mathfrak{B}} + \beta_{\mathfrak{B}}\right)}{\left(\epsilon + P_{\perp}\right)}\left(\partial_{\mu}P_{\perp} - \Delta\partial_{\mu}\log\vartheta\right) - \varsigma_{\mathfrak{B}}\partial_{\mu}\left(\frac{\mu_c}{T}\right) \\
&\quad + \Delta\beta_{\mathfrak{B}}\mathfrak{v}^{\nu}\left(\mathrm{Q}_{\mu\nu} - g_{\mu\nu}\mathbb{Z}\right) = 0 \\
&\frac{\left(\mathbb{D}_{\mathfrak{B}} + \beta_{\mathfrak{B}}\right)\varrho}{\left(\epsilon + P_{\perp}\right)} + \frac{\varsigma_{\mathfrak{B}}}{T} - \mathfrak{c}\frac{\mu_c}{T} = 0
\end{aligned} \tag{65}$$

where the entity $\mathbb{Z}$ could be formally expressed as

$$\mathbb{Z} = \mathbb{N} + \Theta^{(P)} - 2\left(\mathfrak{v}.\mathfrak{a}\right). \tag{66}$$

The above set of (65) precisely corresponds to the *anisotropic* generalization of the earlier results [14] obtained in the context of anomalous hydrodynamics at quantum critical (Lifshitz) point. Our ultimate goal would be to solve (65) in order to obtain parity odd transports away from quantum critical point. In order to proceed further, we however treat the above set of equations perturbatively in the anisotropy and/or the spin wave excitation ($|\Delta| \ll 1$). We consider the following perturbative expansion of anomalous transports, namely,

$$\mathbb{Q}_i = \mathbb{Q}_i^{(0)} + \Delta\mathbb{Q}_i^{(1)} + \mathscr{O}\left(\Delta^2\right) \tag{67}$$

where $\mathbb{Q} = \{\mathbb{D}, \beta, \varsigma\}$ and $i = \{\omega, \mathfrak{B}\}$. The zeroth order solutions are indeed trivial and have been found earlier in [14]. However, the first nontrivial correction appears at the leading order in Δ. The corresponding set of equations at leading order turns out to be (for the sake of simplicity we do not quote the zeroth order solutions here. Interested reader may have a look at [14]. These solutions are purely fixed by the anomaly. However, we will use them explicitly in order to explore solutions at leading order in the anisotropy)

$$\begin{aligned}
&\partial_{\mu}\mathbb{D}_{\omega}^{(1)} - \left(2\mathbb{D}_{\omega}^{(1)} + \beta_{\omega}^{(1)}\right)\left(\frac{\partial_{\mu}P_{\perp}}{\epsilon + P_{\perp}}\right) \\
&\quad + \frac{\left(2\mathbb{D}_{\omega}^{(0)} + \beta_{\omega}^{(0)}\right)}{\left(\epsilon + P_{\perp}\right)}\partial_{\mu}\log\vartheta - \varsigma_{\omega}^{(1)}\partial_{\mu}\left(\frac{\mu_c}{T}\right) \\
&\quad + \beta_{\omega}\mathfrak{v}^{\nu}\left(\mathrm{Q}_{\mu\nu} - g_{\mu\nu}\mathbb{Z}\right) = 0 \\
&\frac{\left(2\mathbb{D}_{\omega}^{(1)} + \beta_{\omega}^{(1)}\right)\varrho}{\left(\epsilon + P_{\perp}\right)} - 2\mathbb{D}_{\mathfrak{B}}^{(1)} + \frac{\varsigma_{\omega}^{(1)}}{T} = 0 \\
&\partial_{\mu}\mathbb{D}_{\mathfrak{B}}^{(1)} - \left(\mathbb{D}_{\mathfrak{B}}^{(1)} + \beta_{\mathfrak{B}}^{(1)}\right)\left(\frac{\partial_{\mu}P_{\perp}}{\epsilon + P_{\perp}}\right) \\
&\quad + \frac{\left(\mathbb{D}_{\mathfrak{B}}^{(0)} + \beta_{\mathfrak{B}}^{(0)}\right)}{\left(\epsilon + P_{\perp}\right)}\partial_{\mu}\log\vartheta - \varsigma_{\mathfrak{B}}^{(1)}\partial_{\mu}\left(\frac{\mu_c}{T}\right) \\
&\quad + \beta_{\mathfrak{B}}\mathfrak{v}^{\nu}\left(\mathrm{Q}_{\mu\nu} - g_{\mu\nu}\mathbb{Z}\right) = 0 \\
&\frac{\left(\mathbb{D}_{\mathfrak{B}}^{(1)} + \beta_{\mathfrak{B}}^{(1)}\right)\varrho}{\left(\epsilon + P_{\perp}\right)} + \frac{\varsigma_{\mathfrak{B}}^{(1)}}{T} = 0.
\end{aligned} \tag{68}$$

The above set of (68) could be simplified further in order to obtain the following reduced set of equations, namely,

$$\begin{aligned}
&\partial_{\mu}\left(\mathbb{D}_{\omega}^{(1)} - \mathbb{D}_{\mathfrak{B}}^{(1)}\right) \\
&\quad - \left(2\mathbb{D}_{\omega}^{(1)} - \mathbb{D}_{\mathfrak{B}}^{(1)} + \beta_{\omega}^{(1)} - \beta_{\mathfrak{B}}^{(1)}\right)\left(\frac{\partial_{\mu}P_{\perp}}{\epsilon + P_{\perp}}\right) \\
&\quad + \frac{\mathbb{X}^{(0)}}{\left(\epsilon + P_{\perp}\right)}\partial_{\mu}\log\vartheta \\
&\quad - \left(\varsigma_{\omega}^{(1)} - \varsigma_{\mathfrak{B}}^{(1)}\right)\partial_{\mu}\left(\frac{\mu_c}{T}\right) = 0 \\
&\frac{\left(2\mathbb{D}_{\omega}^{(1)} + \beta_{\omega}^{(1)}\right)\varrho}{\left(\epsilon + P_{\perp}\right)} - 2\mathbb{D}_{\mathfrak{B}}^{(1)} + \frac{\varsigma_{\omega}^{(1)}}{T} = 0 \\
&\frac{\left(\mathbb{D}_{\mathfrak{B}}^{(1)} + \beta_{\mathfrak{B}}^{(1)}\right)\varrho}{\left(\epsilon + P_{\perp}\right)} + \frac{\varsigma_{\mathfrak{B}}^{(1)}}{T} = 0
\end{aligned} \tag{69}$$

where the entity $\mathbb{X}^{(0)}$ could be formally expressed as

$$\mathbb{X}^{(0)} = 2\mathbb{D}_{\omega}^{(0)} - \mathbb{D}_{\mathfrak{B}}^{(0)} + \beta_{\omega}^{(0)} - \beta_{\mathfrak{B}}^{(0)}. \tag{70}$$

Considering the general identity (here we define $\overline{\mu}_c = \mu_c/T$),

$$\begin{aligned}
\partial_{\mu}\mathbb{D}_i^{(1)} &= \left(\frac{\partial\mathbb{D}_i^{(1)}}{\partial P_{\perp}}\right)_{\overline{\mu}_c,\log\vartheta}\partial_{\mu}P_{\perp} + \left(\frac{\partial\mathbb{D}_i^{(1)}}{\partial\overline{\mu}_c}\right)_{P_{\perp},\log\vartheta}\partial_{\mu}\overline{\mu}_c \\
&\quad + \left(\frac{\partial\mathbb{D}_i^{(1)}}{\partial\log\vartheta}\right)_{P_{\perp},\overline{\mu}_c}\partial_{\mu}\log\vartheta
\end{aligned} \tag{71}$$

From (69), we arrive at the following set of equations:

$$\begin{aligned}
&\left(\frac{\partial \mathbb{D}_{\omega}^{(1)}}{\partial P_{\perp}}\right)_{\bar{\mu}_c,\log\vartheta} - \frac{\left(2\mathbb{D}_{\omega}^{(1)} - \mathbb{D}_{\mathfrak{B}}^{(1)} + \beta_{\omega}^{(1)} - \beta_{\mathfrak{B}}^{(1)}\right)}{(\epsilon + P_{\perp})} = 0 \\
&\left(\frac{\partial \mathbb{D}_{\omega}^{(1)}}{\partial \bar{\mu}_c}\right)_{P_{\perp},\log\vartheta} - \left(\varsigma_{\omega}^{(1)} - \varsigma_{\mathfrak{B}}^{(1)}\right) = 0 \\
&\left(\frac{\partial \mathbb{D}_{\omega}^{(1)}}{\partial \log\vartheta}\right)_{P_{\perp},\bar{\mu}_c} + \frac{\mathbb{X}^{(0)}}{(\epsilon + P_{\perp})} = 0 \\
&\left(\frac{\partial \mathbb{D}_{\mathfrak{B}}^{(1)}}{\partial P_{\perp}}\right)_{\bar{\mu}_c,\log\vartheta} + \frac{\left(2\mathbb{D}_{\omega}^{(1)} - \mathbb{D}_{\mathfrak{B}}^{(1)} + \beta_{\omega}^{(1)} - \beta_{\mathfrak{B}}^{(1)}\right)}{(\epsilon + P_{\perp})} = 0 \\
&\left(\frac{\partial \mathbb{D}_{\mathfrak{B}}^{(1)}}{\partial \bar{\mu}_c}\right)_{P_{\perp},\log\vartheta} + \left(\varsigma_{\omega}^{(1)} - \varsigma_{\mathfrak{B}}^{(1)}\right) = 0 \\
&\left(\frac{\partial \mathbb{D}_{\mathfrak{B}}^{(1)}}{\partial \log\vartheta}\right)_{P_{\perp},\bar{\mu}_c} - \frac{\mathbb{X}^{(0)}}{(\epsilon + P_{\perp})} = 0 \\
&\frac{\left(2\mathbb{D}_{\omega}^{(1)} + \beta_{\omega}^{(1)}\right)\varrho}{(\epsilon + P_{\perp})} - 2\mathbb{D}_{\mathfrak{B}}^{(1)} + \frac{\varsigma_{\omega}^{(1)}}{T} = 0 \\
&\frac{\left(\mathbb{D}_{\mathfrak{B}}^{(1)} + \beta_{\mathfrak{B}}^{(1)}\right)\varrho}{(\epsilon + P_{\perp})} + \frac{\varsigma_{\mathfrak{B}}^{(1)}}{T} = 0.
\end{aligned} \tag{72}$$

Equation (72) is precisely an artifact of the symmetry breaking effect which nontrivially modifies the previously obtained constraint equations [14]. In order to proceed further, from (29) we note

$$\begin{aligned}
\left(\frac{\partial \bar{\mu}_c}{\partial T}\right)_{P_{\perp},\log\vartheta} &= -\frac{(\epsilon + P_{\perp})}{\varrho T^2} \\
\left(\frac{\partial P_{\perp}}{\partial T}\right)_{\bar{\mu}_c,\log\vartheta} &= \frac{(\epsilon + P_{\perp})}{T} \\
\left(\frac{\partial \log\vartheta}{\partial T}\right)_{\bar{\mu}_c,P_{\perp}} &= -\frac{1}{\Delta}\frac{(\epsilon + P_{\perp})}{T}.
\end{aligned} \tag{73}$$

Substituting (73) into (72) we find

$$\begin{aligned}
&\left(\frac{\partial \mathbb{D}_{\omega}^{(1)}}{\partial \log\vartheta}\right)_{T,\bar{\mu}_c} + \left(\frac{\partial \mathbb{D}_{\mathfrak{B}}^{(1)}}{\partial \log\vartheta}\right)_{T,\bar{\mu}_c} + \mathscr{O}\left(\Delta^2, T\right) = 0 \\
&\left(1 - \frac{\varrho T^2}{(\epsilon + P_{\perp})}\right)\left(\left(\frac{\partial \mathbb{D}_{\omega}^{(1)}}{\partial T}\right)_{\bar{\mu}_c,\log\vartheta} + \left(\frac{\partial \mathbb{D}_{\mathfrak{B}}^{(1)}}{\partial T}\right)_{\bar{\mu}_c,\log\vartheta}\right) \\
&\quad + \left(\frac{\partial \mathbb{D}_{\omega}^{(1)}}{\partial \bar{\mu}_c}\right)_{T,\log\vartheta} + \left(\frac{\partial \mathbb{D}_{\mathfrak{B}}^{(1)}}{\partial \bar{\mu}_c}\right)_{T,\log\vartheta} = 0 \\
&\frac{\left(2\mathbb{D}_{\omega}^{(1)} + \beta_{\omega}^{(1)}\right)\varrho}{(\epsilon + P_{\perp})} - 2\mathbb{D}_{\mathfrak{B}}^{(1)} + \frac{\varsigma_{\omega}^{(1)}}{T} = 0 \\
&\frac{\left(\mathbb{D}_{\mathfrak{B}}^{(1)} + \beta_{\mathfrak{B}}^{(1)}\right)\varrho}{(\epsilon + P_{\perp})} + \frac{\varsigma_{\mathfrak{B}}^{(1)}}{T} = 0.
\end{aligned} \tag{74}$$

From the first two equations in (74), we find

$$\mathbb{D}_{\mathfrak{B}}^{(1)} + \mathbb{D}_{\omega}^{(1)} = \mathscr{C} \tag{75}$$

where $\mathscr{C}$ is some integration constant that does not depend on any of the thermodynamic variables. Using (75), the last two equations of (74) could be further modified as

$$\begin{aligned}
&\frac{\left(2\mathscr{C} + \beta_{\omega}^{(1)}\right)\varrho}{(\epsilon + P_{\perp})} - 2\mathbb{D}_{\mathfrak{B}}^{(1)}\left(1 + \frac{\varrho}{(\epsilon + P_{\perp})}\right) + \frac{\varsigma_{\omega}^{(1)}}{T} = 0 \\
&\frac{\left(\mathbb{D}_{\mathfrak{B}}^{(1)} + \beta_{\mathfrak{B}}^{(1)}\right)\varrho}{(\epsilon + P_{\perp})} + \frac{\varsigma_{\mathfrak{B}}^{(1)}}{T} = 0.
\end{aligned} \tag{76}$$

Clearly, the above equation (76) is inadequate to solve all the five different transports in a unique fashion (similar conclusions have been drawn earlier by other authors in [35]). Therefore what we find from the above computation is that the entropy current cannot uniquely fix all the parity odd transports once we break the underlying symmetry of the system. However, it indeed imposes nontrivial constraints among different transports as we have also noticed earlier in the parity even sector.

4. Summary and Final Remarks

We now summarise the key findings of our analysis. The most significant outcome of our analysis is the establishment of the hydrodynamic description away from the quantum criticality. We claim that such hydrodynamic description could be identified with the corresponding hydrodynamic description of *spin waves* in the appropriate limit. The reason for this claim rests over the facts that (1) the spin wave excitations are naturally diminished as the fixed point is approached and (2) they spontaneously break the underlying rotational symmetry of the system. Both of them have been incorporated in the present analysis. Our analysis reveals that it is indeed possible to find out new dissipative effects when we explicitly break the underlying symmetry associated with QCPs. We compute the entropy current in order to fix these arbitrary coefficients in the constitutive relation. It turns out that none of these transports could be fixed uniquely. Nevertheless, they are nontrivially constrained by their respective constraint equations. We perform our analysis for the most general charged dissipative fluids where we consider both parity preserving and parity violating effects at leading order in the derivative expansion.

Finally, as mentioned earlier, for realistic models of strange metal systems one should actually consider the so called *nonrelativistic* limit of the Lifshitz hydrodynamics that has been discussed so far. This will eventually lead us towards a formulation of nonrelativistic QFTs with broken Galilean boost starting from a theory with broken Lorentz boost invariance. This could be done in two different ways. One could either take a (v^i/c) limit of the theory [9] or simply go to some light cone frame [36, 37]. However, one should take care of the fact that in the nonrelativistic limit the so called scaling relations will also get modified leading to a modified Ward identity [9]. We leave all these issues for the purpose of future investigation.

Data Availability

No data were used to support this study.

Conflicts of Interest

The author declares that there are no conflicts of interest.

Acknowledgments

The author would like to acknowledge the financial support from UGC (Project No. UGC/PHY/2014236).

References

[1] N. Iqbal, H. Liu, and M. Mezei, "Lectures on holographic non-fermi liquids and quantum phase transitions," in *Proceedings of the KITPC workshop/school on "AdS/CM duality and other approaches"*, pp. 707–815, 2011.

[2] P. Coleman and A. J. Schofield, "Quantum criticality," *Nature*, vol. 433, no. 7023, pp. 226–229, 2005.

[3] S. Sachdev and B. Keimer, "Quantum criticality," *Physics Today*, vol. 64, no. 2, pp. 29–35, 2011.

[4] P. Gegenwart, Q. Si, and F. Steglich, "Quantum criticality in heavy-fermion metals," *Nature Physics*, vol. 4, no. 3, pp. 186–197, 2008.

[5] Q. Si and F. Steglich, "Heavy fermions and quantum phase transitions," *Science*, vol. 329, no. 5996, pp. 1161–1166, 2010.

[6] E. J. Brynjolfsson, U. H. Danielsson, L. Thorlacius, and T. Zingg, "Black hole thermodynamics and heavy fermion metals," *Journal of High Energy Physics*, vol. 2010, no. 8, article 027, 2010.

[7] S. Kachru, X. Liu, and M. Mulligan, "Gravity duals of Lifshitz-like fixed points," *Physical Review D: Particles, Fields, Gravitation and Cosmology*, vol. 78, no. 10, Article ID 106005, 8 pages, 2008.

[8] M. Taylor, "Lifshitz holography," *Classical and Quantum Gravity*, vol. 33, no. 3, Article ID 033001, 2016.

[9] C. Hoyos, B. S. Kim, and Y. Oz, "Lifshitz hydrodynamics," *Journal of High Energy Physics*, vol. 2013, no. 11, article 145, 2013.

[10] C. Hoyos, B. S. Kim, and Y. Oz, "Lifshitz field theories at non-zero temperature, hydrodynamics and gravity," *Journal of High Energy Physics*, vol. 2014, no. 3, article 029, 2014.

[11] C. Hoyos, B. S. Kim, and Y. Oz, "Bulk viscosity in holographic Lifshitz hydrodynamics," *Journal of High Energy Physics*, vol. 2014, no. 3, article 050, 2014.

[12] C. Eling and Y. Oz, "Horava-Lifshitz black hole hydrodynamics," *Journal of High Energy Physics*, vol. 2014, no. 11, article 067, 2014.

[13] S. Chapman, C. Hoyos, and Y. Oz, "Lifshitz superfluid hydrodynamics," *Journal of High Energy Physics*, vol. 2014, no. 7, article 027, 2014.

[14] C. Hoyos, A. Meyer, and Y. Oz, "Parity breaking transport in Lifshitz hydrodynamics," *Journal of High Energy Physics*, vol. 2015, no. 9, article 031, 2015.

[15] D. Roychowdhury, "Magnetoconductivity in chiral Lifshitz hydrodynamics," *Journal of High Energy Physics*, vol. 2015, no. 9, article 145, 2015.

[16] E. Kiritsis and Y. Matsuo, "Charge-hyperscaling violating Lifshitz hydrodynamics from black-holes," *Journal of High Energy Physics*, vol. 2015, no. 12, article 076, 2015.

[17] A. Dehyadegari, A. Sheykhi, and M. Kord Zangeneh, "Holographic conductivity for logarithmic charged dilaton-Lifshitz solutions," *Physics Letters B*, vol. 758, pp. 226–234, 2016.

[18] D. Pang, "Conductivity and diffusion constant in Lifshitz backgrounds," *Journal of High Energy Physics*, vol. 2010, no. 1, article 120, 2010.

[19] S. Bhattacharyya, "Entropy current from partition function: one example," *Journal of High Energy Physics*, vol. 2014, no. 7, article 139, 2014.

[20] S. Bhattacharyya, "Entropy current and equilibrium partition function in fluid dynamics," *Journal of High Energy Physics*, vol. 2014, no. 8, article 165, 2014.

[21] R. Banerjee, S. Dey, and B. R. Majhi, "Entropy current in two dimensional anomalous hydrodynamics and a bound on the sum of the response parameters," *Physical Review D: Particles, Fields, Gravitation and Cosmology*, vol. 92, no. 4, Article ID 044019, 2015.

[22] R. Loganayagam, "Entropy current in conformal hydrodynamics," *Journal of High Energy Physics*, vol. 2008, no. 5, article 087, 2008.

[23] K. Jensen, M. Kaminski, P. Kovtun, R. Meyer, A. Ritz, and A. Yarom, "Towards hydrodynamics without an entropy current," *Physical Review Letters*, vol. 109, no. 10, Article ID 101601, 2012.

[24] N. Banerjee, J. Bhattacharya, S. Bhattacharyya, S. Jain, S. Minwalla, and T. Sharma, "Constraints on fluid dynamics from equilibrium partition functions," *Journal of High Energy Physics*, vol. 2012, no. 9, article 046, 2012.

[25] I. Gahramanov, T. Kalaydzhyan, and I. Kirsch, "Anisotropic hydrodynamics, holography, and the chiral magnetic effect," *Physical Review D: Particles, Fields, Gravitation and Cosmology*, vol. 85, no. 12, Article ID 126013, 2012.

[26] W. Florkowski, "Anisotropic fluid dynamics in the early stage of relativistic heavy-ion collisions," *Physics Letters B*, vol. 668, no. 32, 2008.

[27] S. Sachdev, "The Quantum phases of matter," 2011, https://arxiv.org/abs/1203.4565.

[28] S. Sachdev, *Quantum Phase Transitions*, Cambridge University Press, Cambridge, UK, 2011.

[29] M. A. Continentino, S. N. de Medeiros, M. T. D. Orlando et al., "Anisotropic quantum critical behavior in $CeCoGe_{3-x}Si_x$," *Physical Review B*, vol. 64, Article ID 012404, 2001.

[30] J. Larrea, J. M. B. Fontes, A. D. Alvarenga et al., "Quantum critical behavior in a CePt ferromagnetic kondo lattice," *Physical Review B*, vol. 72, Article ID 035129, 2005.

[31] E. Verlinde, "On the origin of gravity and the laws of Newton," *Journal of High Energy Physics*, vol. 2011, no. 04, article 029, 2011.

[32] N. Banerjee, J. Bhattacharya, S. Bhattacharyya, S. Dutta, R. Loganayagam, and P. Surówka, "Hydrodynamics from charged

black branes," *Journal of High Energy Physics*, vol. 2011, no. 1, article 094, 2011.

[33] J. Erdmenger, M. Haack, M. Kaminski, and A. Yarom, "Fluid dynamics of *R*-charged black holes," *Journal of High Energy Physics*, vol. 2009, article 055, 2009.

[34] D. T. Son and P. Surowka, "Hydrodynamics with triangle anomalies," *Physical Review Letters*, vol. 103, Article ID 191601, 2009.

[35] Y. Neiman and Y. Oz, "Relativistic hydrodynamics with general anomalous charges," *Journal of High Energy Physics*, vol. 2011, article 023, 2011.

[36] M. Rangamani, S. F. Ross, D. T. Son, and E. G. Thompson, "Conformal non-relativistic hydrodynamics from gravity," *Journal of High Energy Physics. A SISSA Journal*, no. 1, 075, 26 pages, 2009.

[37] N. Banerjee, S. Dutta, A. Jain, and D. Roychowdhury, "Entropy current for non-relativistic fluid," *Journal of High Energy Physics*, vol. 2014, article 037, 2014.

Hindawi
Advances in High Energy Physics
Volume 2019, Article ID 5234014, 11 pages
https://doi.org/10.1155/2019/5234014

Research Article

Dark Energy in Spherically Symmetric Universe Coupled with Brans-Dicke Scalar Field

Koijam Manihar Singh[1] and Gauranga C. Samanta [2]

[1]*Department of Mathematics, Mizoram University, Aizawl, Mizoram 796004, India*
[2]*Department of Mathematics, BITS Pilani K K Birla Goa Campus, Goa 403726, India*

Correspondence should be addressed to Gauranga C. Samanta; gauranga81@gmail.com

Received 5 March 2019; Accepted 27 March 2019; Published 2 May 2019

Guest Editor: Subhajit Saha

Copyright © 2019 Koijam Manihar Singh and Gauranga C. Samanta. This is an open access article distributed under the Creative Commons Attribution License, which permits unrestricted use, distribution, and reproduction in any medium, provided the original work is properly cited.

The phenomenon of dark energy and its manifestations are studied in a spherically symmetric universe considering the Brans-Dicke scalar tensor theory. In the first model, the dark energy behaves like a phantom type and in such a universe the existence of negative time is validated with an indication that our universe started its evolution before $t = 0$. Dark energy prevalent in this universe is found to be more active at times when other types of energies remain passive. The second model of universe begins with big bang. On the other hand, the dark energy prevalent in the third model is found to be of the quintessence type. Here, it is seen that the dark energy triggers the big bang and after that much of the dark energy reduces to dark matter. One peculiarity in such a model is that the scalar field is prevalent eternally; it never tends to zero.

1. Introduction

The type Ia (SNIa) supernovae observations suggested that our universe is not only expanding, but also the rate of expansion is in accelerating way [1, 2] and this acceleration is caused by some mysterious object, so called dark energy. The matter species in the universe are broadly classified into relativistic particle, nonrelativistic particle, and dark energy. Another component, apparently a scalar field, dominated during the period of inflation in the early universe. In the present universe, the sum of the density parameters of baryons, radiation, and dark matter does not exceed 30% [3]; we still need to identify the remaining 70% of the cosmic matter. We call this 70% unknown component as dark energy, and it is supposed to be responsible for the present cosmic acceleration of the universe. According to the cosmological principle, our universe is homogeneous and isotropic in large scale. By assuming isotropicity and homogeneity, the acceleration equation of the universe in general theory of relativity can be written as $\ddot{a}/a = -(1/6)\kappa^2(\rho + 3p)$. The acceleration and deceleration of the universe depend on the sign of $\ddot{a}$; that is, the universe will accelerate if $\rho + 3p < 0$ or decelerate if $\rho + 3p > 0$. So, the condition $\rho + 3p < 0$ has to be satisfied in general relativity to explain accelerated expansion of the universe. This implies that the strong energy condition is violated; moreover, the strong energy condition is violated, meaning that the universe contains some abnormal (something not normal) matter. Hence, without violating strong energy condition, the accelerated expansion of the universe is not possible in general theory of relativity. Therefore, the modification of the general theory of relativity is necessary. Essentially, there are two approaches, out of which one is to modify the right-hand side of Einstein's field equations (i.e., matter part of the universe) by considering some specific forms of the energy momentum tensor $T_{\mu\nu}$ having a huge negative pressure and which is concluded in the form of some mysterious energy dubbed as dark energy. In this approach, the simplest candidate for dark energy is cosmological constant Λ, which is described by the equation of state $p = -\rho$ [4]. The second approach is by modifying Einstein Hilbert action, that is, the geometry of the space-time, which is named as modified gravity theory. So many modifications of general relativity theory have been done, namely, Brans-Dicke (BD) [5] and Saez-Ballester scalar-tensor theories [6], $f(R)$ gravity [7–12], $f(T)$ gravity [13–16], Gauss-Bonnet theory [17–20], Horava-Lifshitz gravity [21–23], and recently $f(R,T)$ gravity [24]. Subsequently, so many authors [25–54] have been studying modified gravity theory to understand the nature of the dark energy and accelerated expansion of the universe.

Apart from this, the Hubble parameter H may provide some important information about the evolution of our universe. It is dynamically determined by the Friedmann equations and then evolves with cosmological red-shift. The evolution of Hubble parameter is closely related with radiation, baryon, cold dark matter, and dark energy or even other exotic components available in the universe. Further, it may be impacted by some interactions between these cosmic inventories. Thus, one can look out upon the evolution of the universe by studying the Hubble parameter. Besides dark energy, there exists a dark matter component of the universe. One can verify whether these two components can interact with each other. Theoretically, there is no evidence against their interaction. Basically, they may exchange their energy which affects the cosmic evolution of the universe. Furthermore, it is not clear whether the nongravitational interactions between two energy sources produced by two different matters in our universe can produce acceleration. We can assume for a while that the origin of nongravitational interaction is related to emergence of the space-time dynamics. However, this is not of much help, since this hypothesis is not more fundamental compared with other phenomenological assumptions within modern cosmology [55–59]. However, the authors [60, 61] studied the finding that the interacting cosmological models make good agreement with observational data. The aim of this paper is to study a cosmological model, where a phenomenological form of nongravitational interactions is involved. In this article, we are interested in the problem of accelerated expansion of the large-scale universe; we follow the well-known approximation of the energy content of the recent universe. Namely, we consider the interaction between dark energy and other matters (including dark matter).

2. Space-Time and Field Equations

We consider the spherically symmetric space-time

$$ds^2 = dt^2 - e^{\lambda}\left(dr^2 + r^2 d\theta^2 + r^2 \sin^2\theta\, d\phi^2\right), \tag{1}$$

where λ is a function of time. The energy momentum tensor for the fluid comprising our universe is taken as

$$T_{\mu\nu} = (p+\rho)\, u_\mu u_\nu - p g_{\mu\nu}, \tag{2}$$

where ρ and p are, respectively, the total energy density and total pressure which are taken as

$$\rho = \rho_m + \rho_d \tag{3}$$

and

$$p = p_m + p_d, \tag{4}$$

with ρ_d and ρ_m being, respectively, the densities of dark energy and other matters in this universe. p_d and p_m are, respectively, the pressures of dark energy and other matters (including dark matter) in this universe. And u_μ is the flow vector satisfying the relations

$$\begin{aligned} u_\mu u^\mu &= 1; \\ u_\mu u^\nu &= 0. \end{aligned} \tag{5}$$

The Brans-Dicke scalar tensor field equations are given by

$$\begin{aligned} R_{\mu\nu} - \frac{1}{2} R g_{\mu\nu} = {} & -8\pi\phi^{-1} T_{\mu\nu} \\ & - \omega\phi^{-2}\left(\phi_{,\mu}\phi_{,\nu} - \frac{1}{2} g_{\mu\nu}\phi_{,\gamma}\phi^{,\gamma}\right) \\ & - \phi^{-1}\left(\phi_{\mu;\nu} - g_{\mu\nu}\phi^{;\gamma}_{;\gamma}\right) \end{aligned} \tag{6}$$

with

$$\phi^{;\gamma}_{;\gamma} = 8\pi (3+2\omega)^{-1} T, \tag{7}$$

where ω is the coupling constant and ϕ is the scalar field. Energy conservation gives the equation

$$T^{\mu\nu}_{;\mu} = 0 \tag{8}$$

Here the field equations take the form

$$\frac{3}{4}\dot{\lambda}^2 - \frac{\omega}{2}\frac{\dot{\phi}^2}{\phi^2} + \frac{3}{2}\dot{\lambda}\frac{\dot{\phi}}{\phi} = 8\pi\phi^{-1}(\rho_m + \rho_d) \tag{9}$$

$$\ddot{\lambda} + \frac{3}{4}\dot{\lambda}^2 + \frac{\omega}{2}\frac{\dot{\phi}^2}{\phi^2} + \dot{\lambda}\frac{\dot{\phi}}{\phi} + \frac{\ddot{\phi}}{\phi} = -8\pi\phi^{-1}(p_m + p_d) \tag{10}$$

$$\frac{3}{2}\left(\ddot{\lambda} + \dot{\lambda}^2\right) + \frac{\omega}{2}\frac{\dot{\phi}^2}{\phi^2} + \frac{\ddot{\phi}}{\phi} + \frac{3}{2}\dot{\lambda}\frac{\dot{\phi}}{\phi} = -8\pi\phi^{-1}(p_m + p_d) \tag{11}$$

$$\ddot{\phi} + \frac{3}{2}\dot{\lambda}\dot{\phi} = 8\pi (3+2\omega)^{-1}(\rho_m + \rho_d - 3p_m - 3p_d) \tag{12}$$

Here, we take the equation of state parameter for dark energy as α so that

$$p_d = \alpha\rho_d. \tag{13}$$

And the conservation equation gives

$$\dot{\rho} + (p+\rho)\frac{3}{2}\dot{\lambda} = 0 \tag{14}$$

Since the dark energy and other matters are interacting in this universe, (14) can be written as

$$\dot{\rho_m} + (\rho_m + p_m)\frac{3}{2}\dot{\lambda} = -Q \tag{15}$$

and

$$\dot{\rho_d} + (\rho_d + p_d)\frac{3}{2}\dot{\lambda} = Q, \tag{16}$$

where Q is the interaction between dark energy and other matters (including dark matter) which this universe comprises. Here Q can take different forms like $3z^2\rho$, $3z^2\rho_m$, $3z^2\rho_d$, and so forth, where z^2 is a coupling constant. It can also take other forms which are functions of ρ and $\dot{\rho}$. Now from (10) and (11) we get the relation

$$\ddot{\lambda}+\frac{3}{4}\dot{\lambda}^2+\dot{\lambda}\frac{\dot{\phi}}{\phi}=\frac{3}{2}\ddot{\lambda}+\frac{3}{2}\dot{\lambda}^2+\frac{3}{2}\dot{\lambda}\frac{\dot{\phi}}{\phi} \tag{17}$$

which gives

$$e^{(3/2)\lambda}\dot{\lambda}=a_0\phi^{-1} \tag{18}$$

where a_0 is an arbitrary constant.

3. Analytical Solutions

In this section, we try to obtain the analytical solutions of the field equations in three different cases based on the different forms of the interaction parameter Q.

3.1. Case-I. From (17) and (18) we get

$$\lambda=\frac{2}{3}\log b_2+\log\left(b_0+b_1t\right)^{a_1} \tag{19}$$

$$\phi=\frac{a_0}{a_1b_1b_2}\left(b_0+b_1t\right)^{1-(3/2)a_1} \tag{20}$$

where a_1, b_0, b_1, and b_2 are arbitrary constants. Here in this case we take

$$Q=3z^2H\rho, \tag{21}$$

where H is Hubble's parameter so that the conservation equation takes the form of the equations

$$\dot{\rho_m}+\left(\rho_m+p_m\right)\frac{3}{2}\dot{\lambda}=-\frac{3}{2}z^2\dot{\lambda}\rho \tag{22}$$

and

$$\dot{\rho_d}+\left(\rho_d+p_d\right)\frac{3}{2}\dot{\lambda}=\frac{3}{2}z^2\dot{\lambda}\rho. \tag{23}$$

Now from (23) we get

$$\begin{aligned}\rho_d&=b_4\left(b_0+b_1t\right)^{-(3/2)(\alpha+1)a_1}\\&\quad+b_3\left(1-\frac{3}{2}a_1\alpha\right)^{-1}\left(b_0+b_1t\right)^{-1-(3/2)a_1}\end{aligned} \tag{24}$$

where b_4 is an arbitrary constant and

$$\begin{aligned}&b_3\\&=\frac{3z^2a_0b_1}{16b_2\pi}\left[\frac{4}{3}a_1^2-\frac{\omega}{2}\left(1-\frac{3}{2}a_1\right)^2+\frac{3}{2}a_1\left(1-\frac{3}{2}a_1\right)\right]\end{aligned} \tag{25}$$

Thus using (24) in (9) we have

$$\begin{aligned}\rho_m&=\frac{2b_3}{3a_1z^2}\left(b_0+b_1t\right)^{-1-(3/2)a_1}\\&\quad+b_3\left(\frac{3}{2}a_1\alpha-1\right)^{-1}\left(b_0+b_1t\right)^{-1-(3/2)a_1}\\&\quad-b_4\left(b_0+b_1t\right)^{-(3/2)(1+\alpha)a_1}\end{aligned} \tag{26}$$

Therefore (22) gives

$$\begin{aligned}p_m&=\left[\frac{z^2a_0b_1}{8\pi a_1b_2}\left\{\frac{\omega}{2}\left(1-\frac{3}{2}a_1\right)^2-\frac{4}{3}a_1^2\right.\right.\\&\quad\left.-\frac{3}{2}a_1\left(1-\frac{3}{2}a_1\right)\right\}-\frac{2}{3a_1b_1}\left\{\frac{2b_1b_3}{3a_1z^2}\right.\\&\quad\left.+b_1b_3\left(\frac{3}{2}a_1\alpha-1\right)^{-1}\right\}-\frac{2b_3}{3a_1z^2}-b_3\left(\frac{3}{2}a_1\alpha\right.\\&\quad\left.\left.-1\right)^{-1}\right]\left(b_0+b_1t\right)^{-1-(3/2)a_1}+\left(b_4+\frac{2b_4}{3a_1}\right)\left(b_0\right.\\&\quad\left.+b_1t\right)^{-(3/2)(1+\alpha)a_1}\end{aligned} \tag{27}$$

Now using (27) in (10) we have

$$\begin{aligned}p_d&=\left[\frac{z^2a_0b_1}{8\pi a_1b_2}\left\{\frac{4}{3}a_1^2-\frac{\omega}{2}\left(1-\frac{3}{2}a_1\right)^2\right.\right.\\&\quad\left.+\frac{3}{2}a_1\left(1-\frac{3}{2}a_1\right)\right\}+\frac{2}{3a_1b_1}\left\{\frac{2b_1b_3}{3a_1z^2}\right.\\&\quad\left.+b_1b_3\left(\frac{3}{2}a_1\alpha-1\right)^{-1}\right\}+b_3\left(\frac{3}{2}a_1\alpha-1\right)^{-1}\\&\quad+\frac{2b_3}{3a_1z^2}-\frac{a_0}{8\pi a_1b_1b_2}\left\{\frac{3}{4}a_1^2b_1^2-a_1b_1^2\right.\\&\quad+\frac{\omega}{2}b_1^2\left(1-\frac{3}{2}a_1\right)^2+a_1b_1^2\left(1-\frac{3}{2}a_1\right)\\&\quad\left.\left.-b_1^2\left(1-\frac{3}{2}a_1\right)\right\}\right]\left(b_0+b_1t\right)^{-1(3/2)a_1}-b_4\left(1\right.\\&\quad\left.+\frac{2}{3a_1}\right)\left(b_0+b_1t\right)^{-(3/2)(1+\alpha)a_1}\end{aligned} \tag{28}$$

Again from (13) and (24) we get

$$\begin{aligned}p_d&=\alpha b_4\left(b_0+b_1t\right)^{-(3/2)(1+\alpha)a_1}\\&\quad+\alpha b_3\left(1-\frac{3}{2}a_1\alpha\right)^{-1}\left(b_0+b_1t\right)^{-1-(3/2)a_1}\end{aligned} \tag{29}$$

Thus comparing coefficients of $(b_0 + b_1 t)^{-(3/2)(1+\alpha)a_1}$ and $(b_0 + b_1 t)^{-(3/2)a_1 - 1}$ of the two expressions of p_d in (28) and (29), we obtain

$$\begin{aligned}
&\frac{z^2 a_0 a_1 b_1}{6\pi b_2} - \frac{z^2 \omega a_0 b_1}{16\pi a_1 b_2}\left(1 - \frac{3}{2}a_1\right)^2 \\
&\quad + \frac{z^2 a_0 b_1}{16\pi b_2}\left(1 - \frac{3}{2}a_1\right) + \frac{4b_3}{9a_1^2 z^2} \\
&\quad + \frac{2b_3}{3a_1}\left(\frac{3}{2}a_1\alpha - 1\right)^{-1} + \frac{2b_3}{3a_1 z^2} \\
&\quad + b_3\left(\frac{3}{2}a_1\alpha - 1\right)^{-1} - \frac{3a_0 a_1 b_1}{32\pi b_2} + \frac{a_0 b_1}{8\pi b_2} \\
&\quad - \frac{\omega a_0 b_1}{16\pi a_1 b_2}\left(1 - \frac{3}{2}a_1\right)^2 - \frac{a_0 b_1}{8\pi b_2}\left(1 - \frac{3}{2}a_1\right) \\
&\quad + \frac{a_0 b_1}{8\pi a_1 b_2}\left(1 - \frac{3}{2}a_1\right) \\
&= \frac{z^2 a_0 a_1 b_1}{6\pi b_2} - \frac{z^2 \omega a_0 b_1}{16\pi a_1 b_2}\left(1 - \frac{3}{2}a_1\right)^2 \\
&\quad + \frac{z^2 a_0 b_1}{16\pi b_2}\left(1 - \frac{3}{2}a_1\right) + \frac{4b_3}{9a_1^2 z^2} + \frac{2b_3}{3a_1 z^2} \\
&\quad + b_3\left(\frac{3}{2}a_1\alpha - 1\right)^{-1}\left(\frac{2}{3a_1} + 1\right) + \frac{3a_0 a_1 b_1}{32\pi b_2} \\
&\quad - \frac{\omega a_0 b_1}{16\pi a_1 b_2}\left(1 - \frac{3}{2}a_1\right)^2 + \frac{a_0 b_1}{8\pi a_1 b_2}\left(1 - \frac{3}{2}a_1\right)
\end{aligned} \tag{30}$$

which is automatically satisfied; and

$$\alpha = -\left(1 + \frac{2}{3a_1}\right) \tag{31}$$

In this case

$$\rho = \frac{2b_3}{3a_1 z^2}(b_0 + b_1 t)^{-1-(3/2)a_1} \tag{32}$$

And the interaction Q is given by

$$\begin{aligned}
Q = \frac{3z^2 a_0 b_1^2}{16 b_2 \pi}&\left[\frac{4}{3}a_1^2 - \frac{\omega}{2}\left(1 - \frac{3}{2}a_1\right)^2\right. \\
&\left. + \frac{3}{2}a_1\left(1 - \frac{3}{2}a_1\right)\right](b_0 + b_1 t)^{-2-(3/2)a_1}
\end{aligned} \tag{33}$$

The physical and kinematical properties of the model are obtained as follows:

Volume is

$$V = b_2 (b_0 b_1 t)^{(3/2)a_1} \tag{34}$$

Hubble's parameter is

$$H = \frac{1}{2}a_1 b_1 (b_0 + b_1 t)^{-1} \tag{35}$$

Expansion factor is

$$\theta = \frac{3}{2}a_1 b_1 (b_0 + b_1 t)^{-1} \tag{36}$$

Deceleration parameter is

$$q = \frac{2}{a_1} - 1 \tag{37}$$

Jerk parameter is

$$j = \frac{2b_1}{a_1}\left(\frac{a_1}{2} - 1\right)\left(\frac{a_1}{2} - 2\right)(b_0 + b_1 t)^{-1} \tag{38}$$

And state-finder parameters $\{r, s\}$ are obtained as

$$r = 4a_1^2\left(\frac{a_1}{2} - 1\right)\left(\frac{a_1}{2} - 2\right) \tag{39}$$

$$s = \frac{2}{3}a_1^{-1}(a_1 - 2)(a_1 - 4)(4 - 3a_1)^{-1} \tag{40}$$

Dark energy parameter is

$$\begin{aligned}
\Omega_d &= \frac{\rho_d}{3H^2} \\
&= a_1^{-2} b_1^{-2} b_3 (4 + 3a_1)(b_0 + b_1 t)^{-1-(3/2)a_1} \\
&\quad + \frac{4}{3}a_1^{-2} b_1^{-2} b_4 (b_0 + b_1 t)^3
\end{aligned} \tag{41}$$

3.2. Case-II. As another solution we get from (17) and (18),

$$\lambda = (c_1 t + c_0)^{c_2} \tag{42}$$

$$\phi = \frac{a_0}{c_1 c_2}(c_1 t + c_0)^{1-c_2} e^{(-3/2)(c_1 t + c_0)^{c_2}} \tag{43}$$

where c_0, c_1, and c_2 are arbitrary constants. Here in the case we take the interaction Q as

$$Q = 3z^2 H \rho_d \tag{44}$$

where H is the mean Hubble's parameter. Then (15) and (16), respectively, take the forms

$$\dot{\rho_m} + (\rho_m + p_m)\frac{3}{2}\dot{\lambda} = -3z^2 \rho_d \frac{\dot{\lambda}}{2} \tag{45}$$

and

$$\dot{\rho_d} + (\rho_d + p_d)\frac{3}{2}\dot{\lambda} = 3z^2 \rho_d \frac{\dot{\lambda}}{2} \tag{46}$$

From (46) we get

$$\rho_d = c_3 e^{(3/2)(z^2 - \alpha - 1)(c_1 t + c_0)^{c_2}} \tag{47}$$

where c_3 is an arbitrary constant. Now using (42), (43), and (47) in (9) we get

$$\begin{aligned}\rho_m &= \frac{a_0c_1c_2}{8\pi}\left(\frac{3}{4}-\frac{9\omega}{8}\right)(c_1t+c_0)^{c_2-1}e^{-(3/2)(c_1t+c_0)^{c_2}} \\ &- \frac{\omega a_0 c_1}{16\pi c_2}(1-c_2)^2(c_1t+c_0)^{-1-c_2}e^{-(3/2)(c_1t+c_0)^{c_2}} \\ &+ \frac{3a_0c_1}{16\pi}(1-c_2)(1+\omega)(c_1t+c_0)^{-1}e^{-(3/2)(c_1t+c_0)^{c_2}} \\ &- \frac{9a_0c_1c_2}{32\pi}(c_1t+c_0)^{c_2-1}e^{-(3/2)(c_1t+c_0)^{c_2}} \\ &- c_3e^{(3/2)(z^2-\alpha-1)(c_1t+c_0)^{c_2}}\end{aligned} \tag{48}$$

Here, using (47), (48) and (13), (12) gives

$$\begin{aligned}p_m &= \left(\frac{21a_0c_1c_2}{96\pi}+\frac{27\omega a_0c_1c_2}{48\pi}-\frac{9}{32\pi}-\frac{9\omega}{48\pi}\right) \\ &\times (c_1t+c_0)^{c_2-1}e^{-(3/2)(c_1t+c_0)^{c_2}}+\frac{a_0c_1}{16\pi}(1-c_2) \\ &\cdot(1+\omega)(c_1t+c_0)^{-1}e^{-(3/2)(c_1t+c_0)^{c_2}} \\ &+\left[\frac{a_0c_1^2(1-c_2)}{24\pi}(3+2\omega)-\frac{\omega a_0c_1(1-c_2)^2}{48\pi c_2}\right] \\ &\cdot(c_1t+c_0)^{-c_2-1}e^{-(3/2)(c_1t+c_0)^{c_2}} \\ &-\alpha c_3 e^{(3/2)(z^2-\alpha-1)(c_1t+c_0)^{c_2}}\end{aligned} \tag{49}$$

In this case

$$\begin{aligned}\rho &= \frac{a_0c_1c_2}{8\pi}\left(\frac{3}{4}-\frac{9\omega}{8}\right)(c_1t+c_0)^{c_2-1}e^{-(3/2)(c_1t+c_0)^{c_2}} \\ &- \frac{\omega a_0 c_1}{16\pi c_2}(1-c_2)^2(c_1t+c_0)^{-1-c_2}e^{-(3/2)(c_1t+c_0)^{c_2}} \\ &+ \frac{3a_0c_1}{16\pi}(1-c_2)(1+\omega)(c_1t+c_0)^{-1}e^{-(3/2)(c_1t+c_0)^{c_2}} \\ &- \frac{9a_0c_1c_2}{32\pi}(c_1t+c_0)^{c_2-1}e^{-(3/2)(c_1t+c_0)^{c_2}}\end{aligned} \tag{50}$$

And the interaction Q is obtained as

$$Q=\frac{3}{2}z^2c_1c_2c_3(c_1t+c_0)^{c_2-1}e^{(3/2)(z^2-\alpha-1)(c_1t+c_0)^{c_2}} \tag{51}$$

3.3. Case-II(a). In this case, we take the interaction Q as $3z^2\rho_m(\dot{\lambda}/2)$, so that the conservation equations take the forms

$$\dot{\rho_m}+(\rho_m+p_m)\frac{3}{2}\dot{\lambda}=-3z^2\rho_m\frac{\dot{\lambda}}{2} \tag{52}$$

$$\dot{\rho_d}+(\rho_d+p_d)\frac{3}{2}\dot{\lambda}=3z^2\rho_m\frac{\dot{\lambda}}{2} \tag{53}$$

Now, from (9), using (42) and (43), we get

$$\begin{aligned}\rho_m &= \frac{a_0}{8\pi c_1c_2}e^{-(3/2)(c_1t+c_0)^{c_2}}\left[\left(\frac{3}{2}\omega c_1^2c_2(1-c_2)\right.\right. \\ &\left.+\frac{3}{2}c_1^1c_2(1-c_2)\right)\times(c_1t+c_0)^{-1}-\frac{\omega}{2}c_1^2(1-c_2)^2 \\ &\left.\cdot(c_1t+c_0)^{-1-c_2}-\left(\frac{3}{2}+\frac{9\omega}{8}\right)c_1^2c_2^2(c_1t+c_0)^{c_2-1}\right] \\ &-\rho_d\end{aligned} \tag{54}$$

From (53), using (54), (13) and (42), we have

$$\begin{aligned}\dot{\rho_d} &= -\frac{3}{2}c_1c_2(c_1t+c_0)^{c_2-1}\rho_d+\frac{3a_0z^2}{16\pi} \\ &\cdot e^{-(3/2)(c_1t+c_0)^{c_2}}\left[-\frac{\omega}{2}c_1^2(1-c_2)^2(c_1t+c_0)^{-2}\right. \\ &+\frac{3}{2}c_1^2c_2(1+\omega)(1-c_2)(c_1t+c_0)^{c_2-2} \\ &\left.-\left(\frac{3}{2}+\frac{9\omega}{8}\right)c_1^2c_2^2(c_1t+c_0)^{2c_2-1}\right],\end{aligned} \tag{55}$$

where

$$\alpha=-z^2 \tag{56}$$

And this is possible without loss of generality as α can take values such that $-1\le\alpha<0$ as well as $\alpha<-1$ which is the characteristic of different forms of dark energy which can be attained according to different values of z^2. Now (55) gives

$$\begin{aligned}\rho_d &= \frac{3a_0z^2}{16\pi}e^{-(3/2)(c_1t+c_0)^{c_2}}\left[\frac{\omega}{2}c_1(1-c_2)^2(c_1t+c_0)^{-1}\right. \\ &-\frac{1}{2}\left(\frac{3}{2}+\frac{9\omega}{8}\right)c_1c_2(c_1t+c_0)^{2c_2} \\ &\left.-\frac{3}{2}(1+\omega)c_1c_2(c_1t+c_0)^{c_2-1}\right]\end{aligned} \tag{57}$$

From (54) and (57), we have

$$\begin{aligned}\rho_m &= e^{-(3/2)(c_1t+c_0)^{c_2}}\left[\left(\frac{3a_0c_1}{16\pi}(1+\omega)(1-c_2)\right.\right. \\ &\left.-\frac{3a_0\omega c_1z^2}{32\pi}(1-c_2)^2\right)\times(c_1t+c_0)^{-1} \\ &+\left(\frac{9a_0c_1c_2}{32\pi}(1+\omega)z^2-\frac{a_0}{8\pi}c_1c_2\left(\frac{3}{2}+\frac{9\omega}{8}\right)\right)(c_1t \\ &+c_0)^{c_2-1}+\frac{3a_0c_1c_2}{32\pi}z^2\left(\frac{3}{2}+\frac{9\omega}{8}\right)(c_1t+c_0)^{2c_2} \\ &\left.-\frac{a_0\omega c_1}{16\pi c_2}(1-c_2)^2(c_1t+c_0)^{-c_2-1}\right]\end{aligned} \tag{58}$$

Now from (57) and (13) we take

$$p_d = \frac{3a_0 z^2 \alpha}{16\pi} e^{-(3/2)(c_1 t + c_0)^{c_2}} \left[\frac{\omega}{2} c_1 (1 - c_2)^2 (c_1 t + c_0)^{-1} - \frac{1}{2} \left(\frac{3}{2} + \frac{9\omega}{8} \right) c_1 c_2 (c_1 t + c_0)^{2c_2} - \frac{3}{2} (1 + \omega) c_1 c_2 (c_1 t + c_0)^{c_2 - 1} \right] \quad (59)$$

Thus, now using (59) in (10), we get

$$p_m = \left[\left\{ \frac{3a_0 \omega c_1}{32\pi} z^4 (1 - c_2)^2 + \frac{3\omega a_0 c_1}{16\pi} (1 - c_2) + \frac{3a_0 c_1}{16\pi} (1 - c_2) \right\} (c_1 t + c_0)^{-1} - \frac{3a_0 z^4 c_1 c_2}{32\pi} \left(\frac{3}{2} + \frac{9\omega}{8} \right) (c_1 t + c_0)^{2c_2} + \left(\frac{9a_0 z^4}{32\pi} (1 + \omega) c_1 c_2 + \frac{3a_0 c_1 c_2}{32\pi} - \frac{9\omega a_0 c_1 c_2}{32\pi} - \frac{9a_0 c_1}{32\pi} \right) (c_1 t + c_0)^{c_2 - 1} + \left(\frac{a_0 c_1 (1 - c_2)}{8\pi} - \frac{\omega a_0 c_1}{16\pi c_2} (1 - c_2)^2 \right) (c_1 t + c_0)^{-1-c_2} \right] e^{-(3/2)(c_1 t + c_0)^{c_2}} \quad (60)$$

And in this case

$$\rho = \frac{a_0}{8\pi c_1 c_2} e^{-(3/2)(c_1 t + c_0)^{c_2}} \left[\left(\frac{3\omega}{2} c_1^2 c_2 (1 - c_2) + \frac{3}{2} c_1^2 c_2 (1 - c_2) \right) \times (c_1 t + c_0)^{-1} - \frac{\omega}{2} c_1^2 (1 - c_2)^2 \cdot (c_1 t + c_0)^{-1-c_2} - \left(\frac{3}{2} + \frac{9\omega}{8} \right) c_1^1 c_2^2 (c_1 t + c_0)^{c_2 - 1} \right] \quad (61)$$

Here the interaction Q is obtained as

$$Q = \frac{3}{2} c_1 c_2 z^2 (c_1 t + c_0)^{c_2 - 1} e^{-(3/2)(c_1 t + c_0)^{c_2}} \times \left[\left(\frac{3a_0 c_1}{16\pi} (1 + \omega)(1 - c_2) - \frac{3a_0 \omega c_1 z^2 (1 - c_2)^2}{32\pi} \right) \cdot (c_1 t + c_0)^{-1} + \left(\frac{9a_0 c_1 c_2}{32\pi} (1 + \omega) z^2 - \frac{a_0}{8\pi} c_1 c_2 \left(\frac{3}{2} + \frac{9\omega}{8} \right) \right) \cdot (c_1 t + c_0)^{c_2 - 1} + \frac{3a_0 c_1 c_2}{32\pi} z^2 \left(\frac{3}{2} + \frac{9\omega}{8} \right) (c_1 t + c_0)^{2c_2} - \frac{a_0 \omega c_1}{16\pi c_2} (1 - c_2)^2 (c_1 t + c_0)^{-1-c_2} \right] \quad (62)$$

The physical and kinematical properties of the models are as follows:

$$V = e^{(3/2)(c_1 t + c_0)^{c_2}} \quad (63)$$

$$H = \frac{1}{2} c_1 c_2 (c_1 t + c_0)^{c_2 - 1} \quad (64)$$

$$\theta = \frac{3}{2} c_1 c_2 (c_1 t + c_0)^{c_2 - 1} \quad (65)$$

$$q = -\frac{2}{c_1 c_2} (c_2 - 1)(c_1 t + c_0)^{-c_2} - 1 \quad (66)$$

$$j = \frac{1}{2} c_1 c_2 (c_1 t + c_0)^{c_2 - 1} + 3c_1 (c_2 - 1)(c_1 t + c_0)^{-1} + 2c_1 c_2^{-1} (c_1 t + c_0)^{-c_2 - 1} \quad (67)$$

$$r = 1 + 4c_2^{-2} (c_2 - 1)(c_2 - 2)(c_1 t + c_0)^{-2c_2} + 6c_2^{-1} (c_2 - 1)(c_1 t + c_0)^{-c_2} \quad (68)$$

$$s = -\frac{1}{3} \left[\frac{2}{c_1 c_2} (c_2 - 1)(c_1 t + c_0)^{-c_2} + \frac{3}{2} \right]^{-1} \times \left[6c_2^{-1} (c_2 - 1)(c_1 t + c_0)^{-c_2} + 4c_2^{-2} (c_2 - 1)(c_2 - 2)(c_1 t + c_0)^{-2c_2} \right] \quad (69)$$

3.4. Case-III. Equations (17) and (18) give

$$\lambda = \beta (\log t)^n, \quad \beta > 0, \; n > 1 \quad (70)$$

$$\phi = a_0 (n\beta)^{-1} t (\log t)^{1-n} e^{-(3\beta/2)(\log t)^n} \quad (71)$$

Here in this case we assume the interaction between dark energy and other matters of the universe in the form

$$Q = 3z^2 H \rho_m \quad (72)$$

so that (15) and (16), respectively, take the forms

$$\dot{\rho_m} + (\rho_m + p_m) 3\frac{\dot{\lambda}}{2} = -3z^2 \rho_m \frac{\dot{\lambda}}{2} \quad (73)$$

$$\dot{\rho_d} + (\rho_d + p_d) 3\frac{\dot{\lambda}}{2} = 3z^2 \rho_m \frac{\dot{\lambda}}{2} \quad (74)$$

Now from (9) we get

$$\begin{aligned}\rho_m = {} & \frac{a_0 n\beta}{8\pi t}(\log t)^{n-1} e^{-(3/2)\beta(\log t)^n} \\ & + \frac{3a_0}{16\pi t}(1-\omega)(1-n)(\log t)^{-1} e^{-(3/2)\beta(\log t)^n} \\ & + \frac{a_0}{8\pi t}\left(1-\frac{\omega}{2}\right) e^{-(3/2)\beta(\log t)^n} \\ & - \frac{a_0\omega}{16\pi n\beta t}(\log t)^{1-n} e^{-(3/2)\beta(\log t)^n} \\ & - \frac{(1-n)^2\omega a_0}{16\pi n\beta t}(\log t)^{-n-1} e^{-(3/2)\beta(\log t)^n} \\ & - \frac{(1-n)\omega a_0}{8\pi n\beta t}(\log t)^{-n} e^{-(3/2)\beta(\log t)^n} - \rho_d\end{aligned} \tag{75}$$

Thus, from (74) and (75), using relation (13), we have

$$\rho_d = e^{-(3/2)\beta(\alpha+1+z^2)(\log t)^n} \times \psi(t) \tag{76}$$

where

$$\begin{aligned}\psi(t) = {} & \int \frac{3z^2 n\beta}{2t^2}(\log t)^{n-1} \\ & \cdot e^{(3/2)\beta(\alpha+z^2)(\log t)^n}\left[\frac{na_0\beta}{8\pi}(\log t)^{n-1}\right. \\ & + \frac{3a_0(1-n)}{16\pi}(1-\omega)(\log t)^{-1} + \left(1-\frac{\omega}{2}\right)\frac{a_0}{8\pi} \\ & - \frac{(1-n)^2\omega a_0}{16\pi n\beta}(\log t)^{-n-1} - \frac{\omega a_0}{16\pi n\beta}(\log t)^{1-n} \\ & \left.- \frac{(1-n)\omega a_0}{8\pi n\beta}(\log t)^{-n}\right] dt\end{aligned} \tag{77}$$

Again using relations (70), (71), (75), (76), and (13) in (12), we have

$$\begin{aligned}p_m = {} & \frac{1}{24\pi t}(3+2\omega) \\ & \cdot e^{-(3/2)\beta(\log t)^n}\left[\frac{a_0}{\beta}(1-n)(\log t)^{-1-n} + \frac{3}{2}a_0\right. \\ & + \frac{3}{2}a_0(1-n)(\log t)^{-1} - \frac{a_0}{n\beta}(1-n)(\log t)^{-n} \\ & \left.- \frac{9na_0\beta}{4}(\log t)^{n-1}\right] - \frac{n\beta(3+2\omega)}{16\pi t}(\log t)^{n-1} \\ & \cdot e^{-(3/2)\beta(\log t)^n} \times \left[\frac{a_0}{n\beta}(\log t)^{1-n} - \frac{3a_0}{2}\right. \\ & \left.+ \frac{a_0}{n\beta}(1-n)(\log t)^{-n}\right] + \frac{1}{3}\left[\frac{na_0\beta}{8\pi t}(\log t)^{n-1}\right. \\ & + \frac{3(1-\omega)a_0(1-n)}{16\pi t}(\log t)^{-1} + \frac{a_0}{8\pi t}\left(1-\frac{\omega}{2}\right) \\ & - \frac{\omega a_0}{16\pi n\beta t}(\log t)^{1-n} - \frac{(1-n)^2\omega a_0}{16\pi n\beta t}(\log t)^{-1-n} \\ & \left.- \frac{(1-n)\omega a_0}{8\pi n\beta t}(\log t)^{-n}\right] e^{-(3/2)\beta(\log t)^n} - \alpha\psi(t) \\ & \cdot e^{-(3/2)\beta(\alpha+1+z^2)(\log t)^n}\end{aligned} \tag{78}$$

Here

$$\begin{aligned}\rho_m = {} & \frac{na_0\beta}{8\pi t}(\log t)^{n-1} e^{-(3/2)\beta(\log t)^n} \\ & + \frac{3a_0}{16\pi t}(1-\omega)(1-n)(\log t)^{-1} e^{-(3/2)\beta(\log t)^n} \\ & + \frac{a_0}{8\pi t}\left(1-\frac{\omega}{2}\right) e^{-(3/2)\beta(\log t)^n} \\ & - \frac{\omega a_0}{16\pi n\beta t}(\log t)^{1-n} e^{-(3/2)\beta(\log t)^n} \\ & - \frac{\omega a_0}{16\pi n\beta t}(1-n)^2(\log t)^{-n-1} e^{-(3/2)\beta(\log t)^n} \\ & - \frac{\omega a_0(1-n)}{8\pi n\beta t}(\log t)^{-n} e^{-(3/2)\beta(\log t)^n} \\ & - e^{-(3/2)\beta(\alpha+1+z^2)(\log t)^n}\psi(t)\end{aligned} \tag{79}$$

And

$$\begin{aligned}\rho = {} & \frac{a_0 n\beta}{8\pi t}(\log t)^{n-1} e^{-(3/2)\beta(\log t)^n} \\ & + \frac{3a_0}{16\pi t}(1-\omega)(1-n)(\log t)^{-1} e^{-(3/2)\beta(\log t)^n} \\ & + \frac{a_0}{8\pi t}\left(1-\frac{\omega}{2}\right) e^{-(3/2)\beta(\log t)^n} \\ & - \frac{\omega a_0}{16\pi n\beta t}(\log t)^{1-n} e^{-(3/2)\beta(\log t)^n} \\ & - \frac{(1-n)^2\omega a_0}{16\pi n\beta t}(\log t)^{-n-1} e^{-(3/2)\beta(\log t)^n} \\ & - \frac{(1-n)\omega a_0}{8\pi n\beta t}(\log t)^{-n} e^{-(3/2)\beta(\log t)^n}\end{aligned} \tag{80}$$

In this case, the interaction Q is given by

$$\begin{aligned}Q = {} & \frac{3z^2 n\beta}{2t}(\log t)^{n-1}\left[\frac{na_0\beta}{8\pi t}(\log t)^{n-1} e^{-(3/2)\beta(\log t)^n}\right. \\ & + \frac{3a_0}{16\pi t}(1-\omega)(1-n)(\log t)^{-1} e^{-(3/2)\beta(\log t)^n}\end{aligned}$$

$$+\frac{a_0}{8\pi t}\left(1-\frac{\omega}{2}\right)e^{-(3/2)\beta(\log t)^n} -\frac{\omega a_0}{16\pi n\beta t}(\log t)^{1-n}e^{-(3/2)\beta(\log t)^n} -\frac{\omega a_0}{16\pi n\beta t}(1-n)^2(\log t)^{-n-1}e^{-(3/2)\beta(\log t)^n} -\frac{\omega a_0(1-n)}{8\pi n\beta t}(\log t)^{-n}e^{-(3/2)\beta(\log t)^n} - e^{-(3/2)\beta(\alpha+1+z^2)(\log t)^n}\psi(t)\Bigg] \quad (81)$$

The physical and kinematical properties of the model are obtained as follows:

$$V = e^{(3/2)\beta(\log t)^n} \quad (82)$$

$$H = \frac{n\beta}{2t}(\log t)^{n-1} \quad (83)$$

$$\theta = \frac{3n\beta}{2t}(\log t)^{n-1} \quad (84)$$

$$q = \frac{2}{n\beta}(\log t)^{n-1} + \frac{2(n-1)}{n\beta}(\log t)^{n-2} - 1 \quad (85)$$

$$j = \frac{n\beta}{2}t^{-1}(\log t)^{n-1} + 3(n-1)t^{-3}(\log t)^{-1} + \frac{4}{n\beta}t^{-1}(\log t)^{-n+1} - 3t^{-3} - \frac{6}{n\beta}(n-1)t^{-1}(\log t)^{-n} + \frac{2}{n\beta}(n-1)(n-2)t^{-1}(\log t)^{n-3} \quad (86)$$

$$r = 1 + \frac{6}{n\beta}(n-1)t^{-2}(\log t)^{-n} - \frac{6}{n\beta}t^{-2}(\log t)^{-n+1} + \frac{8}{n^2\beta^2}(\log t)^{-2n+2} - \frac{12}{n^2\beta^2}(n-1)(\log t)^{-2n+1} + \frac{4}{n^2\beta^2}(n-1)(n-2)(\log t)^{-2} \quad (87)$$

$$s = \frac{1}{3}\left[\frac{2}{n\beta}(\log t)^{n-1} + \frac{2(n-1)}{n\beta}(\log t)^{n-2} - \frac{3}{2}\right]^{-1} \times\left[\frac{6}{n\beta}(n-1)t^{-2}(\log t)^{-n} - \frac{6}{n\beta}t^{-2}(\log t)^{-n+1} + \frac{8}{n^2\beta^2}(\log t)^{-2n+2} - \frac{12}{n^2\beta^2}(n-1)(\log t)^{-2n+1} + \frac{4}{n^2\beta^2}(n-1)(n-2)(\log t)^{-2}\right] \quad (88)$$

4. Study of the Solutions and Conclusions

For the model universe in Case-I, we see that, at $t = 0$, the energy density has finite value dependent on the coupling constant of the interaction between dark energy and other matters in this universe, and the total energy density is found to decrease with time until it tends to zero at infinite time and the interaction term is also found to follow the same behavior with respect to time. But during this time the rate of decrease of the dark energy density is slower in comparison to the rate of decrease of the energy density of other matters in the universe. Therefore, as time passes by, dark energy seems to dominate over other matters. Thus, the scenario in such type of universe is that dark energy plays a vital role and it seems that as the energy density of dark energy increases the expansion of the universe increases.

In this model, it is seen that, at $t = 0, V = b_2(b_0+b_1 t)^{(3/2)a_1}$, which shows that if we have to accept the big bang theory, the universe begins its evolution at time $t \longrightarrow -b_0/b_1$, thereby implying the existence of negative time which is almost possible from the presence of dark energy in this universe. Again the value of the deceleration parameter obtained here implies that the value of a_1 is limited by the condition ($a_1 > 2$). And in this model the expansion of the universe is accelerating though the rate decreases with time. Therefore, this universe may be taken as a reasonable model; otherwise, if the rate of expansion increases with time, there will be a singularity where the universe ends transforming itself into a cloud of dust.

In this universe, we see that the interaction between dark energy and other matters decreases with time, and perhaps there is a tendency where the dark energy decays into cold dark matter. Again it is seen that dark energy density is zero only at time $t = -b_0/b_1$ showing that dark energy exists before $t = 0$ also. Thus perhaps there exists an epoch before our cosmic time begins in the history of evolution of the universe.

Here, in this case, if either $a_1 = 2$ or $a_1 = 4$, then we get the state-finder parameter $\{r, s\}$ as $r = 0$ and $s = 0$ for which the dark energy model reduces to a flat ΛCDM model which predicts a highly accelerated expansion before these events of time. In this model, the interaction between dark energy and other matters is found to exist at these events of time not interrupted by the high speed of expansion.

For this universe, the equation of state parameter for dark energy is found to be less than −1 which indicates that the dark energy contained is of the phantom type. From the study of the interaction, we also see that the action of such type of dark energy is more when the energies from other types of sources remain idle or not so active. It is also opposite to or against the light energy. It acts also against the living energy or the energy possessed by the human beings.

In Case-II, though the universe is expanding and the rate of expansion is accelerating, it depends much on the value of c_1, which indicates that the expansion is related to the dark energy density. There it may be taken that dark energy enhances the accelerated expansion. And this enhancement is also dependent on the value of z^2 which is the coupling constant of the interaction between dark energy and other matters in this universe. This implies that the expansion of the universe is very much interrelated with the interaction between dark energy and other components of the universe. Thus, all the members of this universe may be taken to expand due to also the presence of dark energy. Hence, considering a small-scale structure of the universe, the earth may be taken to expand due to also the presence of dark energy.

In this universe, we see that when $c_2 \longrightarrow 0$, it goes to the asymptotic static era with $r \longrightarrow \infty$ and $s \longrightarrow \infty$. And when $c_2 = 1$, the universe goes to ΛCDM model for which $r = 1$ and $s = 0$. Thus, the state-finder parameters $\{r, s\}$ show the picture of the evolution of our universe, starting from the asymptotic static era and then coming to the ΛCDM model era. Here we see that the interaction $Q \longrightarrow 0$ as $c_2 \longrightarrow 0$ which means that the interaction almost stops at the cosmic time when the scale factor of the universe becomes or takes the value $e^{1/2}$.

Again it is seen that the energy density of this model universe tends to infinity at $c_2 = 0$ and decreases gradually as $c_2 \longrightarrow 1$; thus it seems that our universe started with a big bang. From the above behaviors of this model, it is also implied that at the beginning of the evolution of this universe there was no interaction between dark energy and other components of the universe, and after that the interaction between them becomes active and increases with time, and at present they are highly interacting. But this interaction also depends much on the values of α and z^2 which are, respectively, equation of state parameter of the dark energy contained and the coupling constant of interaction.

Case-III represents the logamediate scenario of the universe where the cosmological solutions have indefinite expansion [62]. In this case, the dark energy has a quintessence-like behavior. Here the matter content of the universe is seen to increase slowly due to the interaction and the cosmic effect. In this universe, there is an interesting event of time, that is, the cosmic time, when $t = 1$. At this point, the universe has the tendency of accelerating expansion, but the expansion suddenly stops at this moment and the volume of the universe takes the value of 1 at this juncture. So it seems that there is a bounce and a new epoch begins from this juncture. Also we see that, at $t = 1$, the state-finder parameters $\{r, s\}$ take the values $r = 1$ and $s = 0$. Thus at this instant our universe will go to that of a ΛCDM model which implies that at this event of time most of the dark energy contained will reduce to cold dark matter.

The energy density of this model universe tends to infinity at $t = 0$ which indicates that this universe begins with a big bang, and it (energy density) decreases gradually until it tends to a finite quantity at infinite time, of course with a bounce at $t = 1$. And at $t = 0$, the dark energy density is found to be exceptionally high which indicates that it helps much in triggering the big bang. It is also seen that the dark energy is highly interacting with other components of the universe at $t = 0$, with the interaction decreasing slowly with the passing away of the cosmic time. In this universe, we see that both the scalar field ϕ and the interaction Q tend to vanish as $a_0 \longrightarrow 0$. Thus, the scalar field is very much interconnected with the dark energy content of this universe and plays a vital role in the production and existence of it. One peculiarity in this model is that the scalar field does not vanish at $t \longrightarrow \infty$; thus, the dark energy seems to be prevalent eternally in this universe due to this scalar field.

Data Availability

No data were used to support this study.

Conflicts of Interest

The authors declare that they have no conflicts of interest.

References

[1] A. G. Riess, A. V. Filippenko, P. Challis et al., "Observational evidence from supernovae for an accelerating universe and a cosmological constant," *The Astronomical Journal*, vol. 116, no. 3, pp. 1009–1038, 1998.

[2] S. Perlmutter, G. Aldering, G. Goldhaber et al., "Measurements of Ω and Λ from 42 high-redshift supernovae," *The Astrophysical Journal*, vol. 517, pp. 565–586, 1999.

[3] L. Amendola and S. Tsujikawa, *Dark Energy: Theory and Observations*, Cambridge University Press, Cambridge, UK, 2010.

[4] S. Weinberg, "The cosmological constant problem," *Reviews of Modern Physics*, vol. 61, no. 1, pp. 1–23, 1989.

[5] C. Brans and R. H. Dicke, "Mach's principle and a relativistic theory of gravitation," *Physical Review*, vol. 124, no. 3, pp. 925–935, 1961.

[6] D. Saez and V. J. Ballester, "A simple coupling with cosmological implications," *Physics Letters A*, vol. 113, no. 9, pp. 467–470, 1986.

[7] D. E. Barraco and V. H. Hamity, "Spherically symmetric solutions in $f(R)$ theories of gravity obtained using the first order formalism," *Physical Review D*, vol. 62, no. 4, Article ID 044027, 6 pages, 2000.

[8] S. Capozziello, "Curvature quintessence," *International Journal of Modern Physics D*, vol. 11, pp. 483–492, 2002.

[9] S. Capozziello, V. F. Cardone, and A. Troisi, "Reconciling dark energy models with *f(R)* theories," *Physical Review D: Particles, Fields, Gravitation and Cosmology*, vol. 71, no. 4, Article ID 043503, 2005.

[10] S. Capozziello, V. F. Cardone, and M. Francaviglia, "$f(R)$ theories of gravity in the Palatini approach matched with observations," *General Relativity and Gravitation*, vol. 38, no. 5, pp. 711–734, 2006.

[11] S. Nojiri and S. D. Odintsov, "Modified $f(R)$ gravity consistent with realistic cosmology: From a matter dominated epoch to a dark energy universe," *Physical Review D*, vol. 74, no. 8, Article ID 046004, 13 pages, 2006.

[12] K. Bamba and C.-Q. Geng, "Thermodynamics in *F(R)* gravity with phantom crossing," *Physics Letters B: Particle Physics, Nuclear Physics and Cosmology*, vol. 679, no. 3, pp. 282–287, 2009.

[13] R. Ferraro and F. Fiorini, "Modified teleparallel gravity: inflation without an inflaton," *Physical Review D: Particles, Fields, Gravitation and Cosmology*, vol. 75, no. 8, Article ID 084031, 2007.

[14] R. Myrzakulov, "Accelerating universe from *F(T)* gravity," *The European Physical Journal C*, vol. 71, article 1752, 2011.

[15] K. Bamba, C.-Q. Geng, C.-C. Lee, and L.-W. Luo, "Equation of state for dark energy in *f(T)* gravity," *Journal of Cosmology and Astroparticle Physics*, vol. 2011, p. 21, 2011.

[16] M. R. Setare and F. Darabi, "Power-law solutions in f (T) gravity," *General Relativity and Gravitation*, vol. 44, no. 10, pp. 2521–2527, 2012.

[17] S. Nojiri, S. D. Odintsov, and M. Sasaki, "Gauss-Bonnet dark energy," *Physical Review D: Particles, Fields, Gravitation and Cosmology*, vol. 71, no. 12, Article ID 123509, 2005.

[18] L. M. Sokołowski, Z. A. Golda, M. Litterio, and L. Amendola, "Classical instability of the einstein-gauss-bonnet gravity theory with compactified higher dimensions," *International Journal of Modern Physics A*, vol. 6, no. 25, pp. 4517–4555, 1991.

[19] A. Iglesias and Z. Kakushadze, "Solitonic brane world with completely localized (super)gravity," *International Journal of Modern Physics A*, vol. 16, no. 21, pp. 3603–3631, 2001.

[20] S. Nojiri, S. D. Odintsov, and S. Ogushi, "Friedmann-Robertson-Walker brane cosmological equations from the five-dimensional bulk (A)dS black hole," *International Journal of Modern Physics A*, vol. 17, no. 32, pp. 4809–4870, 2002.

[21] E. Ó. Colgáin and H. Yavartanoo, "Dyonic solution of Hořava-Lifshitz gravity," *Journal of High Energy Physics*, vol. 2009, no. 08, p. 021, 2009.

[22] A. Ghodsi, "Toroidal solutions in hořava gravity," *International Journal of Modern Physics A*, vol. 26, no. 5, pp. 925–934, 2011.

[23] M. I. Park, "A test of Hořava gravity: the dark energy," *Journal of Cosmology and Astroparticle Physics*, vol. 2010, no. 01, p. 1, 2010.

[24] T. Harko, F. S. N. Lobo, S. Nojiri, and S. D. Odintsov, "*F*(*R*, *T*) gravity," *Physical Review D: Particles, Fields, Gravitation and Cosmology*, vol. 84, no. 2, Article ID 024020, 11 pages, 2011.

[25] M. H. Dehghani, "Accelerated expansion of the Universe in Gauss-Bonnet gravity," *Physical Review D: Particles, Fields, Gravitation and Cosmology*, vol. 70, no. 6, Article ID 064009, 6 pages, 2004.

[26] S. Nojiri and S. D. Odintsov, "Modified gravity with ln *R* terms and cosmic acceleration," *General Relativity and Gravitation*, vol. 36, no. 8, pp. 1765–1780, 2004.

[27] A. Lue, R. Scoccimarro, and G. Starkman, "Probing Newton's constant on vast scales: Dvali-Gabadadze-Porrati gravity, cosmic acceleration, and large scale structure," *Physical Review D: Covering Particles, Fields, Gravitation, and Cosmology*, vol. 69, no. 12, Article ID 044005, 10 pages, 2004.

[28] S. M. Carroll, A. De Felice, V. Duvvuri, D. A. Easson, M. Trodden, and M. S. Turner, "Cosmology of generalized modified gravity models," *Physical Review D: Particles, Fields, Gravitation and Cosmology*, vol. 71, no. 6, Article ID 063513, 2005.

[29] G. C. Samanta and S. N. Dhal, "Higher dimensional cosmological models filled with perfect fluid in *f(R,T)* theory of gravity," *International Journal of Theoretical Physics*, vol. 52, no. 4, p. 1334, 2013.

[30] G. C. Samanta, "Kantowski-sachs universe filled with perfect fluid in *f(R,T)* theory of gravity," *International Journal of Theoretical Physics*, vol. 52, no. 8, pp. 2647–2656, 2013.

[31] G. C. Samanta, "Universe filled with dark energy (DE) from a wet dark fluid (WDF) in *f(R,T)* gravity," *International Journal of Theoretical Physics*, vol. 52, no. 7, pp. 2303–2315, 2013.

[32] G. C. Samanta, "Holographic dark energy (DE) cosmological models with quintessence in bianchi type-V space time," *International Journal of Theoretical Physics*, vol. 52, no. 12, pp. 4389–4402, 2013.

[33] K. M. Singh and K. Priyokumar, "Cosmological model universe consisting of two forms of dark energy," *International Journal of Theoretical Physics*, vol. 53, no. 12, pp. 4360–4365, 2014.

[34] K. M. Singh and K. L. Mahanta, "Do neutrinos contribute to total dark energy," *Astrophysics and Space Science*, vol. 361, no. 85, 2016.

[35] K. Bamba, "Thermodynamic properties of modified gravity theories," *International Journal of Geometric Methods in Modern Physics*, vol. 13, no. 6, Article ID 1630007, 2016.

[36] M. Zubair, M. Syed, and G. Abbas, "Bianchi type I and V solutions in f(R, T) gravity with time-dependent deceleration parameter," *Canadian Journal of Physics*, vol. 94, no. 12, pp. 1289–1296, 2016.

[37] S. D. Maharaj, R. Goswami, S. V. Chervon, and A. V. Nikolaev, "Exact solutions for scalar field cosmology in $f(R)$ gravity," *Modern Physics Letters A*, vol. 32, no. 30, Article ID 1750164, 2017.

[38] K. Priyokumar, K. M. Singh, and M. R. Mollah, "Whether lyra's manifold itself is ahidden source of dark energy," *International Journal of Theoretical Physics*, vol. 56, no. 8, pp. 2607–2621, 2017.

[39] G. C. Samanta and R. Myrzakulov, "Imperfect fluid cosmological model in modified gravity," *Chinese Journal of Physics*, vol. 55, no. 3, pp. 1044–1054, 2017.

[40] J. P. M. Graça, G. I. Salako, and V. B. Bezerra, "Quasi-normal modes of a black hole with a cloud of strings in einstein–gauss–bonnet gravity," *International Journal of Modern Physics D*, vol. 26, no. 10, Article ID 1750113, 2017.

[41] K. Bamba, S. D. Odintsov, and E. N. Saridakis, "Inflationary cosmology in unimodular F(T) gravity," *Modern Physics Letters A*, vol. 32, no. 21, Article ID 1750114, 2017.

[42] I. Noureen and M. Zubair, "Axially symmetric shear-free fluids in *f(R, T)* gravity," *International Journal of Modern Physics D: Gravitation, Astrophysics, Cosmology*, vol. 26, no. 11, Article ID 1750128, 17 pages, 2017.

[43] G. C. Samanta, R. Myrzakulov, and P. Shah, "Kaluza–Klein bulk viscous fluid cosmological models and the validity of the second law of thermodynamics in f(R,T) gravity," *Zeitschrift für Naturforschung A*, vol. 72, no. 4, pp. 365–374, 2017.

[44] E. H. Baffou, M. J. Houndjo, M. Hamani-Daouda, and F. G. Alvarenga, "Late-time cosmological approach in mimetic f(R, T) gravity," *The European Physical Journal C*, vol. 77, p. 708, 2017.

[45] H. Azmat, M. Zubair, and I. Noureen, "Dynamics of shearing viscous fluids in $f(R,T)$ gravity," *International Journal of Modern Physics D: Gravitation, Astrophysics, Cosmology*, vol. 27, no. 1, Article ID 1750181, 2018.

[46] J. K. Singh, R. Nagpal, and S. K. Pacif, "Statefinder diagnostic for modified Chaplygin gas cosmology in $f(R,T)$ gravity with particle creation," *International Journal of Geometric Methods in Modern Physics*, vol. 15, no. 3, Article ID 1850049, 2018.

[47] S. D. Odintsov and V. K. Oikonomou, "Early-time cosmology with stiff era from modified gravity," *Physical Review D: Particles, Fields, Gravitation and Cosmology*, vol. 96, no. 10, Article ID 104059, 2017.

[48] A. Addazi, "Evaporation/antievaporation and energy conditions in alternative gravity," *International Journal of Modern Physics A*, vol. 33, no. 4, Article ID 1850030, 15 pages, 2018.

[49] H. Shabani and A. H. Ziaie, "Interpretation of f(R,T) gravity in terms of a conserved effective fluid," *International Journal of Modern Physics A*, vol. 33, no. 8, Article ID 1850050, 2018.

[50] S. D. Odintsov and V. K. Oikonomou, "Reconstruction of slow-roll *F(R)* gravity inflation from the observational indices," *Annals of Physics*, vol. 388, pp. 267–275, 2018.

[51] M. Zubair, H. Azmat, and I. Noureen, "Anisotropic stellar filaments evolving under expansion-free condition in f(R,T) gravity," *International Journal of Modern Physics D*, vol. 27, no. 4, Article ID 1850047, 2018.

[52] K. Kleidis and V. K. Oikonomou, "Scalar field assisted $f(R)$ gravity inflation," *International Journal of Geometric Methods in Modern Physics*, vol. 15, no. 8, Article ID 1850137, 2018.

[53] R. K. Tiwari, A. Beesham, and B. Shukla, "Cosmological model with variable deceleration parameter in *f(R, T)* modified gravity," *International Journal of Geometric Methods in Modern Physics*, vol. 15, no. 7, Article ID 1850115, p. 10, 2018.

[54] S. Hansraj and A. Banerjee, "Dynamical behavior of the Tolman metrics in $f(R,T)$ gravity," *Physical Review D: Particles, Fields, Gravitation and Cosmology*, vol. 97, no. 10, Article ID 104020, 2018.

[55] D. Rowland and I. B. Whittingham, "Models of interacting dark energy," *Monthly Notices of the Royal Astronomical Society*, vol. 390, no. 4, pp. 1719–1726, 2008.

[56] W. Cui, S. Borgani, and M. Baldi, "The halo mass function in interacting dark energy models," *Monthly Notices of the Royal Astronomical Society*, vol. 424, no. 2, pp. 993–1005, 2012.

[57] M. Baldi, "Clarifying the effects of interacting dark energy on linear and non-linear structure formation processes," *Monthly Notices of the Royal Astronomical Society*, vol. 414, no. 1, pp. 116–128, 2011.

[58] J. Sadeghi, M. Khurshudyan, A. Movsisyan, and H. Farahani, "Interacting ghost dark energy models with variable G and Λ," *Journal of Cosmology and Astroparticle Physics*, vol. 12, p. 31, 2013.

[59] M. Khurshudyan, E. Chubaryan, and B. Pourhassan, "Interacting quintessence models of dark energy," *International Journal of Theoretical Physics*, vol. 53, no. 7, pp. 2370–2378, 2014.

[60] O. Bertolami, F. Gil Pedro, and M. Le Delliou, "Dark energy-dark matter interaction and putative violation of the equivalence principle from the Abell cluster A586," *Physics Letters B*, vol. 654, no. 5-6, pp. 165–169, 2007.

[61] G. Olivares, F. Atrio-Barandela, and D. Pavón, "Observational constraints on interacting quintessence models," *Physical Review D: Particles, Fields, Gravitation and Cosmology*, vol. 71, no. 6, Article ID 063523, pp. 1–7, 2005.

[62] N. Bilic, G. B. Tupper, and R. D. Viollier, "Unification of dark matter and dark energy: the inhomogeneous Chaplygin gas," *Physics Letters B*, vol. 535, pp. 17–21, 2002.

Hindawi
Advances in High Energy Physics
Volume 2019, Article ID 2539217, 15 pages
https://doi.org/10.1155/2019/2539217

Research Article

Reissner-Nordström Black Holes Statistical Ensembles and First-Order Thermodynamic Phase Transition

Hossein Ghaffarnejad and Mohammad Farsam

Faculty of Physics, Semnan University, 35131-19111 Semnan, Iran

Correspondence should be addressed to Hossein Ghaffarnejad; hghafarnejad@semnan.ac.ir

Received 2 November 2018; Accepted 28 February 2019; Published 10 April 2019

Academic Editor: Kazuharu Bamba

Copyright © 2019 Hossein Ghaffarnejad and Mohammad Farsam. This is an open access article distributed under the Creative Commons Attribution License, which permits unrestricted use, distribution, and reproduction in any medium, provided the original work is properly cited.

We apply Debbasch proposal to obtain mean metric of coarse graining (statistical ensemble) of quantum perturbed Reissner-Nordstöm black hole (*RNBH*). Then we seek its thermodynamic phase transition behavior. Our calculations predict first-order phase transition which can take Bose-Einstein's condensation behavior.

1. Introduction

Every observation in any arbitrary system is necessarily finite which deals with a finite number of measured quantities with a finite precision. A given system is therefore generally susceptible of different, equally valid descriptions and building the bridges between those different descriptions is the task of statistical physics (see introduction in [1] for more discussion). Nonlinearity property of Einstein's metric equations causes their averaging to be nontrivial. Various possible ways of averaging the geometry of space time have already been proposed by [2–8], but none of them seems fully satisfactory (see section 7 in [1] for full discussion). Debbasch used an alternative way to averaging Einstein's metric equation in [1]. To do so, he chose a general framework where the mean metric still obeys the equations of general theory of relativity. In his approach averaging and/or coarse graining a gravitational field changes the matter content of space time called "apparent matter" which in cosmological context is related to the dark energy (see [9–12]). So general relativity mean field theory can propose a physical meaning for unknown cosmological dark energy/matter via the "apparent matter". In the Debbasch approach, statistical ensemble of metric is ensembles of histories and not ensembles of states. This is different basically with ordinary statistical mechanics of classical and/or quantum particles. From the latter point of view, it has been known for a long time that black holes in asymptotically flat space times do not admit stable equilibrium states in the canonical ensemble (see introduction in [13]). But from the former point of view the Debbasch gives in [1] general proposal to obtain a mean field theory for the general theory of relativity. In his model members of the ensembles will be labeled by the symbol $\omega \in \Omega$ where Ω is an arbitrary probability space [14]. To each ω, there are corresponding metric tensor $g(\omega)$, compatible connections $\Gamma(\omega)$, and the Einstein metric equation (see [1] and section 2 in [10]). All members of the ensemble correspond to the same macroscopic history of the space time manifold, in particular to a given same mean metric $\overline{g}_{\mu\nu}(x) = \langle g_{\mu\nu}(x,\omega)\rangle$ and corresponding mean connection $\overline{\Gamma}^{\mu}_{\nu\eta} = \langle \Gamma^{\mu}_{\nu\eta}(g, \partial g, \omega)\rangle$. As application of his model Debbasch and coworkers considered statistical ensemble of Schwarzschild black holes as nonvacuum solutions of mean Einstein metric equation by using Kerr-Schild coordinates $R = r-\omega$. They calculated nonvanishing temperature of mean metric where single Schwarzschild black hole is well known which has nonvanishing temperature as a vacuum solution of the Einstein equation. They discussed their results with special emphasis on their connections with the context of astrophysical observations [12]. Extreme RNBH with $m = 1$ has vanishing temperature (see next section) and regular Kerr-Schild coordinates $R = r - \omega$ are not applicable to obtain mean metric similar to the Schwarzschild one because the coarse graining space time turns out not to be a black hole [9]. Hence Chevalier and Debbasch used analytic continuation of the Kerr-Schild coordinates as $R = r - i\omega$ to obtain mean metric of extreme classical black hole in [11]. According to the Debbasch approach we are free to choose types of coarse graining and/or ensemble space to obtain mean metric of the space times ensemble under consideration. We should point that topology of ensemble space times must be similar to topology of their mean metric (see [9]) which restrict us to choose an analytic continuation of Kerr-Schild coordinates for extreme RNBH. In short, with Debbasch proposal the averaging process does not change topology between ensemble of the curved space times and the corresponding mean space time. Precisely, the averaging process modifies the horizon radius and changes the energy-momentum tensor of space time but not total energy or mass of the black holes ensemble. Really the averaging process just redistributes without any change in the total mass which means that the total energy of the black holes dose not change by the coarse graining proposal.

Similar to study of thermodynamic behavior of single RNBH [15], we seek thermodynamic aspect of mean metric of nonextreme RNBHs ensemble in this work, by applying the Debbasch approach to evaluate the mean and/or coarse graining metric. Organization of the paper is as follows.

In Section 2, we calculate mean metric of ensemble of RNBHs. In Section 3 we obtain locations of mean metric horizons. In Section 4 we calculate interior and exterior horizons entropy, temperature, heat capacity, Gibbs free energy, and pressure of RNBHs mean metric. In Section 5 we calculate interior and exterior horizons luminosity and corresponding mass loss equation of quantum perturbed RN mean metric. Section 6 denotes concluding remark and discussion.

2. RNBHs Ensemble and Mean Metric

Exterior metric tensor of a single charged, nonrotating, spherically symmetric body is given by

$$ds^2 = \left(1 - \frac{2M}{r} + \frac{e^2}{r^2}\right) dt^2 - \frac{dr^2}{\left(1 - 2M/r + e^2/r^2\right)} - r^2 \left(d\theta^2 + \sin^2\theta d\varphi^2\right). \quad (1)$$

This is metric solution of Einstein-Maxwell equation and is called RNBH in which M and e are corresponding ADM mass and electric charge defined in units where $c = G = 1$. Equating $g^{\mu\nu}\partial_\mu r \partial_\nu r = 0$ for arbitrary spherically symmetric hypersurface $r = constant$, one can obtain apparent (exterior) horizon radius as $r_+ = M + \sqrt{M^2 - e^2}$ and Cauchy (interior) horizon radius as $r_- = M - \sqrt{M^2 - e^2}$ which appear only for $0 \leq (e/M)^2 \leq 1$. One can obtain mass independent relation between r_+ and r_- as $r_- = e^2/r_+$. With particular choice $e = M$ (called extreme and/or Lukewarm RNBH) these horizons coincide as $r_- = r_+ = M$. Clearly the RNBH metric solution (1) leads to Schwarzschild one by setting $e = 0$ for which we will have $r_+ = 2M$ and $r_- = 0$. Temperature of a single RNBH can be obtained for interior and exterior horizons as $T_\pm = (1/8\pi r_\pm)(\partial r_\pm/\partial M)_e^{-1} = \pm\sqrt{M^2 - e^2}/8\pi(M \pm \sqrt{M^2 - e^2})^2$ [1] which reduce to a zero value for extreme (Lukewarm) RNBH because of $M = e$. They show positive (negative) temperature for exterior (interior) horizons. Negative temperatures of systems have physical meaning and happen under particular conditions. More authors studied conditions where the physical systems are taken to have negative temperatures. See [16] for temperatures of interior and exterior horizons of Kerr-Newman black hole. One can see [17–19] for negative temperature of nongravitational systems. In the nature, materials are obtained which have interesting properties like negative refraction index and reversibility of the Doppler's effect, and so the phase and group velocity (velocity of energy propagation) have opposite singes. In these systems temperature will have negative values (see [17] and references therein). Such systems are called dual system (left-handed) of direct counterpart (right-handed conventional materials). Absolute temperature is usually bounded to be positive but its violation is shown in [18] by Braun et al. They showed, under special conditions, however negative temperatures where high energy states are more occupied than low energy states. Such states have been demonstrated in localized systems with finite, discrete spectra. They used the Bose-Hubbard Hamiltonian and obtained attractively interacting ensemble of ultra-cold bosons at negative temperature which are stable against collapse for arbitrary atom number. Furman et al. studied in [19] behavior of quantum discord of dipole-dipole interacting spins in an external magnetic field in the whole temperature range $-\infty < T < \infty$. They obtained that negative temperatures, which are introduced to describe inversions in the population in a finite level system, provide more favorable conditions for emergence of quantum correlations including entanglement. At negative temperature the correlations become more intense and discord exists between remove spins being in separated states. According to the documentation and looking to diagrams of the present work, one can be convinced that a quantum perturbed mean metric of coarse graining RNBHs will be exhibited finally with a first-order phase transition and Bose-Einstein condensation state microscopically. According to the Debbasch approach [1] ensemble of the nonextreme RNBHs is collection of coarse graining RNBHs indexed by a 3-dimensional real parameter $\vec{\omega} \in \vec{\Omega}$ where $\vec{\Omega}$ is the three balls of radius $\vec{a}$ as follows:

$$\vec{\Omega} = \left\{\vec{\omega} \in \mathbb{R}^3;\ \omega^2 \leq a^2\right\}. \quad (2)$$

The metric solution (1) is convenient to be rewritten with Kerr-Schild coordinates $(\tau, r, \theta, \varphi)$ by transforming

$$dt = d\tau + \frac{h(r)\,dr}{1 - h(r)} \quad (3)$$

as follows (see [10–12]):

$$ds^2 = d\tau^2 - d\vec{r} \cdot d\vec{r} - h(r)\left(d\tau - \frac{\vec{r} \cdot d\vec{r}}{r}\right)^2 \quad (4)$$

where

$$h(r) = \frac{2M}{r} - \frac{e^2}{r^2} \quad (5)$$

and $r = |\overrightarrow{r}|$ is the Euclidean norm of the vector $\overrightarrow{r}$. It should be pointed that all metric solutions of Einstein's field equation will have simple form by using Kerr-Schild coordinates. They are decomposed into the well-known flat Minkowski background metric $\eta_{\mu\nu}$ and null vector fields K_μ as $g_{\mu\nu} = \eta_{\mu\nu} - 2h(x^\mu)K_\mu K_\nu$ where $K_\mu K^\mu = 0 = g_{\mu\nu}K^\mu K^\nu = \eta_{\mu\nu}K^\mu K^\nu$ and $h(x^\mu)$ is a scalar function (see [20] and references therein). Now, we must choose a probability measure. Hence we follow the assumption presented in [11] and choose uniform probability measure $d\mathsf{p}_\omega$ in which p is probability density of this measure with respect to Lebesgue measure $d^3\omega$ as $\mathsf{p}(\omega) = 1/V_a$ with $V_a = (4/3)\pi a^3$. Applying the Kerr-Schild radial coordinate (in case of extreme RNBH where $M = e$ we must use analytic continuation of the Kerr-Schild coordinates as $R = r - i\omega$ (see discussion given in the introduction)) $\overrightarrow{R}(\overrightarrow{r}, \overrightarrow{\omega}) = \overrightarrow{r} - \overrightarrow{\omega}$, we extend single RNBH metric (4) to obtain metric of coarse graining and/or statistical ensemble of RNBHs as follows:

$$ds^2 = d\tau^2 - d\overrightarrow{r} \cdot d\overrightarrow{r} - h(R)\left(d\tau - \frac{\overrightarrow{R}.d\overrightarrow{r}}{R}\right)^2 \tag{6}$$

where $h(R) = 2M/R - e^2/R^2$ and $R = \sqrt{\overrightarrow{R} \cdot \overrightarrow{R}}$. Using perturbation series expansion method and averaging the metric (6) against $\overrightarrow{\omega}$ we obtain mean metric of (6) such that (see [21] for details of calculations)

$$\begin{aligned}\left\langle ds^2\right\rangle_\omega = {} & b_1(r)\,d\tau^2 + b_2(r)\,d\overrightarrow{r} \cdot d\overrightarrow{r} + b_3(r)\,dr^2 \\ & + b_4(r)\,dr\,d\tau\end{aligned} \tag{7}$$

where $|e| < M$, $d\overrightarrow{r} \cdot d\overrightarrow{r} = dr^2 + r^2(d\theta^2 + \sin^2\theta d\varphi^2)$,

$$b_1(r) = 1 - \frac{2M}{r} + \frac{e^2}{r^2}\left(1 + \frac{a^2}{5r^2}\right), \tag{8}$$

$$b_2(r) = -1 - \frac{2a^2M}{5r^3} + \frac{a^2e^2}{5r^4}, \tag{9}$$

$$b_3(r) = -\frac{2M}{r}\left(1 - \frac{3a^2}{5r^2}\right) + \frac{e^2}{r^2}\left(1 - \frac{2a^2}{5r^2}\right), \tag{10}$$

and

$$b_4(r) = \frac{4M}{r}\left(1 - \frac{a^2}{5r^2}\right) - \frac{2e^2}{r^2}. \tag{11}$$

It is simple to show that the mean metric (7) reduces to a single RNBH metric (4) by setting $a = 0$. We can rewrite the mean metric (7) in the static frame by defining the Schwarzschild coordinates. To do so, we first choose a suitable local frame with coordinates $(t, \rho, \theta, \varphi)$ as

$$\rho(r) = r\sqrt{-b_2(r)} \tag{12}$$

and

$$d\tau = dt - \alpha(\rho)\,d\rho \tag{13}$$

where

$$\alpha(\rho) = \frac{b_4(r)}{2b_1(r)}\left(\frac{\partial\rho}{\partial r}\right)^{-1}. \tag{14}$$

In the latter case the mean metric (7) reads

$$\begin{aligned}\left\langle ds^2\right\rangle = {} & F(\rho)\,d\tau^2 - f(\rho)\,d\rho^2 \\ & - \rho^2\left(d\theta^2 + \sin^2\theta d\varphi^2\right)\end{aligned} \tag{15}$$

where we defined

$$F(\rho) = 1 - \frac{2M}{r(\rho)} + \frac{e^2}{r^2(\rho)}\left(1 + \frac{a^2}{5r^2(\rho)}\right) \tag{16}$$

and

$$f(\rho) = \frac{1}{F(\rho)}\left(1 - \frac{e^2a^2}{5r^4(\rho)}\right). \tag{17}$$

We now seek location of mean metric horizons.

3. Horizons Location for Mean Metric

One can obtain event horizon location of the mean metric (15) by solving $F(\rho_{EH}) = 0$ and location of apparent (interior and exterior) horizons by solving null condition $g^{\mu\nu}\partial_\mu\rho\partial_\nu\rho = 0$ which leads to the equation $F(\rho_{AH}) = 0$ such that

$$1 - \frac{2M}{r_H} + \frac{e^2}{r_H^2} + \frac{e^2a^2}{5r_H^4} = 0. \tag{18}$$

The above equation has not exactly analytic solution for $a \neq 0$ but for small a we can use perturbation series expansion to evaluate the event horizon location. To do so we first define $\epsilon = a/r_H$ for which the horizon equation (18) can be written as $r_H^2 - 2Mr_H + e^2(1 + \epsilon^2) = 0$. The latter equation has a real solution as $r_H = M\{1 + \sqrt{1 - (e^2/M^2)(1 + \epsilon^2/5)}\}$ for $(e^2/M^2)(1 + \epsilon^2/5) < 1$. We know that for a single RN black hole $e/M < 1$ and so the condition $(e^2/M^2)(1 + \epsilon^2/5) < 1$ reads $\epsilon < 1 (a < r_H)$ for which horizon of the ensemble of statistical RN black holes is not destructed by raising $0 < \epsilon < 1$ if we want to apply perturbation series expansion method to obtain asymptotically behavior of the event horizon solution versus the parameters (a, e, M). Thus we must obtain perturbation series expansion form of the event horizon but for $a < r_H$ as follows. Inserting

$$r_H^\pm = r_0^\pm + ar_1^\pm + a^2r_2^\pm + O\left(a^3\right) \tag{19}$$

and solving (18) as order by order, we obtain

$$r_0^\pm = M \pm \sqrt{M^2 - e^2},$$

$$r_1^\pm = 0,$$

$$r_2^{\pm} = \frac{\mp e^2}{10\sqrt{M^2-e^2}\left(M \pm \sqrt{M^2-e^2}\right)^2} \tag{20}$$

where r_H^+ and r_H^- denote apparent exterior and Cauchy (interior) horizon radiuses of the mean metric (7), respectively. Inserting (9) and (19), one can obtain perturbation series expansion of (12) which up to terms in order of $O(a^3)$ becomes

$$\rho_H = \rho_0^{\pm} + a^2 \rho_2^{\pm} \tag{21}$$

where we defined

$$\begin{aligned} \rho_0^{\pm} &= r_0^{\pm}, \\ \rho_2^{\pm} &= r_2^{\pm} + \frac{2Mr_0^{\pm} - e^2}{10 r_0^{\pm 3}}. \end{aligned} \tag{22}$$

Area equation of apparent horizon hypersurface of the spherically symmetric static mean metric (15) is defined by $A = 4\pi\rho_H^2$ which up to terms in order of $O(a^3)$ reads

$$A^{\pm} = A_0^{\pm} + a^2 A_2^{\pm} \tag{23}$$

where we defined

$$\begin{aligned} A_0^{\pm} &= 4\pi\left(r_0^{\pm}\right)^2, \\ A_2^{\pm} &= 8\pi\left[r_0^{\pm} r_2^{\pm} + \frac{1}{10 r_0^{\pm}}\left(2M - \frac{e^2}{r_0^{\pm}}\right)\right]. \end{aligned} \tag{24}$$

According to Bekenstein-Hawking entropy theorem we have the result that $A_+(A_-)$ given by (23) will be entropy function of exterior (interior) horizon of the mean metric (15). Black holes containing multiple horizons have several corresponding temperatures. Such a black hole will be in-equilibrium thermally throughout the space time where the temperature has a gradient between the horizons. Thermal equilibrium is possible only if horizon radiuses and so the corresponding temperatures become equal (see, for instance, [22, 23]). The latter situations happen for an extreme RNBH where $M = e$ and so $r_H^+ = r_H^-$. We now calculate thermodynamic characteristics of interior and exterior horizons of the nonextreme mean metric of RNBHs statistical ensemble.

4. Mean Metric Thermodynamics

In the next section we will consider massless, chargeless quantum scalar field effects on luminosity of the quantum perturbed coarse graining RNBHs where its electric charge becomes invariant quantity. Hence it is useful to define dimensionless black hole mass $m = M/e$ and ensemble factor $\delta = a/e$ in what follows. In the latter case exterior horizon entropy of mean metric (15) can be obtained up to terms in order of $O(\delta^3)$ as follows:

$$\begin{aligned} S_+(m,\delta) &= \left(m + \sqrt{m^2-1}\right)^2 \\ &\quad + \frac{\delta^2}{5}\left[\frac{2\left(m^2-1\right)^{3/2} + m\left(2m^2-3\right)}{\sqrt{m^2-1}\left(m+\sqrt{m^2-1}\right)^2}\right] \end{aligned} \tag{25}$$

and its interior horizon entropy becomes

$$\begin{aligned} S_-(m,\delta) &= \left(m - \sqrt{m^2-1}\right)^2 \\ &\quad + \frac{\delta^2}{5}\left[\frac{2\left(m^2-1\right)^{3/2} - m\left(2m^2-3\right)}{\sqrt{m^2-1}\left(m-\sqrt{m^2-1}\right)^2}\right] \end{aligned} \tag{26}$$

where $0 < \delta < 1$ and

$$S_{\pm} = \frac{A_{\pm}}{4\pi e^2} > 0. \tag{27}$$

Diagrams of entropies (25) and (26) are plotted versus m in Figure 4. They show that $S_{\pm} > 0$ for a single RNBH ($\delta = 0$) in limits $m \longrightarrow 1$ but for an ensemble of RNBHs for which we use $\delta = 0.9$, they reach infinity $S_{\pm} \longrightarrow \mp\infty$. In fact for physical systems the entropy itself must be positive function but its variations may reach some negative values. Hence we define difference between interior horizon entropy and exterior horizon entropy as

$$\begin{aligned} \Delta S = S_+ - S_- &= 4m\sqrt{m^2-1} \\ &\quad + \frac{2\delta^2}{5}\left[\frac{m\left(2m^2-1\right)\left(2m^2-3\right)}{\sqrt{m^2-1}} \right. \\ &\quad \left. - 4m\left(m^2-1\right)^{3/2}\right] \end{aligned} \tag{28}$$

and total entropy such as follows:

$$S_{tot} = S_+ + S_- = 4m^2 - 2 + \frac{4\delta^2}{5}\left(4m^4 - 6m^2 + 1\right). \tag{29}$$

Diagrams of ΔS and S_{tot} are plotted in Figure 3. Fortunately these diagrams show that, for a single RNBH where $\delta = 0$, we will have $\Delta S > 0$ by decreasing $m \longrightarrow 1$ and $S_{tot} > 0$ but for ensemble of RNBHs with $\delta = 0.9$ we have $\Delta S < 0$ while $S_{tot} > 0$. Hence ΔS and S_{tot} should be considered as physical entropies of coarse graining RNBHs. Decrease of entropy causes some negative temperatures (see Figure 2) in thermodynamic systems containing bounded energy levels. In the latter case there is a critical temperature for which the system exhibits a phase transition reaching Bose-Einstein condensation state microscopically. In thermodynamics, increase of entropy $\Delta S > 0$ means an increase of disorder or randomness in natural systems. It measures heat transfer of the system for which heat flows naturally from a warmer to a cooler substance. Decrease of entropy $\Delta S < 0$ means an increase of orderliness or organization of microstates of a system. To do so the substance of a system must loose heat in the transfer process. Individual systems can experience negative entropy, but overall, natural processes in the universe trend toward positive entropy. Negative entropy was first introduced for living things by Ervin Schrödinger in 1944 as the reverse concept of entropy, to describe the order that can emerge from chaos [24]. The heat generated by computations in the information theory is other applications for negative entropy concept (see [25–28] for more discussions). However we consider ΔS and S_{tot} to be physical entropies of RNBHs statistical ensemble containing two horizons which is in accord with positivity condition of the Bekenstein-Hawking entropy theorem. Our coarse graining RNBHs can be considered as a two-level thermodynamical system with upper bound finite energy M because it has two dual (interior and exterior) horizons. We now calculate exterior (interior) horizon temperature $T_+(T_-)$ of the RNBHs mean metric (15) as follows:

$$T^*_\pm = (4\pi e)\, T_\pm = \frac{1}{(\partial S_\pm/\partial m)_\delta} = \pm\frac{1}{2}\frac{\sqrt{m^2-1}}{\left(m \pm \sqrt{m^2-1}\right)^2} + \frac{\delta^2}{60}\left[\frac{4m - 2m^3 - 2m^5 \mp \sqrt{m^2-1}\left(2m^4+3m^2-3\right)}{(m^2-1)^{5/6}\left(m\pm\sqrt{m^2-1}\right)^6}\right] \quad (30)$$

Their diagrams are plotted against m in Figure 2 for $\delta = 0; 0.9$. For $m \gg 1$ we see that $T^*_-(T^*_+)$ has some negative (positive) values and their sign is changed when $m \longrightarrow 1$. We also plotted diagram for $T^*_\pm$ versus $\Delta T^* = T^*_+ - T^*_-$ in Figure 2. They show that $T^*_- < 0$ for $\Delta T^* > 0$ reaching zero value at $\Delta T^* = 0$ for $\delta = 0, 0.9$. While $T^*_+ > 0(T^*_+ < 0)$, $\Delta T^* \longrightarrow 0^+$ for $\delta = 0(0.9)$ after that to obtain a finite positive maximum value. This maximum has smaller value for $\delta = 0.9$ with respect to situations where we choose $\delta = 0$. In ordinary statistical physics, negative temperatures are taken into account when the system has upper bound (maximum finite) energy for which entropy is continuously increasing but the energy and temperature decrease and vice versa. In the latter case the system reaches Bose-Einstein condensation state microscopically. Energy upper bound of our system is its total mass M for which we have $m > 1$. Regarding quantum matter effects on mean metric we will show in Section 5 that mass of mean metric decreases finally as $m_{final} = 1$ (see Figure 1). Bose-Einstein condensation state needs a phase transition which happens when sign of heat capacity is changed. Hence we now calculate interior and exterior horizon of mean metric heat capacity $C^*_\pm$ which up to terms in order of $O(\delta^3)$, at constant electric charge e and ensemble radius a, become

$$C_\pm{}^* = \frac{C^\pm_\delta}{4\pi e^2} = \left(T_\pm\frac{\partial S_\pm}{\partial T_\pm}\right)_\delta = \left(\frac{\partial T^*_\pm}{\partial m}\right)^{-1}_\delta = -\frac{2\sqrt{m^2-1}\left(m\pm\sqrt{m^2-1}\right)^2}{2\sqrt{m^2-1}\mp m} + \frac{2\delta^2}{45}\left[\frac{2m\sqrt{m^2-1}\left(4m^4+12m^2-15\right) \pm 8m^6 \pm 20m^4 \mp 49m^2 \pm 21}{\left(m^2-2\pm m\sqrt{m^2-1}\right)^2(m^2-1)^{5/6}}\right]. \quad (31)$$

Their diagrams are plotted against m in Figure 5. They show that sign of C^*_+ is changed at $m_c = 1.15(1.2)$ for $\delta = 0(0.9)$ but sign of C^*_- is changed at $m = 1$ for $\delta = 0, 0.9$. We plot also diagrams of $C^*_\pm$ versus ΔT^* in Figure 5. They show a changing of sign for C^*_+ when $\Delta T^* \longrightarrow 0$ and $\delta = 0, 0.9$ but not for C^*_-. In case $\delta = 0.9$ we see $C^*_- < 0$ for $\Delta T^* > 0$ but its absolute value exhibits a minimum value. When $\Delta T^* \longrightarrow 0$ we see C^*_- which decreases monotonically to negative infinite value for $\delta = 0$. Changing of sign of exterior horizon heat capacity means that a phase transition happens when the quantum perturbed RNBHs ensemble reaches its stable state with minimum mass $m_{final} = 1$. To determine order kind of this phase transition we should study behavior of the corresponding Gibbs free energy as follows.

Exterior and interior horizon Gibbs free energies are defined by

$$G_\pm = M - T_\pm A_\pm - \Phi_\pm \quad (32)$$

where entropy $A_\pm$ is given by (24) and electric potential $\Phi_\pm$ is defined by

$$\Phi_\pm = -T_\pm\left(\frac{\partial A_\pm}{\partial e}\right)_{a,M}. \quad (33)$$

Inserting $M = em$, $A_\pm = 4\pi e^2 S_\pm$, and (30), the above Gibbs energy equation reads

$$G^*_\pm = \frac{G_\pm}{e} = m - T^*_\pm S_\pm - 8\pi S_\pm - 4\pi e\frac{\partial S_\pm}{\partial e} \quad (34)$$

in which we have

$$e\frac{\partial S_\pm}{\partial e} = \mp\frac{2m\left(m\pm\sqrt{m^2-1}\right)^2}{\sqrt{m^2-1}} - \frac{\delta^2}{15(m^2-1)^{11/6}\left(m\pm\sqrt{m^2-1}\right)^2}\times\Big[28m^7 - 75m^5 + 74m^3 - 27m \pm \sqrt{m^2-1}\left(26m^6 - 61m^4 + 47m^2 - 12\right)\Big]. \quad (35)$$

We plot diagrams of the above equations against m in Figure 6. They show that G^*_- has minimum zero value at $m = 1$ but G^*_+ raises to $+\infty$ by decreasing $m \longrightarrow 1$ for $\delta = 0.9$. In case $\delta = 0$, we see $G^*_\pm \longrightarrow \pm\infty$ when $m \longrightarrow 1$. Furthermore we plot diagrams of $G^*_\pm$ versus ΔT^* in Figure 6. We see $G^*_- \longrightarrow -\infty$ when $\Delta T^* \longrightarrow 0$ for $\delta = 0$ but $G^*_- \longrightarrow 0^+$ for $\delta = 0$. G^*_+ decreases to a positive minimum value by decreasing $\Delta T^* \longrightarrow 0$ and then reaches positive infinite value.

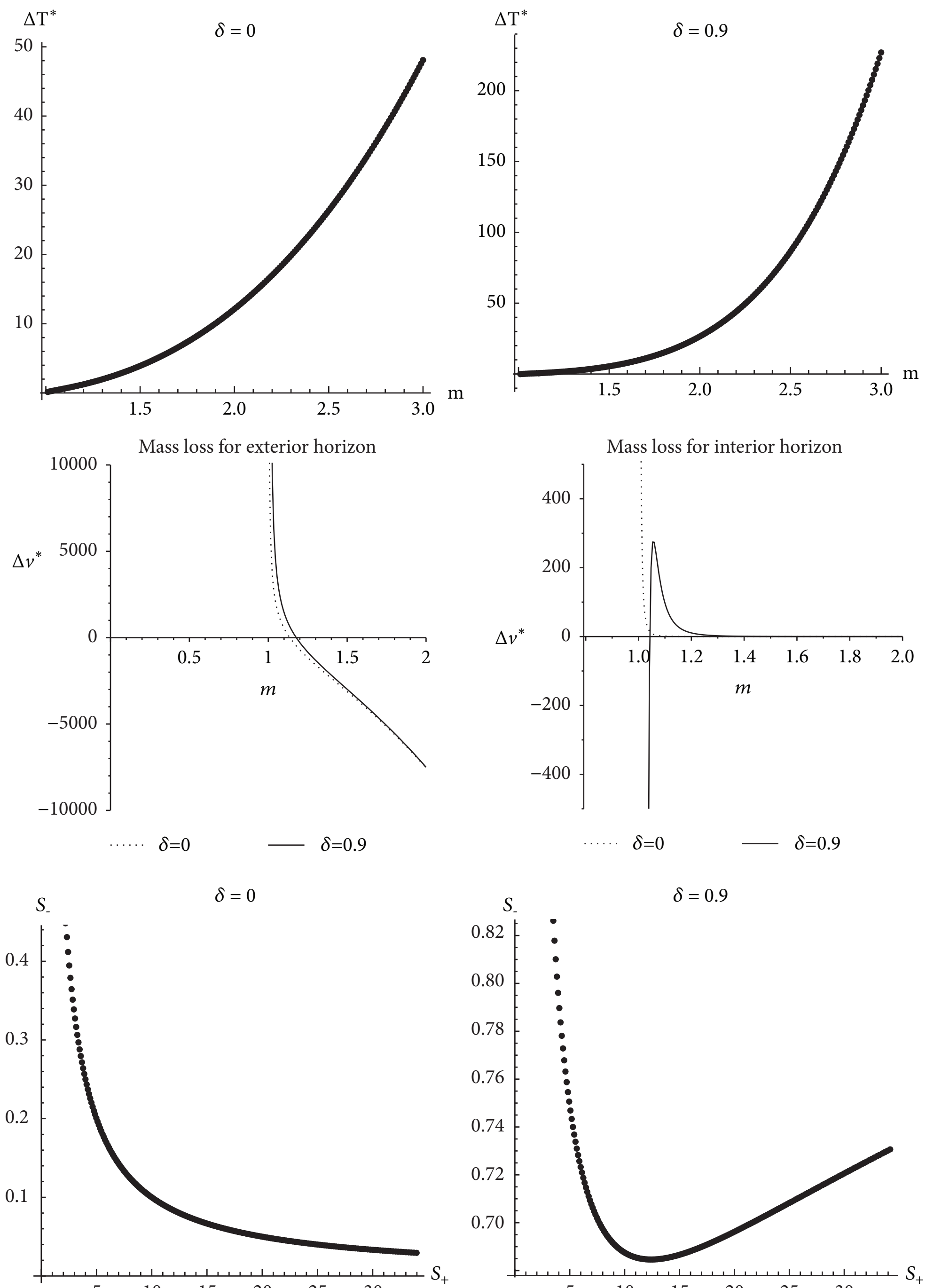

Figure 1: Diagram of mass loss $m(v)$, interior (exterior) horizon entropy $S_-(S_+)$, and difference of temperatures between interior and exterior horizons $\Delta T^*(m)$ is plotted against for single RNBH $\delta = 0$ and mean metric of coarse graining RNBHs $\delta = 0.9$.

The latter behavior shows changing the sign of first derivative of G_+^* when decreases m and/or ΔT^* which means that the phase transition is first order.

One of other suitable quantities which should be calculated is pressure of black hole microparticles which coincide with the interior horizon as follows. If a quantum particle is collapsed inside of the interior (exterior) horizon then its de Broglie wave length must be at least $\lambda_- \approx 2\rho_-(\lambda_+ \approx 2\rho_+)$. We use de Broglie quantization condition on quantum particles as $p_\pm = h/\lambda_\pm$ where h is Planck constant and $p_\pm$ is momentum of in-falling quantum particles inside of the horizons. In Plank units where $c = h = G = 1$ we can write

$$\Delta p = p_- - p_+ = \frac{1}{2}\left(\frac{1}{\rho_-} - \frac{1}{\rho_+}\right) \tag{36}$$

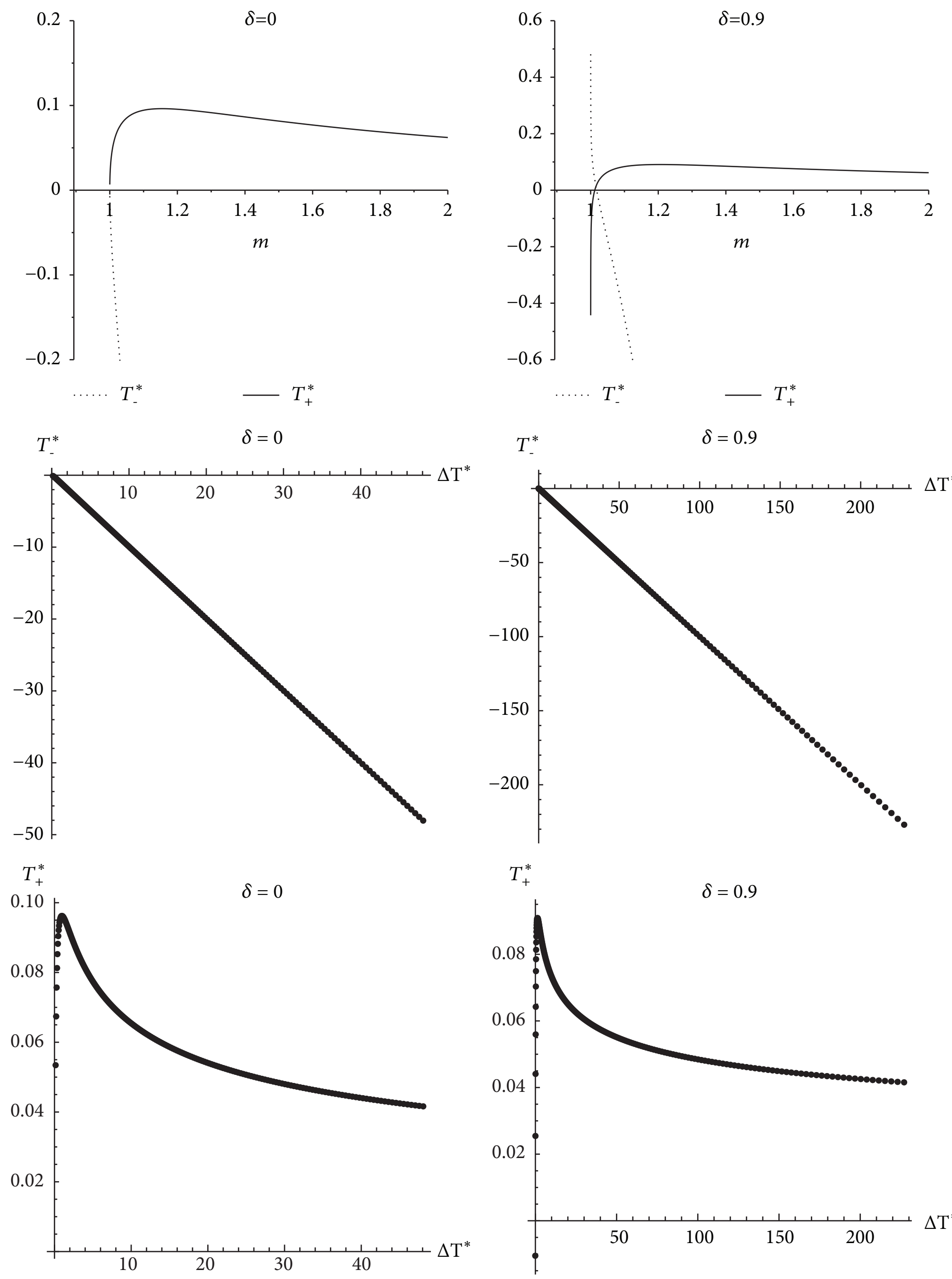

FIGURE 2: Diagram of $T^*_\pm$ is plotted against m and ΔT^* for $\delta = 0$ and $\delta = 0.9$.

in which Δp is difference of momentum of quantum particles which move from exterior horizon ρ_+ to interior ρ_- horizon. For $c = 1$ they move for durations $\Delta t = \rho_+ - \rho_-$. We now use the latter assumptions to rewrite Newton's second law as

$$F = \frac{\Delta p}{\Delta t} = \frac{1}{2\rho_+\rho_-}. \quad (37)$$

F is dimensionless force which affects interior horizon surface. When the system becomes stable mechanically, then F must be balanced by the electric force of the system defined by $F_E = e((\Phi_- - \Phi_+)/(\rho_+ - \rho_-))$. Spherically symmetric condition of the system causes choosing some radial motions for quantum particles located inside of the statistical ensemble of RNBHs. However one can define pressure of moving charged quantum particle on the interior horizon as

$$P_- = \frac{F}{4\pi\rho_-^2} = \frac{1}{8\pi\rho_+\rho_-^3} \quad (38)$$

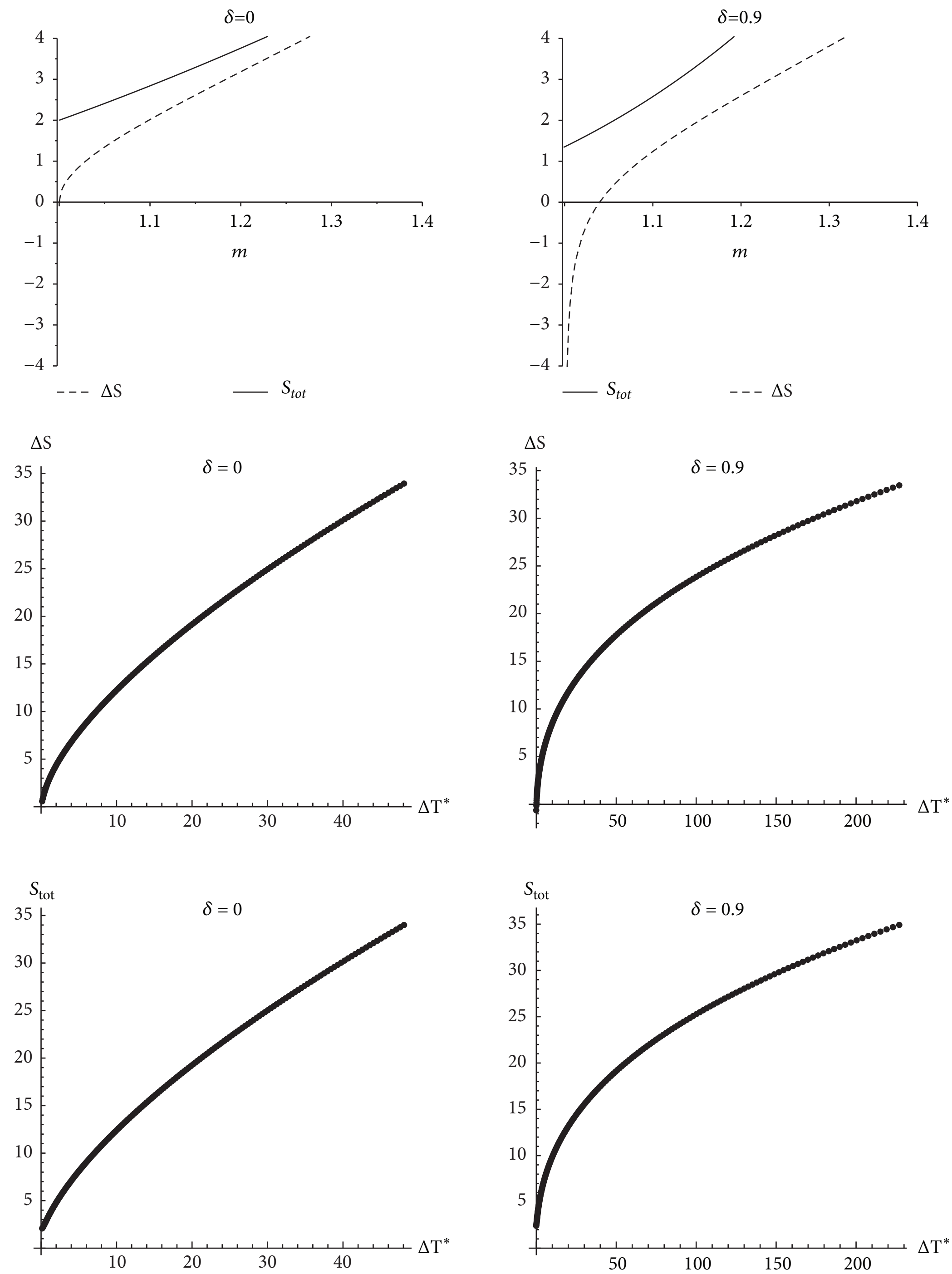

FIGURE 3: Diagram of ΔS and S_{tot} is plotted against m and ΔT^* for $\delta = 0$ and $\delta = 0.9$.

which by inserting (22) and using some simple calculations reads

$$P_-^*(m) = 8\pi e^4 P_- = \left(m - \sqrt{m^2-1}\right)^{-2} \left\{1 + \frac{\delta^2}{5} \times \left[\frac{24m^5 - 26m^3 + 2m^2 - 6m - 2}{\left(m - \sqrt{m^2-1}\right)^3} - \frac{\left(24m^6 - 38m^4 + 2m^3 + 16m^2 - 3m - 2\right)}{\sqrt{m^2-1}\left(m - \sqrt{m^2-1}\right)^3}\right]\right\}. \tag{39}$$

We plot diagram of the above pressure in Figure 8. They show that $P_-^* > 0 (< 0)$ in case $\delta = 0(0.9)$ for all values of $\Delta T^* > 0$. Diagrams show that P_-^* is vanishing when $\Delta T^* \longrightarrow 0$. Also we plot diagram for P_-^* versus m. It shows

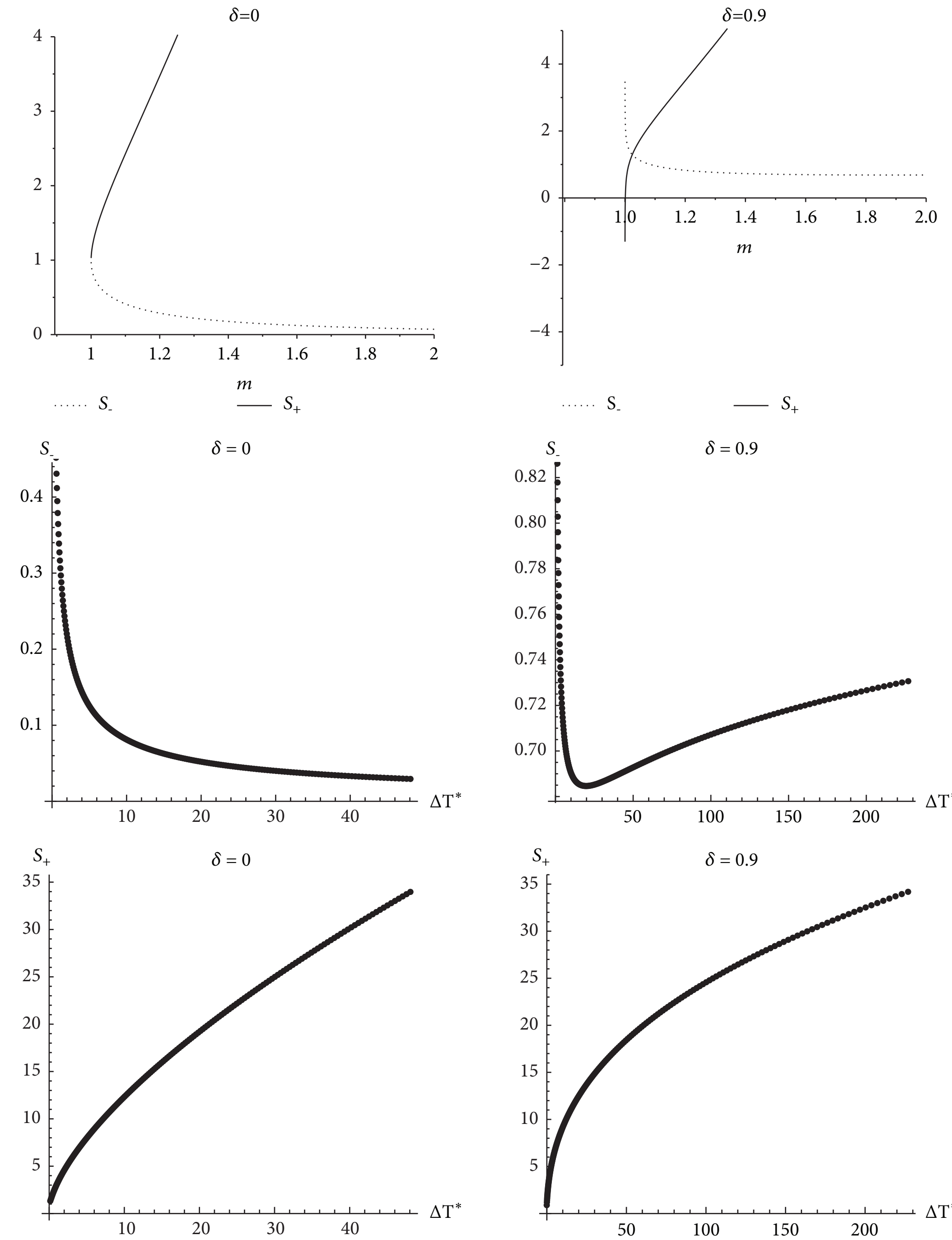

Figure 4: Diagram of $S_{\pm}$ is plotted against m and ΔT^* for $\delta = 0$ and $\delta = 0.9$.

$P_-^* \longrightarrow 0^+$ for $\delta = 0$. In case where $\delta = 0.9$ one can see $P_-^* < 0$ when $m \longrightarrow 1$ for $m > 1$ but $P_-^* \longrightarrow +\infty$. The latter results predict dark matter behavior of the interior horizon matter counterpart where for positive mass $m > 1$ there is some "negative" pressure. How can mass of mean metric RNBHs decrease? Dynamically this is possible if we consider corrections of quantum matter field interacting with the mean metric of RNBHs as follows. This makes the mean metric of RNBHs unstable quantum mechanically. In the next section we assume interaction of the mean metric of RNBHs statistical ensemble with massless, chargeless quantum scalar field for which e will be invariant of the system and so there is not any electromagnetic radiation. In other words there will be only mass interaction between quantum scalar field and ensemble of the RNBHs. They reduce usually to the well-known Hawking thermal radiation of the quantum perturbed mean metric which is causing mass loss of the mean RNBHs. For such a quantum mechanically unstable mean metric we now calculate its luminosity, mass loss process, and switching off effect.

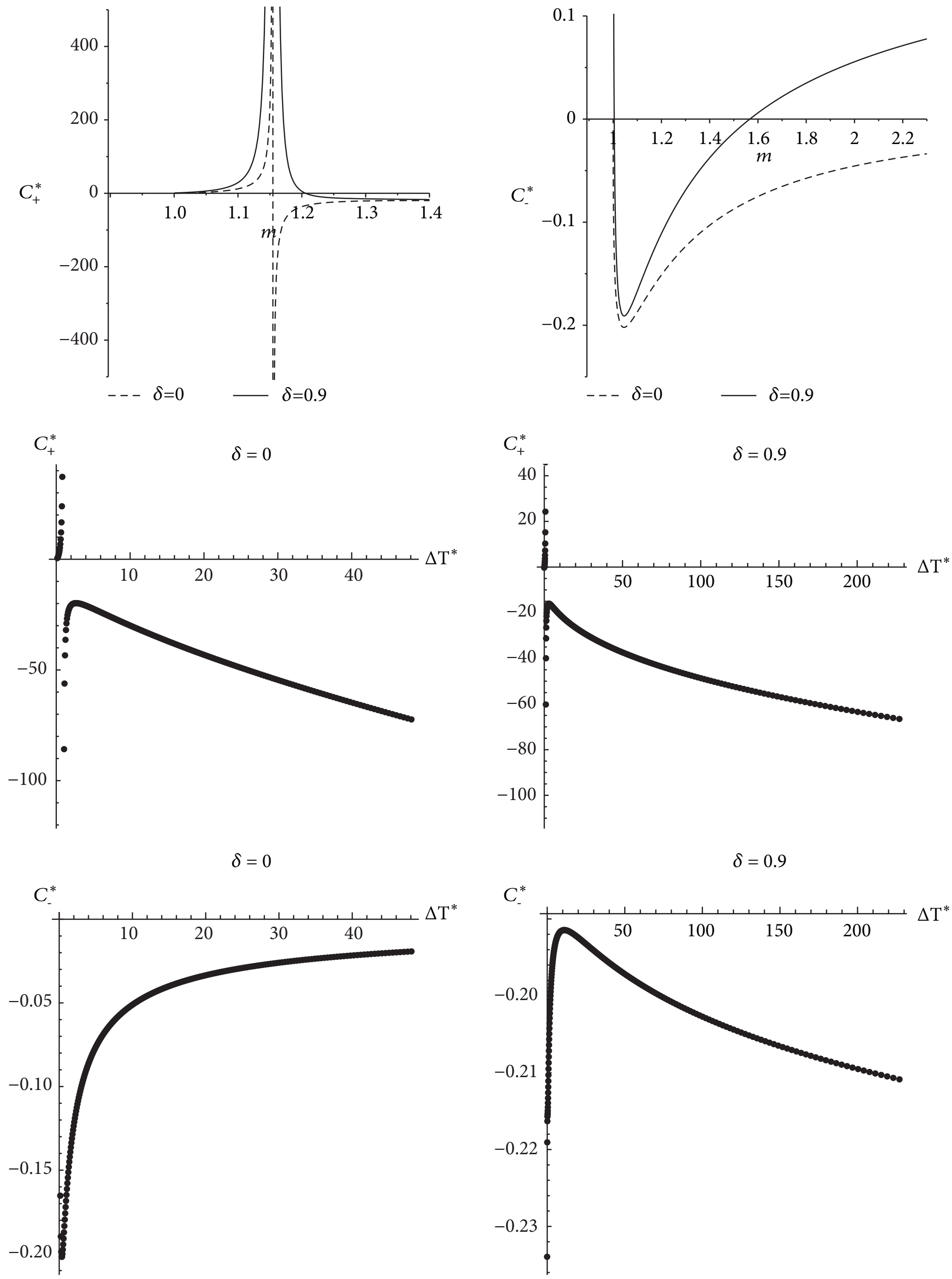

Figure 5: Diagram of interior and exterior horizons heat capacities $C_\pm^*$ is plotted against m and ΔT^* for $\delta = 0$ and $\delta = 0.9$.

5. Mean Quantum RNBH Mass Loss

We applied massless, chargeless quantum scalar field Hawking thermal radiation effects on single quantum unstable RNBH and calculated time dependence mass loss function in [15]. We obtained that the evaporating quantum perturbed RNBH exhibits switching off effect before its mass disappears completely. It should be pointed that electric charge of the black hole is invariant of the system because there is no electromagnetic interaction between its electric charge and chargeless quantum matter scalar field. Thus mass of the RNBH decreases to reach nonvanishing remnant stable mini Lukewarm black hole with $m_{final} = 1$. In other words its luminosity is eliminated while its mass is not eliminated completely (see figures 9, 10, and 11 given in [15]). Here we study mass loss and switching off effect of quantum perturbed mean metric (15). This is a dynamical approach to describe that how mean metric of RNBHs statistical ensemble exhibits a phase

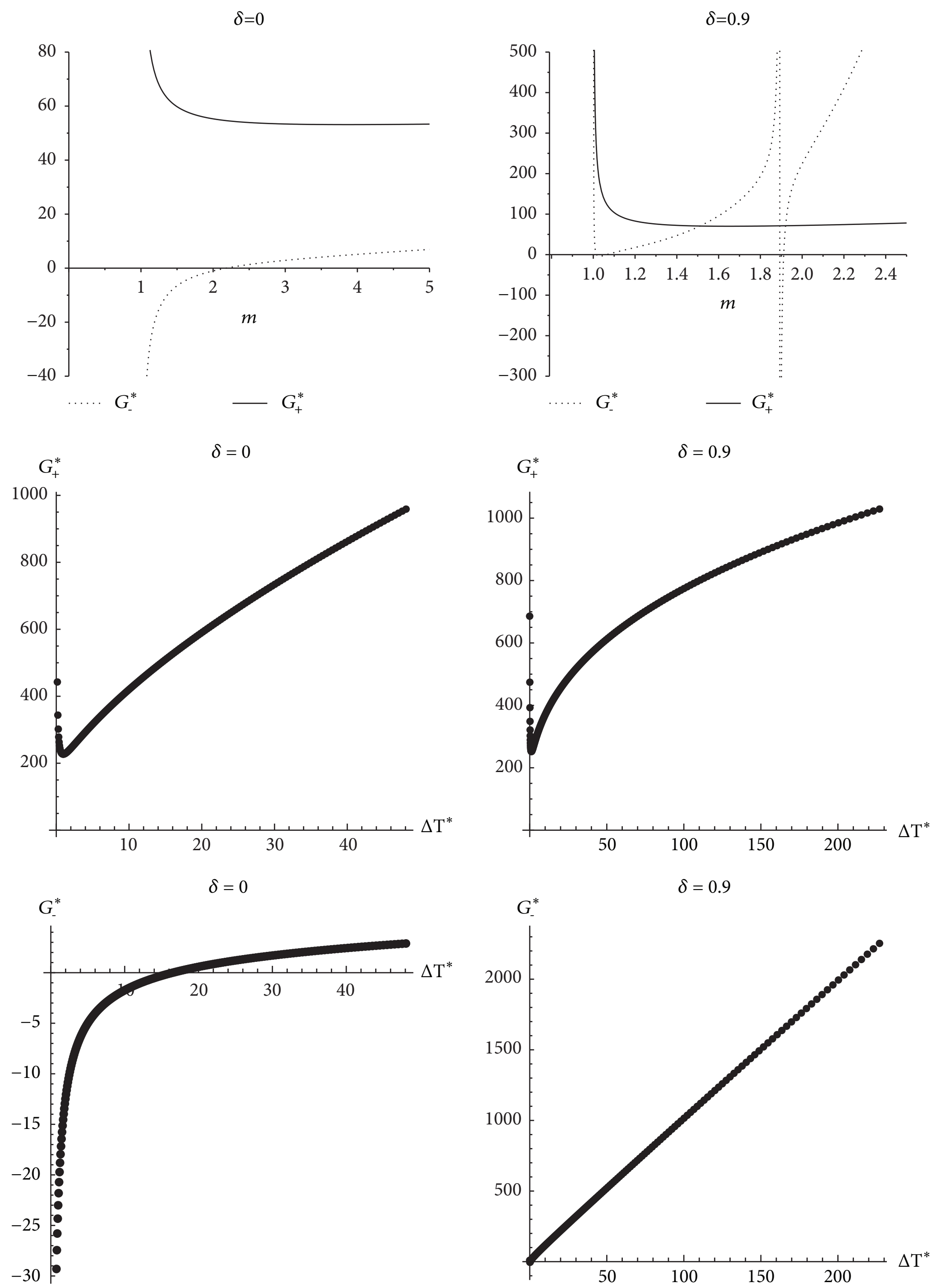

Figure 6: Diagram of interior and exterior horizons Gibbs free energies $G^*_{\pm}$ is plotted against m and ΔT^* for $\delta = 0$ and $\delta = 0.9$.

transition leading to a possible Bose-Einstein condensation state microscopically. Line element of the evaporating mean metric (15) can be written near the exterior horizon as Vaida form (see, for instance, [29]):

$$ds^2 \simeq \left(1 - \frac{r_+(v)}{r}\right) dv^2 - 2dvdr - r^2\left(d\theta^2 + \sin^2\theta d\varphi^2\right) \quad (40)$$

with the associated stress energy tensor

$$\left\langle \widehat{T}^{quant}_{\mu\nu} \right\rangle_{ren} = \frac{1}{4\pi r^2} \frac{dr_+(v)}{dv} \delta_{\mu v} \delta_{\nu v} \quad (41)$$

where (v, r) is advance Eddington-Finkelstein coordinates system. Subscript *ren* denotes the word *Renormalization*, and $\langle\rangle$ denotes expectation value of quantum matter scalar field stress tensor operator evaluated in its vacuum state. The

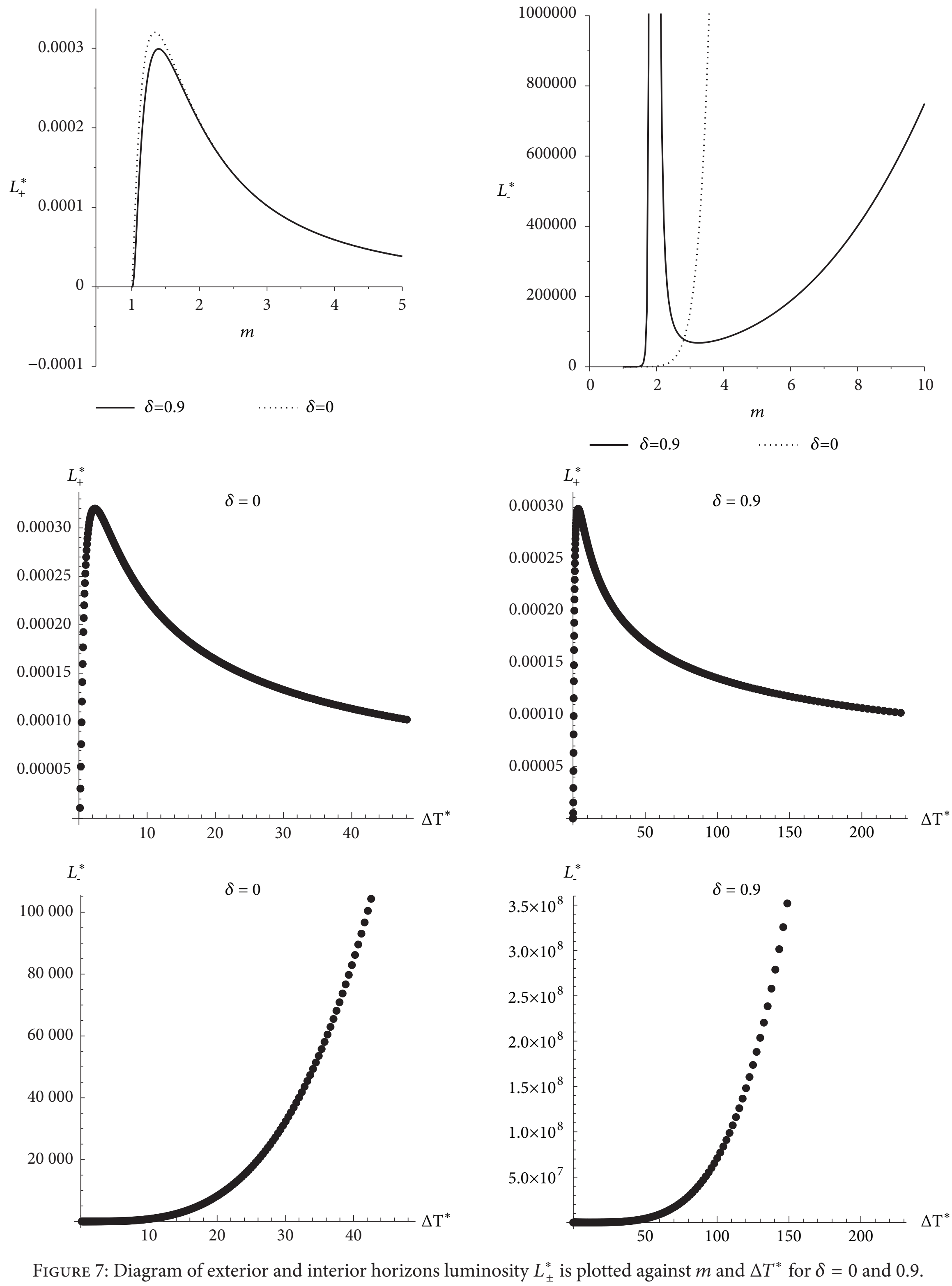

FIGURE 7: Diagram of exterior and interior horizons luminosity $L_{\pm}^*$ is plotted against m and ΔT^* for $\delta = 0$ and 0.9.

black hole luminosity is defined by the following equation from point of view of distant observer located in r.

$$L(r, v) = 4\pi r^2 \left\langle \widehat{T}_v^r \right\rangle_{ren}^{quant}. \tag{42}$$

Applying (40) and (41), (42) becomes

$$L = -\frac{1}{2} \frac{dr_+(v)}{dv} \tag{43}$$

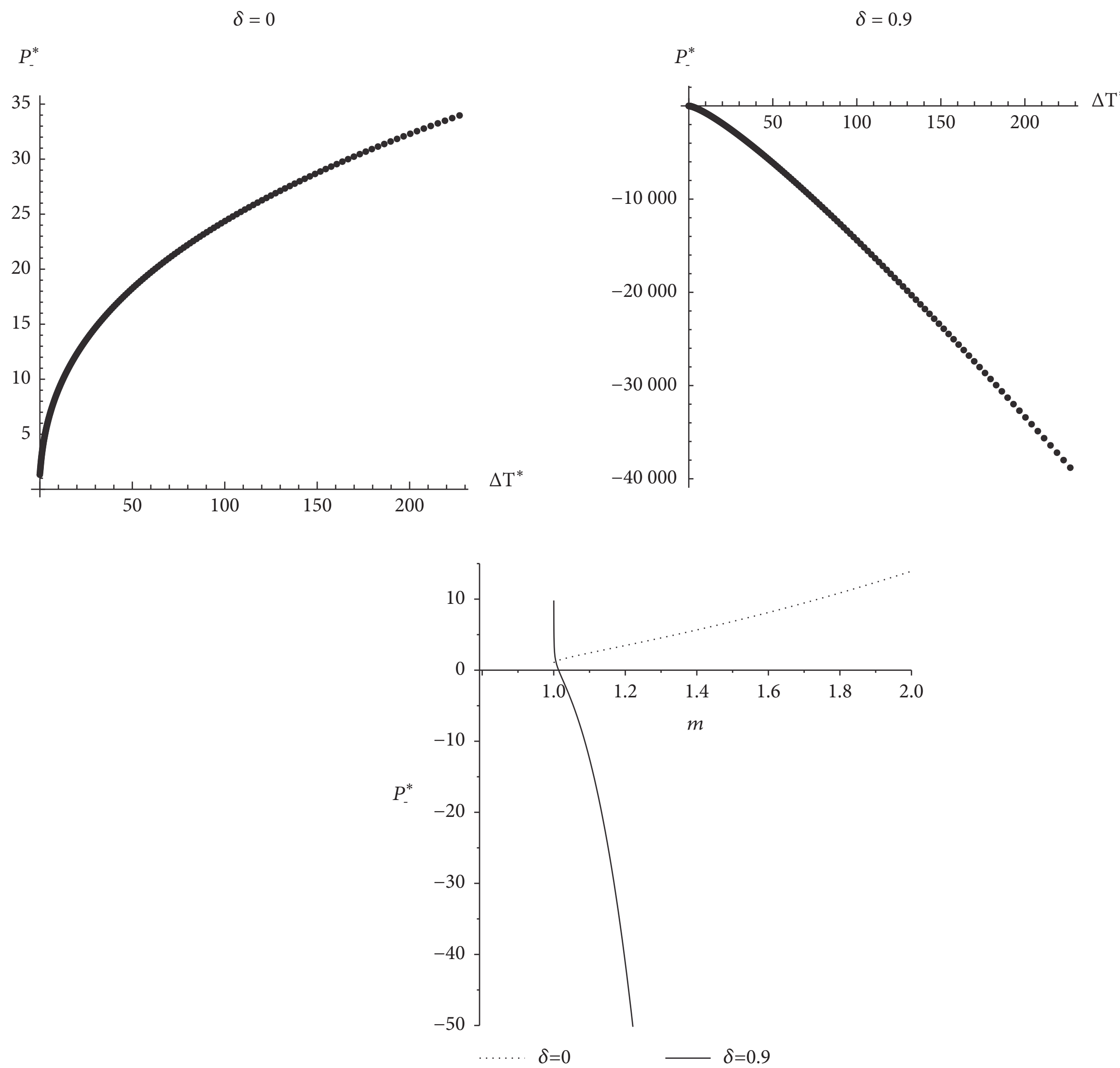

FIGURE 8: Diagram of interior horizon pressure P_-^* is plotted against m and ΔT^* for $\delta = 0$ and $\delta = 0.9$.

where negative sign describes inward flux of negative energy across the horizon. This causes the mean metric horizon of RNBHs statistical ensemble to shrink. In the latter case quantum particles of matter content of the black hole are in high energy state and so one can assume that the quantum black hole behaves as a black body radiation of which luminosity is defined by well-known Stefan-Boltzman law as follows:

$$L = \sigma_{SB} A T^4 \tag{44}$$

where A is surface area of the black body and T is its temperature. $\sigma_{SB} = 5.67 \times 10^{-8} (J/(m^2 \times {}^\circ K^4 \times Sec))$ is Stefan-Boltzman coupling constant of which dimensions become as $(length)^2$ in units $G = c = 1$. If (44) satisfies (43), then we can obtain mass loss equation of the mean metric of RNBHs statistical ensemble such that

$$\frac{dr_+(v)}{dv} = -2\sigma_{SB} \xi A_+(v) T_+^4(v) \tag{45}$$

where the normalization constant ξ depends linearity on the number of massless, chargeless quantum matter fields and will control the rate of evaporation. Inserting (27) one can show that the luminosity (44) for RNBHs mean metric (15) becomes

$$L_+^*(m) = \frac{(4\pi)^3 e^2}{\sigma_{SB}} L = S_+(m) T^{*4}_+(m) \tag{46}$$

where $S_+(m)$ and $T_+^*(m)$ should be inserted from (25) and (30), respectively. Applying (19), (20), (21), (22), (27), and some simple calculations, we can show that the mean mass loss equation (45) for RNBHs mean metric (15) reads

$$\Delta v^* = v^*(m) - v_\infty^* = -\frac{1}{2} \int_m^1 \left(\frac{dr_+}{d\rho_+} \right) \frac{dm}{S_+^{3/2} T_+^{*5}} \tag{47}$$

where we used (19), (20), (21), (22), (27), $\delta = a/e$, $m = M/e$, and $\rho_+ = e\sqrt{S_+}$ to calculate $dr_+/d\rho_+$ which up to terms in order of $O(\delta^3)$ become

$$\frac{dr_+}{d\rho_+} = 1 + \frac{\delta^2}{5}\left(\frac{2}{\left(m+\sqrt{m^2-1}\right)^3} - \frac{3}{\left(m+\sqrt{m^2-1}\right)^4}\right). \tag{48}$$

$v^*_\infty = v^*(1)$ given in (47) is integral constant for which evaporating mean mass of RNBHs statistical ensemble reaches its final value as $m_{final} = 1$. Also we defined dimensionless advance Eddington-Finkelstein time coordinate v^* as follows:

$$\frac{v^*}{v} = \frac{2\xi\sigma_{SB}}{(4\pi e)^3}. \tag{49}$$

When exterior horizon of quantum evaporating RNBHs mean metric reduces to scale of its interior horizon as $r_+(v) \longrightarrow r_-$ then one can use similar equations for luminosity and mass loss equations (46) and (47) for interior horizon as follows:

$$L^*_-(m) = \frac{(4\pi)^3 e^2}{\sigma_{SB}} L = S_-(m)\, T^{*4}_-(m) \tag{50}$$

$$\Delta v^* = v^*(m) - v^*_\infty = -\frac{1}{2}\int_m^1 \left(\frac{dr_-}{d\rho_-}\right)\left(\frac{dS_-}{dm}\right)\frac{dm}{S_-^{3/2} T^{*4}_-} \tag{51}$$

where

$$\frac{dr_-}{d\rho_-} = 1 + \frac{\delta^2}{5}\left(\frac{2}{\left(m-\sqrt{m^2-1}\right)^3} - \frac{3}{\left(m-\sqrt{m^2-1}\right)^4}\right). \tag{52}$$

Diagrams of the luminosities (46) and (50) and the evaporating mean RNBHs mass loss equations (47) and (51) are plotted versus mass parameter m in Figure 7. They show that evaporating quantum unstable mean mass of RNBHs final state reaches remnant stable cold mini Lukewarm RNBH with final mass $m_{final} = 1$ where its causal singularity is still covered by its shrunken horizon and its luminosity reaches zero value. We see that invariant conditions on the black hole electric charge e causes the Penrose cosmic censorship hypothesis to be valid while the black hole metric is evaporated where the casual singularity of mean metric (15) defined by $\rho = 0$ is still covered by their smallest scale horizons hypersurface with no naked singularity.

6. Summary and Discussion

According to the Debbasch approach we calculated mean metric of RNBHs statistical ensemble to obtain locations of interior and exterior horizons. We calculated corresponding entropy, temperature, heat capacity, Gibbs free energy, and pressure. At last section of the paper we considered interaction of massless, chargeless quantum scalar matter field on quantum perturbed mean metric of coarse graining RNBHs. Our mathematical calculations predict evaporation of the mean metric which reduces to a remnant stable mini black hole metric with nonvanishing mass. Before the evaporation reaches its final state, the mean metric exhibits a first-order phase transition and Bose-Einstein condensation state happens microscopically. Our results approve outputs of the published work [15] qualitatively in which the author studied thermodynamic behavior of a single RN black hole.

Data Availability

The data used to support the findings of this study are available from the corresponding author upon request.

Conflicts of Interest

The authors declare that they have no conflicts of interest.

References

[1] F. Debbasch, "What is a mean gravitational field?" *The European Physical Journal B - Condensed Matter*, vol. 37, no. 2, pp. 257–269, 2003.

[2] T. Buchert, "On average properties of inhomogeneous fluids in general relativity: dust cosmologies," *General Relativity and Gravitation*, vol. 32, no. 1, pp. 105–125, 2000.

[3] T. Buchert, "On average properties of inhomogeneous fluids in general relativity: perfect fluid cosmologies," *General Relativity and Gravitation*, vol. 33, no. 8, pp. 1381–1405, 2001.

[4] T. Futamase, "A new description for a realistic inhomogeneous universe in general relativity," *Progress of Theoretical and Experimental Physics*, vol. 86, no. 2, pp. 389–399, 1991.

[5] T. Futamase, "General relativistic description of a realistic inhomogeneous universe," *Progress of Theoretical and Experimental Physics*, vol. 89, no. 3, pp. 581–597, 1993.

[6] T. Futamase, "Averaging of a locally inhomogeneous realistic universe," *Physical Review D: Particles, Fields, Gravitation and Cosmology*, vol. 53, no. 2, pp. 681–689, 1996.

[7] M. Kasai, "Construction of inhomogeneous universes which are Friedmann-Lematre-Robertson-Walker on average," *Physical Review Letters*, vol. 69, no. 16, pp. 2330–2332, 1992.

[8] R. M. Zalaletdinov, "Averaging problem in general relativity, macroscopic gravity and using Einstein's equations in cosmology," *Bulletin of the Astronomical Society of India*, vol. 25, p. 401, 1997.

[9] C. Chevalier and F. Debbasch, "Is matter an emergent property of Space time?" 2010, https://www.semanticscholar.org/paper/Is-Matter-an-emergent-property-of-Space-Time-Chevalier-Debbasch/170660f108a1eaaa463144dcdeeec9d10f1c6a26.

[10] F. Debbasch and Y. Ollivier, “Observing a Schwarzschild black hole with finite precision,” *Astronomy & Astrophysics* , vol. 433, no. 2, pp. 397–404, 2005.

[11] C. Chevalier and F. Debbasch, “Thermal statistical ensembles of classical extreme black holes,” *Physica A: Statistical Mechanics and Its Applications*, vol. 388, no. 5, pp. 628–638, 2009.

[12] C. Chevalier, M. Bustamante, and F. Debbasch, “Thermal statistical ensembles of black holes,” *Physica A: Statistical Mechanics and Its Applications*, vol. 376, pp. 293–307, 2007.

[13] S. W. Hawking and D. N. Page, “Thermodynamics of black holes in anti-de Sitter space,” *Communications in Mathematical Physics*, vol. 87, no. 4, pp. 577–588, 1983.

[14] G. Grimmett and D. Stiraker, *Probability and Random Process*, Oxford University Press, Oxford, UK, 2nd edition, 1994.

[15] H. Ghaffarnejad, “Classical and quantum Reissner-Nordström black hole thermodynamics and first order phase transition,” *Astrophysics and Space Science*, vol. 361, article 7, 2016.

[16] L. Bo and L. Wen-Biao, “Negative temperature of inner horizon and planck absolute entropy of a Kerr-Newman black hole,” *Communications in Theoretical Physics*, vol. 53, no. 1, pp. 83–86, 2010.

[17] J. C. Flores and L. P. Chilla, “Theoretical thermodynamics connections between dual (left-handed) and direct (right-handed) system: entropy, temperatue, pressure and heat capacity,” *Physca B*, vol. 476, p. 88, 2015.

[18] S. Braun, J. P. Ronzheimer, M. Schreiber et al., “Negative absolute temperature for motional degrees of freedom,” *Science*, vol. 339, no. 6115, pp. 52–55, 2013.

[19] G. B. Furman, S. D. Goren, V. M. Meerovich, and V. L. Sokolovsky, “Quantum correlations at negative absolute temperatures,” *Quantum Information Processing*, vol. 13, no. 12, pp. 2759–2768, 2014.

[20] H. Stephani, D. Kramer, M. MacCallum, C. Hoenselaers, and E. Herlt, *Exact Solutions of Einstein's Equations*, Cambridge University Press, Cambridge, UK, 2nd edition, 2009.

[21] H. Ghaffarnejad and M. Farsam, “Statistical ensembles of Reissner-Nordstrom black holes and thermodynamical first order phase transition,” https://arxiv.org/abs/1603.08408.

[22] H. Nariai, “On some static solutions of Einstein's gravitational field equations in a spherically symmetric case,” *Science Reports of Tohoku University*, vol. 34, pp. 160–167, 1950.

[23] R. Bousso and S. W. Hawking, “(Anti-)evaporation of Schwarzschild-de SITter black holes,” *Physical Review D: Particles, Fields, Gravitation and Cosmology*, vol. 57, no. 4, pp. 2436–2442, 1998.

[24] E. Schrödinger, *What Is Life - The Physical Aspect of the Living Cell*, Cambridge University Press, 1944.

[25] L. del Rio, J. Aberg, R. Renner, O. Dahlsten, and V. Vedral, “The thermodynamic meaning of negative entropy,” *Nautre*, vol. 474, p. 61, 2011.

[26] S. P. Mahulikar and H. Herwig, “Exact thermodynamic principles for dynamic order existence and evolution in chaos,” *Chaos, Solitons & Fractals*, vol. 41, no. 4, pp. 1939–1948, 2009.

[27] E. Oliva, “Entropy and negentropy: applications in game theory,” in *Dynamics, Games and Science*, J.-P. Bourguignon, R. Jeltsch, A. A. Pinto, and M. Viana, Eds., vol. 1 of *CIM Series in Mathematical Sciences*, pp. 513–525, Springer, Cham, Switzerland, 2015.

[28] L. F. del Castillo and P. V. Cruz, “Thermodynamical formulation of living systems and their evolution,” *Journal of Modern Physics*, vol. 2, p. 379, 2012.

[29] P. Hajicek and W. Israel, “What, no black hole evaporation?” *Physics Letters A*, vol. 80, no. 1, pp. 9-10, 1980.

Hindawi
Advances in High Energy Physics
Volume 2019, Article ID 6825104, 28 pages
https://doi.org/10.1155/2019/6825104

Research Article

A New Mechanism for Generating Particle Number Asymmetry through Interactions

Takuya Morozumi,[1,2] Keiko I. Nagao,[3,4] Apriadi Salim Adam,[1] and Hiroyuki Takata[5]

[1] *Graduate School of Science, Hiroshima University, Higashi-Hiroshima, 739-8526, Japan*
[2] *Core of Research for Energetic Universe, Hiroshima University, Higashi-Hiroshima, 739-8526, Japan*
[3] *National Institute of Technology, Niihama College, Ehime, 792-8580, Japan*
[4] *Okayama University of Science, Ridaicho, Kita-ku, Okayama, 700-0005, Japan*
[5] *Tomsk State Pedagogical University, Tomsk, 634061, Russia*

Correspondence should be addressed to Apriadi Salim Adam; apriadiadam@hiroshima-u.ac.jp

Received 27 December 2018; Accepted 19 February 2019; Published 7 April 2019

Guest Editor: Subhajit Saha

Copyright © 2019 Takuya Morozumi et al. This is an open access article distributed under the Creative Commons Attribution License, which permits unrestricted use, distribution, and reproduction in any medium, provided the original work is properly cited. The publication of this article was funded by SCOAP[3].

A new mechanism for generating particle number asymmetry (PNA) has been developed. This mechanism is realized with a Lagrangian including a complex scalar field and a neutral scalar field. The complex scalar carries U(1) charge which is associated with the PNA. It is written in terms of the condensation and Green's function, which is obtained with two-particle irreducible (2PI) closed time path (CTP) effective action (EA). In the spatially flat universe with a time-dependent scale factor, the time evolution of the PNA is computed. We start with an initial condition where only the condensation of the neutral scalar is nonzero. The initial condition for the fields is specified by a density operator parameterized by the temperature of the universe. With the above initial conditions, the PNA vanishes at the initial time and later it is generated through the interaction between the complex scalar and the condensation of the neutral scalar. We investigate the case that both the interaction and the expansion rate of the universe are small and include their effects up to the first order of the perturbation. The expanding universe causes the effects of the dilution of the PNA, freezing interaction, and the redshift of the particle energy. As for the time dependence of the PNA, we found that PNA oscillates at the early time and it begins to dump at the later time. The period and the amplitude of the oscillation depend on the mass spectrum of the model, the temperature, and the expansion rate of the universe.

1. Introduction

The origin of BAU has long been a question of great interest in explaining why there is more baryon than antibaryon in nature. Big bang nucleosynthesis (BBN) [1] and cosmic microwave background [2] measurements give the BAU as $\eta \equiv n_B/s \simeq 10^{-10}$, where n_B is the baryon number density and s is the entropy density. In order to address this issue, many different models and mechanisms have been proposed [3–7]. The mechanisms discussed in the literature satisfy the three Sakharov conditions [3], namely, (i) baryon number (B) violation, (ii) charge (C) and charge-parity (CP) violations, and (iii) a departure from the thermal equilibrium. For reviews of different types of models and mechanisms, see, for example, [8–10]. Recently, the variety of the method for the calculation of BAU has been also developed [11–13].

In the present paper, we further extend the model of scalar fields [14] so that it generates the PNA through interactions. In many of the previous works, the mechanism generating BAU relies on the heavy particle decays. Another mechanism uses U(1) phase of the complex scalar field [6]. In this work, we develop a new mechanism to generate PNA. The new feature of our approach is briefly explained below.

The model which we have proposed [15] consists of a complex scalar field and a neutral scalar field. The PNA is related to the U(1) current of the complex field. In our model, the neutral scalar field has a time-dependent expectation value which is called condensation. In the new mechanism, the oscillating condensation of the neutral scalar interacts with the complex scalar field. Since the complex scalar field carries U(1) charge, the interactions with the condensation of the neutral scalar generate PNA. The interactions break U(1) symmetry as well as charge conjugation symmetry. At the initial time, the condensation of the neutral scalar is nonzero. We propose a way which realizes such initial condition.

As for the computation of the PNA, we use 2PI formalism combined with density operator formulation of quantum field theory [16]. The initial conditions of the quantum fields are specified with the density operator. The density operator is parameterized by the temperature of the universe at the initial time. We also include the effect of the expansion of the universe. It is treated perturbatively and the leading order term which is proportional to the Hubble parameter at the initial time is considered. With this method, the time dependence of the PNA is computed and the numerical analysis is carried out. The dependence, especially, on the various parameters of the model such as masses and strength of interactions is investigated. We also study the dependence on the temperature and the Hubble parameter at the initial time. We first carry out the numerical simulation without specifying the unit of parameter sets. Later, in a radiation dominated era, we specify the unit of the parameters and estimate the numerical value of the PNA over entropy density.

This paper is organized as follows. In Section 2, we introduce our model with CP and particle number violating interactions. We also specify the density operator as the initial state. In Section 3, we derive the equation of motion for Green's function and field by using 2PI CTP EA formalism. We also provide the initial condition for Green's function and field. In Section 4, using the solution of Green's function and field, we compute the expectation value of the PNA. Section 5 provides the numerical study of the time dependence of the PNA. We will also discuss the dependence on the parameters of the model. Section 6 is devoted to conclusion and discussion. In Appendix A, we introduce a differential equation which is a prototype for Green's function and field equations. Applying the solutions of the prototype, we obtain the solutions for both Green's function and field equations. In Appendices B–D, the useful formulas to obtain the PNA for nonvanishing Hubble parameter case are derived.

2. A Model with CP and Particle Number Violating Interaction

In this section, we present a model which consists of scalar fields [15]. It has both CP and particle number violating features. As an initial statistical state for scalar fields, we employ the density operator for thermal equilibrium.

Let us start by introducing a model consisting of a neutral scalar, N, and a complex scalar, ϕ. The action is given by

$$\begin{aligned} S &= \int d^4x\sqrt{-g}\left(\mathcal{L}_{\text{free}} + \mathcal{L}_{\text{int}}\right), \\ \mathcal{L}_{\text{free}} &= g^{\mu\nu}\nabla_\mu\phi^\dagger\nabla_\nu\phi - m_\phi^2|\phi|^2 + \frac{1}{2}\nabla_\mu N\nabla^\mu N \\ &\quad - \frac{M_N^2}{2}N^2 + \frac{B^2}{2}\left(\phi^2 + \phi^{\dagger 2}\right) \\ &\quad + \left(\frac{\alpha_2}{2}\phi^2 + h.c.\right)R + \alpha_3|\phi|^2 R, \\ \mathcal{L}_{\text{int}} &= A\phi^2 N + A^*\phi^{\dagger 2}N + A_0|\phi|^2 N, \end{aligned} \tag{1}$$

where $g_{\mu\nu}$ is the metric and R is the Riemann curvature. With this Lagrangian, we aim to produce the PNA through the soft-breaking terms of U(1) symmetry whose coefficients are denoted by A and B^2. One may add the quartic terms to the Lagrangian which are invariant under the U(1) symmetry. Though those terms preserve the stability of the potential for large field configuration and are also important for the renormalizability, we assume they do not lead to the leading contribution for the generation of the PNA. We also set the coefficients of the odd power terms for N^n $(n = 1, 3)$ zero in order to obtain a simple oscillating behavior for the time dependence of the condensation of N. We assume that our universe is homogeneous for space and employ the Friedmann-Lemaître-Robertson-Walker metric,

$$g_{\mu\nu} = \left(1, -a^2\left(x^0\right), -a^2\left(x^0\right), -a^2\left(x^0\right)\right), \tag{2}$$

where $a(x^0)$ is the scale factor at time x^0. Correspondingly the Riemann curvature is given by

$$R\left(x^0\right) = 6\left[\frac{\ddot{a}\left(x^0\right)}{a\left(x^0\right)} + \left(\frac{\dot{a}\left(x^0\right)}{a\left(x^0\right)}\right)^2\right]. \tag{3}$$

In (1), the terms proportional to A, B, and α_2 are the particle number violating interactions. In general, only one of the phases of those parameters can be rotated away. Throughout this paper, we study the special case that B and α_2 are real numbers and A is a complex number. Since only A is a complex number, it is a unique source of the CP violation.

We rewrite all the fields in terms of real scalar fields, ϕ_i $(i = 1, 2, 3)$, defined as

$$\phi = \frac{\phi_1 + i\phi_2}{\sqrt{2}}, \quad N = \phi_3. \tag{4}$$

With these definitions, the free part of the Lagrangian is rewritten as

$$\mathcal{L}_{\text{free}} = \frac{1}{2}\sqrt{-g}\left[g^{\mu\nu}\nabla_\mu\phi_i\nabla_\nu\phi_i - \widetilde{m}_i^2\left(x^0\right)\phi_i^2\right], \tag{5}$$

where the kinetic term is given by

$$g^{\mu\nu}\nabla_\mu\phi_i\nabla_\nu\phi_i = \frac{\partial\phi_i}{\partial x^0}\frac{\partial\phi_i}{\partial x^0} - \frac{1}{a\left(x^0\right)^2}\frac{\partial\phi_i}{\partial x^j}\frac{\partial\phi_i}{\partial x^j}, \tag{6}$$

and their effective masses are given as follows:

$$\widetilde{m}_1^2\left(x^0\right) = m_\phi^2 - B^2 - \left(\alpha_2 + \alpha_3\right)R\left(x^0\right), \tag{7}$$

$$\widetilde{m}_2^2\left(x^0\right) = m_\phi^2 + B^2 + \left(\alpha_2 - \alpha_3\right)R\left(x^0\right), \tag{8}$$

$$\widetilde{m}_3^2\left(x^0\right) = m_N^2. \tag{9}$$

Nonzero B^2 or α_2 leads to the nondegenerate mass spectrum for ϕ_1 and ϕ_2. The interaction Lagrangian is rewritten with a totally symmetric coefficient A_{ijk},

$$\mathcal{L}_{\text{int}} = \sum_{ijk=1}^{3}\frac{1}{3}A_{ijk}\phi_i\phi_j\phi_k \tag{10}$$

Table 1: The cubic interactions and their properties.

Cubic interaction coupling	Property
$A_{113} = \dfrac{A_0}{2} + \mathrm{Re.}(A)$	–
$A_{223} = \dfrac{A_0}{2} - \mathrm{Re.}(A)$	–
$A_{113} - A_{223} = 2\mathrm{Re.}(A)$	U(1) violation
$A_{123} = -\mathrm{Im.}(A)$	U(1), CP violation

with $i, j, k = 1, 2, 3$. The nonzero components of A_{ijk} are written with the couplings for cubic interaction, A and A_0, as shown in Table 1. We also summarize the qubic interactions and their properties according to U(1) symmetry and CP symmetry.

Nöether current related to the U(1) transformation is

$$j_\mu(x) = \frac{i}{2}\left(\phi^\dagger \overleftrightarrow{\partial_\mu} \phi - \phi \overleftrightarrow{\partial_\mu} \phi^\dagger\right). \tag{11}$$

In terms of real scalar fields, the Nöether current alters into

$$j_\mu = \frac{1}{2}\left(\phi_2 \overleftrightarrow{\partial_\mu} \phi_1 - \phi_1 \overleftrightarrow{\partial_\mu} \phi_2\right). \tag{12}$$

The ordering of the operators in (11) is arranged so that it is Hermite and the particle number operator,

$$Q\left(x^0\right) = \int d^3\mathbf{x}\sqrt{-g}\, j_0(x), \tag{13}$$

has a normal ordered expression. Then, in the vanishing limit of interaction terms and particle number violating terms, the vacuum expectation value of the particle number vanishes. With the above definition, $j_0(x)$ is the PNA per unit comoving volume. The expectation value of the PNA is written with a density operator,

$$\langle j_0(x)\rangle = \mathrm{Tr}\left(j_0(x)\,\rho(t_0)\right). \tag{14}$$

Note that, the PNA is a Heisenberg operator and $\rho(t_0)$ is a density operator which specifies the state at the initial time $x^0 = t_0$. In this work, we use the density operator with zero chemical potential. It is specifically given by

$$\rho(t_0) = \frac{e^{-\beta H}}{\mathrm{Tr}\left(e^{-\beta H}\right)}, \tag{15}$$

where β denotes inverse temperature, $1/T$, and H is a Hamiltonian which includes linear term of fields,

$$\begin{aligned} H = {} & \frac{1}{2}\sum_{i=1}^{3}\int d^3\mathbf{x}\, a(t_0)^3 \\ & \cdot \left[\pi_{\phi_i}\pi_{\phi_i} + \frac{\nabla\phi_i\cdot\nabla\phi_i}{a(t_0)^2} + \widetilde{m}_i^2(\phi_i - v_i)^2\right], \end{aligned} \tag{16}$$

where v_i is a constant. The linear term of fields in (16) is prepared for the nonzero expectation value of fields. Note that the density operator in (15) is not exactly the same as the thermal equilibrium one since, in the Hamiltonian, the interaction parts are not included. Since we assume three-dimensional space is translational invariant, then the expectation value of the PNA depends on time x^0 and the initial time t_0. As we will show later, the nonzero expectation value for the field ϕ_3 leads to the time-dependent condensation which is the origin of the nonequilibrium time evolution of the system.

Below we consider the matrix element of the density operator given in (15). We start with the following density operator for one component real scalar field as an example,

$$\rho(t_0) = \frac{e^{-\beta H_{\text{example}}}}{\mathrm{Tr}\left(e^{-\beta H_{\text{example}}}\right)}, \tag{17}$$

$$\begin{aligned} & H_{\text{example}} \\ & \quad = \frac{1}{2}\int d^3\mathbf{x}\, a(t_0)^3\left[\pi_\phi\pi_\phi + \frac{\nabla\phi\cdot\nabla\phi}{a(t_0)^2} + \widetilde{m}^2(\phi - v)^2\right]. \end{aligned} \tag{18}$$

The above Hamiltonian is obtained from that of (16) by keeping only one of the real scalar fields. The matrix element of the initial density operator in (17) is written in terms of the path integral form of the imaginary time formalism given as

$$\langle\phi^1|\rho(t_0)|\phi^2\rangle = \frac{\int_{\phi(0)=\phi^2,\phi(\beta)=\phi^1} d\phi\, e^{-S_E^{\text{example}}[\phi]}}{\int d\phi^1 \int_{\phi(0)=\phi^1,\phi(\beta)=\phi^1} d\phi\, e^{-S_E^{\text{example}}[\phi]}}, \tag{19}$$

where S_E^{example} is an Euclidean action which corresponds to the Hamiltonian in (18) and it is given by

$$\begin{aligned} S_E^{\text{example}}[\phi(\mathbf{x},u)] = {} & \frac{1}{2}\int_0^\beta du \int d^3\mathbf{x}\left\{\left(\frac{\partial\phi}{\partial u}\right)^2\right. \\ & \left. + \frac{\nabla\phi\cdot\nabla\phi}{a(t_0)^2} + \widetilde{m}^2(\phi - v)^2\right\}. \end{aligned} \tag{20}$$

After carrying out the path integral, the density matrix is written with $S_E^{\text{example}}[\phi_{\text{cl}}(\mathbf{x},u)]$ which is the action for the classical orbit ϕ_{cl} satisfying the boundary conditions, $\phi_{\text{cl}}(u = 0) = \phi^2, \phi_{\text{cl}}(u = \beta) = \phi^1$. It is given as the functional of the boundary fields ϕ^i $(i = 1, 2)$ and vacuum expectation value v as

$$\langle\phi^1|\rho(t_0)|\phi^2\rangle = \frac{\exp\left[-S_{\text{Ecl}}^{\text{example}}\left[\phi^1,\phi^2\right]\right]}{\int d\phi^1 \exp\left[-S_{\text{Ecl}}^{\text{example}}\left[\phi^1,\phi^1\right]\right]}, \tag{21}$$

where $S_{\text{Ecl}}^{\text{example}}[\phi^1,\phi^2] \simeq S_E^{\text{example}}[\phi_{\text{cl}}(\mathbf{x},u)]$ is given by

$$S^{\text{example}}_{\text{Ecl}}\left[\phi^1,\phi^2\right] = -\frac{a(t_0)^6}{2} \cdot \int \frac{d^3\mathbf{k}}{(2\pi)^3}\left\{\sum_{i=1}^{2}\phi^i(\mathbf{k})\kappa^{ii}(-\mathbf{k})\phi^i(-\mathbf{k}) - \phi^1(\mathbf{k})\kappa^{12}(-\mathbf{k})\phi^2(-\mathbf{k}) - \phi^2(\mathbf{k})\kappa^{21}(-\mathbf{k})\phi^1(-\mathbf{k})\right\} + a(t_0)^6\left\{\sum_{i=1}^{2}\phi^i(0) \cdot \kappa^{ii}(0) - \phi^1(0)\kappa^{12}(0) - \phi^2(0)\kappa^{21}(0)\right\}\nu. \tag{22}$$

In the above expression, we drop the terms which are proportional to ν^2 because they do not contribute to the normalized density matrix. $\kappa^{bd}(\mathbf{k})$ is defined as [14]

$$\begin{aligned}\kappa^{11}(\mathbf{k}) = \kappa^{22}(\mathbf{k}) &:= -\frac{1}{a(t_0)^3}\frac{\omega(\mathbf{k})\cosh\beta\omega(\mathbf{k})}{\sinh\beta\omega(\mathbf{k})},\\ \kappa^{12}(\mathbf{k}) = \kappa^{21}(\mathbf{k}) &:= -\frac{1}{a(t_0)^3}\frac{\omega(\mathrm{k})}{\sinh\beta\omega(\mathbf{k})},\\ \omega(\mathbf{k}) &:= \sqrt{\frac{\mathbf{k}^2}{a(t_0)^2}+\widetilde{m}^2}.\end{aligned} \tag{23}$$

Using the above definitions, one can write the density matrix in (21) as the following form,

$$\left\langle\phi^1\left|\rho(t_0)\right|\phi^2\right\rangle = N\exp\left[\int\sqrt{-g(x)}d^4xJ^a(x) \cdot c^{ab}\phi^b(x) + \frac{1}{2}\int d^4xd^4y\sqrt{-g(x)}\phi^a(x) \cdot c^{ab}K^{bd}(x,y)c^{de}\phi^e(y)\sqrt{-g(y)}\right], \tag{24}$$

with $\phi^1(t_0) = \phi^1$ and $\phi^2(t_0) = \phi^2$. The upper indices a and b are 1 or 2. c^{ab} is the metric of CTP formalism [16] and $c^{11} = -c^{22} = 1$ and $c^{12} = c^{21} = 0$. In the above expression, the source terms J and K do not vanish only at the initial time t_0 and they are given by

$$\begin{aligned}J^b(x) &:= -i\delta\left(x^0-t_0\right)j^b,\\ j^b &= -a_{t_0}^3\kappa^{bd}(\mathbf{k}=0)c^{de}\nu^e,\end{aligned} \tag{25}$$

$$\begin{aligned}K^{bd}(x,y) &:= -i\delta\left(x^0-t_0\right)\delta\left(y^0-t_0\right)\kappa^{bd}(\mathbf{x}-\mathbf{y}),\\ \kappa^{ab}(\mathbf{x}) &= \int\frac{d^3k}{(2\pi)^3}\kappa^{ab}(\mathbf{k})e^{-i\mathbf{k}\cdot\mathbf{x}},\end{aligned} \tag{26}$$

where $\kappa^{ab}(\mathbf{k})$ is given in (23). In (24), N is a normalization constant which is given as

$$\frac{1}{N} = \int d\phi^1\int d\phi^2\delta\left(\phi^1-\phi^2\right) \cdot \exp\left[\int\sqrt{-g(x)}d^4xJ^a(x)c^{ab}\phi^b(x) + \frac{1}{2} \cdot \int d^4xd^4y\sqrt{-g(x)}\phi^a(x)c^{ab}K^{bd}(x,y)c^{de}\phi^e(y) \cdot \sqrt{-g(y)}\right]. \tag{27}$$

3. Two-Particle Irreducible Closed Time Path Effective Action

In this section, we derive the equations of motion, i.e., the Schwinger-Dyson equations (SDEs) for both Green's function and field. SDEs are obtained by taking the variation of 2PI EA with respect to fields and Green's functions, respectively. In addition, we also provide the initial condition for Green's function and field to solve SDEs.

3.1. 2PI Formalism in Curved Space-Time. 2PI CTP EA in curved space-time has been investigated in [17] and their formulations can be applied to the present model. In 2PI formalism, one introduces nonlocal source term denoted as K and local source term denoted as J,

$$e^{iW[J,K]} = \int d\phi\exp\left(i\left[S[\phi,g] + \int\sqrt{-g(x)}d^4xJ_i^a(x)c^{ab}\phi_i^b(x) + \frac{1}{2}\int d^4xd^4y\sqrt{-g(x)} \times \phi_i^a(x)c^{ab}K_{ij}^{bd}(x,y)c^{de}\phi_j^e(y)\sqrt{-g(y)}\right]\right), \tag{28}$$

where $i, j = 1$ or 2 and $S[\phi,g]$ is given by

$$S[\phi,g] = \int d^4x\sqrt{-g(x)} \cdot \left[\frac{1}{2}c^{ab}\left(g^{\mu\nu}\nabla_\mu\phi_i^a\nabla_\nu\phi_i^b - \widetilde{m}_{ii}^2\phi_i^a\phi_i^b\right) + \frac{1}{3}D_{abc}A_{ijk}\phi_i^a\phi_j^b\phi_k^c\right], \tag{29}$$

where $D_{111} = -D_{222} = 1$ and the other components are zero. The upper indices of the field and the source terms distinguish two different time paths in closed time path formalism [16]. One can define the mean fields $\overline{\phi_i^a}$ and Green's function by taking the functional derivative with respect to the source terms J and K, respectively,

$$\overline{\phi}_i^a(x) = \frac{c^{ab}}{\sqrt{-g(x)}}\frac{\delta W[J,K]}{\delta J_i^b(x)}, \quad (30)$$

$$\overline{\phi}_i^a(x)\overline{\phi}_j^e(y) + G_{ij}^{ae}(x,y) = 2\frac{c^{ab}}{\sqrt{-g(x)}}\frac{\delta W[J,K]}{\delta K_{ij}^{bd}(x,y)}\frac{c^{de}}{\sqrt{-g(y)}}. \quad (31)$$

If one sets the source terms to be the ones given in (25) and (26), one can show that the expectation value of the product of the field operators with the initial density operator is related to the Green function and mean fields. Definitely, we can prove the following relations,

$$\overline{\phi}_i^a(x) = \frac{\int d\phi^1 \int d\phi^2 \langle \phi^2 | \phi_i(x) | \phi^1 \rangle \exp\left(-S_{E\mathrm{cl}}[\phi^1,\phi^2]\right)}{\int d\phi^1 \int d\phi^2 \delta(\phi^1-\phi^2)\exp\left(-S_{E\mathrm{cl}}[\phi^1,\phi^2]\right)} \quad (32)$$

$$= \mathrm{Tr}\left[\phi_i(x)\rho(t_0)\right], \quad (33)$$

$$G_{ij}^{12}(x,y) = \frac{\int\int d\phi^1 d\phi^2 \langle \phi^2 | \Phi_j(y)\Phi_i(x) | \phi^1 \rangle e^{-S_{E\mathrm{cl}}[\phi^1,\phi^2]}}{\int\int d\phi^1 d\phi^2 \delta(\phi^2-\phi^1) e^{-S_{E\mathrm{cl}}[\phi^1,\phi^2]}} \quad (34)$$

$$= \mathrm{Tr}\left[\phi_j(y)\phi_i(x)\rho(t_0)\right] - \overline{\phi}_j^2(y)\overline{\phi}_i^1(x), \quad (35)$$

with $\overline{\phi}^a(x) = \overline{\phi}(x)$ and $\Phi(x)$ is a Heisenberg operator which has form as $\Phi(x^0,\mathbf{x}) \equiv \phi(x^0,\mathbf{x}) - \overline{\phi}(x^0)$. With (35), one can write the expectation value of the current as the sum of the contribution from Green's function and the current of the mean fields. Then (14) alters into

$$\langle j_0(x)\rangle = \mathrm{Re}\left[\left(\frac{\partial}{\partial x^0} - \frac{\partial}{\partial y^0}\right) G_{12}^{12}(x,y)\Big|_{y\longrightarrow x} + \overline{\phi}_2^2(x)\overleftrightarrow{\partial_0}\overline{\phi}_1^1(x)\right], \quad (36)$$

where we have used (12) and the following relations

$$G_{ij}^{ab*}(x,y) = \tau^{1ac}G_{ij}^{cd}(x,y)\tau^{1db}, \quad (37)$$

$$\overline{\phi}_i^{a*}(x) = \tau^{1ab}\overline{\phi}_i^b(x), \quad (38)$$

where τ is the Pauli matrix.

The Green's functions and expectation value of fields are derived as solutions of the SDEs which are obtained with 2PI EA. The 2PI EA is related to the generating functional $W[J,K]$ by Legendre transformation as [18, 19]

$$\Gamma_2\left[G,\overline{\phi},g\right] = W[J,K] - \int d^4x\sqrt{-g(x)}J_i^a(x) \cdot c^{ab}\overline{\phi}_i^b(x) - \frac{1}{2}\int d^4x\int d^4y\sqrt{-g(x)}c^{ab}K_{ij}^{bd}(x,y) \cdot c^{de}\left\{\overline{\phi}_i^a(x)\overline{\phi}_j^e(y) + G_{ij}^{ae}(x,y)\right\}\sqrt{-g(y)}. \quad (39)$$

Let us write the 2PI EA Γ_2 in our model, in which we only keep the interaction term up to the first order of cubic interaction, A_{ijk}. It is given as

$$\Gamma_2\left[G,\overline{\phi},g\right] = S\left[\overline{\phi},g\right] + \frac{1}{2}\int d^4x\int d^4y\frac{\delta^2 S\left[\overline{\phi},g\right]}{\delta\overline{\phi}_i^a(x)\delta\overline{\phi}_j^b(y)}G_{ij}^{ab}(x,y) + \frac{i}{2}\mathrm{TrLn}\,G^{-1}, \quad (40)$$

where $S[\overline{\phi},g]$ is the action written in terms of mean fields as

$$S\left[\overline{\phi},g\right] = \int d^4x\sqrt{-g(x)}\left[-\overline{\phi}_i^a\frac{1}{2}c^{ab}\left(\Box + \widetilde{m}_{ii}^2\right)\overline{\phi}_i^b + \frac{1}{3} \cdot D_{abc}A_{ijk}\overline{\phi}_i^a\overline{\phi}_j^b\overline{\phi}_k^c\right] + \frac{1}{2} \cdot \int d^4x\sqrt{-g(x)}\left[\delta\left(x^0-T\right) - \delta\left(x^0-t_0\right)\right]\overline{\phi}_i^a c^{ab}\dot{\overline{\phi}}_i^b. \quad (41)$$

In (40), the interactions are included in the first term as well as in the second term. In the action above, we have also taken into account the surface term at the boundary which corresponds to the last term of (41). T and t_0 in (41) are the upper bound and the lower bound of the time integration, respectively.

3.2. Schwinger Dyson Equations. Now let us derive SDEs for both Green's function and field. These equations can be obtained by taking the variation of the 2PI EA, Γ_2, with respect to the scalar field $\overline{\phi}$ and Green's function G.

In the following, we first derive SDEs for the field. The variation of the 2PI EA in (39) with respect to the scalar field $\overline{\phi}$ leads to

$$\frac{1}{\sqrt{-g(x)}}\frac{\delta\Gamma_2}{\delta\overline{\phi}_i^a(x)} = -c^{ab}J_i^b(x) - \int d^4z\, c^{ab}K_{ij}^{bc}(x,z)\,c^{cd}\sqrt{-g(z)}\overline{\phi}_j^d(z). \quad (42)$$

Using (25) and (26), one computes the right-hand side of the above equation as

$$
\begin{aligned}
& c^{ab} J_i^b(x) + \int d^4 z c^{ab} K_{ij}^{bc}(x,z) c^{cd} \sqrt{-g(z)} \overline{\phi}_j^d(z) \\
& = -i\delta\left(x^0 - t_0\right) \\
& \cdot \left(v_i \widetilde{m}_i \tanh \frac{\beta \widetilde{m}_i}{2} + c^{ab} \kappa_{ii}^{bc}(\mathbf{k}=0) c^{cd} a\left(t_0\right)^3 v_i^d\right) \\
& = 0,
\end{aligned} \tag{43}
$$

where we have used $\kappa^{ab}(\mathbf{k})$ given in (23). The left-hand side of Eq. (42) is computed using (40) and one obtains the following equation of motion of the scalar field $\overline{\phi}$,

$$
\begin{aligned}
& \left(\delta_{ij}\Box + \widetilde{m}_{ij}^2\right) \overline{\phi}_j^d(x) \\
& = c^{da} D_{abc} A_{ijk} \left\{\overline{\phi}_j^b(x) \overline{\phi}_k^c(x) + G_{jk}^{bc}(x,x)\right\},
\end{aligned} \tag{44}
$$

where the Laplacian of Friedman-Lemaître-Robertson-Walker metric is given by

$$
\Box = \nabla_\mu \nabla^\mu = \frac{\partial^2}{\partial x^{02}} - \frac{1}{a\left(x^0\right)^2} \nabla \cdot \nabla + 3\frac{\dot{a}}{a}\frac{\partial}{\partial x^0}. \tag{45}
$$

Next, the equation of motion for Green's function is derived in the following way. The variation of the 2PI EA in (39) with respect to Green's function G leads to

$$
\frac{\delta \Gamma_2}{\delta G_{ij}^{ab}(x,y)} = -\frac{1}{2} c^{ac} \sqrt{-g(x)} K_{ij}^{cd}(x,y) \sqrt{-g(y)} c^{db}. \tag{46}
$$

The left-hand side of the above equation is obtained by taking variation of Eq. (40) with respect to Green's function as,

$$
\begin{aligned}
\frac{\delta \Gamma_2}{\delta G_{ij}^{ab}(x,y)} = & -\frac{i}{2}\left(G^{-1}\right)_{ji}^{ba}(y,x) \\
& + \frac{1}{2} \frac{\delta^2 S\left[\overline{\phi}, g\right]}{\delta \overline{\phi}_i^a(x) \delta \overline{\phi}_j^b(y)},
\end{aligned} \tag{47}
$$

where the second term of above expression is computed using action in (41). Taking all together (46) and (47), one obtains the following two differential equations for Green's function,

$$
\begin{aligned}
& \left(\overrightarrow{\Box}_x + \widetilde{m}_i^2\right) G_{ij}^{ab}(x,y) \\
& = -i\delta_{ij} \frac{c^{ab}}{\sqrt{-g(x)}} \delta(x-y) \\
& + 2c^{ad} D_{dce} A_{ikl} \overline{\phi}_{l,x}^e G_{kj,xy}^{cb} \\
& + \int d^4 z K_{ik}^{ae}(x,z) \sqrt{-g(z)} c^{ef} G_{kj}^{fb}(z,y),
\end{aligned} \tag{48}
$$

$$
\begin{aligned}
& \left(\overleftarrow{\Box}_y + \widetilde{m}_j^2\right) G_{ij}^{ab}(x,y) \\
& = -i\delta_{ij} \delta(x-y) \frac{c^{ab}}{\sqrt{-g(y)}} \\
& + 2G_{ik,xy}^{ac} D_{cef} A_{kjl} \overline{\phi}_{l,y}^f c^{eb} \\
& + \int d^4 z G_{ik}^{ae}(x,z) c^{ef} \sqrt{-g(z)} K_{kj}^{fb}(z,y),
\end{aligned} \tag{49}
$$

where $\Box_x = \nabla_x^\mu \nabla_\mu^x$ and $\Box_y = \nabla_y^\mu \nabla_\mu^y$.

Next, we rescale Green's function, field and coupling constant of interaction as follows:

$$
\overline{\phi}\left(x^0\right) =: \left(\frac{a_{t_0}}{a\left(x^0\right)}\right)^{3/2} \widehat{\varphi}\left(x^0\right), \tag{50}
$$

$$
\begin{aligned}
& G\left(x^0, y^0, \mathbf{k}\right) \\
& =: \left(\frac{a_{t_0}}{a\left(x^0\right)}\right)^{3/2} \widehat{G}\left(x^0, y^0, \mathbf{k}\right) \left(\frac{a_{t_0}}{a\left(y^0\right)}\right)^{3/2},
\end{aligned} \tag{51}
$$

$$
\widehat{A}\left(x^0\right) := \left(\frac{a_{t_0}}{a\left(x^0\right)}\right)^{3/2} A, \tag{52}
$$

where a_{t_0} stands for the initial value for the scale factor and we have defined $a_{t_0} := a(t_0)$ and we have used Fourier transformation for Green's function as

$$
G\left(x^0, y^0, \mathbf{k}\right) = \int d^3\mathbf{r}\, G\left(x^0, \mathbf{r}, y^0, 0\right) e^{i\mathbf{k}\cdot\mathbf{r}}. \tag{53}
$$

By using these new definitions, SDEs in (44) are written as

$$
\begin{aligned}
& \left[\frac{\partial^2}{\partial x^{02}} + \overline{m}_i^2\left(x^0\right)\right] \widehat{\varphi}_i^d\left(x^0\right) \\
& = c^{da} D_{abc} \widehat{A}_{ijk}\left(x^0\right) \left\{\widehat{\varphi}_j^b\left(x^0\right) \widehat{\varphi}_k^c\left(x^0\right) + \widehat{G}_{jk}^{bc}(x,x)\right\}.
\end{aligned} \tag{54}
$$

Next SDEs for the rescaled Green's function in (48) and (49) are written as

$$\left[\frac{\partial^2}{\partial x^{0\,2}} + \Omega_{i,\mathbf{k}}^2\left(x^0\right)\right]\widehat{G}^{ab}_{ij,x^0y^0}(\mathbf{k}) = 2c^{ad}D_{dce}\widehat{A}_{ikl,x^0}\widehat{\varphi}^{e}_{l,x^0}\widehat{G}^{cb}_{kj,x^0y^0}(\mathbf{k}) - i\delta_{ij}\delta_{x^0y^0}\frac{c^{ab}}{a_{t_0}^3} - i\delta_{t_0x^0}\kappa^{ae}_{ik}(\mathbf{k})\,a_{t_0}^3c^{ef}\widehat{G}^{fb}_{kj,t_0y^0}(\mathbf{k}), \tag{55}$$

$$\left[\frac{\partial^2}{\partial y^{0\,2}} + \Omega_{i,\mathbf{k}}^2\left(y^0\right)\right]\widehat{G}^{ab}_{ij,x^0y^0}(\mathbf{k}) = 2\widehat{G}^{ac}_{ik,x^0y^0}(\mathbf{k})\,D_{cef}\widehat{A}_{kjl,y^0}\widehat{\varphi}^{f}_{l,y^0}c^{eb} - i\delta_{ij}\delta_{x^0y^0}\frac{c^{ab}}{a_{t_0}^3} - i\widehat{G}^{ae}_{ik,x^0t_0}(\mathbf{k})\,c^{ef}a_{t_0}^3\kappa^{fb}_{kj}(\mathbf{k})\,\delta_{t_0y^0}, \tag{56}$$

where we have defined

$$\Omega_{i,\mathbf{k}}^2\left(x^0\right) := \frac{\mathbf{k}^2}{a\left(x^0\right)^2} + \overline{m}_i^2\left(x^0\right), \tag{57}$$

$$\overline{m}_i^2\left(x^0\right) := \widetilde{m}_i^2\left(x^0\right) - \frac{3}{2}\left(\frac{\ddot{a}\left(x^0\right)}{a\left(x^0\right)}\right) - \frac{3}{4}\left(\frac{\dot{a}\left(x^0\right)}{a\left(x^0\right)}\right)^2. \tag{58}$$

Note that the first derivative with respect to time which is originally presented in the expression of Laplacian (45) is now absent in the expression of SDEs for the rescaled fields and Green's functions.

3.3. The Initial Condition for Green's Function and Field. In this subsection, the initial conditions for Green's function and field are determined. For simplicity, let us look back to example model for one real scalar field. We first compute the initial condensation of the field $\overline{\phi}(t_0) = \widehat{\varphi}(t_0)$ (see (50)). Using (32) and setting $x^0 = t_0$, we compute it as follows:

$$\begin{aligned}\overline{\phi}(t_0) \equiv \langle\phi(t_0,\mathbf{x})\rangle &:= \frac{\int d\phi\,\phi(t_0,\mathbf{x})\exp\left[-S^{\text{example}}_{\text{Ecl}}[\phi,\phi]\right]}{\int d\phi\exp\left[-S^{\text{example}}_{\text{Ecl}}[\phi,\phi]\right]} \\ &= \frac{\int d\phi\,\phi(\mathbf{x})\exp\left[-(1/2)\int d^3\mathbf{x}d^3\mathbf{y}\phi(\mathbf{x})D(\mathbf{x}-\mathbf{y})\phi(\mathbf{y}) + 2a_{t_0}^3\int d^3\mathbf{x}\phi(\mathbf{x})\,j^1\right]}{\int d\phi\exp\left[-(1/2)\int d^3\mathbf{x}d^3\mathbf{y}\phi(\mathbf{x})D(\mathbf{x}-\mathbf{y})\phi(\mathbf{y}) + 2a_{t_0}^3\int d^3\mathbf{x}\phi(\mathbf{x})\,j^1\right]},\end{aligned} \tag{59}$$

where we have computed the last term of (22) using (25) and $D(\mathbf{r})$ is defined as [14]

$$D(\mathbf{r}) = 2a_{t_0}^3\int\frac{d^3\mathbf{k}}{(2\pi)^3}\frac{\omega(\mathbf{k})\left(\cosh\beta\omega(\mathbf{k})-1\right)}{\sinh\beta\omega(\mathbf{k})}e^{-i\mathbf{r}\cdot\mathbf{k}}. \tag{60}$$

To proceed the calculation, we denote $J(\mathbf{x})$ as $J(\mathbf{x}) = 2a_{t_0}^3 j^1$. Then the initial condensation of field $\langle\phi(t_0,\mathbf{x})\rangle$ is given by

$$\langle\phi(t_0,\mathbf{x})\rangle = \frac{\int d\phi'(\mathbf{x})\left\{\phi'(\mathbf{x}) + \int d^3\mathbf{z}D^{-1}(\mathbf{x}-\mathbf{z})J(\mathbf{z})\right\}\exp\left[-(1/2)\int d^3\mathbf{x}d^3\mathbf{y}\phi'(\mathbf{x})D(\mathbf{x}-\mathbf{y})\phi'(\mathbf{y})\right]}{\int d\phi'(\mathbf{x})\exp\left[-(1/2)\int d^3\mathbf{x}d^3\mathbf{y}\phi'(\mathbf{x})D(\mathbf{x}-\mathbf{y})\phi'(\mathbf{y})\right]} = v, \tag{61}$$

where we have defined $\phi'(\mathbf{x}) = \phi(\mathbf{x}) - \int d^3\mathbf{z}D^{-1}(\mathbf{z}-\mathbf{x})J(\mathbf{z})$ and $D^{-1}(\mathbf{z}-\mathbf{x})$ satisfies

$$\int d^3\mathbf{x}D^{-1}(\mathbf{z}-\mathbf{x})\,D(\mathbf{x}-\mathbf{y}) = \delta(\mathbf{z}-\mathbf{y}). \tag{62}$$

Next we will compute the initial condition for Green's function $G(t_0,t_0,\mathbf{k}) = \widehat{G}(t_0,t_0,\mathbf{k})$ (see (51)). By using (34) and setting $x^0 = t_0$ and $y^0 = t_0$, one computes it as follows:

$$\begin{aligned}G^{ab}(t_0,\mathbf{x},t_0,\mathbf{y}) &= \frac{\int\int d\phi^1d\phi^2\left\langle\phi^2\left|\Phi(t_0,\mathbf{y})\Phi(t_0,\mathbf{x})\right|\phi^1\right\rangle\exp\left[-S^{\text{example}}_{\text{Ecl}}\left[\phi^1,\phi^2\right]\right]}{\int d\phi\exp\left[-S^{\text{example}}_{\text{Ecl}}[\phi,\phi]\right]} \\ &= \frac{\int d\phi'\,\phi'(\mathbf{y})\,\phi'(\mathbf{x})\exp\left[-(1/2)\int d^3\mathbf{x}d^3\mathbf{y}\phi'(\mathbf{x})D(\mathbf{x}-\mathbf{y})\phi'(\mathbf{y})\right]}{\int d\phi'\exp\left[-(1/2)\int d^3\mathbf{x}d^3\mathbf{y}\phi'(\mathbf{x})D(\mathbf{x}-\mathbf{y})\phi'(\mathbf{y})\right]}, \\ &= D^{-1}(\mathbf{y}-\mathbf{x}).\end{aligned} \tag{63}$$

Using (53) and (60), (63) becomes

$$G^{ab}(t_0,t_0,\mathbf{k}) = D^{-1}(\mathbf{k}) = \frac{1}{2\omega(\mathbf{k})a_{t_0}^3}\left[\frac{\sinh\beta\omega(\mathbf{k})}{\cosh\beta\omega(\mathbf{k})-1}\right]. \tag{64}$$

The above results with the example model can be extended to our model and we summarize them as

$$\widehat{G}^{ab}_{ij,t_0t_0}(\mathbf{k}) = \delta_{ij}\frac{1}{2\omega_i(\mathbf{k})a_{t_0}^3}\left[\frac{\sinh\beta\omega_i(\mathbf{k})}{\cosh\beta\omega_i(\mathbf{k})-1}\right], \tag{65}$$

$$\widehat{\varphi}^a_i(t_0) = v_i. \tag{66}$$

Next we derive the time derivative of the field and Green's function at the initial time t_0. First we integrate the field equation in (54) with respect to time. By setting $x^0 = t_0$, we obtain

$$\left.\frac{\partial\widehat{\varphi}_{i,x^0}}{\partial x^0}\right|_{x^0=t_0} = 0. \tag{67}$$

Similarly, we integrate (55) with respect to time x^0. By setting both x^0 and y^0 equal to t_0, we obtain the following initial condition

$$\lim_{x^0\to t_0}\frac{\partial}{\partial x^0}\widehat{G}^{ab}_{ij,x^0t_0}(\mathbf{k}) = -i\delta_{ij}\frac{c^{ab}}{a_{t_0}^3} - i\kappa^{ae}_{ik}(\mathbf{k})a_{t_0}^3c^{ef}\widehat{G}^{fb}_{kj,t_0t_0}(\mathbf{k}). \tag{68}$$

Finally, we integrate (56) with respect to time y^0. By setting both x^0 and y^0 equal to t_0, we obtain another initial condition,

$$\lim_{y^0\to t_0}\frac{\partial}{\partial y^0}\widehat{G}^{ab}_{ij,t_0y^0}(\mathbf{k}) = -i\delta_{ij}\frac{c^{ab}}{a_{t_0}^3} - i\widehat{G}^{ae}_{ik,t_0t_0}(\mathbf{k})c^{ef}a_{t_0}^3\kappa^{fb}_{kj}(\mathbf{k}). \tag{69}$$

4. The Expectation Value of PNA

The SDEs obtained in the previous section allow us to write the solutions for both Green's functions and fields in the form of integral equations. In this section, we present the correction to the expectation value of the PNA up to the first order contribution with respect to the cubic interaction. For this purpose, in Subsection 4.1, we show how one analytically obtains the solutions of SDEs. We write down the solutions up to the first order of the cubic interaction. In the Subsection 4.2, we also write the expectation value of the PNA up to the first order of the cubic interaction and investigate it by taking into account of the time dependence of the scale factor.

4.1. The Solution of Green's Function and Fields including $o(A)$ Corrections. The SDEs in present work are inhomogeneous differential equations of the second order. To solve the differential equation, the variation of constants method is used. With the method, the solutions of SDEs are written in the form of integral equations. We solve the integral equation perturbatively and the solutions up to the first order of the cubic interaction are obtained. We first write the solutions of fields as

$$\widehat{\varphi}^d_{i,x^0} = \widehat{\varphi}^{d,\text{free}}_{i,x^0} + \widehat{\varphi}^{d,o(A)}_{i,x^0}, \tag{70}$$

$$\widehat{\varphi}^{d,\text{free}}_{i,x^0} = -\overline{K}'_{i,x^0t_0}\widehat{\varphi}^d_{i,t_0}, \tag{71}$$

$$\widehat{\varphi}^{d,o(A)}_{i,x^0} = \int_{t_0}^{x^0}\overline{K}_{i,x^0t}c^{da}D_{abc}\widehat{A}_{ijk}(t)\cdot\left\{\widehat{\varphi}^{b,\text{free}}_j(t)\widehat{\varphi}^{c,\text{free}}_k(t) + \int\frac{d^3k}{(2\pi)^3}\widehat{G}^{bc,\text{free}}_{jk,tt}(\mathbf{k})\right\}dt, \tag{72}$$

where $\widehat{\varphi}^{\text{free}}$ denotes the free part contribution while $\widehat{\varphi}^{o(A)}$ is the contribution due to the first order of the cubic interaction. In Appendix A.2, (70)-(72) are derived in detail. $\overline{K}_{i,x^0y^0} := \overline{K}_{i,x^0y^0,\mathbf{k}=\mathbf{0}}$ and $\overline{K}_{i,x^0y^0,\mathbf{k}}$ is defined by

$$\overline{K}_{i,x^0y^0,\mathbf{k}} := \frac{1}{W_{i,\mathbf{k}}}\left\{f_{i,\mathbf{k}}(x^0)g_{i,\mathbf{k}}(y^0) - g_{i,\mathbf{k}}(x^0)f_{i,\mathbf{k}}(y^0)\right\}, \tag{73}$$

where $W_{i,\mathbf{k}}$ is defined as

$$W_{i,\mathbf{k}} := \dot{f}_{i,\mathbf{k}}(x^0)g_{i,\mathbf{k}}(x^0) - f_{i,\mathbf{k}}(x^0)\dot{g}_{i,\mathbf{k}}(x^0). \tag{74}$$

$f_{i,\mathbf{k}}$ and $g_{i,\mathbf{k}}$ are the solutions which satisfy the following homogeneous differential equations:

$$\left[\frac{\partial^2}{\partial x^{0\,2}} + \Omega^2_{i,\mathbf{k}}(x^0)\right]f_{i,\mathbf{k}}(x^0) = 0, \tag{75}$$

$$\left[\frac{\partial^2}{\partial x^{0\,2}} + \Omega^2_{i,\mathbf{k}}(x^0)\right]g_{i,\mathbf{k}}(x^0) = 0, \tag{76}$$

where $\Omega^2_{i,\mathbf{k}}(x^0)$ is given in (57). In Appendix B, $f_{i,\mathbf{k}}$ and $g_{i,\mathbf{k}}$ are derived in detail. $\overline{K'}_{i,x^0y^0} := \overline{K'}_{i,x^0y^0,\mathbf{k}=0}$ and $\overline{K'}_{i,x^0y^0,\mathbf{k}}$ is also defined as follows:

$$\overline{K'}_{i,x^0y^0,\mathbf{k}} := \frac{\partial\overline{K}_{i,x^0y^0,\mathbf{k}}}{\partial y^0}. \tag{77}$$

Next we write down the solution of Green's function as follows:

$$\widehat{G}^{ab}_{ij,x^0y^0}(\mathbf{k}) = \widehat{G}^{ab,\text{free}}_{ij,x^0y^0}(\mathbf{k}) + \widehat{G}^{ab,o(A)}_{ij,x^0y^0}(\mathbf{k}), \tag{78}$$

$$\begin{aligned}\widehat{G}^{ab,\text{free}}_{ij,x^0y^0}(\mathbf{k}) &= \frac{\delta_{ij}}{2\omega_{i,\mathbf{k}}a_{t_0}^3}\coth\frac{\beta\omega_{i,\mathbf{k}}}{2}\begin{pmatrix}1 & 1\\ 1 & 1\end{pmatrix}^{ab}\\ &\cdot\left[\overline{K}'_{i,x^0t_0,\mathbf{k}}\overline{K}'_{i,y^0t_0,\mathbf{k}} + \omega^2_{i,\mathbf{k}}\overline{K}_{i,x^0t_0,\mathbf{k}}\overline{K}_{y^0t_0,\mathbf{k}}\right] + \frac{i\delta_{ij}}{2a_{t_0}^3}\\ &\cdot\overline{K}_{i,x^0y^0,\mathbf{k}}\left\{\epsilon^{ab} + c^{ab}\left(\theta(y^0-x^0) - \theta(x^0-y^0)\right)\right\},\end{aligned} \tag{79}$$

where ϵ^{ab} is an antisymmetric tensor and its nonzero components are given as $\epsilon^{12} = 1$ while $\theta(t)$ denotes a unit step function,

$$\widehat{G}^{ab,o(A)}_{ij,x^0y^0}(\mathbf{k}) = \int_{t_0}^{y^0} R^{ab,o(A)}_{ij,x^0t,\mathbf{k}} \overline{K}_{j,y^0t,\mathbf{k}} dt + \int_{t_0}^{x^0} \overline{K}_{i,x^0t,\mathbf{k}} Q^{ac,o(A)}_{ij,tt_0,\mathbf{k}} \left(E^{T,cb}_{jj,\mathbf{k}} \overline{K}_{j,y^0t_0,\mathbf{k}} - \overline{K}'_{j,y^0t_0,\mathbf{k}} \delta^{cb} \right) dt, \tag{80}$$

where $Q^{o(A)}$, $R^{o(A)}$, and $E_{\mathbf{k}}$ are given as

$$Q^{ab,o(A)}_{ij,x^0y^0,\mathbf{k}} = 2c^{ad} D_{dce} \widehat{A}_{ikl,x^0} \widehat{\varphi}^{e,\mathrm{free}}_{l,x^0} \widehat{G}^{cb,\mathrm{free}}_{kj,x^0y^0}(\mathbf{k}), \tag{81}$$

$$R^{ab,o(A)}_{ij,x^0y^0,\mathbf{k}} = 2\widehat{G}^{ac,\mathrm{free}}_{ik,x^0y^0}(\mathbf{k}) D_{cef} \widehat{A}_{kjl,y^0} \widehat{\varphi}^{f,\mathrm{free}}_{l,y^0} c^{eb}, \tag{82}$$

$$E^{ac}_{ik,\mathbf{k}} = -i\kappa^{ae}_{ik}(\mathbf{k}) a^3_{t_0} c^{ec}, \tag{83}$$

and $\kappa^{ab}_{ij}(\mathbf{k})$ is given in (23). In Appendices A.4 and A.5, we derive (79) and (80) in detail, respectively.

4.2. The Expectation Value of PNA including $o(A)$ Corrections and the First Order of the Hubble Parameter. Next we compute the PNA in (36) including the first order correction with respect to A ($o(A)$) and the effect of expansion up to the first order of the Hubble parameter. By using rescaled fields, Green's function, and coupling constant in (50)-(52), one can write down total contribution to the expectation value of PNA with order $o(A)$ corrections as

$$\begin{aligned}
\left(\frac{a(x^0)}{a_{t_0}}\right)^3 \langle j_0(x^0)\rangle &= \mathrm{Re}\left[\widehat{\varphi}^{1,\mathrm{free}}_2(x^0)\dot{\widehat{\varphi}}^{1*,\mathrm{free}}_1(x^0) - \widehat{\varphi}^{1,\mathrm{free}}_1(x^0)\dot{\widehat{\varphi}}^{1*,\mathrm{free}}_2(x^0)\right] \\
&+ \int \frac{d^3\mathbf{k}}{(2\pi)^3}\left(\frac{\partial}{\partial x^0} - \frac{\partial}{\partial y^0}\right)\mathrm{Re}\left[\widehat{G}^{12,o(A)}_{12}(x^0,y^0,\mathbf{k})\right]\Big|_{y^0\to x^0} \\
&+\mathrm{Re}\left[\widehat{\varphi}^{1,\mathrm{free}}_2(x^0)\dot{\widehat{\varphi}}^{1*,o(A)}_1(x^0) - \widehat{\varphi}^{1,\mathrm{free}}_1(x^0)\dot{\widehat{\varphi}}^{1*,o(A)}_2(x^0)\right] \\
&+\mathrm{Re}\left[\widehat{\varphi}^{1,o(A)}_2(x^0)\dot{\widehat{\varphi}}^{1*,\mathrm{free}}_1(x^0) - \widehat{\varphi}^{1,o(A)}_1(x^0)\dot{\widehat{\varphi}}^{1*,\mathrm{free}}_2(x^0)\right]
\end{aligned} \tag{84}$$

The first line of the above equation is the zeroth order of the cubic interaction while the next three terms are the first order.

As was indicated previously, we will further investigate the expectation value of the PNA for the case of time-dependent scale factor. For that purpose, one can expand scale factor around t_0 for $0 < t_0 \leqslant x^0$ as follows:

$$\begin{aligned}
a(x^0) &= a(t_0) + (x^0 - t_0)\dot{a}(t_0) + \frac{1}{2}(x^0 - t_0)^2 \ddot{a}(t_0) + \dots \\
&= a^{(0)} + a^{(1)}(x^0) + a^{(2)}(x^0) + \dots.
\end{aligned} \tag{85}$$

We first assume that $a^{(n+1)}(x^0) < a^{(n)}(x^0)$ when x^0 is near t_0. Then one can keep only the following terms:

$$a(x^0) \simeq a^{(0)} + a^{(1)}(x^0), \tag{86}$$

and $a^{(n)}(x^0)$ for ($n \geqslant 2$) are set to be zero. $a^{(0)}$ corresponds to the constant scale factor and $a^{(1)}(x^0)$ corresponds to linear Hubble parameter $H(t_0)$. Thus it can be written as

$$\frac{a(x^0)}{a(t_0)} = 1 + (x^0 - t_0) H(t_0), \tag{87}$$

where $H(t_0)$ is given by

$$H(t_0) = \frac{\dot{a}(t_0)}{a(t_0)}, \tag{88}$$

and $t_0 > 0$. Throughout this study, we only keep first order of $H(t_0)$ as the first nontrivial approximation. For the case that Hubble parameter is positive, it corresponds to the case for the expanding universe. Under this situation, $\dot{a}(x^0) = a(t_0)H(t_0)$ and $\ddot{a}(x^0) = 0$.

Now let us briefly go back to (58). With these approximations, the second term of (58) is apparently vanished. Since $\dot{a}(x^0)$ is proportional to linear $H(t_0)$, the third term of (58) involves second order of $H(t_0)$. Hence, one can neglect it and the Riemann curvature $R(x^0)$ in (3) is also vanished. Therefore, $\overline{m}^2_i(x^0)$ is simply written as $\widetilde{m}^2_i$. Now $\widetilde{m}^2_i$ are given as

$$\widetilde{m}^2_1 = m^2_\phi - B^2, \tag{89}$$

$$\widetilde{m}^2_2 = m^2_\phi + B^2, \tag{90}$$

$$\widetilde{m}^2_3 = m^2_N. \tag{91}$$

Next we define $\omega_{i,\mathbf{k}}$ as

$$\omega_{i,\mathbf{k}} := \sqrt{\frac{\mathbf{k}^2}{a^2_{t_0}} + \widetilde{m}^2_i}. \tag{92}$$

We consider $\Omega_{i,\mathbf{k}}(x^0)$ defined in (57). One can expand it around time t_0 as

$$\begin{aligned}\Omega_{i,\mathbf{k}}\left(x^0\right) &\simeq \omega_{i,\mathbf{k}} + \left(x^0 - t_0\right)\frac{\partial}{\partial x^0}\Omega_{i,\mathbf{k}}\left(x^0\right)\Big|_{x^0=t_0} \\ &= \omega_{i,\mathbf{k}}\left\{1 - H\left(t_0\right)\left(x^0 - t_0\right)\frac{\mathbf{k}^2}{\left[a\left(t_0\right)\omega_{i,\mathbf{k}}\left(t_0\right)\right]^2}\right\}.\end{aligned} \tag{93}$$

Now let us investigate the expectation value of PNA under these approximations. For the case that $\widehat{\varphi}_{1,t_0} = \widehat{\varphi}_{2,t_0} = 0$ and $\widehat{\varphi}_{3,t_0} \neq 0$, the nonzero contribution to the expectation value of PNA comes only from $o(A)$ corrections to Green's function. From (84), we can obtain

$$\begin{aligned}\left\langle j_0\left(x^0\right)\right\rangle &= \frac{2}{a\left(x^0\right)^3}\widehat{\varphi}_{3,t_0}\int\frac{d^3\mathbf{k}}{(2\pi)^3}\int_{t_0}^{x^0}\widehat{A}_{123,t}\left(-\overline{K}'_{3,tt_0,\mathbf{0}}\right)\left[\left\{\frac{1}{2\omega_{2,\mathbf{k}}\left(t_0\right)}\times\coth\frac{\beta\omega_{2,\mathbf{k}}\left(t_0\right)}{2}\right.\right. \\ &\quad\cdot\left.\left[\left(\dot{\overline{K}}_{1,x^0t,\mathbf{k}}\overline{K}'_{2,x^0t_0,\mathbf{k}} - \overline{K}_{1,x^0t,\mathbf{k}}\dot{\overline{K}}'_{2,x^0t_0,\mathbf{k}}\right)\overline{K}'_{2,tt_0,\mathbf{k}} + \omega^2_{2,\mathbf{k}}\left(t_0\right)\left(\dot{\overline{K}}_{1,x^0t,\mathbf{k}}\overline{K}_{2,x^0t_0,\mathbf{k}} - \overline{K}_{1,x^0t,\mathbf{k}}\dot{\overline{K}}_{2,x^0t_0,\mathbf{k}}\right)\overline{K}_{2,tt_0,\mathbf{k}}\right]\right\} - \{1 \\ &\quad\left.\longleftrightarrow 2\text{ for lower indices}\}\right]dt,\end{aligned} \tag{94}$$

where we have used (71) and (80). Following the expression of the scale factor in (87), $\overline{K}$ is also divided into the part of the constant scale factor and the part which is proportional to $H(t_0)$. In Appendix C, $\overline{K}$ and its derivative are derived in detail. In the above expression, $H(t_0)$ is also included in $\widehat{A}(t)$. Since we are interested in the PNA up to the first order of $H(t_0)$, we expand it as follows:

$$\widehat{A}(t) \simeq A\left\{1 - \frac{3}{2}\left(t - t_0\right)H\left(t_0\right)\right\}. \tag{95}$$

Furthermore, substituting (87), (95) and $\overline{K}$ and its derivative in (C.7), (C.8), (C.11)-(C.16) into Eq. (94), one can divide the PNA into two parts,

$$\left\langle j_0\left(x^0\right)\right\rangle = \left\langle j_0\left(x^0\right)\right\rangle_{1\text{st}} + \left\langle j_0\left(x^0\right)\right\rangle_{2\text{nd}}, \tag{96}$$

$$\begin{aligned}\left\langle j_0\left(x^0\right)\right\rangle_{1\text{st}} &= \frac{2\widehat{\varphi}_{3,t_0}A_{123}}{a^3_{t_0}}\int\frac{d^3\mathbf{k}}{(2\pi)^3}\int_{t_0}^{x^0}\left\{1 - 3\left(x^0 - t_0\right)H\left(t_0\right) - \frac{3}{2}\left(t - t_0\right)H\left(t_0\right)\right\}\times\left[\left\{\frac{\left(-\overline{K}^{(0)\prime}_{3,tt_0,\mathbf{0}}\right)}{2\omega_{2,\mathbf{k}}\left(t_0\right)}\coth\frac{\beta\omega_{2,\mathbf{k}}\left(t_0\right)}{2}\left[\left(\overline{K}^{(0)\prime}_{2,x^0t_0,\mathbf{k}}\overleftrightarrow{\partial}\overline{K}^{(0)}_{1,x^0t,\mathbf{k}}\right)\overline{K}^{(0)\prime}_{2,tt_0,\mathbf{k}}\right.\right.\right. \\ &\quad\left.\left.+\,\omega^2_{2,\mathbf{k}}\left(t_0\right)\left(\overline{K}^{(0)}_{2,x^0t_0,\mathbf{k}}\overleftrightarrow{\partial}\overline{K}^{(0)}_{1,x^0t,\mathbf{k}}\right)\overline{K}^{(0)}_{2,tt_0,\mathbf{k}}\right]\right\} - \{1\longleftrightarrow 2\text{ for lower indices}\}\Bigg]dt,\end{aligned} \tag{97}$$

$$\begin{aligned}\left\langle j_0\left(x^0\right)\right\rangle_{2\text{nd}} &= \frac{2\widehat{\varphi}_{3,t_0}A_{123}}{a^3_{t_0}}\int\frac{d^3\mathbf{k}}{(2\pi)^3}\int_{t_0}^{x^0}\left[\left\{\frac{\left(-\overline{K}^{(0)\prime}_{3,tt_0,\mathbf{0}}\right)}{2\omega_{2,\mathbf{k}}\left(t_0\right)}\coth\frac{\beta\omega_{2,\mathbf{k}}\left(t_0\right)}{2}\right.\right. \\ &\quad\times\left[\left(\overline{K}^{(0)\prime}_{2,x^0t_0,\mathbf{k}}\overleftrightarrow{\partial}\overline{K}^{(0)}_{1,x^0t,\mathbf{k}}\right)\overline{K}^{(1)\prime}_{2,tt_0,\mathbf{k}} + \left(\overline{K}^{(1)\prime}_{2,x^0t_0,\mathbf{k}}\overleftrightarrow{\partial}\overline{K}^{(0)}_{1,x^0t,\mathbf{k}} + \overline{K}^{(0)\prime}_{2,x^0t_0,\mathbf{k}}\overleftrightarrow{\partial}\overline{K}^{(1)}_{1,x^0t,\mathbf{k}}\right)\overline{K}^{(0)\prime}_{2,tt_0,\mathbf{k}} + \omega^2_{2,\mathbf{k}}\left(t_0\right)\left[\left(\overline{K}^{(0)}_{2,x^0t_0,\mathbf{k}}\overleftrightarrow{\partial}\overline{K}^{(0)}_{1,x^0t,\mathbf{k}}\right)\overline{K}^{(1)}_{2,tt_0,\mathbf{k}} + \left(\overline{K}^{(1)}_{2,x^0t_0,\mathbf{k}}\overleftrightarrow{\partial}\overline{K}^{(0)}_{1,x^0t,\mathbf{k}} + \overline{K}^{(0)}_{2,x^0t_0,\mathbf{k}}\overleftrightarrow{\partial}\overline{K}^{(1)}_{1,x^0t,\mathbf{k}}\right)\overline{K}^{(0)}_{2,tt_0,\mathbf{k}}\right]\right]\Bigg\} \\ &\quad - \{1\longleftrightarrow 2\text{ for lower indices}\}\Bigg]dt,\end{aligned} \tag{98}$$

and the derivative $\overleftrightarrow{\partial}$ acts on the first argument of $\overline{K}$ and is defined as follows:

$$\begin{aligned}\overline{K}_{2,x^0t,\mathbf{k}}\overleftrightarrow{\partial}\overline{K}_{1,x^0t,\mathbf{k}} &= \overline{K}_{2,x^0t,\mathbf{k}}\left(\frac{\partial}{\partial x^0}\overline{K}_{1,x^0t,\mathbf{k}}\right) \\ &\quad - \left(\frac{\partial}{\partial x^0}\overline{K}_{2,x^0t,\mathbf{k}}\right)\overline{K}_{1,x^0t,\mathbf{k}}.\end{aligned} \tag{99}$$

Each term of the PNA shown in (97) and (98) can be understood as follows. The first term is the PNA with the constant scale factor. The second term with a prefactor $-3H(t_0)(x^0 - t_0)(1/a^3_{t_0}) \simeq 1/a(x^0)^3 - 1/a^3_{t_0}$ is called the dilution effect. The third term with a prefactor $-(3/2)A_{123}(t-t_0)H(t_0) \simeq \widehat{A}_{123}(t) - A_{123}$ is called the freezing interaction effect. The fourth term which corresponds to $\langle j_0(x^0)\rangle_{2\text{nd}}$ is called the redshift effect. Below we explain their physical origins. The dilution of the PNA is caused by the increase of the volume of the universe. The origin of the freezing interaction effect can be understood with (95). It implies that the strength of the cubic interaction $\widehat{A}(t)$ controlling the size of PNA decreases as the scale factor grows. The origin of the redshift can be explained as follows. As shown in (57), as the scale factor grows, the physical wavelength becomes large. Therefore, the momentum and the energy of the particles become small. Note that this effect does not apply to the zero-mode such as condensate which is homogeneous and is a constant in the space.

Before closing this section, we compute the production rate of the PNA per unit time which is a useful expression when we understand the numerical results of the PNA. We compute the time derivative of the PNA for the case of the constant scale factor $H_{t_0} = 0$. By setting $H_{t_0} = 0$, one obtains it at the initial time $x^1 = x^0 - t_0 = 0$,

$$\begin{aligned}\frac{\partial}{\partial x^1}\left\langle j_0\left(x^1+t_0\right)\right\rangle\Big|_{x^1=0} &= \frac{v_3 A_{123}}{a_{t_0}^3} \\ &\cdot \int_0^\infty \frac{k^2 dk}{2\pi^2}\frac{1}{\omega_{1,\mathbf{k}}\omega_{2,\mathbf{k}}} \times \left[\left(n_2-n_1\right)\left(\omega_{1,\mathbf{k}}+\omega_{2,\mathbf{k}}\right)\right. \\ &\left. + \left(n_2+n_1+1\right)\left(\omega_{1,\mathbf{k}}-\omega_{2,\mathbf{k}}\right)\right],\end{aligned} \tag{100}$$

where n_i is the distribution functions for the Bose particles,

$$n_i = \frac{e^{-\beta\omega_{i,\mathbf{k}}}}{1-e^{-\beta\omega_{i,\mathbf{k}}}}, \quad (i=1,2). \tag{101}$$

In Appendix D, we derive (100) in detail. Because we assume $\widetilde{m}_1 < \widetilde{m}_2$, one obtains inequality $n_2 < n_1$. From the expression above, the production rate of PNA at the initial time is negative for $v_3 A_{123} > 0$. One also finds the rate is logarithmically divergent for the momentum ($\mathbf{k}$) integration,

$$\begin{aligned}&\frac{\partial}{\partial x^1}\left\langle j_0\left(x^1+t_0\right)\right\rangle\Bigg|_{x^1=0}^{\text{divergent}} \\ &\simeq \frac{v_3 A_{123}}{2\pi^2 a_{t_0}^3}\frac{\widetilde{m}_1^2-\widetilde{m}_2^2}{2}\log\left(\frac{k_{\max}}{\mu}\right),\end{aligned} \tag{102}$$

where $\mu = O(\widetilde{m}_i)$ $(i = 1,2)$ and $k_{\max}$ is an ultraviolet cut off for the momentum integration. With the expression, one expects that for the positive $v_3 A_{123}$, the PNA becomes negative from zero just after the initial time and the behavior will be confirmed in the numerical simulation.

5. Numerical Results

In this section, we numerically study the time dependence of the PNA. The PNA depends on the parameters of the model such as masses and coupling constants. It also depends on the initial conditions and the expansion rates of the universe. Since the PNA is linearly proportional to the coupling constant A_{123} and the initial value of the field $\widehat{\varphi}_{3,t_0}$, we can set these parameters as unity in the unit of energy and later on one can multiply their values. As for the initial scale factor a_{t_0}, without loss of generality, one can set this dimensionless factor as unity. For the other parameters of the model, we choose $\widetilde{m}_2$, B, and $\omega_{3,\mathbf{0}} = \widetilde{m}_3$ as independent parameters since the mass $\widetilde{m}_1$ is written as

$$\widetilde{m}_1^2 = \widetilde{m}_2^2 - 2B^2. \tag{103}$$

The temperature T and the expansion rate $H(t_0)$ determine the environment for the universe. The former determines the thermal distribution of the scalar fields. Within the approximation for the time dependence of the scale factor in (87), $H(t_0)$ is the only parameter which controls the expansion rate of the universe. The approximation is good for the time range which satisfies the following inequality:

$$x^0 - t_0 \ll \frac{1}{3H\left(t_0\right)}. \tag{104}$$

The time dependence of PNA is plotted as a function of the dimensionless time defined as

$$t = \omega_{3,\mathbf{0}}^r\left(x^0 - t_0\right), \tag{105}$$

where $\omega_{3,\mathbf{0}}^r$ is a reference frequency. In terms of the dimensionless time, the condition of (104) is written as

$$t \ll t_{\max} \equiv \frac{\omega_{3,\mathbf{0}}^r}{3H\left(t_0\right)}. \tag{106}$$

How the PNA behaves with respect to time is discussed in the following Subsections 5.1–5.3. The results, as will be shown later, revealed that the PNA has an oscillatory behavior. We also investigate the parameter dependence for two typical cases, one of which corresponds to the longer period and the other corresponds to the shorter period. In the numerical simulation, we do not specify the unit of parameters. Note that the numerical values for the dimensionless quantities such as ratio of masses do not depend on the choice of the unit as far as the quantities in the ratio are given in the same unit. In Subsection 5.4, we assign the unit for the parameters and estimate the ratio of the PNA over entropy density.

5.1. The PNA with the Longer Period. Let us now consider the PNA which has the longer period. While we investigate the dependence of several parameters, we fix two parameters as $(\widetilde{m}_2, H_{t_0}) = (0.05, 10^{-3})$. In Figure 1, the temperature (T) dependence of PNA is shown. It depends on the temperature only through hyperbolic function as shown in (94). In this figure, $t_{\max}$ in (106) is around 110. What stands out of this figure is the change of the amplitude for PNA among the three curves. As the temperature increases, the amplitude of the oscillation becomes larger. In Figure 2, we show the B dependence. Interestingly, both of the amplitude and the period of the oscillation change when we alter the parameter B. As it increases, the amplitude becomes larger and its period becomes shorter. Figure 3 shows the dependence of the PNA on $\omega_{3,\mathbf{0}}$. As shown in the black, blue, and dot-dashed blue lines, the position of the first node does not change when $\omega_{3,\mathbf{0}}$ takes its value within the difference of $\widetilde{m}_1$ and $\widetilde{m}_2$. However, the amplitude of oscillation gradually decreases as $\omega_{3,\mathbf{0}}$ increases up to the mass difference. The more interesting findings were observed when $\omega_{3,\mathbf{0}}$ becomes larger than the mass difference. As $\omega_{3,\mathbf{0}}$ becomes larger, the amplitude decreases and the new node is formed at once. The dashed and dotted blue lines show this behavior. The dependence on the expansion rate (H_{t_0}) is shown in Figure 4. There is an interesting aspect of this figure at the fixed time t. As the expansion rate becomes larger, the size of PNA becomes smaller.

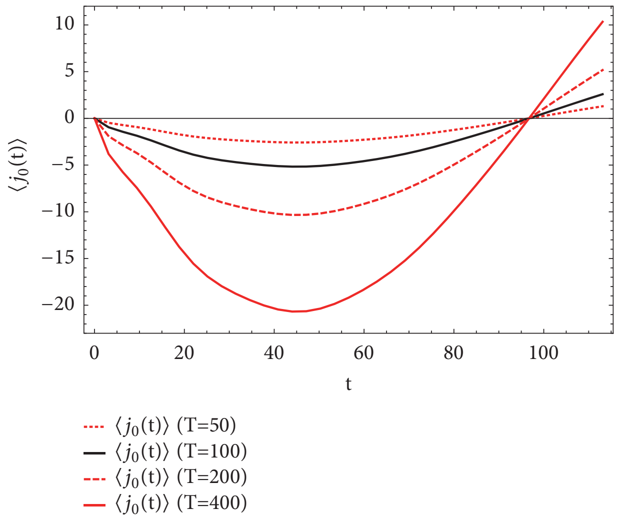

FIGURE 1: Dependence on temperature T of the time evolution of PNA. In horizontal axis, we use the dimensionless time $t = \omega_{3,\mathbf{0}}^{r}(x^0 - t_0)$ where we choose $\omega_{3,\mathbf{0}}^{r} = 0.35$. We fix a set of parameters as $(\widetilde{m}_1, \widetilde{m}_2, B, H_{t_0}, \omega_{3,\mathbf{0}}) = (0.04, 0.05, 0.021, 10^{-3}, 0.0035)$ for all of the lines. The dotted red, black, dashed red, and red lines show the cases $T = 50, 100, 200$, and 400, respectively.

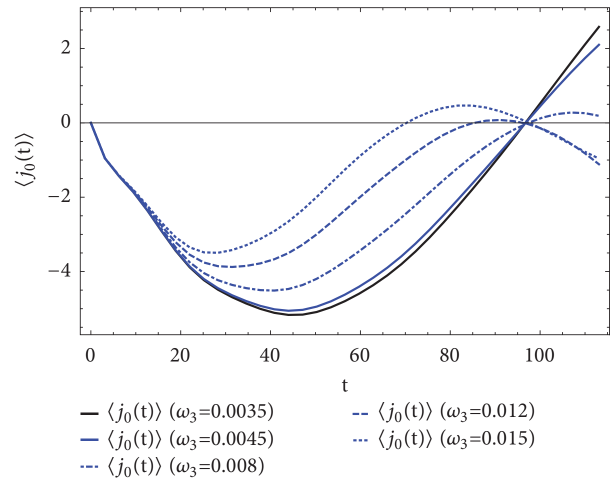

FIGURE 3: The $\omega_{3,\mathbf{0}}$ dependence of the time evolution of PNA. In horizontal axis, we use the dimensionless time $t = \omega_{3,\mathbf{0}}^{r}(x^0 - t_0)$ where we choose $\omega_{3,\mathbf{0}}^{r} = 0.35$. We use a set of parameters as $(\widetilde{m}_1, \widetilde{m}_2, B, T, H_{t_0}) = (0.04, 0.05, 0.021, 100, 10^{-3})$ for all of the lines. The black, blue, dot-dashed blue, dashed blue and dotted blue lines show the cases $\omega_{3,\mathbf{0}} = 0.0035, 0.0045, 0.008, 0.012$ and 0.015, respectively.

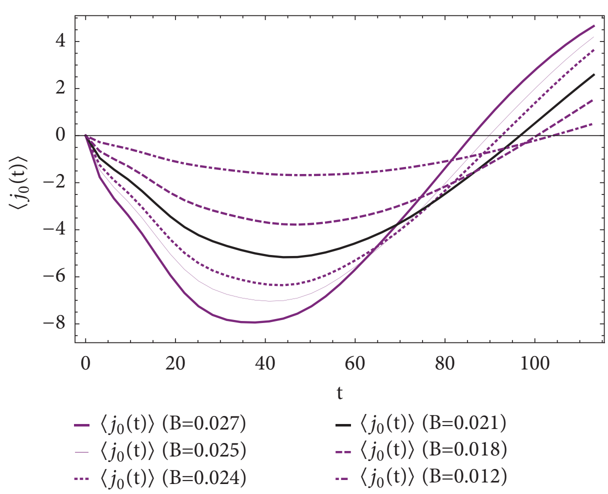

FIGURE 2: Dependence on parameter B of the time evolution of PNA. The horizontal axis is the dimensionless time defined as $t = \omega_{3,\mathbf{0}}^{r}(x^0 - t_0)$. As a reference angular frequency, we choose $\omega_{3,\mathbf{0}}^{r} = 0.35$. We fix a set of parameters as $(\widetilde{m}_2, T, H_{t_0}, \omega_{3,\mathbf{0}}) = (0.05, 100, 10^{-3}, 0.0035)$ for all of the lines. The purple, thin purple, dotted purple, black, dashed purple, and dot-dashed purple lines show the cases $B = 0.027, 0.025, 0.024, 0.021, 0.018$ and 0.012, respectively.

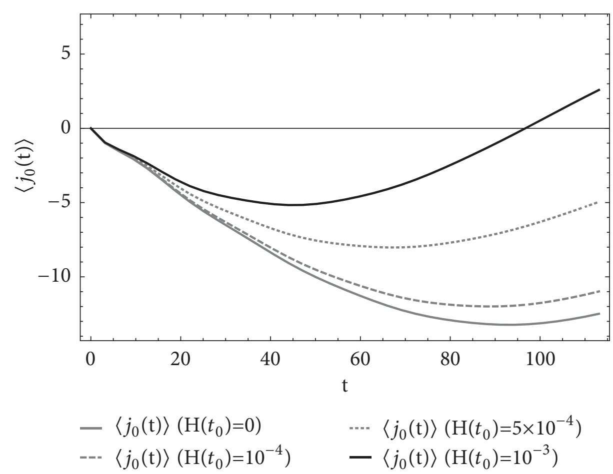

FIGURE 4: Dependence on the expansion rate H_{t_0} of the time evolution of PNA. In the horizontal axis, we use the dimensionless time $t = \omega_{3,\mathbf{0}}^{r}(x^0 - t_0)$ where we choose $\omega_{3,\mathbf{0}}^{r} = 0.35$. We fix a set of parameters as $(\widetilde{m}_1, \widetilde{m}_2, B, T, \omega_{3,\mathbf{0}}) = (0.04, 0.05, 0.021, 100, 0.0035)$ for all of the lines. The gray, dashed gray, dotted gray, and black lines show the cases $H_{t_0} = 0, 10^{-4}, 5 \times 10^{-4}$ and 10^{-3}, respectively.

5.2. The PNA with the Shorter Period. Now we investigate the PNA with the shorter period. In Figure 5, we show the temperature (T) dependence for the time evolution of PNA. In this regard, the temperature dependence is similar to the one with the longer period. Namely, the amplitude of oscillation becomes larger as the temperature increases. Figure 6 shows the B dependence. As B parameter decreases, the period of oscillation becomes longer. However, there were different effects on the amplitude of oscillation. In the left plot, we show the cases that the mass difference $\widetilde{m}_2 - \widetilde{m}_1$ is larger than the frequency $\omega_{3,\mathbf{0}}$. Since B^2, proportional to mass squared difference $\widetilde{m}_2^2 - \widetilde{m}_1^2$, of the magenta line is smaller than that of the black line, the mass difference $\widetilde{m}_2 - \widetilde{m}_1$ of the magenta line is closer to $\omega_{3,\mathbf{0}}$. At the beginning ($0 < t < 22$), the black line of large B has the larger amplitude than that of the magenta line of small B. At time $t \sim 22$, the amplitude of the magenta line becomes larger than that of the black line. We also observed that when the mass difference is near to the $\omega_{3,\mathbf{0}}$, that is for the case of magenta line, the amplitude grows slowly compared with that of the black line and reaches its

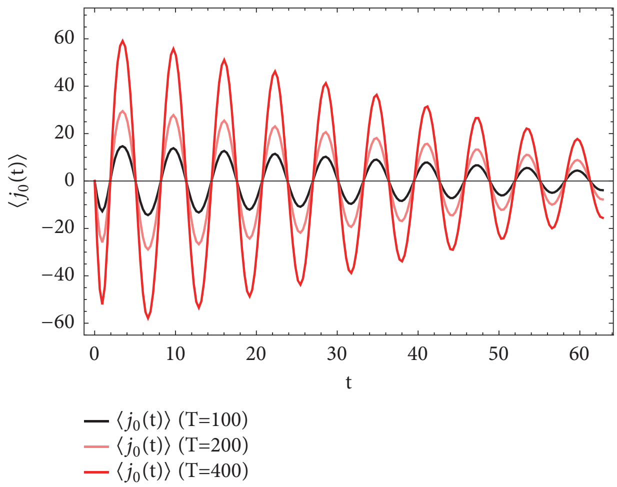

FIGURE 5: Dependence on temperature T of the time evolution of PNA. As for horizontal axis, we use the dimensionless time $t = \omega^r_{3,\mathbf{0}}(x^0 - t_0)$ where we choose $\omega^r_{3,\mathbf{0}} = 0.35$. We fix a set of parameters as $(\widetilde{m}_1, \widetilde{m}_2, B, \omega_3, H_{t_0}) = (2, 3, 1.58, 0.35, 10^{-3})$ for all the lines. The black, light red, and red lines show the cases $T = 100, 200$, and 400, respectively.

maximal value between one and a half period and twice of the period. After taking its maximal value, it slowly decreases. In the right plot, the blue line shows the case that the mass difference $\widetilde{m}_2 - \widetilde{m}_1$ is smaller than the frequency $\omega_{3,\mathbf{0}}$. In comparison with the black line, the phase shift of $\pi/2$ was observed in the blue line. The dependence on the parameter B is similar to that of the magenta line. Namely, as B becomes smaller, the amplitude gradually grows at the beginning and slowly decreases at the later time.

In Figure 7, we show the dependence on $\omega_{3,\mathbf{0}}$. In the left plot, we show the cases that $\omega_{3,\mathbf{0}}$'s are smaller than the mass difference as, $\omega^{\text{black}}_{3,\mathbf{0}} < \omega^{\text{orange}}_{3,\mathbf{0}} < \widetilde{m}_2 - \widetilde{m}_1$. As $\omega_{3,\mathbf{0}}$ increases, the period of the oscillation becomes shorter. There is also a different behavior of the amplitudes as follows. At the beginning, the amplitudes of both black and orange lines increase. After that, in comparison with the black lines, the amplitude of the orange line slowly decreases. In the right plot, the green line shows the case that $\omega_{3,\mathbf{0}}$ is larger than the mass difference. We observe that the amplitude of the green line is smaller than that of the black line and the period of the green one is shorter than that of the black one. Figure 8 shows the dependence of expansion rate (H_{t_0}). In this plot, the PNA gradually decreases as the expansion rate increases.

5.3. The Comparison of Two Different Periods. In this subsection, we present a comparison of two different periods of the time evolution of the PNA. In Figure 9, the black line shows the case of the shorter period and the dotted black line shows the case of the longer one. As can be seen in this figure, the PNA with the shorter period frequently changes the sign and the magnitude also strongly depends on the time. In contrast to the shorter period case, both the sign and magnitude of the longer period case are stable if restricted to the time range $t = 30 \sim 60$ in Figure 9.

5.4. The Evolution of the PNA with the Scale Factor of a Specific Time Dependence. In this subsection, we interpret the numerical simulation in a specific situation. We assume that the time dependence of the scale factor is given by the one in radiation dominated era. We also specify the unit of the parameters, time and temperature. By doing so, we can clarify implication of the numerical simulation in a more concrete situation.

Specifically, the time dependence of the scale factor is given as follows:

$$a\left(x^0\right) = \sqrt{1 + 2H_{t_0}\left(x^0 - t_0\right)}. \tag{107}$$

The above equation is derived as follows. The Einstein's equations without cosmological constant lead to the following equation:

$$\left(\frac{\dot{a}}{a}\right)^2 = \frac{8\pi}{3}G\rho, \tag{108}$$

where G is the Newton's constant. ρ is the energy density for radiation and it is given by

$$\rho\left(x^0\right) = \rho_0 a^{-4}\left(x^0\right), \tag{109}$$

where ρ_0 is the initial energy density and we set $a_{t_0} = 1$. By setting $x^0 = t_0$ in (108), the initial Hubble parameter is given by

$$H^2_{t_0} = \frac{8\pi}{3}G\rho_0. \tag{110}$$

Then using (110), (108) becomes

$$\frac{d}{dx^0}\left\{a\left(x^0\right)^2\right\} = 2H_{t_0}. \tag{111}$$

Solving the equation above, one can obtain (107).

From the expression in (107), one needs to specify the unit of the Hubble parameter at t_0. Through (110), it is related to the initial energy density ρ_0. Assuming ρ_0 is given by radiation with an effective degree of freedom g_* and a temperature $T(t_0)$, one can write ρ_0 as follows:

$$\rho_0 = g_*\frac{\pi^2}{30}T^4\left(t_0\right). \tag{112}$$

Hereafter, we assume that the temperature of the radiation $T(t_0)$ is equal to the temperature T in the density operator for the scalar fields. Then one can write the ratio of the initial Hubble parameter and temperature T as follows:

$$\frac{H_{t_0}}{T} = \frac{\pi}{3}\sqrt{\frac{4\pi g_*}{5}}\frac{T}{M_{\text{Pl}}}, \tag{113}$$

where M_{Pl} is the Planck mass and $M_{\text{Pl}} = 1.2 \times 10^{19}$ (GeV). Then one can write the temperature T in GeV unit as follows:

$$T\,(\text{GeV}) = \frac{3}{\pi}\sqrt{\frac{5}{4\pi g_*}}\left(\frac{H_{t_0}}{T}\right)M_{\text{Pl}}\,(\text{GeV}). \tag{114}$$

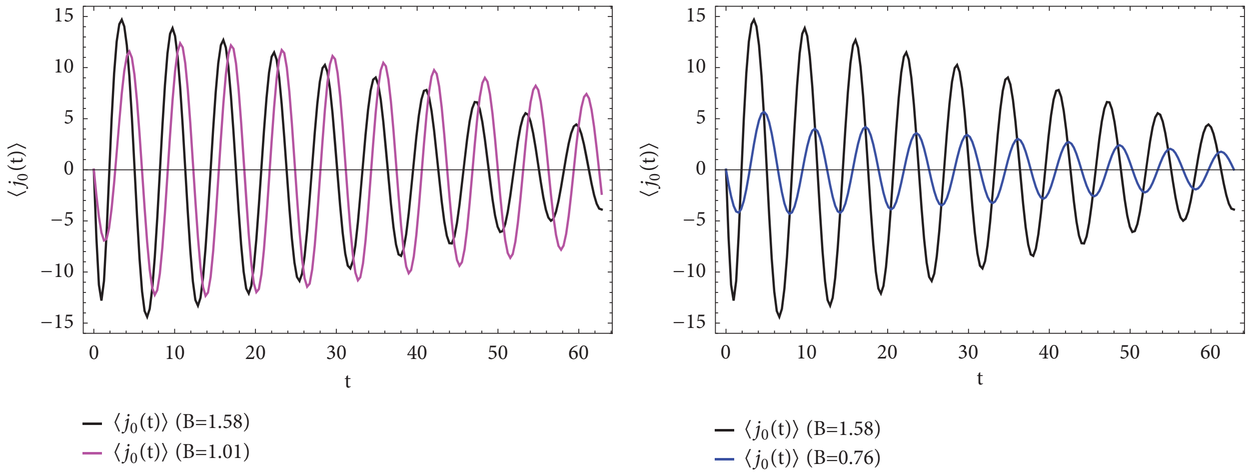

Figure 6: B dependence for the time evolution of PNA. The horizontal axis is the dimensionless time defined as $t = \omega^r_{3,\mathbf{0}}(x^0 - t_0)$. As a reference angular frequency, we choose $\omega^r_{3,\mathbf{0}} = 0.35$. We use a set of parameters as $(\widetilde{m}_2, T, H_{t_0}, \omega_{3,\mathbf{0}}) = (3, 100, 10^{-3}, 0.35)$ for all the lines. In the left plot, the black and magenta lines display the cases $B = 1.58$ and 1.01, respectively. For the right plot, the black and blue lines display the cases $B = 1.58$ and 0.76, respectively.

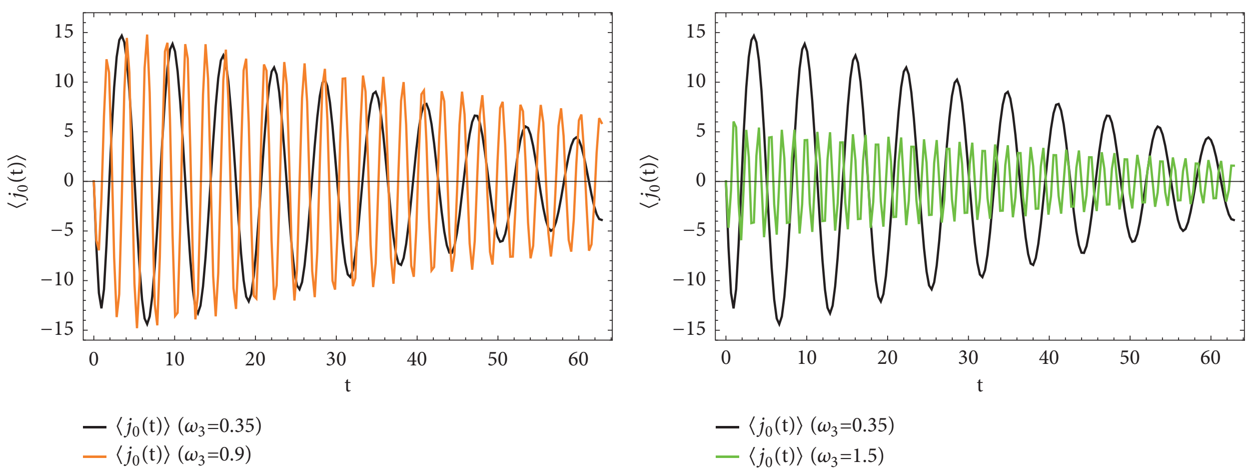

Figure 7: Dependence on frequency $\omega_{3,0}$ of the time evolution of the PNA. We use the dimensionless time $t = \omega^r_{3,\mathbf{0}}(x^0 - t_0)$ for horizontal axis and as a reference angular frequency, we choose $\omega^r_{3,\mathbf{0}} = 0.35$. We fix parameters $(\widetilde{m}_1, \widetilde{m}_2, B, T, H_{t_0}) = (2, 3, 1.58, 100, 10^{-3})$ for all the lines. The black and orange lines show the cases $\omega_{3,\mathbf{0}} = 0.35$ and 0.9, respectively (left plot). The black and green lines show the cases $\omega_{3,\mathbf{0}} = 0.35$ and 1.5, respectively (right plot).

In the numerical simulation, the ratio H_{t_0}/T is given. Therefore, for the given ratio and g_*, the temperature T in terms of GeV unit is determined. Then H_{t_0} in GeV unit also becomes

$$H_{t_0}\,(\mathrm{GeV}) = T\,(\mathrm{GeV}) \times \left(\frac{H_{t_0}}{T}\right). \tag{115}$$

The masses of the scalar fields $\widetilde{m}_i$ $(i = 1, 2, 3)$ can be also expressed in GeV unit as

$$\widetilde{m}_i\,(\mathrm{GeV}) = H_{t_0}\,(\mathrm{GeV}) \times \left(\frac{\widetilde{m}_i}{H_{t_0}}\right), \tag{116}$$

where we use the ratios $\widetilde{m}_i/H_{t_0}$ given in the numerical simulation.

As an example, we study the implication of the numerical simulation shown in Figure 9 by specifying the mass parameter in GeV unit. We also determine the unit of time scale. We first determine the temperature in GeV unit using (114). As for the degree of freedom, we can take $g_* \simeq 100$ which corresponds to the case that all the standard model particles are regarded as radiation. Then, substituting the ratio $H_{t_0}/T = 10^{-5}$ adapted in Figure 9 to (114) and (115), one obtains $T \sim 10^{13}$ (GeV) and $H(t_0) \sim 10^8$ (GeV), respectively. The mass parameters are different between the longer period case (the dotted line) and the shorter period case (the solid line). They are also given in GeV unit shown in Table 2. The time scale $\Delta t = 100$ corresponds to 3×10^{-9} $(\mathrm{GeV})^{-1}$ which is about 2×10^{-33} (sec).

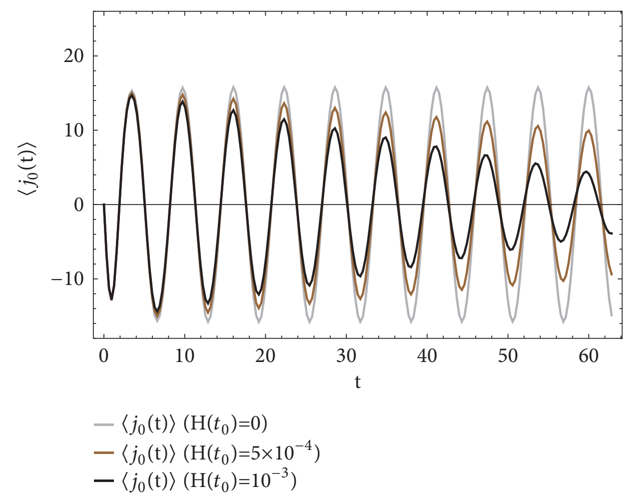

FIGURE 8: The expansion rate $H(t_0)$ dependence of the time evolution PNA. In horizontal axes, we use the dimensionless time $t = \omega^r_{3,\mathbf{0}}(x^0 - t_0)$ where we choose $\omega^r_{3,\mathbf{0}} = 0.35$. We fix parameters as $(\widetilde{m}_1, \widetilde{m}_2, B, \omega_{3,\mathbf{0}}, T) = (2, 3, 1.58, 0.35, 100)$ for all the lines. The light gray, brown, and black lines display the cases $H(t_0) = 0, 5\times10^{-4}$ and 10^{-3}, respectively.

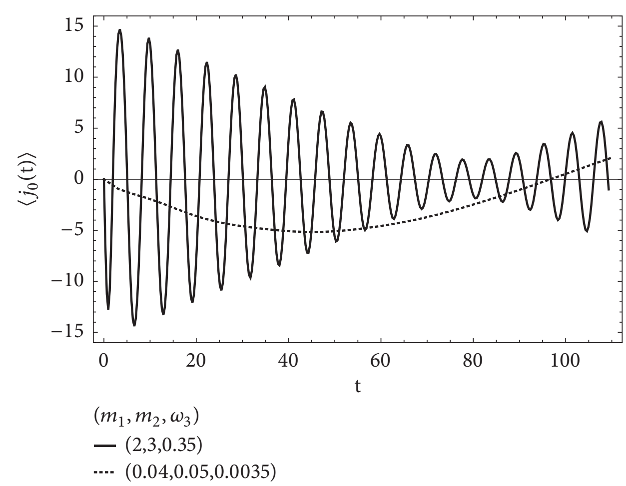

FIGURE 9: Comparison between two different periods of the time evolution of the PNA. We use the dimensionless time $t = \omega^r_{3,\mathbf{0}}(x^0 - t_0)$ for horizontal axis and as a reference we choose $\omega^r_{3,\mathbf{0}} = 0.35$. We fix parameters $(T, H_{t_0}) = (100, 10^{-3})$ for all the lines. The black (shorter period) and black dotted (longer period) lines show the set parameters $(\widetilde{m}_1, \widetilde{m}_2, B, \omega_{3,\mathbf{0}})$ as $(2, 3, 1.58, 0.35)$ and $(0.04, 0.05, 0.021, 0.0035)$, respectively. Notice that our approximation will break down after $t = 80$.

One can also estimate the size of PNA. Here, we consider the maximum value of the PNA for the longer period case in Figure 9. We evaluate the ratio of the PNA over entropy density s,

$$\frac{\langle j_0 (t \simeq 50)\rangle}{s} = -\frac{5\times10^{11}\,(\mathrm{GeV})}{T\,(\mathrm{GeV})} \times \frac{A_{123}\,(\mathrm{GeV})}{T\,(\mathrm{GeV})} \times \frac{v_3\,(\mathrm{GeV})}{T\,(\mathrm{GeV})} \times \frac{45}{2\pi^2 g_*}, \tag{117}$$

TABLE 2: The mass parameters in GeV unit for both longer and shorter period cases in Figure 9.

Mass parameter (GeV)	The shorter period	The longer period
m_1	2×10^{11}	4×10^{9}
m_2	3×10^{11}	5×10^{9}
$\omega_{3,\mathbf{0}}$	3.5×10^{10}	3.5×10^{8}

where s is given by

$$s = g_* \frac{2\pi^2}{45} T^3 \left(\mathrm{GeV}^3\right). \tag{118}$$

In (117), the first numerical factor, -5×10^{11}(GeV), is obtained in the following way:

$$\frac{A_{123}\,(\mathrm{GeV})}{T\,(\mathrm{GeV})} = \frac{A_{123}}{T}, \tag{119}$$

$$\frac{v_3\,(\mathrm{GeV})}{T\,(\mathrm{GeV})} = \frac{v_3}{T}, \tag{120}$$

$$\frac{-5\times10^{11}\,(\mathrm{GeV})}{T\,(\mathrm{GeV})} = \frac{-5}{T}. \tag{121}$$

In the right-hand side of the above equations, T denotes the temperature in the universal unit of the simulation in Figure 9 where $T = 100$ is used. In the left-hand side, T denotes the corresponding temperature in GeV unit and it is $T = 10^{13}$ (GeV). Substituting the temperature $T = 10^{13}$ (GeV) into (117), one obtains

$$\frac{\langle j_0 (t \simeq 50)\rangle}{s} = -1\times10^{-11} \times \left(\frac{A_{123}\,(\mathrm{GeV})}{10^8\,(\mathrm{GeV})}\right) \times \left(\frac{v_3\,(\mathrm{GeV})}{10^{10}\,(\mathrm{GeV})}\right). \tag{122}$$

From the equation above, we can achieve the ratio as 10^{-10} by taking $A_{123} = 10^8$ (GeV) and $v_3 = 10^{11}$ (GeV).

6. Discussion and Conclusion

In this paper, we developed a new mechanism for generating the PNA. This mechanism is realized with the specific model Lagrangian which we have proposed. The model includes a complex scalar. The PNA is associated with U(1) charge of the complex scalar. In addition, we introduce a neutral scalar which interacts with the complex scalar. The U(1) charge is not conserved due to particle number violating interaction. As another source of particle number violation, the U(1) symmetry breaking mass term for the complex scalar is introduced. The initial value for the condensation of the neutral scalar is nonzero. Using 2PI formalism and specifying the initial condition with density operator, the time-dependent PNA is obtained. To include the effect of the time dependence of the scale factor, we approximate it up to the first order of Hubble parameter.

The results show that the PNA depends on the interaction coupling A_{123} and the initial value of the condensation of

Table 3: The classification of $o(H_{t_0})$ contributions to the PNA.

The effect	The origin
Dilution	The increase of volume of the universe due to expansion, $1/a(x^0)^3 - 1/a_{t_0}^3$
Freezing interaction	The decrease of the strength of the cubic interaction $\widehat{A}$ as $\widehat{A}_{123} - A_{123}$
Redshift	The effective energy of particle as indicated in Eq. (57), $\mathbf{k}^2/a(x^0)^2 + \overline{m}_i^2(x^0)$

the neutral scalar $\widehat{\varphi}_{3,t_0}$. It also depends on the mass squared difference of two real scalars which originally form a complex scalar. We found that the interaction coupling A_{123} and the mass squared difference play a key role to give rise to non-vanishing PNA. Even if the initial value of the neutral scalar is nonzero, in the vanishing limit of interaction terms and the mass squared difference, the PNA will vanish. Another important finding is that the contribution to the PNA is divided into four types. The constant scale factor which is the zeroth order of Hubble parameter is the leading contribution. The rest which are the first order term contribute according to their origins. Those are summarized in Table 3.

We have numerically calculated time evolution of the PNA and have investigated its dependence on the temperature, parameter B, the angular frequency $\omega_{3,\mathbf{0}}$, and the expansion rate of the universe. Starting with the null PNA at the initial time, it is generated by particle number violating interaction. Once the nonzero PNA is generated, it starts to oscillate. The amplitude decreases as the time gets larger. The dumping rate of the amplitude increases as the Hubble parameter becomes larger. The period of the oscillation depends on the angular frequency $\omega_{3,\mathbf{0}}$ and the parameter B. The former determines the oscillation period for the condensation of the neutral scalar. The latter determines the mass difference of ϕ_1 and ϕ_2. In the simulation, we focus on the two cases for the oscillation period, one of which corresponds to the longer period case and the other is the shorter period case. The longer period is about half of the Hubble time $(1/H_{t_0})$ and the shorter period is one percent of the Hubble time. The set of parameters $(\omega_{3,\mathbf{0}}, B)$ which corresponds to the longer period is typically one percent of the values for the shorter period. In both cases, the amplitude gets larger as the temperature increases. For the longer period, as parameter B becomes larger, the amplitude increases. For the shorter period, in order to have large amplitude, the parameter B is taken so that the mass difference $\widetilde{m}_2 - \widetilde{m}_1$ is near to $\omega_{3,\mathbf{0}}$. In other words, when the resonance condition $\omega_{3,\mathbf{0}} \simeq \widetilde{m}_2 - \widetilde{m}_1$ is satisfied, the amplitude becomes large. For the longer period case, as the angular frequency $\omega_{3,\mathbf{0}}$ decreases, the amplitude becomes large.

To show how the mechanism can be applied to a realistic situation, we study the simulated results for radiation dominated era when the degree of freedom of light particles is assumed to be $g_* \simeq O(100)$. Then when the initial temperature of the scalar fields is the same as that of the light particles, the simulation with $H_{t_0}/T = 10^{-5}$ corresponds to the case that the temperature of the universe is 10^{13} (GeV) which is slightly lower than GUT scale $\sim 10^{16}$ (GeV) [20, 21]. The masses of the scalar fields in Figure 9 are different between the shorter period case and the longer period case as shown in Table 2. In the shorter period case, the mass spectrum of the scalar ranges from 10^{10} (GeV) to 10^{11} (GeV) while for the longer period case, it is lower than that of the shorter period case by two orders of magnitude. For the longer period case, the maximum asymmetry is achieved at 10^{-33} (sec) after the initial time. For shorter period, it is achieved at about 10^{-34} (sec). We have estimated the ratio of the PNA over entropy density by substituting the numerical values of the coupling constant (A_{123}) and the initial expectation value (v_3).

Compared with the previous works [13, 14, 22, 23], instead of assuming the nonzero PNA at the initial time, the PNA is created through interactions. These interactions have the following unique feature; namely, the interaction between the complex scalars and oscillating condensation of a neutral scalar leads to the PNA. In our work, by assuming the initial condensation of the neutral scalar is away from the equilibrium point, the condensation starts to oscillate. In the expression of the amplitude of PNA, one finds that it is proportional to the CP violating coupling between the scalars and the condensation, the initial condensation of the neutral scalars, and mass difference between mass eigenstates of the two neutral scalars which are originally introduced as a complex scalar with the particle number violating mass and curvature terms. One of the distinctive features of the present mechanism from the one which utilizes the PNA created through the heavy particle decays is as follows. In the mechanism which utilizes the heavy particle decays, the temperature must be high enough so that it once brings the heavy particle to the state of the thermal equilibrium. Therefore the temperature of the universe at reheating era must be as high as the mass of the heavy particle. In contrast to this class of the models, the present model is not restricted by such condition. In place of the condition, the initial condensation must be large enough to explain the asymmetry.

In our model, even for the longer period case, the oscillation period is shorter than the Hubble time $(1/H_{t_0})$. It implies that one of Sakharov conditions for BAU, namely, nonequilibrium condition, is not satisfied. In this respect, we expect that due to the finite life time of the condensation of the neutral scalar, the interaction between the condensation and complex scalars will vanish and eventually the oscillation of the PNA may terminate. The detailed study will be given in the future work. The relation between the PNA and the observed BAU should be also studied. In particular, we need to consider the mechanism how the created PNA is transferred to the observed BAU.

Appendix

A. The Solution of SDEs for Both Green's Function and Field

A.1. The General Solutions of SDEs. In this subsection, we provide the general solution of SDEs. Let us introduce the following differential equation for a field φ,

$$\left[\frac{\partial^2}{\partial x^{0\,2}} + m^2\left(x^0\right)\right]\varphi\left(x^0\right) = S\left(x^0\right) + E\left(t_0\right)\delta\left(x^0 - t_0\right) + F\left(T\right)\delta\left(x^0 - T\right), \quad \text{(A.1)}$$

where S is an arbitrary function of time x^0 and we will find the solution within the time range from $x^0 = t_0$ to $x^0 = T$. At the boundaries $x^0 = t_0$ and $x^0 = T$, we introduce the source terms of the form of delta function. The strength of the delta function is denoted as $E(t_0)$ and $F(T)$, respectively. One may assume that field vanishes at $x^0 < t_0$,

$$\varphi\left(x^0 < t_0\right) = 0, \qquad \left.\frac{\partial\varphi\left(x^0\right)}{\partial x^0}\right|_{x^0<t_0} = 0. \quad \text{(A.2)}$$

One integrates (A.1) with respect to time x^0 from $t_0 - \epsilon$ to $t_0 + \epsilon$ and obtains initial condition for the first derivative of the field as

$$\left.\frac{\partial\varphi\left(x^0\right)}{\partial x^0}\right|_{t_0^+} = E\left(t_0\right), \quad \text{(A.3)}$$

where we have used the above assumption and taken limit $\epsilon \longrightarrow 0$. t_0^+ denotes $t_0 + 0$.

The method of variation of constants has been employed to determine the solution of (A.1) and it is written as

$$\varphi\left(x^0\right) = C_1\left(x^0\right) f\left(x^0\right) + C_2\left(x^0\right) g\left(x^0\right), \quad \text{(A.4)}$$

where $f(x^0)$ and $g(x^0)$ are two linear independent solutions of the following homogeneous equation:

$$\left[\frac{\partial^2}{\left(\partial x^0\right)^2} + m^2\left(x^0\right)\right]\varphi_{\text{homo}}\left(x^0\right) = 0. \quad \text{(A.5)}$$

Firstly, the following condition is imposed:

$$\dot{C}_1\left(x^0\right) f\left(x^0\right) + \dot{C}_2\left(x^0\right) g\left(x^0\right) = 0. \quad \text{(A.6)}$$

Equation (A.4) becomes the solution of the differential equation (A.1) when $C_i(x^0)$ satisfies another condition,

$$\dot{C}_1\left(x^0\right)\dot{f}\left(x^0\right) + \dot{C}_2\left(x^0\right)\dot{g}\left(x^0\right) = S\left(x^0\right) + F\left(T\right)\delta\left(x^0 - T\right). \quad \text{(A.7)}$$

The remaining task is to find $C_i(x^0)$ which satisfy the conditions in (A.6) and (A.7). It is convenient to write these conditions in matrix form as

$$\begin{pmatrix}\dot{C}_1\left(x^0\right)\\ \dot{C}_2\left(x^0\right)\end{pmatrix} = \frac{1}{W} \cdot \begin{pmatrix} g\left(x^0\right) & -\dot{g}\left(x^0\right) \\ -f\left(x^0\right) & \dot{f}\left(x^0\right)\end{pmatrix}\begin{pmatrix} S\left(x^0\right) + F\left(T\right)\delta\left(x^0 - T\right) \\ 0\end{pmatrix}, \quad \text{(A.8)}$$

where we have defined

$$W = \dot{f}\left(x^0\right) g\left(x^0\right) - f\left(x^0\right)\dot{g}\left(x^0\right). \quad \text{(A.9)}$$

and it is a constant with respect to time. Integrating (A.8) with respect to time from t_0^+ to x^0, one obtains

$$C_1\left(x^0\right) = \int_{t_0^+}^{x^0}\frac{1}{W}\left(g\left(t\right)\left\{S\left(t\right) + F\left(t\right)\delta\left(t - T\right)\right\}\right)dt + C_1\left(t_0^+\right) \quad \text{(A.10)}$$

$$C_2\left(x^0\right) = -\int_{t_0^+}^{x^0}\frac{1}{W}\left(f\left(t\right)\left\{S\left(t\right) + F\left(t\right)\delta\left(t - T\right)\right\}\right)dt + C_2\left(t_0^+\right) \quad \text{(A.11)}$$

Therefore (A.4) becomes

$$\varphi\left(x^0\right) = \frac{1}{W}\int_{t_0^+}^{x^0}\left[f\left(x^0\right) g\left(t\right) - g\left(x^0\right) f\left(t\right)\right] \cdot \left\{S\left(t\right) + F\left(t\right)\delta\left(t - T\right)\right\}dt + C_1\left(t_0^+\right) f\left(x^0\right) + C_2\left(t_0^+\right) g\left(x^0\right). \quad \text{(A.12)}$$

In this regard, it enables us to define

$$\overline{K}\left[x^0, y^0\right] \coloneqq \frac{1}{W}\left[f\left(x^0\right) g\left(y^0\right) - g\left(x^0\right) f\left(y^0\right)\right]. \quad \text{(A.13)}$$

Then (A.12) alters into

$$\varphi\left(x^0\right) = \int_{t_0^+}^{x^0}\overline{K}\left[x^0, t\right]\left\{S\left(t\right) + F\left(t\right)\delta\left(t - T\right)\right\}dt + C_1\left(t_0^+\right) f\left(x^0\right) + C_2\left(t_0^+\right) g\left(x^0\right). \quad \text{(A.14)}$$

To determine $C_i(t_0^+)$, the first derivative of field is required,

$$\frac{\partial}{\partial x^0}\varphi\left(x^0\right) = \int_{t_0^+}^{x^0}\left(\frac{\partial\overline{K}\left[x^0, t\right]}{\partial x^0}\right)\left\{S\left(t\right) + F\left(t\right)\delta\left(t - T\right)\right\}dt + C_1\left(t_0^+\right)\dot{f}\left(x^0\right) + C_2\left(t_0^+\right)\dot{g}\left(x^0\right). \quad \text{(A.15)}$$

Consequently, using definition (A.13), the term which includes $S(t_0)$ vanishes after integration. From now on, we will denote $\dot{\varphi}(x^0)$ as $\partial\varphi(x^0)/\partial x^0$.

Let us now write $C_i(t_0^+)$ in terms of $\varphi(t_0)$ and $\dot{\varphi}(t_0)$. We consider the following equations:

$$\varphi\left(t_0^+\right) = C_1\left(t_0^+\right) f\left(t_0^+\right) + C_2\left(t_0^+\right) g\left(t_0^+\right), \quad (A.16)$$

$$\dot{\varphi}\left(t_0^+\right) = C_1\left(t_0^+\right) \dot{f}\left(t_0^+\right) + C_2\left(t_0^+\right) \dot{g}\left(t_0^+\right). \quad (A.17)$$

Next, one can write $C_i(t_0^+)$ in matrix form as

$$\begin{pmatrix} C_1\left(t_0^+\right) \\ C_2\left(t_0^+\right) \end{pmatrix} = -\frac{1}{W}\begin{pmatrix} \dot{g}\left(t_0^+\right) & -g\left(t_0^+\right) \\ -\dot{f}\left(t_0^+\right) & f\left(t_0^+\right) \end{pmatrix}\begin{pmatrix} \varphi\left(t_0^+\right) \\ \dot{\varphi}\left(t_0^+\right) \end{pmatrix}. \quad (A.18)$$

Thus one substitutes these $C_i(t_0^+)$ into (A.14) and obtains

$$\begin{aligned} \varphi\left(x^0\right) = &\int_{t_0^+}^{x^0} \overline{K}\left[x^0, t\right] S(t)\, dt \\ &+ \overline{K}\left[x^0, T\right] F(T)\, \theta\left(x^0 - T\right) \\ &- \overline{K'}\left[x^0, t_0\right] \varphi\left(t_0\right) + \overline{K}\left[x^0, t_0\right] E\left(t_0\right), \end{aligned} \quad (A.19)$$

where we have used the initial condition in (A.3) and $\overline{K'}[x^0, y^0]$ is defined as

$$\overline{K'}\left[x^0, y^0\right] := \frac{\partial \overline{K}\left[x^0, y^0\right]}{\partial y^0}. \quad (A.20)$$

In the next subsection, we will use the obtained solution to provide the solution of SDEs.

A.2. The SDEs for the Field. Next we move to consider the SDEs for the field in (54). It is rewritten as

$$\left[\frac{\partial^2}{\partial x^{02}} + \Omega^2_{i,x^0,\mathbf{k}=0}\right] \widehat{\varphi}^d_{i,x^0} = S^d_{i,x^0}, \quad (A.21)$$

where we have defined S^d_{i,x^0} as

$$\begin{aligned} S^d_{i,x^0} := &\, c^{da} D_{abc} \widehat{A}_{ijk}\left(x^0\right) \\ &\cdot \left\{\widehat{\varphi}^b_j\left(x^0\right)\widehat{\varphi}^c_k\left(x^0\right) + \widehat{G}^{bc}_{jk}(x, x)\right\}. \end{aligned} \quad (A.22)$$

To solve (A.21), one first sets $E(t_0) = 0$ and $F(T) = 0$ in (A.1). Then, the general differential equation is similar to the SDEs for the field. The SDEs of the field in the form of integral equation are given by

$$\widehat{\varphi}^d_{i,x^0} = -\overline{K}'_{i,x^0 t_0}\widehat{\varphi}^d_{i,t_0} + \int_{t_0^+}^{x^0} \overline{K}_{i,x^0 t} S^d_{i,t}\, dt, \quad (A.23)$$

$$\widehat{\varphi}^{d,\text{free}}_{i,x^0} = -\overline{K}'_{i,x^0 t_0}\widehat{\varphi}^d_{i,t_0}, \quad (A.24)$$

$$\widehat{\varphi}^{d,\text{int}}_{i,x^0} = \int_{t_0^+}^{x^0} \overline{K}_{i,x^0 t} S^d_{i,t}\, dt. \quad (A.25)$$

By using the above equations and keeping the solutions up to the first order of the cubic interaction, one obtains (70)-(72).

A.3. The SDEs for Green's Function. In this subsection, we consider the SDEs for Green's function in (55) and (56). They are simply rewritten as

$$\begin{aligned} &\left[\frac{\overrightarrow{\partial^2}}{\partial x^{02}} + \Omega^2_{i,x^0,\mathbf{k}}\right]\widehat{G}^{ab}_{ij,x^0 y^0,\mathbf{k}} \\ &\quad = Q^{ab}_{ij,x^0 y^0,\mathbf{k}} + E^{ac}_{ik,\mathbf{k}}\widehat{G}^{cb}_{kj,t_0 y^0,\mathbf{k}}\delta_{t_0 x^0} + F^{ab}_{ij}\delta_{x^0 y^0}, \end{aligned} \quad (A.26)$$

$$\begin{aligned} &\widehat{G}^{ab}_{ij,x^0 y^0,\mathbf{k}}\left[\frac{\overleftarrow{\partial^2}}{\partial y^{02}} + \Omega^2_{i,y^0,\mathbf{k}}\right] \\ &\quad = R^{ab}_{ij,x^0 y^0,\mathbf{k}} + \widehat{G}^{ac}_{ik,x^0 t_0,\mathbf{k}} E^{Tcb}_{kj,\mathbf{k}}\delta_{t_0 y^0} + F^{ab}_{ij}\delta_{x^0 y^0}, \end{aligned} \quad (A.27)$$

where we have defined

$$F^{ab}_{ij} := -i\delta_{ij}\frac{c^{ab}}{a^3_{t_0}}, \quad (A.28)$$

$$Q^{ab}_{ij,x^0 y^0}(\mathbf{k}) := 2c^{ad} D_{dce}\widehat{A}_{ikl,x^0}\widehat{\varphi}^e_{l,x^0}\widehat{G}^{cb}_{kj,x^0 y^0}(\mathbf{k}), \quad (A.29)$$

$$R^{ab}_{ij,x^0 y^0}(\mathbf{k}) := 2\widehat{G}^{ac}_{ik,x^0 y^0}(\mathbf{k}) D_{cef}\widehat{A}_{kjl,y^0}\widehat{\varphi}^f_{l,y^0} c^{eb}, \quad (A.30)$$

and $E^{ac}_{ik,\mathbf{k}}$ is given in (83).

In the following, we will obtain SDEs for Green's functions at (x^0, y^0) in the form of integral equation. Starting with the initial condition for Green's function at (t_0, t_0), we obtain two expressions for Green's function at (x^0, y^0). The two expressions correspond to two paths shown in Figure 10 which are used to integrate the differential equation in (A.26) and (A.27). They are given by (dot multiplication describes matrix product corresponding their indices)

$$\begin{aligned} \widehat{G}^{br}_{x^0 y^0} = &\left\{\overline{K}_{x^0 t_0}\cdot\left(E\cdot\widehat{G}_{t_0 t_0} + F\right) - \overline{K}'_{x^0 t_0}\cdot\widehat{G}_{t_0 t_0}\right\} \\ &\cdot\left(E^T\cdot\overline{K}_{y^0 t_0} - \overline{K}'_{y^0 t_0}\right) + \theta\left(y^0 - x^0\right) F \\ &\cdot\overline{K}_{y^0 x^0} + \int_{t_0^+}^{y^0} R_{x^0 t}\cdot\overline{K}_{y^0 t}\, dt \\ &+ \int_{t_0^+}^{x^0} \overline{K}_{x^0 t}\cdot Q_{t t_0}\, dt \\ &\cdot\left(E^T\cdot\overline{K}_{y^0 t_0} - \overline{K}'_{y^0 t_0}\right), \end{aligned} \quad (A.31)$$

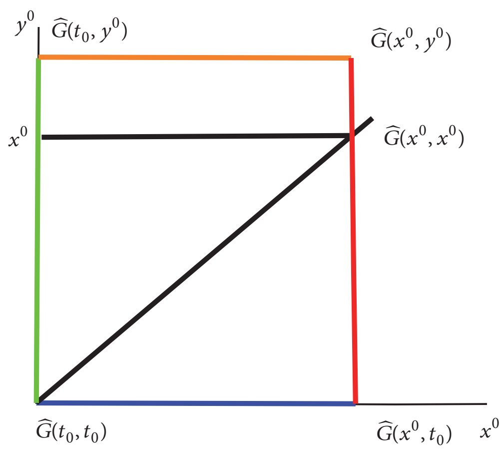

FIGURE 10: Two paths to obtain $\widehat{G}(x^0, y^0)$. We show the paths for the case $x^0 < y^0$.

$$\begin{aligned}\widehat{G}^{go}_{x^0y^0} &= \left(\overline{K}_{x^0t_0} \cdot E - \overline{K}'_{x^0t_0}\right) \\ &\cdot \left\{\left(\widehat{G}_{t_0t_0} \cdot E^T + F\right) \cdot \overline{K}_{y^0t_0} - \widehat{G}_{t_0t_0} \cdot \overline{K}'_{y^0t_0}\right\} \\ &+ \theta\left(x^0 - y^0\right) \overline{K}_{x^0y^0} \cdot F \\ &+ \int_{t_0^+}^{x^0} \overline{K}_{x^0t} \cdot Q_{ty^0}\, dt \\ &+ \left(\overline{K}_{x^0t_0} \cdot E - \overline{K}'_{x^0t_0}\right) \\ &\cdot \int_{t_0^+}^{y^0} R_{t_0t} \cdot \overline{K}_{y^0t}\, dt,\end{aligned} \tag{A.32}$$

where the upper indices "*br*" and "*go*" denote the blue red path and the green orange path, respectively.

Now let us explain how one can derive (A.31). The steps are summarized below.

(i) We first consider the differential equation in (A.26) which Green's function $\widehat{G}(t, t_0)$ on the blue line $(t_0 \le t \le x^0)$ satisfies. Using the solution of the general differential equation in (A.19), we obtain the expression

$$\begin{aligned}\widehat{G}_{x^0t_0} &= \int_{t_0^+}^{x^0} \overline{K}_{x^0t} \cdot Q_{tt_0}\, dt + \overline{K}_{x^0t_0} \cdot \left(E \cdot \widehat{G}_{t_0t_0} + F\right) \\ &- \overline{K}'_{x^0t_0} \cdot \widehat{G}_{t_0t_0},\end{aligned} \tag{A.33}$$

where $\widehat{G}_{t_0t_0}$ denotes the initial condition.

(ii) Next we consider the differential equation in (A.27) which Green's function $\widehat{G}(x^0, t)$ on the red line $(t_0 \le t \le y^0)$ satisfies. Using the solution of the general differential equation in (A.19), we obtain the expression

$$\begin{aligned}\widehat{G}_{x^0y^0} &= \int_{t_0^+}^{y^0} R_{x^0t} \cdot \overline{K}_{y^0t}\, dt + \widehat{G}_{x^0t_0} \\ &\cdot \left(E \cdot \overline{K}_{y^0t_0} - \overline{K}'_{y^0t_0}\right) + \theta\left(y^0 - x^0\right) F \\ &\cdot \overline{K}_{y^0x^0},\end{aligned} \tag{A.34}$$

where $\widehat{G}_{x^0t_0}$ denotes the initial condition.

(iii) Substituting (A.33) to (A.34), we obtain (A.31).

Equation (A.32) is obtained through the steps similar to the above. The difference is as follows. We first integrate the differential equation on the green line with the initial condition at (t_0, t_0) and obtain the expression for $\widehat{G}_{t_0y^0}$. Using it as the initial condition, we integrate the differential equation on the orange line and obtain the expression in (A.32).

A.4. The Derivation of Free Part for Green's Function and Its Path Independence. In the following subsection, we derive the free parts of Green's function which are the zeroth order of cubic interaction. From (A.31) and (A.32), we can write them respectively as

$$\begin{aligned}\widehat{G}^{br,\text{free}}_{x^0y^0} &= \left\{\overline{K}_{x^0t_0} \cdot \left(E \cdot \widehat{G}_{t_0t_0} + F\right) - \overline{K}'_{x^0t_0} \cdot \widehat{G}_{t_0t_0}\right\} \\ &\cdot \left(E^T \cdot \overline{K}_{y^0t_0} - \overline{K}'_{y^0t_0}\right) + \theta\left(y^0 - x^0\right) F \\ &\cdot \overline{K}_{y^0x^0},\end{aligned} \tag{A.35}$$

$$\begin{aligned}\widehat{G}^{go,\text{free}}_{x^0y^0} &= \left(\overline{K}_{x^0t_0} \cdot E - \overline{K}'_{x^0t_0}\right) \\ &\cdot \left\{\left(\widehat{G}_{t_0t_0} \cdot E^T + F\right) \cdot \overline{K}_{y^0t_0} - \widehat{G}_{t_0t_0} \cdot \overline{K}'_{y^0t_0}\right\} \\ &+ \theta\left(x^0 - y^0\right) \overline{K}_{x^0y^0} \cdot F.\end{aligned} \tag{A.36}$$

Both of the above expressions satisfy the differential equations in which we turn off the interaction part, namely,

$$\begin{aligned}&\left[\frac{\overrightarrow{\partial}^2}{\partial x^{0\,2}} + \Omega^2_{i,x^0,\mathbf{k}}\right] \widehat{G}^{ab,\text{free}}_{ij,x^0y^0,\mathbf{k}} \\ &\quad = E^{ac}_{ik,\mathbf{k}} \widehat{G}^{cb,\text{free}}_{kj,t_0y^0,\mathbf{k}} \delta_{t_0x^0} + F^{ab}_{ij} \delta_{x^0y^0},\end{aligned} \tag{A.37}$$

$$\begin{aligned}&\widehat{G}^{ab,\text{free}}_{ij,x^0y^0,\mathbf{k}} \left[\frac{\overleftarrow{\partial}^2}{\partial y^{0\,2}} + \Omega^2_{i,y^0,\mathbf{k}}\right] \\ &\quad = \widehat{G}^{ac,\text{free}}_{ik,x^0t_0,\mathbf{k}} E^{Tcb}_{kj,\mathbf{k}} \delta_{t_0y^0} + F^{ab}_{ij} \delta_{x^0y^0},\end{aligned} \tag{A.38}$$

Below we show both expressions in (A.35) and (A.36) lead to a single expression. Using (66), (83), and (A.28), we can rewrite them as follows:

$$\widehat{G}^{ab,br,\text{free}}_{ij,x^0y^0}(\mathbf{k}) = \frac{\delta_{ij}}{2\omega_i(\mathbf{k})\,a^3_{t_0}}\left[\frac{\sinh\beta\omega_i(\mathbf{k})}{\cosh\beta\omega_i(\mathbf{k})-1}\right] \cdot \begin{pmatrix}1&1\\1&1\end{pmatrix}^{ab} \times\left[\overline{K}'_{i,x^0t_0}\overline{K}'_{i,y^0t_0}+\omega_i^2(\mathbf{k})\,\overline{K}_{i,x^0t_0}\overline{K}_{i,y^0t_0}\right] + \frac{i\delta_{ij}}{2a^3_{t_0}}\left(\overline{K}'_{i,x^0t_0}\overline{K}_{i,y^0t_0}-\overline{K}_{i,x^0t_0}\overline{K}'_{i,y^0t_0}\right)\begin{pmatrix}-1&1\\-1&1\end{pmatrix}^{ab} - \frac{i\delta_{ij}}{2a^3_{t_0}}\theta\left(y^0-x^0\right)\overline{K}_{i,y^0x^0}c^{ab}, \quad (A.39)$$

$$\widehat{G}^{ab,go,\text{free}}_{ij,x^0y^0}(\mathbf{k}) = \frac{\delta_{ij}}{2\omega_i(\mathbf{k})\,a^3_{t_0}}\left[\frac{\sinh\beta\omega_i(\mathbf{k})}{\cosh\beta\omega_i(\mathbf{k})-1}\right] \cdot \begin{pmatrix}1&1\\1&1\end{pmatrix}^{ab} \times\left[\overline{K}'_{i,x^0t_0}\overline{K}'_{i,y^0t_0}+\omega_i^2(\mathbf{k})\,\overline{K}_{i,x^0t_0}\overline{K}_{i,y^0t_0}\right] + \frac{i\delta_{ij}}{2a^3_{t_0}}\left(\overline{K}'_{i,x^0t_0}\overline{K}_{i,y^0t_0}-\overline{K}_{i,x^0t_0}\overline{K}'_{i,y^0t_0}\right) \cdot\begin{pmatrix}1&1\\-1&-1\end{pmatrix}^{ab} - \frac{i\delta_{ij}}{2a^3_{t_0}}\theta\left(x^0-y^0\right)\overline{K}_{i,x^0y^0}c^{ab}. \quad (A.40)$$

By using the following relation,

$$\overline{K}'_{i,x^0t_0}\overline{K}_{i,y^0t_0}-\overline{K}_{i,x^0t_0}\overline{K}'_{i,y^0t_0}=\overline{K}_{i,x^0y^0}, \quad (A.41)$$

we can show that two expressions are identical to each other. Therefore, they can be summarized into a single expression which is (79).

A.5. The Interaction Part of Green's Function and Its Path Independence. Now we move to consider the interaction parts of Green's function. From (A.31) and (A.32), we can temporary define them, respectively, as

$$\widehat{G}^{br,\text{int}}_{x^0y^0} := \int_{t_0^+}^{y^0} R_{x^0t}\cdot\overline{K}_{y^0t}\,dt + \int_{t_0^+}^{x^0}\overline{K}_{x^0t}\cdot Q_{tt_0}\,dt \cdot\left(E^T\cdot\overline{K}_{y^0t_0}-\overline{K}'_{y^0t_0}\right), \quad (A.42)$$

$$\widehat{G}^{go,\text{int}}_{x^0y^0} := \int_{t_0^+}^{x^0}\overline{K}_{x^0t}\cdot Q_{ty^0}\,dt + \left(\overline{K}_{x^0t_0}\cdot E-\overline{K}'_{x^0t_0}\right) \cdot\int_{t_0^+}^{y^0}R_{t_0t}\cdot\overline{K}_{y^0t}\,dt, \quad (A.43)$$

where Q and R are written in terms of the same $\widehat{G}$ and $\widehat{\varphi}$ in (A.29) and (A.30). Below, we will show the two expressions are similar to each other. Remind us that Q and R in (A.42) and (A.43) are written in terms of $\widehat{G}_{x^0y^0,\text{int}}$ in (78) through the following differential equation:

$$Q_{x^0y^0} = \left[\frac{\overrightarrow{\partial}^2}{\partial x^{0\,2}}+\Omega^2_{x^0}\right]\widehat{G}^{\text{int}}_{x^0y^0} - E\cdot\widehat{G}^{\text{int}}_{t_0y^0}\delta_{t_0x^0}, \quad (A.44)$$

$$R_{x^0y^0} = \widehat{G}^{\text{int}}_{x^0y^0}\left[\frac{\overleftarrow{\partial}^2}{\partial y^{0\,2}}+\Omega^2_{y^0}\right] - \widehat{G}^{\text{int}}_{x^0t_0}\cdot E^T\delta_{t_0y^0}. \quad (A.45)$$

Substituting these expressions to (A.42) and (A.43), we obtain

$$\widehat{G}^{go,\text{int}}_{x^0y^0} = \widehat{G}^{\text{int}}_{x^0y^0} + \overline{K}_{x^0t_0}\cdot\left(E\cdot\widehat{G}^{\text{int}}_{t_0y^0} - \lim_{t\to t_0}\frac{\partial\widehat{G}^{\text{int}}_{ty^0}}{\partial t}\right) + \left(\overline{K}_{x^0t_0}\cdot E-\overline{K}'_{x^0t_0}\right)\cdot\widehat{G}^{\text{int}}_{t_0t_0}\cdot\overline{K}'_{y^0t_0} + \left(\overline{K}'_{x^0t_0}-\overline{K}_{x^0t_0}\cdot E\right)\cdot\lim_{t\to t_0}\frac{\partial\widehat{G}^{\text{int}}_{t_0t}}{\partial t} \cdot\overline{K}_{y^0t_0}, \quad (A.46)$$

$$= \widehat{G}^{\text{int}}_{x^0y^0}, \quad (A.47)$$

$$\widehat{G}^{br,\text{int}}_{x^0y^0} = \widehat{G}^{\text{int}}_{x^0y^0} + \left(\widehat{G}^{\text{int}}_{x^0t_0}\cdot E^T - \lim_{t\to t_0}\frac{\partial\widehat{G}^{\text{int}}_{x^0t}}{\partial t}\right)\cdot\overline{K}_{y^0t_0} + \overline{K}'_{x^0t_0}\cdot\widehat{G}^{\text{int}}_{t_0t_0}\cdot\left(E^T\cdot\overline{K}_{y^0t_0}-\overline{K}'_{y^0t_0}\right) + \overline{K}_{x^0t_0}\cdot\lim_{t\to t_0}\frac{\partial\widehat{G}^{\text{int}}_{tt_0}}{\partial t} \cdot\left(\overline{K}'_{y^0t_0}-E^T\cdot\overline{K}_{y^0t_0}\right), \quad (A.48)$$

$$= \widehat{G}^{\text{int}}_{x^0y^0}, \quad (A.49)$$

respectively. To show the equalities of (A.47) and (A.49), we have used the following relations:

$$\widehat{G}^{\text{int}}_{t_0t_0} = 0, \quad (A.50)$$

$$\lim_{t\to t_0}\frac{\partial}{\partial t}\widehat{G}^{\text{int}}_{t_0t} = 0, \quad (A.51)$$

$$\lim_{t\to t_0}\frac{\partial\widehat{G}^{\text{int}}_{tt_0}}{\partial t} = 0, \quad (A.52)$$

$$E\cdot\widehat{G}^{\text{int}}_{t_0y^0} = \lim_{t\to t_0}\frac{\partial\widehat{G}^{\text{int}}_{ty^0}}{\partial t}, \quad (A.53)$$

$$\widehat{G}^{\text{int}}_{x^0t_0}\cdot E^T = \lim_{t\to t_0}\frac{\partial\widehat{G}^{\text{int}}_{x^0t}}{\partial t}. \quad (A.54)$$

We complete the proof of equality of two expressions given in (A.42) and (A.43). Since they are identical to each other, from now on, we will use $\widehat{G}^{br,\text{int}}_{x^0y^0}$ in (A.42).

To summarize this subsection, let us write the SDEs of Green's functions in the form of integral equations. Omitting the upper and lower indices i, j, a, and b, the interaction part of Green's function is written as

$$\begin{aligned} &\widehat{G}^{\text{int}}_{x^0 y^0} \\ &= \int_{t_0^+}^{y^0} R_{x^0 t} \cdot \overline{K}_{y^0 t}\, dt \\ &\quad - \int_{t_0^+}^{x^0} \overline{K}_{x^0 t} \cdot \left[Q_{tt_0} \cdot \overline{K}'_{y^0 t_0} - Q_{tt_0} \cdot E^T \cdot \overline{K}_{y^0 t_0} \right] dt, \end{aligned} \tag{A.55}$$

where Q and R are given in (A.29) and (A.30). Using the above equations and keeping the solutions up to the first order of the cubic interaction, one can obtain (80).

B. Derivation for $f(x^0)$ and $g(x^0)$ up to First Order of $H(t_0)$

$f(x^0)$ and $g(x^0)$ are the solutions of a homogeneous differential equation given in (75) and (76). In this appendix, we derive those solutions for the case that the scale factor is given in (87). We present them within linear approximation with respect to $H(t_0)$.

One first considers a couple of general homogeneous differential equations given in (75) and (76). As for $\Omega_{i,\mathbf{k}}(x^0)$, we substitute the expression given in (93). The solutions are expanded up to the first order with respect to $H(t_0)$,

$$f_{i,\mathbf{k}}\left(x^0\right) = f^{(0)}_{i,\mathbf{k}}\left(x^0\right) + f^{(1)}_{i,\mathbf{k}}\left(x^0\right), \tag{B.1}$$

$$g_{i,\mathbf{k}}\left(x^0\right) = g^{(0)}_{i,\mathbf{k}}\left(x^0\right) + g^{(1)}_{i,\mathbf{k}}\left(x^0\right), \tag{B.2}$$

where $f^{(0)}(x^0)$ and $g^{(0)}(x^0)$ are the solutions which correspond to the zeroth order of $H(t_0)$ while $f^{(1)}(x^0)$ and $g^{(1)}(x^0)$ are the solutions which correspond to the first order correction with respect to $H(t_0)$.

We first compute solution for $f(x^0)$. The differential equations of $f(x^0)$ in (75) can be rewritten as

$$\left[\frac{1}{\omega^2_{i,\mathbf{k}}} \frac{\partial^2}{\partial x^{0 2}} + \frac{\Omega^2_{i,\mathbf{k}}\left(x^0\right)}{\omega^2_{i,\mathbf{k}}} \right] f_{i,\mathbf{k}}\left(x^0\right) = 0. \tag{B.3}$$

Using (93), the second term in parentheses of above expression is rewritten as

$$\frac{\Omega^2_{i,\mathbf{k}}\left(x^0\right)}{\omega^2_{i,\mathbf{k}}} = 1 - 2H\left(t_0\right)\left(x^0 - t_0\right) \frac{\mathbf{k}^2}{\left[a\left(t_0\right)\omega_{i,\mathbf{k}}\right]^2}. \tag{B.4}$$

Then using (B.4), (B.3) alters into

$$\begin{aligned} &\left[\frac{1}{\omega^2_{i,\mathbf{k}}} \frac{\partial^2}{\partial x^{0 2}} + 1 - 2H\left(t_0\right)\left(x^0 - t_0\right) \frac{\mathbf{k}^2}{\left[a\left(t_0\right)\omega_{i,\mathbf{k}}\right]^2} \right] \\ &\quad \cdot f_{i,\mathbf{k}}\left(x^0\right) = 0. \end{aligned} \tag{B.5}$$

One can define several dimensionless parameters as

$$\begin{aligned} s &:= \omega_{i,\mathbf{k}} x^0, \\ s_0 &:= \omega_{i,\mathbf{k}} t_0, \\ h_0 &:= \frac{H\left(t_0\right)}{\omega_{i,\mathbf{k}}}, \\ \mathbf{l} &:= \frac{\mathbf{k}}{a\left(t_0\right)\omega_{i,\mathbf{k}}} \end{aligned} \tag{B.6}$$

Then using the above dimensionless parameters, (B.5) is rewritten as (for simplicity, we omit the lower indices, i and $\mathbf{k}$)

$$\left[\frac{\partial^2}{\partial s^2} + 1 - 2h_0\left(s - s_0\right)\mathbf{l}^2 \right] f\left(s\right) = 0. \tag{B.7}$$

The above equation leads to the following leading equations:

$$\left[\frac{\partial^2}{\partial s^2} + 1 \right] f^{(0)}\left(s\right) = 0, \tag{B.8}$$

$$\left[\frac{\partial^2}{\partial s^2} + 1 \right] f^{(1)}\left(s\right) = 2h_0\left(s - s_0\right)\mathbf{l}^2 f^{(0)}\left(s\right). \tag{B.9}$$

As for the solution of (B.8), we choose

$$f^{(0)}\left(s\right) = \sin\left(s\right). \tag{B.10}$$

Next one needs to solve $f^{(1)}(s)$. The solution is written in terms of linear combination of sine and cosine functions,

$$f^{(1)}\left(s\right) = C_1\left(s\right)\sin\left(s\right) + C_2\left(s\right)\cos\left(s\right), \tag{B.11}$$

where their coefficients C_i depend on time. Since we can impose the following condition,

$$C_1'\left(s\right)\sin\left(s\right) + C_2'\left(s\right)\cos\left(s\right) = 0, \tag{B.12}$$

one can show that $C_i(s)$ satisfy

$$\begin{aligned} &C_1'\left(s\right)\cos\left(s\right) - C_2'\left(s\right)\sin\left(s\right) \\ &\quad = 2h_0\left(s - s_0\right)\mathbf{l}^2 \sin\left(s\right), \end{aligned} \tag{B.13}$$

where $C_i'(s)$ are defined as

$$C_i'\left(s\right) := \frac{dC_i\left(s\right)}{ds}. \tag{B.14}$$

From (B.12) and (B.13), one can write $C_i'(s)$ as

$$\begin{aligned} C_1'\left(s\right) &= h_0\left(s - s_0\right)\mathbf{l}^2 \sin\left(2s\right), \\ C_2'\left(s\right) &= h_0\left(s - s_0\right)\mathbf{l}^2 \left\{\cos\left(2s\right) - 1\right\}. \end{aligned} \tag{B.15}$$

With the initial conditions $C_i(s_0) = 0$, $C_i(s)$ are written as

$$\begin{aligned} C_1\left(s\right) &= -\frac{h_0\mathbf{l}^2}{2}\left[\left(s - s_0\right)\cos\left(2s\right) \right. \\ &\quad \left. - \frac{1}{2}\left\{\sin\left(2s\right) - \sin\left(2s_0\right)\right\}\right], \end{aligned} \tag{B.16}$$

$$\begin{aligned} C_2\left(s\right) &= \frac{h_0\mathbf{l}^2}{2}\left[\left(s - s_0\right)\left\{\sin\left(2s\right) - 2s\right\} \right. \\ &\quad \left. + \frac{1}{2}\left\{\cos\left(2s\right) - \cos\left(2s_0\right)\right\} + \left(s^2 - s_0^2\right)\right]. \end{aligned} \tag{B.17}$$

Now using (B.16) and (B.17), the solution of $f^{(1)}(s)$ is written as

$$f^{(1)}(s)=\frac{h_0\mathbf{l}^2}{2}(s-s_0)\left\{\sin(s)-\frac{\sin(s-s_0)}{(s-s_0)}\sin(s_0)-(s-s_0)\cos(s)\right\}. \tag{B.18}$$

To summarize this part, let us write $f^{(0)}(s)$ and $f^{(1)}(s)$ in terms of original dimensional parameters. They are given by

$$f^{(0)}\left(x^0\right)=\sin\left[\omega_{i,\mathbf{k}}x^0\right], \tag{B.19}$$

$$f^{(1)}\left(x^0\right)=\frac{H(t_0)\mathbf{k}^2\left(x^0-t_0\right)}{2\left\{a(t_0)\omega_{i,\mathbf{k}}\right\}^2}\left\{\sin\left[\omega_{i,\mathbf{k}}x^0\right]-\frac{\sin\left[\omega_{i,\mathbf{k}}\left(x^0-t_0\right)\right]}{\omega_{i,\mathbf{k}}\left(x^0-t_0\right)}\sin\left[\omega_{i,\mathbf{k}}t_0\right]-\omega_{i,\mathbf{k}}\left(x^0-t_0\right)\cos\left[\omega_{i,\mathbf{k}}x^0\right]\right\}. \tag{B.20}$$

Now we move to compute for $g(x^0)$. In this regard, $g(s)$ satisfies the same equation in (B.7) which $f(s)$ satisfies. The difference is that $g^0(s)$ is a cosine function,

$$g^{(0)}(s)=\cos(s). \tag{B.21}$$

Applying the same procedure which we have used for the derivation of $f^1(s)$, we obtain

$$g^{(1)}(s)=\frac{h_0\mathbf{l}^2}{2}(s-s_0)\left[\cos(s)-\frac{\sin(s-s_0)}{(s-s_0)}\cos(s_0)+(s-s_0)\sin(s)\right]. \tag{B.22}$$

Finally, one rewrites $g^{(0)}(s)$ and $g^{(1)}(s)$ in terms of original variables. They are given by

$$g^{(0)}\left(x^0\right)=\cos\left[\omega_{i,\mathbf{k}}x^0\right], \tag{B.23}$$

$$g^{(1)}\left(x^0\right)=\frac{H(t_0)\mathbf{k}^2\left(x^0-t_0\right)}{2\left\{a(t_0)\omega_{i,\mathbf{k}}\right\}^2}\left\{\cos\left[\omega_{i,\mathbf{k}}x^0\right]-\frac{\sin\left[\omega_{i,\mathbf{k}}\left(x^0-t_0\right)\right]}{\omega_{i,\mathbf{k}}\left(x^0-t_0\right)}\cos\left[\omega_{i,\mathbf{k}}t_0\right]+\omega_{i,\mathbf{k}}\left(x^0-t_0\right)\sin\left[\omega_{i,\mathbf{k}}x^0\right]\right\}. \tag{B.24}$$

C. Derivation of $\overline{K}_i[x^0,y^0]$ up to First Order of $H(t_0)$

In this appendix, we present $\overline{K}_{i,x^0y^0,\mathbf{k}}$ given in (73) within the linear approximation with respect to $H(t_0)$. For simplicity, momentum index $\mathbf{k}$ is suppressed. $\overline{K}_{i,x^0y^0,\mathbf{k}}$ is also expanded up to the first order with respect to $H(t_0)$, namely,

$$\overline{K}_i\left[x^0,y^0\right]=\overline{K}_i^{(0)}\left[x^0,y^0\right]+\overline{K}_i^{(1)}\left[x^0,y^0\right], \tag{C.1}$$

where we have defined

$$\overline{K}_i^{(0)}\left[x^0,y^0\right]\coloneqq\frac{1}{W_i}\left\{f_i^{(0)}\left(x^0\right)g_i^{(0)}\left(y^0\right)-f_i^{(0)}\left(y^0\right)g_i^{(0)}\left(x^0\right)\right\}, \tag{C.2}$$

$$\overline{K}_i^{(1)}\left[x^0,y^0\right]\coloneqq\frac{1}{W_i}\left\{f_i^{(0)}\left(x^0\right)g_i^{(1)}\left(y^0\right)-f_i^{(0)}\left(y^0\right)g_i^{(1)}\left(x^0\right)+f_i^{(1)}\left(x^0\right)g_i^{(0)}\left(y^0\right)-f_i^{(1)}\left(y^0\right)g_i^{(0)}\left(x^0\right)\right\}. \tag{C.3}$$

One can show that W is written in terms of the zeroth order solutions $f_i^{(0)}$, $g_i^{(0)}$, and their derivatives.

$$W_i=\dot{f}_i^{(0)}(t_0)\,g_i^{(0)}(t_0)-f_i^{(0)}(t_0)\,\dot{g}_i^{(0)}(t_0)=\omega_{i,\mathbf{k}}, \tag{C.4}$$

because $f^{(1)}(t_0)$, $\dot{f}^{(1)}(t_0)$, $g^{(1)}(t_0)$, and $\dot{g}^{(1)}(t_0)$ vanish. Substituting the zeroth order function and the first order function of f and g in (B.10), (B.18), (B.21), and (B.22), equations (C.2) and (C.3) alter into

$$\begin{aligned}\overline{K}_i^{(0)}\left[x^0,y^0\right]&=\frac{\sin(s-u)}{\omega_{i,\mathbf{k}}}\\ \overline{K}_i^{(1)}\left[x^0,y^0\right]&=\frac{h_0\mathbf{l}^2}{2\omega_{i,\mathbf{k}}}\{u+s-2s_0\}\cdot[\sin(s-u)+(u-s)\cos(s-u)]\end{aligned} \tag{C.5}$$

where we have defined the following dimensionless parameters as

$$\begin{aligned}u&\coloneqq\omega_{i,\mathbf{k}}y^0,\\ s_0&\coloneqq u_0=\omega_{i,\mathbf{k}}t_0.\end{aligned} \tag{C.6}$$

and s, s_0, h_0, and $\mathbf{l}$ are defined in (B.6), respectively. Therefore, $\overline{K}_i[x^0,y^0]$ in (C.1) is written in terms of original parameters as

$$\begin{aligned}\overline{K}_i\left[x^0,y^0\right]&=\overline{K}_i^{(0)}\left[x^0,y^0\right]+\overline{K}_i^{(1)}\left[x^0,y^0\right]\\ \overline{K}_i^{(0)}\left[x^0,y^0\right]&=\frac{\sin\left[\omega_{i,\mathbf{k}}\left(x^0-y^0\right)\right]}{\omega_{i,\mathbf{k}}},\end{aligned} \tag{C.7}$$

$$\overline{K}_i^{(1)}\left[x^0,y^0\right]=\frac{H(t_0)}{2}\frac{\mathbf{k}^2}{\omega_{i,\mathbf{k}}^2a(t_0)^2}\left(x^0+y^0-2t_0\right)\times\left(\frac{\sin\left[\omega_{i,\mathbf{k}}\left(x^0-y^0\right)\right]}{\omega_{i,\mathbf{k}}}-\left(x^0-y^0\right)\cos\left[\omega_{i,\mathbf{k}}\left(x^0-y^0\right)\right]\right). \tag{C.8}$$

We define $\dot{\overline{K}}_i$ and $\dot{\overline{K}}_i'$ as

$$\dot{\overline{K}}_i\left[x^0, y^0\right] := \frac{\partial \overline{K}_i\left[x^0, y^0\right]}{\partial x^0}, \tag{C.9}$$

$$\dot{\overline{K}}_i'\left[x^0, y^0\right] := \frac{\partial^2 \overline{K}_i\left[x^0, y^0\right]}{\partial x^0 \partial y^0}. \tag{C.10}$$

Then $\overline{K}_i'$ in (A.20), $\dot{\overline{K}}_i$, and $\dot{\overline{K}}_i'$ are given in terms of original parameters by

$$\begin{aligned}\overline{K}_i'\left[x^0, y^0\right] &= \overline{K}_i^{(0)\prime}\left[x^0, y^0\right] + \overline{K}_i^{(1)\prime}\left[x^0, y^0\right],\\ \overline{K}_i^{(0)\prime}\left[x^0, y^0\right] &= -\cos(s-u)\\ &= -\cos\left[\omega_{i,\mathbf{k}}\left(x^0 - y^0\right)\right],\end{aligned} \tag{C.11}$$

$$\begin{aligned}\overline{K}_i^{(1)\prime}\left[x^0, y^0\right] &= \frac{h_0 \mathbf{l}^2}{2}\left[(u-s)\cos(s-u)\right.\\ &\quad \left.+\left\{1+\left(u+s-2s_0\right)(u-s)\right\}\sin(s-u)\right],\\ &= H\left(t_0\right)\frac{\mathbf{k}^2}{2\omega_{i,\mathbf{k}}^3 a\left(t_0\right)^2}\left[\omega_{i,\mathbf{k}}\left(y^0 - x^0\right)\right.\\ &\quad \cdot\cos\left[\omega_{i,\mathbf{k}}\left(x^0 - y^0\right)\right]\\ &\quad + \left\{1+\omega_{i,\mathbf{k}}^2\left(y^0 + x^0 - 2t_0\right)\left(y^0 - x^0\right)\right\}\\ &\quad \left.\cdot\sin\left[\omega_{i,\mathbf{k}}\left(x^0 - y^0\right)\right]\right],\end{aligned} \tag{C.12}$$

$$\begin{aligned}\dot{\overline{K}}_i\left[x^0, y^0\right] &= \dot{\overline{K}}_i^{(0)}\left[x^0, y^0\right] + \dot{\overline{K}}_i^{(1)}\left[x^0, y^0\right],\\ \dot{\overline{K}}_i^{(0)}\left[x^0, y^0\right] &= \cos(s-u) = \cos\left[\omega_{i,\mathbf{k}}\left(x^0 - y^0\right)\right],\end{aligned} \tag{C.13}$$

$$\begin{aligned}\dot{\overline{K}}_i^{(1)}\left[x^0, y^0\right] &= \frac{h_0 \mathbf{l}^2}{2}\left[(u-s)\cos(s-u)\right.\\ &\quad \left.+\left\{1-\left(u+s-2s_0\right)(u-s)\right\}\sin(s-u)\right]\\ &= H\left(t_0\right)\frac{\mathbf{k}^2}{2\omega_{i,\mathbf{k}}^3 a\left(t_0\right)^2}\left[\omega_{i,\mathbf{k}}\left(y^0 - x^0\right)\right.\\ &\quad \cdot\cos\left[\omega_{i,\mathbf{k}}\left(x^0 - y^0\right)\right]\\ &\quad + \left\{1-\omega_{i,\mathbf{k}}^2\left(y^0 + x^0 - 2t_0\right)\left(y^0 - x^0\right)\right\}\\ &\quad \left.\cdot\sin\left[\omega_{i,\mathbf{k}}\left(x^0 - y^0\right)\right]\right],\end{aligned} \tag{C.14}$$

$$\begin{aligned}\dot{\overline{K}}_i'\left[x^0, y^0\right] &= \dot{\overline{K}}_i^{(0)\prime}\left[x^0, y^0\right] + \dot{\overline{K}}_i^{(1)\prime}\left[x^0, y^0\right],\\ \dot{\overline{K}}_i^{(0)\prime}\left[x^0, y^0\right] &= \omega_{i,\mathbf{k}}\sin(s-u) = \omega_{i,\mathbf{k}}\\ &\quad \cdot\sin\left[\omega_{i,\mathbf{k}}\left(x^0 - y^0\right)\right],\end{aligned} \tag{C.15}$$

$$\begin{aligned}\dot{\overline{K}}_i^{(1)\prime}\left[x^0, y^0\right] &= \frac{h_0 \mathbf{l}^2}{2}\omega_{i,\mathbf{k}}\left(u+s-2s_0\right)\left[(u-s)\right.\\ &\quad \left.\cdot\cos(s-u) - \sin(s-u)\right] = H\left(t_0\right)\\ &\quad \cdot\frac{\mathbf{k}^2}{2\omega_{i,\mathbf{k}} a\left(t_0\right)^2}\left(y^0 + x^0 - 2t_0\right)\\ &\quad \times\left\{\omega_{i,\mathbf{k}}\left(y^0 - x^0\right)\cos\left[\omega_{i,\mathbf{k}}\left(x^0 - y^0\right)\right]\right.\\ &\quad \left.- \sin\left[\omega_{i,\mathbf{k}}\left(x^0 - y^0\right)\right]\right\}.\end{aligned} \tag{C.16}$$

D. Calculation of the Expectation Value of PNA

D.1. Time Integration and Momentum Integration of $\langle \boldsymbol{j}_0(\boldsymbol{x}^0)\rangle_{1st}$.

In this section, we provide both time and momentum integrations in the expression of the expectation value of the PNA. Let us first consider (97). It can be rewritten as

$$\left\langle j_0\left(x^0\right)\right\rangle_{\mathrm{1st}} = \left\langle j_0\left(x^0\right)\right\rangle_{\mathrm{1st},A} + \left\langle j_0\left(x^0\right)\right\rangle_{\mathrm{1st},B}, \tag{D.1}$$

where $\langle j_0(x^0)\rangle_{\mathrm{1st},A}$ and $\langle j_0(x^0)\rangle_{\mathrm{1st},B}$ are given by

$$\begin{aligned}\left\langle j_0\left(x^0\right)\right\rangle_{\mathrm{1st},A} &= \frac{1}{a_{t_0}^3}\widehat{\varphi}_{3,t_0}A_{123}\left\{1 - 3\left(x^0 - t_0\right)\right.\\ &\quad \left.\cdot H\left(t_0\right)\right\}\int\frac{d^3\mathbf{k}}{(2\pi)^3}\left[\frac{1}{2}\left(\frac{1}{\omega_{2,\mathbf{k}}} + \frac{1}{\omega_{1,\mathbf{k}}}\right)\right.\\ &\quad \times\left(\coth\frac{\beta\omega_{2,\mathbf{k}}}{2} - \coth\frac{\beta\omega_{1,\mathbf{k}}}{2}\right)\\ &\quad \cdot\int_{t_0}^{x^0}\cos\omega_{3,\mathbf{0}}t\cos\left(\omega_{1,\mathbf{k}} - \omega_{2,\mathbf{k}}\right)\left(x^0 - t\right)dt\\ &\quad + \frac{1}{2}\left(\frac{1}{\omega_{2,\mathbf{k}}} - \frac{1}{\omega_{1,\mathbf{k}}}\right)\left(\coth\frac{\beta\omega_{2,\mathbf{k}}}{2} + \coth\frac{\beta\omega_{1,\mathbf{k}}}{2}\right)\\ &\quad \left.\times\int_{t_0}^{x^0}\cos\omega_{3,\mathbf{0}}t\cos\left(\omega_{1,\mathbf{k}} + \omega_{2,\mathbf{k}}\right)\left(x^0 - t\right)dt\right],\end{aligned} \tag{D.2}$$

$$\begin{aligned}\left\langle j_0\left(x^0\right)\right\rangle_{\mathrm{1st},B} &= -\frac{3}{2}\frac{H\left(t_0\right)}{a_{t_0}^3}\\ &\quad \cdot\widehat{\varphi}_{3,t_0}A_{123}\int\frac{d^3\mathbf{k}}{(2\pi)^3}\left[\frac{1}{2}\left(\frac{1}{\omega_{2,\mathbf{k}}} + \frac{1}{\omega_{1,\mathbf{k}}}\right)\right.\\ &\quad \cdot\left(\coth\frac{\beta\omega_{2,\mathbf{k}}}{2} - \coth\frac{\beta\omega_{1,\mathbf{k}}}{2}\right)\times\int_{t_0}^{x^0}\left(t - t_0\right)\\ &\quad \cdot\cos\omega_{3,\mathbf{0}}\left(t - t_0\right)\cos\left(\omega_{1,\mathbf{k}} - \omega_{2,\mathbf{k}}\right)\left(x^0 - t\right)dt\\ &\quad + \frac{1}{2}\left(\frac{1}{\omega_{2,\mathbf{k}}} - \frac{1}{\omega_{1,\mathbf{k}}}\right)\left(\coth\frac{\beta\omega_{2,\mathbf{k}}}{2} + \coth\frac{\beta\omega_{1,\mathbf{k}}}{2}\right)\\ &\quad \times\int_{t_0}^{x^0}\left(t - t_0\right)\\ &\quad \left.\cdot\cos\omega_{3,\mathbf{0}}\left(t - t_0\right)\cos\left(\omega_{1,\mathbf{k}} + \omega_{2,\mathbf{k}}\right)\left(x^0 - t\right)dt\right].\end{aligned} \tag{D.3}$$

$\langle j_0(x^0)\rangle_{\mathrm{1st},A}$ is the part which includes the PNA with constant scale factor and dilution effect while $\langle j_0(x^0)\rangle_{\mathrm{1st},B}$ is the part which includes the freezing interaction effect. One can derive (D.2) and (D.3) by substituting (C.7), (C.11), (C.13), and (C.15) into (97).

Below we first carry out time integration of $\langle j_0(x^0)\rangle_{1\text{st},A}$. One defines the new variable of integration as

$$s := x^0 - t, \tag{D.4}$$

$$x^1 := x^0 - t_0. \tag{D.5}$$

Then one obtains that

$$\begin{aligned}
&\left\langle j_0\left(x^1+t_0\right)\right\rangle_{1\text{st},A} \\
&= \frac{\omega_{3,\mathbf{0}}}{2a_{t_0}^3}\widehat{\varphi}_{3,t_0}A_{123}\left(\widetilde{m}_1^2-\widetilde{m}_2^2\right)\left\{1-3x^1H\left(t_0\right)\right\}\int\frac{d^3\mathbf{k}}{(2\pi)^3}\frac{1}{\omega_{1,\mathbf{k}}\omega_{2,\mathbf{k}}} \\
&\times\left[\left(\frac{2e^{-\beta\omega_{2,\mathbf{k}}}}{1-e^{-\beta\omega_{2,\mathbf{k}}}}\right.\right. \\
&\left.-\frac{2e^{-\beta\omega_{1,\mathbf{k}}}}{1-e^{-\beta\omega_{1,\mathbf{k}}}}\right) \\
&\cdot\frac{\sin\left[\omega_{3,\mathbf{0}}x^1\right]/\left(\omega_{1,\mathbf{k}}-\omega_{2,\mathbf{k}}\right)-\sin\left[\left(\omega_{1,\mathbf{k}}-\omega_{2,\mathbf{k}}\right)x^1\right]/\omega_{3,\mathbf{0}}}{\omega_{3,\mathbf{0}}^2-\left(\omega_{1,\mathbf{k}}-\omega_{2,\mathbf{k}}\right)^2}+\left(\frac{1+e^{-\beta\omega_{2,\mathbf{k}}}}{1-e^{-\beta\omega_{2,\mathbf{k}}}}\right. \\
&\left.+\frac{1+e^{-\beta\omega_{1,\mathbf{k}}}}{1-e^{-\beta\omega_{1,\mathbf{k}}}}\right) \\
&\left.\cdot\frac{\sin\left[\omega_{3,\mathbf{0}}x^1\right]/\left(\omega_{1,\mathbf{k}}+\omega_{2,\mathbf{k}}\right)-\sin\left[\left(\omega_{1,\mathbf{k}}+\omega_{2,\mathbf{k}}\right)x^1\right]/\omega_{3,\mathbf{0}}}{\omega_{3,\mathbf{0}}^2-\left(\omega_{1,\mathbf{k}}+\omega_{2,\mathbf{k}}\right)^2}\right].
\end{aligned} \tag{D.6}$$

By taking first time derivative of the above expression, setting $x^1 = 0$, using the initial expectation value of $\widehat{\varphi}_{3,t_0} = v_3$ and setting $H(t_0) = 0$, we obtain (100).

We move now to compute $\langle j_0(x^0)\rangle_{1\text{st},B}$. To perform time integration for $\langle j_0(x^0)\rangle_{1\text{st},B}$, one introduces the new variable of integration,

$$s := t - t_0, \tag{D.7}$$

and obtains

$$\begin{aligned}
&\left\langle j_0\left(x^1+t_0\right)\right\rangle_{1\text{st},B} = -\frac{3H\left(t_0\right)\omega_{3,\mathbf{0}}}{4a_{t_0}^3}\widehat{\varphi}_{3,t_0}A_{123}\left(\widetilde{m}_1^2-\widetilde{m}_2^2\right) \\
&\cdot\int\frac{d^3\mathbf{k}}{(2\pi)^3}\frac{1}{\omega_{1,\mathbf{k}}\omega_{2,\mathbf{k}}}\left[\left(\frac{\coth\left(\beta\omega_{2,\mathbf{k}}/2\right)-\coth\left(\beta\omega_{1,\mathbf{k}}/2\right)}{\omega_{12,\mathbf{k}}^-}\right)\right. \\
&\times\left(\frac{x^1\sin\omega_{3,\mathbf{0}}x^1}{\left(\omega_{3,\mathbf{0}}^2-\omega_{12,\mathbf{k}}^{-\,2}\right)}\right. \\
&\left.+\frac{\left(\left(\omega_{3,\mathbf{0}}^2+\omega_{12,\mathbf{k}}^{-\,2}\right)/\omega_{3,\mathbf{0}}\right)\left\{\cos\omega_{3,\mathbf{0}}x^1-\cos\left[\omega_{12,\mathbf{k}}^-x^1\right]\right\}}{\left(\omega_{3,\mathbf{0}}^2-\omega_{12,\mathbf{k}}^{-\,2}\right)^2}\right) \\
&+\left(\frac{\coth\left(\beta\omega_{2,\mathbf{k}}/2\right)+\coth\left(\beta\omega_{1,\mathbf{k}}/2\right)}{\omega_{12,\mathbf{k}}^+}\right)\left(\frac{x^1\sin\omega_{3,\mathbf{0}}x^1}{\left(\omega_{3,\mathbf{0}}^2-\omega_{12,\mathbf{k}}^{+\,2}\right)}\right. \\
&\left.\left.+\frac{\left(\left(\omega_{3,\mathbf{0}}^2+\omega_{12,\mathbf{k}}^{+\,2}\right)/\omega_{3,\mathbf{0}}\right)\left\{\cos\omega_{3,\mathbf{0}}x^1-\cos\left[\omega_{12,\mathbf{k}}^+x^1\right]\right\}}{\left(\omega_{3,\mathbf{0}}^2-\omega_{12,\mathbf{k}}^{+\,2}\right)^2}\right)\right],
\end{aligned} \tag{D.8}$$

where we have defined $\omega_{12,\mathbf{k}}^{\pm}$ as

$$\omega_{12,\mathbf{k}}^{\pm} := \omega_{1,\mathbf{k}} \pm \omega_{2,\mathbf{k}}. \tag{D.9}$$

The next task is to integrate (D.6) and (D.8) with respect to spatial momentum. Using those equations, (D.1) leads to the following expression:

$$\begin{aligned}
&\left\langle j_0\left(x^1+t_0\right)\right\rangle_{1\text{st}} = -\frac{\widehat{\varphi}_{3,t_0}A_{123}}{a_{t_0}^3}\frac{\left(\widetilde{m}_1^2-\widetilde{m}_2^2\right)}{\omega_{3,\mathbf{0}}}\left[\left\{1\right.\right. \\
&\left.-3x^1H\left(t_0\right)\right\}\left\{J_1\left(x^1,\widetilde{m}_1,\widetilde{m}_2,\omega_{3,\mathbf{0}}\right)\right. \\
&\left.+J_2\left(x^1,\widetilde{m}_1,\widetilde{m}_2,\omega_{3,\mathbf{0}}\right)\right\}+\frac{3}{4}H\left(t_0\right) \\
&\left.\cdot\left\{J_3\left(x^1,\widetilde{m}_1,\widetilde{m}_2,\omega_{3,\mathbf{0}}\right)+J_4\left(x^1,\widetilde{m}_1,\widetilde{m}_2,\omega_{3,\mathbf{0}}\right)\right\}\right],
\end{aligned} \tag{D.10}$$

where auxiliary functions $J_i(x^1,\widetilde{m}_1,\widetilde{m}_2,\omega_{3,\mathbf{0}})$ $(i = 1,\ldots,4)$ are defined as

$$\begin{aligned}
J_1\left(x^1,\widetilde{m}_1,\widetilde{m}_2,\omega_{3,\mathbf{0}}\right) &:= -\frac{\sin\left[\omega_{3,\mathbf{0}}x^1\right]}{2}\int\frac{d^3\mathbf{k}}{(2\pi)^3}\frac{1}{\omega_{2,\mathbf{k}}\omega_{1,\mathbf{k}}}\frac{\left(\left(1+e^{-\beta\omega_{2,\mathbf{k}}}\right)/\left(1-e^{-\beta\omega_{2,\mathbf{k}}}\right)+\left(1+e^{-\beta\omega_{1,\mathbf{k}}}\right)/\left(1-e^{-\beta\omega_{1,\mathbf{k}}}\right)\right)}{1-\left(\omega_{12,\mathbf{k}}^+\right)^2/\omega_{3,\mathbf{0}}^2} \\
&\cdot\frac{1}{\omega_{12,\mathbf{k}}^+}+\frac{1}{2\omega_{3,\mathbf{0}}}\int\frac{d^3\mathbf{k}}{(2\pi)^3}\frac{1}{\omega_{2,\mathbf{k}}\omega_{1,\mathbf{k}}}\frac{\left(\left(1+e^{-\beta\omega_{2,\mathbf{k}}}\right)/\left(1-e^{-\beta\omega_{2,\mathbf{k}}}\right)+\left(1+e^{-\beta\omega_{1,\mathbf{k}}}\right)/\left(1-e^{-\beta\omega_{1,\mathbf{k}}}\right)\right)\sin\left[\omega_{12,\mathbf{k}}^+x^1\right]}{1-\left(\omega_{12,\mathbf{k}}^+\right)^2/\omega_{3,\mathbf{0}}^2},
\end{aligned} \tag{D.11}$$

$$\begin{aligned}
J_2\left(x^1,\widetilde{m}_1,\widetilde{m}_2,\omega_{3,\mathbf{0}}\right) &:= -\frac{\sin\left[\omega_{3,\mathbf{0}}x^1\right]}{2\left(\widetilde{m}_1^2-\widetilde{m}_2^2\right)}\int\frac{d^3\mathbf{k}}{(2\pi)^3}\frac{\omega_{12,\mathbf{k}}^+}{\omega_{1,\mathbf{k}}\omega_{2,\mathbf{k}}}\frac{\left(\left(1+e^{-\beta\omega_{2,\mathbf{k}}}\right)/\left(1-e^{-\beta\omega_{2,\mathbf{k}}}\right)-\left(1+e^{-\beta\omega_{1,\mathbf{k}}}\right)/\left(1-e^{-\beta\omega_{1,\mathbf{k}}}\right)\right)}{1-\left(\omega_{12,\mathbf{k}}^-\right)^2/\omega_{3,\mathbf{0}}^2} \\
&+\frac{1}{2\omega_{3,\mathbf{0}}}\int\frac{d^3\mathbf{k}}{(2\pi)^3}\frac{1}{\omega_{2,\mathbf{k}}\omega_{1,\mathbf{k}}}\frac{\left(\left(1+e^{-\beta\omega_{2,\mathbf{k}}}\right)/\left(1-e^{-\beta\omega_{2,\mathbf{k}}}\right)-\left(1+e^{-\beta\omega_{1,\mathbf{k}}}\right)/\left(1-e^{-\beta\omega_{1,\mathbf{k}}}\right)\right)\sin\left[\omega_{12,\mathbf{k}}^-x^1\right]}{1-\left(\omega_{12,\mathbf{k}}^-\right)^2/\omega_{3,\mathbf{0}}^2},
\end{aligned} \tag{D.12}$$

$$J_3\left(x^1,\widetilde{m}_1,\widetilde{m}_2,\omega_{3,\mathbf{0}}\right) := \int \frac{d^3\mathbf{k}}{(2\pi)^3}\frac{1}{\omega_{1,\mathbf{k}}\omega_{2,\mathbf{k}}}\frac{\omega^{+\,2}_{12,\mathbf{k}}\left(\coth\left(\beta\omega_{2,\mathbf{k}}/2\right)-\coth\left(\beta\omega_{1,\mathbf{k}}/2\right)\right)}{\omega^{+\,2}_{12,\mathbf{k}}-\left(\widetilde{m}_1^2-\widetilde{m}_2^2\right)^2/\omega_{3,\mathbf{0}}^2}\left[\frac{x^1\sin\left[\omega_{3,\mathbf{0}}x^1\right]}{\omega^-_{12,\mathbf{k}}}\right.$$
$$\left.+\frac{\left(\omega^{+\,2}_{12,\mathbf{k}}+\left(\widetilde{m}_1^2-\widetilde{m}_2^2\right)^2/\omega_{3,\mathbf{0}}^2\right)\left(\cos\left[\omega_{3,\mathbf{0}}x^1\right]/\omega^-_{12,\mathbf{k}}-\cos\left[\left(\widetilde{m}_1^2-\widetilde{m}_2^2\right)x^1/\omega^+_{12,\mathbf{k}}\right]/\omega^-_{12,\mathbf{k}}\right)}{\omega_{3,\mathbf{0}}\left(\omega^{+\,2}_{12,\mathbf{k}}-\left(\widetilde{m}_1^2-\widetilde{m}_2^2\right)^2/\omega_{3,\mathbf{0}}^2\right)}\right], \tag{D.13}$$

$$J_4\left(x^1,\widetilde{m}_1,\widetilde{m}_2,\omega_{3,\mathbf{0}}\right) := \int \frac{d^3\mathbf{k}}{(2\pi)^3}\frac{1}{\omega_{1,\mathbf{k}}\omega_{2,\mathbf{k}}}\frac{\left(\left(1+e^{-\beta\omega_{2,\mathbf{k}}}\right)/\left(1-e^{-\beta\omega_{2,\mathbf{k}}}\right)+\left(1+e^{-\beta\omega_{1,\mathbf{k}}}\right)/\left(1-e^{-\beta\omega_{1,\mathbf{k}}}\right)\right)}{1-\omega^{+\,2}_{12,\mathbf{k}}/\omega_{3,\mathbf{0}}^2}\left[\frac{x^1\sin\left[\omega_{3,\mathbf{0}}x^1\right]}{\omega^+_{12,\mathbf{k}}}\right.$$
$$\left.+\left(1+\frac{\omega^{+\,2}_{12,\mathbf{k}}}{\omega_{3,\mathbf{0}}^2}\right)\frac{\left\{\cos\left[\omega_{3,\mathbf{0}}x^1\right]-\cos\left[\omega^+_{12,\mathbf{k}}x^1\right]\right\}}{\omega_{3,\mathbf{0}}\omega^+_{12,\mathbf{k}}\left(1-\omega^{+\,2}_{12,\mathbf{k}}/\omega_{3,\mathbf{0}}^2\right)}\right]. \tag{D.14}$$

We carry out the momentum integration of the above expressions numerically.

D.2. Time Integration and Momentum Integration of $\langle \boldsymbol{j}_0(\boldsymbol{x}^0)\rangle_{\boldsymbol{2nd}}$. Below we consider time and momentum integrations of the second part of PNA which is (98). Substituting (C.7), (C.8), (C.11)-(C.16) into (98) and performing time integration, we obtain

$$\begin{aligned}
&\left\langle j_0\left(x^1+t_0\right)\right\rangle_{\text{2nd}} = -\frac{2\widehat{\varphi}_{3,t_0}A_{123}}{a^3_{t_0}}\int\frac{d^3\mathbf{k}}{(2\pi)^3}\left[\left[\left\{\frac{1}{2\omega_2}\right.\right.\right.\\
&\cdot\coth\frac{\beta\omega_2}{2}\frac{\sqrt{\Delta'_1\Delta'_2}}{2}\left[\frac{1}{\omega_2^2}\left\{\frac{\omega^{-2}_{12}\cos\left[\omega^+_{12}x^1\right]}{\omega_3^2-\omega^{-2}_{12}}\right.\right.\\
&-\frac{\omega^{+2}_{12}\cos\left[\omega^-_{12}x^1\right]}{\omega_3^2-\omega^{+2}_{12}}-\cos\left[\omega_3x^1\right]\cos\left[2\omega_2x^1\right]\\
&\cdot\left(\frac{\omega^{-2}_{12}}{\omega_3^2-\omega^{-2}_{12}}-\frac{\omega^{+2}_{12}}{\omega_3^2-\omega^{+2}_{12}}\right)+\omega_3\sin\left[\omega_3x^1\right]\\
&\left.\cdot\sin\left[2\omega_2x^1\right]\times\left(\frac{\omega^-_{12}}{\omega_3^2-\omega^{-2}_{12}}+\frac{\omega^+_{12}}{\omega_3^2-\omega^{+2}_{12}}\right)\right\}\\
&+\frac{\left(\widetilde{m}_1^2-\widetilde{m}_2^2\right)}{\omega_1}\left\{4\omega_3x^1\sin\left[\omega_3x^1\right]\left(\frac{\omega^+_{12}}{\left(\omega_3^2-\omega^{+2}_{12}\right)^2}\right.\right.\\
&\left.-\frac{\omega^-_{12}}{\left(\omega_3^2-\omega^{-2}_{12}\right)^2}\right)\\
&-\frac{2\omega^+_{12}\left\{\cos\left[\omega_3x^1\right]-\cos\left[\omega^+_{12}x^1\right]\right\}}{\left(\omega_3^2-\omega^{+2}_{12}\right)^2}\\
&+\frac{2\omega^-_{12}\left\{\cos\left[\omega_3x^1\right]-\cos\left[\omega^-_{12}x^1\right]\right\}}{\left(\omega_3^2-\omega^{-2}_{12}\right)^2}-\left(\left(x^1\right)^2\right.\\
&\left.-\frac{1}{\omega_1\omega_2}\right)\frac{\omega^+_{12}\cos\left[\omega^+_{12}x^1\right]}{\omega_3^2-\omega^{+2}_{12}}\\
&+8\omega_3^2\left(\frac{\omega^+_{12}\left\{\cos\left[\omega_3x^1\right]-\cos\left[\omega^+_{12}x^1\right]\right\}}{\left(\omega_3^2-\omega^{+2}_{12}\right)^3}\right.\\
&\left.-\frac{\omega^-_{12}\left\{\cos\left[\omega_3x^1\right]-\cos\left[\omega^-_{12}x^1\right]\right\}}{\left(\omega_3^2-\omega^{-2}_{12}\right)^3}\right)+\left(\left(x^1\right)^2\right.\\
&\left.+\frac{1}{\omega_1\omega_2}\right)\frac{\omega^-_{12}\cos\left[\omega^-_{12}x^1\right]}{\omega_3^2-\omega^{-2}_{12}}\\
&\left.-\frac{\cos\left[\omega_3x^1\right]}{\omega_1\omega_2}\left(\frac{\omega^+_{12}}{\omega_3^2-\omega^{+2}_{12}}+\frac{\omega^-_{12}}{\omega_3^2-\omega^{-2}_{12}}\right)\right\}\\
&-\frac{\left(x^1/\omega_1\right)\left(\widetilde{m}_1^2-\widetilde{m}_2^2\right)}{\omega_1\omega_2}\left\{\left(\frac{\omega^+_{12}}{\omega_3^2-\omega^{+2}_{12}}\right.\right.\\
&\left.+\frac{\omega^-_{12}}{\omega_3^2-\omega^{-2}_{12}}\right)\omega_3\sin\left[\omega_3x^1\right]-\frac{\omega^{+2}_{12}\sin\left[\omega^+_{12}x^1\right]}{\omega_3^2-\omega^{+2}_{12}}\\
&\left.-\frac{\omega^{-2}_{12}\sin\left[\omega^-_{12}x^1\right]}{\omega_3^2-\omega^{-2}_{12}}\right\}-\frac{1}{\omega_1}\left(\frac{\omega_1}{\omega_2}+\frac{\omega_2}{\omega_1}\right)\\
&\cdot\left\{\frac{\left(\omega_3^2+\omega^{+2}_{12}\right)\omega^-_{12}}{\left(\omega_3^2-\omega^{+2}_{12}\right)^2}\left\{\cos\left[\omega_3x^1\right]-\cos\left[\omega^+_{12}x^1\right]\right\}\right.\\
&+\frac{\left(\omega_3^2+\omega^{-2}_{12}\right)\omega^+_{12}}{\left(\omega_3^2-\omega^{-2}_{12}\right)^2}\\
&\times\left\{\cos\left[\omega_3x^1\right]-\cos\left[\omega^-_{12}x^1\right]\right\}\\
&\left.\left.\left.+\left(\frac{\omega^-_{12}}{\omega_3^2-\omega^{+2}_{12}}+\frac{\omega^+_{12}}{\omega_3^2-\omega^{-2}_{12}}\right)\omega_3x^1\sin\left[\omega_3x^1\right]\right\}\right]\right]\\
&-\left\{1\longleftrightarrow 2 \text{ for lower indices}\right\}\right],
\end{aligned} \tag{D.15}$$

where we have introduced $\Delta'_{i,\mathbf{k}}$ defined by

$$\Delta'_{i,\mathbf{k}} = \frac{H(t_0)}{2} \frac{\mathbf{k}^2}{\omega_{i,\mathbf{k}}^2 a(t_0)^2}. \tag{D.16}$$

For notational simplicity, $\omega_{i,\mathbf{k}}$ is denoted by ω_i ($i = 1, 2$) and $\omega^{\pm}_{12,\mathbf{k}}$ is denoted by $\omega^{\pm}_{12}$ in (D.15).

The next task is to integrate (D.15) with respect to spatial momentum. Equation (D.15) leads to the following expression:

$$\begin{aligned}\left\langle j_0\left(x^1 + t_0\right)\right\rangle_{2\text{nd}} &= \frac{\widehat{\varphi}_{3,t_0} A_{123}}{a_{t_0}^3} \frac{H(t_0)}{4} \left(\widetilde{m}_1^2 - \widetilde{m}_2^2\right) \\ &\cdot \left[J_{11}\left(x^1, \widetilde{m}_1, \widetilde{m}_2, \omega_{3,\mathbf{0}}\right) + J_{12}\left(x^1, \widetilde{m}_1, \widetilde{m}_2, \omega_{3,\mathbf{0}}\right)\right. \\ &+ J_{13}\left(x^1, \widetilde{m}_1, \widetilde{m}_2, \omega_{3,\mathbf{0}}\right) + J_{14}\left(x^1, \widetilde{m}_1, \widetilde{m}_2, \omega_{3,\mathbf{0}}\right) \\ &\left.+ J_{15}\left(x^1, \widetilde{m}_1, \widetilde{m}_2, \omega_{3,\mathbf{0}}\right)\right],\end{aligned} \tag{D.17}$$

where we have defined auxiliary functions $J_i(x^1, \widetilde{m}_1, \widetilde{m}_2, \omega_{3,\mathbf{0}})$ ($i = 11, \ldots, 15$) as

$$\begin{aligned}&J_{11}\left(x^1, \widetilde{m}_1, \widetilde{m}_2, \omega_{3,\mathbf{0}}\right) \\ &\quad := \int \frac{d^3\mathbf{k}}{(2\pi)^3} \frac{\mathbf{k}^2}{a(t_0)^2} \frac{x^1}{(\omega_1\omega_2)^3} \left[\left(\coth\frac{\beta\omega_2}{2}\right.\right. \\ &\quad + \left.\coth\frac{\beta\omega_1}{2}\right) \times \left(\frac{\omega^+_{12}\omega_3 \sin\left[\omega_3 x^1\right]}{\omega_3^2 - \omega^{+2}_{12}}\right. \\ &\quad - \left.\frac{\omega^{+2}_{12} \sin\left[\omega^+_{12} x^1\right]}{\omega_3^2 - \omega^{+2}_{12}}\right) + \left(\coth\frac{\beta\omega_2}{2} - \coth\frac{\beta\omega_1}{2}\right) \\ &\quad \times \left.\left(\frac{\omega^-_{12}\omega_3 \sin\left[\omega_3 x^1\right]}{\omega_3^2 - \omega^{-2}_{12}} - \frac{\omega^{-2}_{12} \sin\left[\omega^-_{12} x^1\right]}{\omega_3^2 - \omega^{-2}_{12}}\right)\right],\end{aligned} \tag{D.18}$$

$$\begin{aligned}&J_{12}\left(x^1, \widetilde{m}_1, \widetilde{m}_2, \omega_{3,\mathbf{0}}\right) := \left(\widetilde{m}_1^2 - \widetilde{m}_2^2\right)^{-1} \\ &\quad \cdot \int \frac{d^3\mathbf{k}}{(2\pi)^3} \frac{\mathbf{k}^2}{a(t_0)^2} \frac{1}{\omega_1\omega_2} \left[\left(\coth\frac{\beta\omega_1}{2}\frac{1}{\omega_1^3}\right.\right. \\ &\quad - \left.\coth\frac{\beta\omega_2}{2}\frac{1}{\omega_2^3}\right) \times \left(\frac{\omega^{-2}_{12} \cos\left[\omega^+_{12} x^1\right]}{\omega_3^2 - \omega^{-2}_{12}}\right. \\ &\quad - \left.\frac{\omega^{+2}_{12} \cos\left[\omega^-_{12} x^1\right]}{\omega_3^2 - \omega^{+2}_{12}}\right) + \left(\coth\frac{\beta\omega_2}{2}\frac{\cos\left[2\omega_2 x^1\right]}{\omega_2^3}\right. \\ &\quad - \left.\coth\frac{\beta\omega_1}{2}\frac{\cos\left[2\omega_1 x^1\right]}{\omega_1^3}\right)\left(\frac{\omega^{-2}_{12}}{\omega_3^2 - \omega^{-2}_{12}}\right. \\ &\quad - \left.\frac{\omega^{+2}_{12}}{\omega_3^2 - \omega^{+2}_{12}}\right)\cos\left[\omega_3 x^1\right] \\ &\quad - \left(\coth\frac{\beta\omega_2}{2}\frac{\sin\left[2\omega_2 x^1\right]}{\omega_2^3}\right. \\ &\quad + \left.\coth\frac{\beta\omega_1}{2}\frac{\sin\left[2\omega_1 x^1\right]}{\omega_1^3}\right)\frac{\omega^-_{12}\omega_3 \sin\left[\omega_3 x^1\right]}{\omega_3^2 - \omega^{-2}_{12}} \\ &\quad - \left(\coth\frac{\beta\omega_2}{2}\frac{\sin\left[2\omega_2 x^1\right]}{\omega_2^3}\right. \\ &\quad - \left.\left.\coth\frac{\beta\omega_1}{2}\frac{\sin\left[2\omega_1 x^1\right]}{\omega_1^3}\right)\frac{\omega^+_{12}\omega_3 \sin\left[\omega_3 x^1\right]}{\omega_3^2 - \omega^{+2}_{12}}\right],\end{aligned} \tag{D.19}$$

$$\begin{aligned}&J_{13}\left(x^1, \widetilde{m}_1, \widetilde{m}_2, \omega_{3,\mathbf{0}}\right) := \left(\widetilde{m}_1^2 - \widetilde{m}_2^2\right)^{-1} \\ &\quad \cdot \int \frac{d^3\mathbf{k}}{(2\pi)^3} \frac{\mathbf{k}^2}{a(t_0)^2} \frac{\left(\omega_1^2 + \omega_2^2\right)}{(\omega_1\omega_2)^3} \left[\left(\coth\frac{\beta\omega_2}{2}\right.\right. \\ &\quad + \left.\coth\frac{\beta\omega_1}{2}\right) \\ &\quad \times \left(\frac{\left(\omega_3^2 + \omega^{+2}_{12}\right)\omega^-_{12}\left\{\cos\left[\omega_3 x^1\right] - \cos\left[\omega^+_{12} x^1\right]\right\}}{\left(\omega_3^2 - \omega^{+2}_{12}\right)^2}\right. \\ &\quad + \left.\frac{\omega^-_{12}\omega_3 x^1 \sin\left[\omega_3 x^1\right]}{\omega_3^2 - \omega^{+2}_{12}}\right) + 2\left(\frac{e^{-\beta\omega_2}}{1 - e^{-\beta\omega_2}}\right. \\ &\quad - \left.\frac{e^{-\beta\omega_1}}{1 - e^{-\beta\omega_1}}\right) \\ &\quad \cdot \left(\frac{\left(\omega_3^2 + \omega^{-2}_{12}\right)\omega^+_{12}\left\{\cos\left[\omega_3 x^1\right] - \cos\left[\omega^-_{12} x^1\right]\right\}}{\left(\omega_3^2 - \omega^{-2}_{12}\right)^2}\right. \\ &\quad + \left.\left.\frac{\omega^+_{12}\omega_3 x^1 \sin\left[\omega_3 x^1\right]}{\omega_3^2 - \omega^{-2}_{12}}\right)\right],\end{aligned} \tag{D.20}$$

$$\begin{aligned}&J_{14}\left(x^1, \widetilde{m}_1, \widetilde{m}_2, \omega_{3,\mathbf{0}}\right) \\ &\quad := -\int \frac{d^3\mathbf{k}}{(2\pi)^3} \frac{\mathbf{k}^2}{a(t_0)^2} \frac{1}{(\omega_1\omega_2)^2} \left(\coth\frac{\beta\omega_1}{2}\right. \\ &\quad + \left.\coth\frac{\beta\omega_2}{2}\right) \times \left[4\omega_3 x^1 \sin\left[\omega_3 x^1\right] \frac{\omega^+_{12}}{\left(\omega_3^2 - \omega^{+2}_{12}\right)^2}\right. \\ &\quad - \frac{2\omega^+_{12}\left\{\cos\left[\omega_3 x^1\right] - \cos\left[\omega^+_{12} x^1\right]\right\}}{\left(\omega_3^2 - \omega^{+2}_{12}\right)^2}\end{aligned}$$

$$+\frac{8\omega_3^2\omega_{12}^+\left\{\cos\left[\omega_3 x^1\right]-\cos\left[\omega_{12}^+ x^1\right]\right\}}{\left(\omega_3^2-\omega_{12}^{+2}\right)^3}-\left(\left(x^1\right)^2-\frac{1}{\omega_1\omega_2}\right)\frac{\omega_{12}^+\cos\left[\omega_{12}^+ x^1\right]}{\omega_3^2-\omega_{12}^{+2}}-\frac{\cos\left[\omega_3 x^1\right]}{\omega_1\omega_2}\cdot\frac{\omega_{12}^+}{\omega_3^2-\omega_{12}^{+2}}\Bigg], \tag{D.21}$$

$$J_{15}\left(x^1,\widetilde{m}_1,\widetilde{m}_2,\omega_{3,\mathbf{0}}\right):=-2\int\frac{d^3\mathbf{k}}{(2\pi)^3}\frac{\mathbf{k}^2}{a\left(t_0\right)^2}\frac{1}{\left(\omega_1\omega_2\right)^2}\left(\frac{e^{-\beta\omega_1}}{1-e^{-\beta\omega_1}}-\frac{e^{-\beta\omega_2}}{1-e^{-\beta\omega_2}}\right)\times\left[4\omega_3 x^1\sin\left[\omega_3 x^1\right]\frac{\omega_{12}^-}{\left(\omega_3^2-\omega_{12}^{-2}\right)^2}-\frac{2\omega_{12}^-\left\{\cos\left[\omega_3 x^1\right]-\cos\left[\omega_{12}^- x^1\right]\right\}}{\left(\omega_3^2-\omega_{12}^{-2}\right)^2}\right. \tag{D.22}$$

$$\left.+\frac{8\omega_3^2\omega_{12}^-\left\{\cos\left[\omega_3 x^1\right]-\cos\left[\omega_{12}^- x^1\right]\right\}}{\left(\omega_3^2-\omega_{12}^{-2}\right)^3}-\left(\left(x^1\right)^2+\frac{1}{\omega_1\omega_2}\right)\frac{\omega_{12}^-\cos\left[\omega_{12}^- x^1\right]}{\omega_3^2-\omega_{12}^{-2}}+\frac{\cos\left[\omega_3 x^1\right]}{\omega_1\omega_2}\cdot\frac{\omega_{12}^-}{\omega_3^2-\omega_{12}^{-2}}\right].$$

We carry out the momentum integration of the above expressions numerically.

Data Availability

No data were used to support this study.

Conflicts of Interest

The authors declare that they have no conflicts of interest.

Acknowledgments

Hiroyuki Takata and Keiko I. Nagao would like to thank the theoretical particle physics group in Hiroshima University for its kind hospitality. Apriadi Salim Adam would like to thank Summer Institute (SI) 2017 for stimulating discussion where the part of this work has been completed. This work is supported by JSPS KAKENHI Grant Number JP17K05418 (Takuya Morozumi) and supported in part by JSPS Grant-in-Aid for Scientific Research for Young Scientists (B) 26800151 (Keiko I. Nagao).

References

[1] J. P. Kneller and G. Steigman, "BBN for pedestrians," *New Journal of Physics*, vol. 6, article 117, 2004.

[2] P. A. R. Ade, N. Aghanim, M. Arnaud et al., "Cosmological parameters," *Astronomy & Astrophysics*, vol. 594, Article ID A13, 2016.

[3] A. D. Sakharov, "Violation of CP invariance, c asymmetry, and baryon asymmetry of the universe," *Soviet Physics Uspekhi*, vol. 34, no. 5, pp. 392-393, 1991.

[4] M. Yoshimura, "Unified Gauge theories and the baryon number of the universe," *Physical Review Letters*, vol. 281, no. 41, 1978.

[5] M. Fukugita and T. Yanagida, "Barygenesis without grand unification," *Physics Letters B*, vol. 174, no. 1, pp. 45–47, 1986.

[6] I. Affleck and M. Dine, "A new mechanism for baryogenesis," *Nuclear Physics B*, vol. 249, no. 2, pp. 361–380, 1985.

[7] A. G. Cohen and D. B. Kaplan, "Spontaneous baryogenesis," *Nuclear Physics B*, vol. 308, no. 4, pp. 913–928, 1988.

[8] S. Davidson, E. Nardi, and Y. Nir, "Leptogenesis," *Physics Reports*, vol. 466, no. 4-5, pp. 105–177, 2008.

[9] M. Trodden, "Electroweak baryogenesis," *Reviews of Modern Physics*, vol. 71, pp. 1463–1500, 1999.

[10] K. M. Zurek, "Asymmetric Dark Matter: Theories, signatures, and constraints," *Physics Reports*, vol. 537, no. 3, pp. 91–121, 2013.

[11] A. Kobakhidze and A. Manning, "Cosmological matter-antimatter asymmetry as a quantum fluctuation," *Physical Review D*, vol. 91, Article ID 123529, 2015.

[12] D. Zhuridov, "Baryogenesis from leptomesons," *Physical Review D*, vol. 94, Article ID 035007, 2016.

[13] N. Blinov and A. Hook, "Particle asymmetries from quantum statistics," *Physical Review D: Particles, Fields, Gravitation and Cosmology*, vol. 95, Article ID 095014, 2017.

[14] R. Hotta, T. Morozumi, and H. Takata, "Time variation of particle and antiparticle asymmetry in an expanding universe," *Physical Review D: Particles, Fields, Gravitation and Cosmology*, vol. 90, Article ID 016008, 2014.

[15] T. Morozumi, K. I. Nagao, A. S. Adam, and H. Takata, "Creation and evolution of particle number asymmetry in an expanding universe," *Russian Physics Journal*, vol. 59, no. 11, pp. 1852–1856, 2017.

[16] E. Calzetta and B. L. Hu, "Nonequilibrium quantum fields: closed-time-path effective action, Wigner function, and Boltzmann equation," *Physical Review D: Particles, Fields, Gravitation and Cosmology*, vol. 37, no. 10, pp. 2878–2900, 1988.

[17] S. A. Ramsey and B. L. Hu, "*O(N)* quantum fields in curved spacetime," *Physical Review D: Particles, Fields, Gravitation and Cosmology*, vol. 56, no. 2, pp. 661–677, 1997.

[18] E. A. Calzetta and B. B. Hu, *Nonequilibrium Quantum Field Theory*, Cambridge University Press, Cambridge, UK, 2008.

[19] J. M. Cornwall, R. Jackiw, and E. Tomboulis, "Effective action for composite operators," *Physical Review D: Particles, Fields, Gravitation and Cosmology*, vol. 10, no. 8, pp. 2428–2445, 1974.

[20] U. Amaldi, W. de Boer, and H. Furstenau, "Comparison of grand unified theories with electroweak and strong coupling constants measured at LEP," *Physics Letters B*, vol. 260, no. 3-4, pp. 447–455, 1991.

[21] D. I. Kazakov, "Beyond the Standard Model (In Search of Supersymmetry)," https://arxiv.org/abs/hep-ph/0012288.

[22] M. Cirelli, P. Panci, G. Servant, and G. Zaharijas, "Consequences of DM/antiDM oscillations for asymmetric WIMP dark matter,"

Journal of Cosmology and Astroparticle Physics, vol. 2012, no. 3, 2012.

[23] S. Tulin, H.-B. Yu, and K. M. Zurek, "Oscillating asymmetric dark matter," *Journal of Cosmology and Astroparticle Physics*, vol. 2012, no. 5, p. 13, 2012.

Hindawi
Advances in High Energy Physics
Volume 2019, Article ID 5769564, 8 pages
https://doi.org/10.1155/2019/5769564

Research Article

Heun-Type Solutions of the Klein-Gordon and Dirac Equations in the Garfinkle-Horowitz-Strominger Dilaton Black Hole Background

Marina-Aura Dariescu,[1] **Ciprian Dariescu**,[1] **and Cristian Stelea**[2]

[1] *Faculty of Physics, "Alexandru Ioan Cuza" University, 11 Blvd. Carol I, Iasi 700506, Romania*
[2] *Research Department, Faculty of Physics, "Alexandru Ioan Cuza" University, 11 Blvd. Carol I, Iasi 700506, Romania*

Correspondence should be addressed to Cristian Stelea; cristian.stelea@uaic.ro

Received 20 December 2018; Revised 28 January 2019; Accepted 11 February 2019; Published 26 February 2019

Guest Editor: Subhajit Saha

Copyright © 2019 Marina-Aura Dariescu et al. This is an open access article distributed under the Creative Commons Attribution License, which permits unrestricted use, distribution, and reproduction in any medium, provided the original work is properly cited. The publication of this article was funded by SCOAP[3].

We study the Klein-Gordon and the Dirac equations in the background of the Garfinkle-Horowitz-Strominger black hole in the Einstein frame. Using a $SO(3,1) \times U(1)$−gauge covariant approach, as an alternative to the Newman-Penrose formalism for the Dirac equation, it turns out that these solutions can be expressed in terms of Heun confluent functions and we discuss some of their properties.

1. Introduction

In recent years, black holes with electric or magnetic charge, in presence of a scalar field called *dilaton*, have been studied mainly in string theories. These charged black holes are solutions of the low-energy four-dimensional effective theories obtained by dimensional compactification of the heterotic string theories. Generically, the effective action of these theories describes a massless dilaton coupled to an abelian vector field [1]. Due to the dimensional compactification process, the dilaton is also nonminimally coupled to the Ricci scalar, with the effective solution being described in the so-called string frame. However, to facilitate comparison with the standard black holes in general relativity, it is convenient to go to the so-called Einstein frame by performing conformal rescaling of the metric (for a review, see [2]).

A remarkable black hole solution of the effective four-dimensional compactified theory was found by Gibbons and Maeda [3, 4] and independently rediscovered in a simpler form, few years later, by Garfinkle, Horowitz, and Strominger (GHS) [5] (for a review of its properties, see [6]). Even though, in terms of the string metric, the electric and magnetic black holes have very different properties, in the Einstein frame the metric does not change when we go from an electrically charged to a magnetically charged black hole (this is basically due to the electromagnetic duality present in the Einstein frame; in the string frame, the electromagnetic field strength is also modified by the dilaton field [7]).

Using the GHS metric in the Einstein frame, the present work is devoted to a study of the Klein-Gordon and Dirac equations, which describe charged particles evolving in the Garfinkle-Horowitz-Strominger (GHS) dilaton black hole spacetime. Within a $SO(3,1) \times U(1)$−gauge covariant approach, it turns out that the solutions can be expressed in terms of Heun confluent functions [8, 9]. Special attention is given to the resonant frequencies, which arise here by imposing a polynomial form of the Heun functions. In general, the so-called quasi-normal modes have discrete spectra of complex characteristic frequencies, with the real part representing the actual frequency of the oscillation and the imaginary part representing the damping. By comparing these modes with the gravitational waves observed in the universe, one should be able to identify the presence of a GHS black hole [10, 11] (see also in [12] the effect of the dilaton field imprint on the gravitational waves emitted in the collision of two GHS black holes).

When the parameter related to the dilaton field goes to zero, one obtains the Klein-Gordon and Dirac equations for the usual Schwarzschild metric, which have been intensively worked out both in their original form and in different types of extensions. For instance, recently, for the Schwarzschild metric in the presence of an electromagnetic field, the Klein-Gordon and Dirac equations for massless particles have been put into a Heun-type form [13, 14]. One should note that Heun functions are often encountered when studying the propagation of various test fields in the background of various black holes or relativistic stars [15–20] and also in cosmology in the context of extended effective field theories of inflation [21].

The method used in the present paper, while based on Cartan's formalism, is an alternative to the Newman-Penrose (NP) formalism [22], which is usually employed for solving Dirac equation describing fermions in the vicinity of different types of black holes [23–27].

The structure of this paper is as follows: in the next section, we present the solutions of the Klein-Gordon and Dirac equations in the background of the GHS dilatonic black hole. In Section 3, we discuss the solutions of the massless Dirac equations in this background and show how to recover the expression of the Hawking temperature. The final section is dedicated to conclusions.

2. Klein-Gordon and Dirac Equations on the GHS Dilaton Black Hole Metric

In Einstein frame, the static and spherically symmetric GHS dilaton black hole metric is given by [5]

$$ds^2 = -R\,dt^2 + \frac{dr^2}{R} + r(r-a)\left[d\theta^2 + \sin^2\theta\, d\varphi^2\right], \quad (1)$$

where

$$R = 1 - \frac{2M}{r}, \qquad \text{and } a = \frac{Q^2}{M}, \quad (2)$$

with M and Q being the mass and the charge of this black hole, which has an event horizon at $r = 2M$ and two singularities located at $r = 0$ and $r = a$. Obviously, if the electric charge of the GHS black hole is zero, the metric in (1) reduces to the Schwarzschild one.

The parameter a is related to the dilaton field ϕ as (Note that we set the asymptotic value of the dilaton field $\phi_0 = 0$.)

$$e^{-2\phi} = 1 \mp \frac{a}{r}, \quad (3)$$

where the *minus* and *plus* signs are for, respectively, the magnetically electrically charged black holes.

Within the $SO(3,1)$–gauge covariant formulation, we introduce the pseudoorthonormal frame $\{E_a\}_{(a=\overline{1,4})}$; that is,

$$\begin{aligned} E_1 &= \sqrt{R}\partial_r, \\ E_2 &= \frac{1}{\sqrt{r(r-a)}}\partial_\theta, \\ E_3 &= \frac{1}{\sqrt{r(r-a)}\sin\theta}\partial_\varphi, \\ E_4 &= \frac{1}{\sqrt{R}}\partial_t, \end{aligned} \quad (4)$$

whose corresponding dual base is

$$\begin{aligned} \omega^1 &= \frac{1}{\sqrt{R}}dr, \\ \omega^2 &= \sqrt{r(r-a)}d\theta, \\ \omega^3 &= \sqrt{r(r-a)}\sin\theta\, d\varphi, \\ \omega^4 &= \sqrt{R}\,dt, \end{aligned} \quad (5)$$

so that the metric in (1) becomes the usual Minkowsky metric $ds^2 = \eta_{ab}\ \omega^a\omega^b$, with $\eta_{ab} = \mathrm{diag}[1,1,1,-1]$.

Using the first Cartan's equation,

$$d\omega^a = \Gamma^a_{.[bc]}\omega^b \wedge \omega^c, \quad (6)$$

with $1 \le b < c \le 4$ and $\Gamma^a_{.[bc]} = \Gamma^a_{.bc} - \Gamma^a_{.cb}$, we obtain the following connection one-forms $\Gamma_{ab} = \Gamma_{abc}\omega^c$, where $\Gamma_{abc} = -\Gamma_{bac}$; namely,

$$\begin{aligned} \Gamma_{212} = \Gamma_{313} &= \frac{r-a/2}{r(r-a)}\sqrt{R}, \\ \Gamma_{323} &= \frac{\cot\theta}{\sqrt{r(r-a)}}, \\ \Gamma_{414} &= -\frac{M}{r^2\sqrt{R}} \end{aligned} \quad (7)$$

In the pseudoorthonormal bases (with $\eta_{44} = -1$), the fourth component of the one-form potential is

$$A_4 = -\frac{1}{\sqrt{R}}\frac{Q}{r}, \quad (8)$$

and it corresponds to an electric field:

$$F_{14} = E_1 A_4 - E_4 A_1 + A_c\Gamma^c{}_{ab} - A_c\Gamma^c{}_{ba} = \frac{Q}{r^2}. \quad (9)$$

2.1. The Klein-Gordon Equation. For the complex scalar field of mass m_0, minimally coupled to gravity, the Klein-Gordon equation has the general $SO(3,1)\times U(1)$-gauge covariant form

$$\eta^{ab}\Phi_{;ab} - m_0^2\Phi = 0; \quad (10)$$

that is,

$$\eta^{ab}\Phi_{|ab} - \eta^{ab}\Phi_{|c}\Gamma^c{}_{ab} = m_0^2\Phi + 2iqA^a\Phi_{|a} + q^2A_aA^a\Phi, \quad (11)$$

where

$$\Phi_{;a} = \Phi_{|a} - iqA_a\Phi, \tag{12}$$

with $\Phi_{|a} = E_a\Phi$.

The two terms in the left-hand side of relation (11) are, respectively, given by

$$\begin{aligned}\eta^{ab}\Phi_{|ab} = {} & R\frac{\partial^2\Phi}{\partial r^2} + \frac{M}{r^2}\frac{\partial\Phi}{\partial r} \\ & + \frac{1}{r(r-a)}\left[\frac{\partial^2\Phi}{\partial\theta^2} + \frac{1}{\sin^2\theta}\frac{\partial^2\Phi}{\partial\varphi^2}\right] - \frac{1}{R}\frac{\partial^2\Phi}{\partial t^2}\end{aligned} \tag{13}$$

and

$$\begin{aligned}\eta^{ab}\Phi_{|c}\Gamma^{c}{}_{ab} = {} & -\left[\frac{M}{r^2} + \frac{R(2r-a)}{r(r-a)}\right]\frac{\partial\Phi}{\partial r} \\ & - \frac{\cot\theta}{r(r-a)}\frac{\partial\Phi}{\partial\theta},\end{aligned} \tag{14}$$

and the Klein-Gordon equation in (11) can be cast into the following explicit form:

$$\begin{aligned} & r(r-a)R\frac{\partial^2\Phi}{\partial r^2} + (2r-2M-a)\frac{\partial\Phi}{\partial r} \\ & + \left[\frac{\partial^2\Phi}{\partial\theta^2} + \cot\theta\frac{\partial\Phi}{\partial\theta} + \frac{1}{\sin^2\theta}\frac{\partial^2\Phi}{\partial\varphi^2}\right] \\ & - \left[r(r-a)m_0^2 + \frac{r(r-a)}{R}\left(\frac{\partial}{\partial t} + i\frac{qQ}{r}\right)^2\right]\Phi \\ & = 0.\end{aligned} \tag{15}$$

Using the separation of the variables with the ansatz

$$\Phi(r,\theta,\varphi,t) = G(r)\,Y_\ell^m(\theta,\varphi)\,e^{-i\omega t}, \tag{16}$$

where Y_ℓ^m are the spherical harmonics, it turns out that the unknown function $G(r)$ is the solution of the differential equation

$$\begin{aligned} & r(r-a)R\frac{d^2G}{dr^2} + (2r-2M-a)\frac{dG}{dr} \\ & - \left[\ell(\ell+1) + r(r-a)m_0^2 - \frac{r-a}{r-2M}(\omega r - qQ)^2\right]G \\ & = 0.\end{aligned} \tag{17}$$

This equation can be solved exactly, with its solutions being expressed in terms of the confluent Heun functions [8, 9] as

$$\begin{aligned}G = e^{\alpha x/2}\{ & C_1 x^{\beta/2}\mathit{HeunC}[\alpha,\beta,\gamma,\delta,\eta,x] \\ & + C_2 x^{-\beta/2}\mathit{HeunC}[\alpha,-\beta,\gamma,\delta,\eta,x]\}\end{aligned} \tag{18}$$

with the variable

$$x = \frac{r-2M}{a-2M} \tag{19}$$

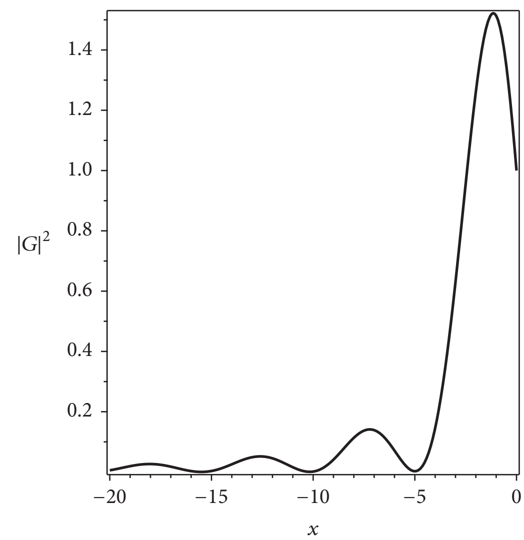

FIGURE 1: The square modulus of the function $G(r)$ given in (18).

and parameters

$$\begin{aligned}\alpha &= 2i(a-2M)\sqrt{\omega^2 - m_0^2}, \\ \beta &= 2i(2M\omega - qQ), \\ \gamma &= 0, \\ \delta &= 2\left[Mm_0^2 - 2M\omega^2 + qQ\omega\right](2M-a), \\ \eta &= -\delta - \ell(\ell+1).\end{aligned} \tag{20}$$

The parameters α and β are purely imaginary, and the radial part of the density probability is given by the square modulus of the Heun functions in (18). The two independent solutions have the generic behavior represented in Figure 1, for $r > 2M > a$. The main features of the probability curve are quite nice; that is, it satisfies all the text-book requirements imposed to physically meaningful wave functions. In this respect, $|G(r)|^2 = 1$ on the horizon and it gets a series of local decreasing maxima, finally vanishing rapidly, at the spatial infinity. If the number of these maxima was finite, the state would be bounded. Otherwise, it could asymptotically radiate. More details on the physical phenomena related to these properties are thoroughly discussed in [28], where the authors are computing the complex values of the energy spectrum coming from the polynomial condition imposed on the Heun functions. In [19, 28], the authors were working in coordinate bases, with

$$A_4^{(c)} = -\frac{Q}{r}, \tag{21}$$

so that $A_4^{(c)}dt = A_4\omega^4$, where A_4 is given in (8).

In the particular case $a = 0$, corresponding to the familiar Schwarzschild black hole, the function G has the same expression as in (18) but with the variable and parameters computed for $a = 0$.

2.2. The Dirac Equation. The spinor of mass μ minimally coupled to gravity is described by the Dirac equation

$$\gamma^a \Psi_{;a} + \mu\Psi = 0 \tag{22}$$

with

$$\Psi_{;a} = \Psi_{|a} + \frac{1}{4}\Gamma_{bca}\gamma^b\gamma^c\Psi - iqA_a\Psi. \tag{23}$$

In contrast to the Klein-Gordon case, the situation is more complicated in the case of the Dirac equation (22) and this complication is basically due to the square root $\sqrt{r(r-a)}$, which appears in the expressions of E_2 and E_3. Thus, with the term expressing the Ricci spin-connection given by

$$\begin{aligned}\frac{1}{4}\Gamma_{bca}\gamma^a\gamma^b\gamma^c = \frac{1}{2}\left[\frac{2r-a}{r(r-a)}\sqrt{R} + \frac{M}{r^2\sqrt{R}}\right]\gamma^1 \\ + \frac{\cot\theta}{2\sqrt{r(r-a)}}\gamma^2,\end{aligned} \tag{24}$$

the Dirac equation becomes

$$\begin{aligned}&\gamma^1\left[\sqrt{R}\frac{\partial\Psi}{\partial r} + \frac{2r-a-3M+aM/r}{2\sqrt{R}r(r-a)}\Psi\right] \\ &\quad + \frac{\gamma^2}{\sqrt{r(r-a)}}\left[\frac{\partial\Psi}{\partial\theta} + \frac{\cot\theta}{2}\Psi\right] \\ &\quad + \frac{\gamma^3}{\sqrt{r(r-a)}\sin\theta}\frac{\partial\Psi}{\partial\varphi} + \frac{\gamma^4}{\sqrt{R}}\left[\frac{\partial\Psi}{\partial t} + iq\frac{Q}{r}\Psi\right] \\ &\quad + \mu\Psi = 0.\end{aligned} \tag{25}$$

As in the previous Klein-Gordon case, one can use the separation of the variables

$$\Psi = \psi(r,\theta)\,e^{i(m\varphi-\omega t)}, \tag{26}$$

with the function $\psi(r,\theta)$ defined as

$$\psi(r,\theta) = \left[r(r-a)\sqrt{R}\right]^{-1/2}\chi(r,\theta) \tag{27}$$

and one obtains the explicit expression of the differential equation satisfied by $\chi(r,\theta)$:

$$\begin{aligned}&\sqrt{Rr(r-a)}\gamma^1\frac{\partial\chi}{\partial r} + \gamma^2 D_\theta\chi + \frac{im}{\sin\theta}\gamma^3\chi \\ &\quad + i\sqrt{\frac{r(r-a)}{R}}\left(\frac{qQ}{r} - \omega\right)\gamma^4\chi + \mu\sqrt{r(r-a)}\chi \\ &= 0,\end{aligned} \tag{28}$$

where

$$D_\theta = \frac{\partial}{\partial\theta} + \frac{\cot\theta}{2}. \tag{29}$$

Using the Weyl representation for the γ^i matrices,

$$\begin{aligned}\gamma^1 &= -i\beta\alpha^3, \\ \gamma^2 &= -i\beta\alpha^1, \\ \gamma^3 &= -i\beta\alpha^2, \\ \gamma^4 &= -i\beta,\end{aligned} \tag{30}$$

with

$$\begin{aligned}\alpha^\mu &= \begin{pmatrix}\sigma^\mu & 0 \\ 0 & -\sigma^\mu\end{pmatrix}, \\ \beta &= \begin{pmatrix}0 & -\mathrm{I} \\ -\mathrm{I} & 0\end{pmatrix}, \\ \text{so that } \gamma^5 &= \begin{pmatrix}\mathrm{I} & 0 \\ 0 & -\mathrm{I}\end{pmatrix},\end{aligned} \tag{31}$$

where σ^μ denote the usual Pauli matrices and (28) becomes

$$\begin{aligned}&\sqrt{Rr(r-a)}\alpha^3\frac{\partial\chi}{\partial r} + \alpha^1 D_\theta\chi + \frac{im}{\sin\theta}\alpha^2\chi \\ &\quad + i\sqrt{\frac{r(r-a)}{R}}\left(\frac{qQ}{r} - \omega\right)\chi + i\mu\sqrt{r(r-a)}\beta\chi \\ &= 0,\end{aligned} \tag{32}$$

and one may use again the standard procedure based on the separation of the variables. Thus, with the bi-spinor χ written in terms of two components spinors as

$$\chi(r,\theta) = \begin{bmatrix}\zeta(r,\theta) \\ \eta(r,\theta)\end{bmatrix}, \tag{33}$$

where

$$\begin{aligned}\zeta_1 &= S_1(r)\,T_1(\theta), \\ \zeta_2 &= S_2(r)\,T_2(\theta), \\ \eta_1 &= S_2(r)\,T_1(\theta), \\ \eta_2 &= S_1(r)\,T_2(\theta),\end{aligned} \tag{34}$$

one obtains the following system of coupled radial equations for the components S_1 and S_2, that is,

$$\begin{aligned}S_1' + \frac{i(qQ-\omega r)}{rR}S_1 + \frac{1}{\sqrt{R}}\left[\frac{\lambda}{\sqrt{r(r-a)}} - i\mu\right]S_2 = 0, \\ S_2' - \frac{i(qQ-\omega r)}{rR}S_2 + \frac{1}{\sqrt{R}}\left[\frac{\lambda}{\sqrt{r(r-a)}} + i\mu\right]S_1 = 0,\end{aligned} \tag{35}$$

and take into account the following essential relations:

$$\begin{aligned}\left[\frac{d}{d\theta} + \frac{\cot\theta}{2} + \frac{m}{\sin\theta}\right]T_2 = \lambda T_1, \\ \left[\frac{d}{d\theta} + \frac{\cot\theta}{2} - \frac{m}{\sin\theta}\right]T_1 = -\lambda T_2.\end{aligned} \tag{36}$$

Thus, the angular parts T_A, with $A = 1, 2$, are satisfying the decoupled equations

$$\frac{d^2 T_A}{d\theta^2} + \cot\theta \frac{dT_A}{d\theta} - \left[\frac{(\cos\theta \mp 2m)^2}{4\sin^2\theta} - \lambda^2 + \frac{1}{2}\right] T_A = 0, \quad (37)$$

with the solutions given by the spin-weighted spherical harmonics [29], for $\lambda = \ell + 1/2$.

As for the radial equations, we employ the auxiliary function method and consider S_1 and S_2 as

$$S_1 = e^{i\omega r}\left(\frac{r}{2M} - 1\right)^{2i\omega M - iqQ} \Sigma_1(r),$$
$$S_2 = e^{-i\omega r}\left(\frac{r}{2M} - 1\right)^{-2i\omega M + iqQ} \Sigma_2(r), \quad (38)$$

so that system (35) leads to the following simpler equations for the unknown functions Σ_A:

$$\Sigma_1' + \left(\frac{r}{2M} - 1\right)^{-4i\omega M + 2iqQ} \frac{e^{-2i\omega r}}{\sqrt{R}}\left[\frac{\lambda}{\sqrt{r(r-a)}} - i\mu\right] \cdot \Sigma_2 = 0,$$
$$\Sigma_2' + \left(\frac{r}{2M} - 1\right)^{4i\omega M - 2iqQ} \frac{e^{2i\omega r}}{\sqrt{R}}\left[\frac{\lambda}{\sqrt{r(r-a)}} + i\mu\right] \Sigma_1 = 0. \quad (39)$$

The differential equation for Σ_1, that is,

$$\Sigma_1'' + \left[\frac{4i\omega r - 4iqQ + 1}{2(r - 2M)} + \frac{1}{2(r-a)} + \frac{i\mu(2r - a)}{2\sqrt{r(r-a)}\left[\lambda - i\mu\sqrt{r(r-a)}\right]}\right]\Sigma_1' - \frac{r}{r - 2M}\left[\frac{\lambda^2}{r(r-a)} + \mu^2\right]\Sigma_1 = 0, \quad (40)$$

can not be analytically solved. Numerically, using Mathematica [30], with the initial conditions

$$\Sigma_1(2M_+) = 0,$$
$$\Sigma_1'(2M_+) = 1, \quad (41)$$

the absolute value of the radial part of $|\psi|^2$ given in (26), namely,

$$F(r) = \frac{1}{r(r-a)\sqrt{R}}\left|S_1\right|^2, \quad (42)$$

is represented in Figure 2, for $r > 2M > a$.

This is describing the fermionic ground state in the outer region, with just one maximum (as it should) and exponentially vanishing at infinity. We have not analyzed the corresponding modes located within the black hole, since, in the limit $a \longrightarrow 0$, the area of the sphere $r = a$ is zero so that this surface is singular. Once Q increases, the singular surface moves towards the event horizon $r = 2M$, and one has to solve the problems related to the physically meaningful boundary conditions.

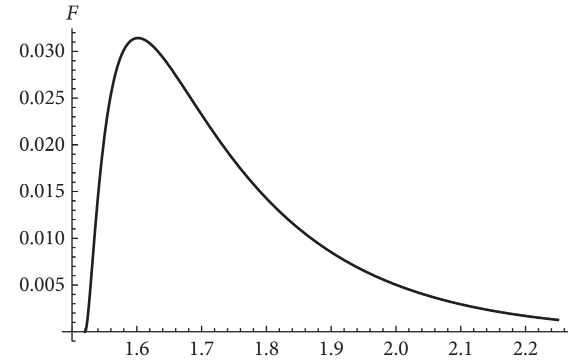

Figure 2: Function (42), for $a = 1$ and $2M = 1.5$.

If one imposes $\lambda \ll \mu r$ and performs a series expansion of the last term multiplying Σ_1' in (40), to first order in a/r, this last term can be approximated to $1/(r-a)$ and the solution is given by the Heun confluent functions [8, 9] as

$$\Sigma_1 = C_1 e^{-\mu r} HeunC\left[\alpha, \beta, \gamma, \delta, \eta, \frac{r - 2M}{a - 2M}\right] + C_2 e^{-\mu r}\left(\frac{r}{2M} - 1\right)^{-2i\omega M + 2iqQ + 1/2} \cdot HeunC\left[\alpha, -\beta, \gamma, \delta, \eta, \frac{r - 2M}{a - 2M}\right], \quad (43)$$

with the parameters

$$\alpha = 2\mu(2M - a),$$
$$\beta = 2i(\omega M - qQ) - \frac{1}{2},$$
$$\gamma = -\frac{3}{2},$$
$$\delta = 2\mu^2 M(2M - a)$$
$$\eta = -\delta + \frac{i(\omega M - qQ)}{2} + \frac{5}{8} - \lambda^2. \quad (44)$$

Near the exterior event horizon, $r \longrightarrow 2M$; that is, $x \longrightarrow 0$; the Heun confluent functions in (43) have a polynomial form if their parameters are satisfying the condition [8, 9]

$$\frac{\delta}{\alpha} = -\left[n + 1 + \frac{\beta + \gamma}{2}\right]. \quad (45)$$

By replacing the expressions of (44) in (45), one gets the relation

$$i(\omega M - qQ) + \mu M = -n, \quad (46)$$

for the Heun function multiplied by C_1, and the relation

$$i(\omega M - qQ) - \mu M = n + \frac{1}{2}, \tag{47}$$

for the one multiplied by C_2. These relations are pointing out a quantized part of the imaginary part of ω, which corresponds to resonant frequencies [28].

3. The Massless Case

The Dirac equation has been worked out for several physically important metrics, mainly using the NP formalism [25] and some of the solutions, especially in the massless case, have been expressed in terms of Heun confluent functions [13].

In view of the analysis developed in the previous section, the massless and chargeless fermions are described by the radial equations coming from system (35); namely,

$$\begin{aligned} S_1' - \frac{i\omega}{R} S_1 + \frac{\lambda}{\sqrt{Rr(r-a)}} S_2 &= 0, \\ S_2' + \frac{i\omega}{R} S_2 + \frac{\lambda}{\sqrt{Rr(r-a)}} S_1 &= 0, \end{aligned} \tag{48}$$

with

$$\begin{aligned} S_1 &= e^{i\omega r} \left(\frac{r}{2M} - 1 \right)^{2i\omega M} \Sigma_1(r), \\ S_2 &= e^{-i\omega r} \left(\frac{r}{2M} - 1 \right)^{-2i\omega M} \Sigma_2(r). \end{aligned} \tag{49}$$

Thus, system (48) turns into the simpler form

$$\begin{aligned} \Sigma_1' + e^{-2i\omega r} \left(\frac{r}{2M} - 1 \right)^{-4i\omega M} \frac{\lambda}{\sqrt{Rr(r-a)}} \Sigma_2 &= 0, \\ \Sigma_2' + e^{2i\omega r} \left(\frac{r}{2M} - 1 \right)^{4i\omega M} \frac{\lambda}{\sqrt{Rr(r-a)}} \Sigma_1 &= 0, \end{aligned} \tag{50}$$

which leads to the following differential equation for Σ_1:

$$\begin{aligned} \Sigma_1'' + \left[\frac{4i\omega r + 1}{2(r-2M)} + \frac{1}{2(r-a)} \right] \Sigma_1' \\ - \frac{\lambda^2}{(r-2M)(r-a)} \Sigma_1 = 0 \end{aligned} \tag{51}$$

and similarly for Σ_2. The solution of this equation is expressed in terms of Heun confluent functions as

$$\begin{aligned} \Sigma_1 = e^{-2i\omega r} \{ & C_1 \mathit{HeunC}[\alpha, \beta, \gamma, \delta, \eta, x] \\ & + C_2 x^{-\beta} \mathit{HeunC}[\alpha, -\beta, \gamma, \delta, \eta, x] \} \end{aligned} \tag{52}$$

where the variable is

$$x = \frac{r - 2M}{a - 2M} \tag{53}$$

and the corresponding parameters are

$$\begin{aligned} \alpha &= 2i\omega(2M - a), \\ \beta &= 4i\omega M - \frac{1}{2}, \\ \gamma &= -\frac{1}{2}, \\ \delta &= i\omega(4i\omega M + 1)(2M - a) \\ \eta &= -\delta - \frac{i\omega a}{2} + \frac{3}{8} - \lambda^2. \end{aligned} \tag{54}$$

The solutions to Heun confluent equations are computed as power series expansions around the regular singular point $x = 0$; that is, $r = 2M$. The series converges for $r < a$ (the second regular singularity) and the analytic continuation is obtained by expanding the solution around the regular singularity $r = a$ and overlapping the series.

For large x values, one may use the formula [8, 28]

$$\begin{aligned} & \mathit{HeunC}[\alpha, \beta, \gamma, \delta, \eta, x] \\ & \quad \approx D_1 x^{-[(\beta+\gamma+2)/2 + \delta/\alpha]} + D_2 e^{-\alpha x} x^{-[(\beta+\gamma+2)/2 - \delta/\alpha]} \\ & \quad = e^{-\alpha x/2} x^{-(\beta+\gamma+2)/2} \{ D_1 e^{\alpha x/2} x^{-\delta/\alpha} + D_2 e^{-\alpha x/2} x^{\delta/\alpha} \} \\ & \quad = D e^{-\alpha x/2} x^{-(\beta+\gamma+2)/2} \sin \left[-\frac{i\alpha x}{2} + \frac{i\delta}{\alpha} \ln x + \sigma \right], \end{aligned} \tag{55}$$

where D is an arbitrary constant and σ is the phase shift. With the parameters given in (54), the component S_1 from (49) gets the asymptotic form

$$S_1 \approx \frac{D}{\sqrt{r}} \sin \left[\omega r + 2\omega M \ln r - \frac{i}{2} \ln r + \sigma \right] \tag{56}$$

which, for large r values, behaves like

$$S_1 \sim \exp[i(\omega r + 2\omega M \ln r + \sigma)]. \tag{57}$$

The necessary condition for a polynomial form of the Heun confluent functions in (45) leads to the following quantized imaginary quasi-spectrum:

$$\omega = i \frac{(n+1)}{4M}. \tag{58}$$

In order to study the radiation emitted by the GHS black hole, one has to take the radial solution near the exterior event horizon, $r \longrightarrow r_h = 2M$. For $x \longrightarrow 0$, the Heun functions can be approximated to 1 and the (radial) components of Ψ defined in (26) and (33), with S_A given in (49), can be written as

$$\begin{aligned} \Psi_1 \approx e^{-i\omega t} e^{-i\omega r} \frac{1}{\sqrt{r(r-a)}} \{ & C_1 (r - 2M)^{2i\omega M - 1/4} \\ & + C_2 (r - 2M)^{-2i\omega M + 1/4} \} \end{aligned} \tag{59}$$

and

$$\Psi_2 \approx e^{-i\omega t} e^{i\omega r} \frac{1}{\sqrt{r(r-a)}} \left\{ C_1 (r-2M)^{-2i\omega M-1/4} + C_2 (r-2M)^{2i\omega M+1/4} \right\}, \tag{60}$$

pointing out the *in* and *out* modes

$$\Psi_{in} \sim e^{-i\omega t} (r-2M)^{-2i\omega M+1/4}, \quad \Psi_{out} \sim e^{-i\omega t} (r-2M)^{2i\omega M-1/4}. \tag{61}$$

By definition, the component ψ_{out} should asymptotically have the form

$$\Psi_{out} \sim (r-r_h)^{(i/2\kappa_h)(\omega-\omega_h)} \tag{62}$$

so that the relative scattering probability at the exterior event horizon surface is given by

$$\Gamma = \left| \frac{\Psi_{out}(r>2M)}{\Psi_{out}(r<2M)} \right|^2 = \exp\left[-\frac{2\pi}{\kappa_h} (\omega-\omega_h) \right]. \tag{63}$$

Inspecting the above relations, it yields the well-known results: $\kappa_h = 1/(4M)$,

$$\Gamma = e^{-8\pi M\omega} \tag{64}$$

and the mean number of emitted particles

$$N = \frac{\Gamma}{1-\Gamma} = \frac{1}{e^{\omega/T_h}-1}, \tag{65}$$

where $T_h = 1/(8\pi M)$ is the Hawking temperature.

4. Conclusions

In the present paper, we have used the free-of-coordinates formalism to write down both the Klein-Gordon and the Dirac equations, in their $SO(3,1) \times U(1)$ expression, for the GHS metric in (1).

Unlike the case for bosons, it turns out that, for the charged massive fermions interacting with the GHS dilaton black hole, the radial equation (40) does not have an analytic solution. However, to first order in a/r, the corresponding equations are satisfied by the Heun confluent functions (43).

In the massless case, the Dirac equation can be analytically solved and the derived solution, given by (52), is valid for the whole space, which includes not only the near-horizon region but also the far-away-from-the-black-hole region. Once the relation in (45) among the Heun function's parameters is imposed, the confluent Heun functions can be cast into a polynomial form and the energy spectrum is given by the imaginary quantized expression (58).

Finally, by identifying the *out* modes near the event horizon, we identified the Hawking black body radiation and the expected Hawking temperature is correctly recovered.

Data Availability

No data were used to support this study.

Conflicts of Interest

The authors declare that they have no conflicts of interest.

Acknowledgments

This work was supported by a grant of Ministry of Research and Innovation, CNCS-UEFISCDI, Project no. PN-III-P4-ID-PCE-2016-0131, within PNCDI III.

References

[1] M. J. Duff and J. Rahmfeld, "Massive string states as extreme black holes," *Physics Letters. B. Particle Physics, Nuclear Physics and Cosmology*, vol. 345, no. 4, pp. 441–447, 1995.

[2] V. Faraoni, E. Gunzig, and P. Nardone, "Conformal transformations in classical gravitational theories and in cosmology," *Fundamentals of Cosmic Physics*, vol. 20, p. 121, 1999.

[3] G. W. Gibbons, "Antigravitating black hole solitons with scalar hair in $N = 4$ supergravity," *Nuclear Physics B*, vol. 207, no. 2, pp. 337–349, 1982.

[4] G. W. Gibbons and K. Maeda, "Black holes and membranes in higher-dimensional theories with dilaton fields," *Nuclear Physics B*, vol. 298, no. 4, pp. 741–775, 1988.

[5] D. Garfinkle, G. T. Horowitz, and A. Strominger, "Charged black holes in string theory," *Physical Review D: Particles, Fields, Gravitation and Cosmology*, vol. 43, no. 10, p. 3140, 1991, Erratum: Physical Review D, vol. 45, pp. 3888, 1992.

[6] G. T. Horowitz, "The dark side of string theory: black holes and black strings," in *Proceedings of the Trieste Spring School and Workshop*, J. Harvey, R. Iengo, K. S. Narain, S. Randjbar-Daemi, and H. Verlinde, Eds., pp. 55–99, Trieste, Italy, 1992.

[7] R. Casadio and B. Harms, "Charged dilatonic black holes: string frame versus Einstein frame," *Modern Physics Letters A*, vol. 14, no. 17, pp. 1089–1103, 1999.

[8] A. Ronveaux, Ed., *Heun's Differential Equations*, Oxford University Press, New York, NY, USA, 1995.

[9] S. Y. Slavyanov and W. Lay, *Special Functions, A Unified Theory Based on Singularities*, Oxford Mathematical Monographs, Oxford University Press, 2000.

[10] S. B. Chen and J. L. Jing, "Asymptotic quasinormal modes of a coupled scalar field in the Garfinkle–Horowitz–Strominger dilaton spacetime," *Classical and Quantum Gravity*, vol. 22, no. 3, p. 533, 2005.

[11] S. Chen and J. Jing, "Dirac quasinormal modes of the Garfinkle–Horowitz–Strominger dilaton black-hole spacetime," *Classical and Quantum Gravity*, vol. 22, no. 6, pp. 1129–1141, 2005.

[12] F. McCarthy, D. Kubizňák, and R. B. Mann, "Dilatonic imprints on exact gravitational wave signatures," *Physical Review D: Particles, Fields, Gravitation and Cosmology*, vol. 97, no. 10, Article ID 104025, 2018.

[13] T. Birkandan and M. Hortaçsu, "Heun-type solutions for Schwarzschild metric with electromagnetic fields," *EPL (Europhysics Letters)*, vol. 119, no. 2, Article ID 20002, 2017.

[14] M. Hortaçsu, "Heun functions and some of their applications in physics," *Advances in High Energy Physics*, vol. 2018, Article ID 8621573, 14 pages, 2018.

[15] R. A. Konoplya, "Decay of a charged scalar field around a black hole: quasinormal modes of RN, RNAdS and dilaton black holes," *Physical Review D: Particles, Fields, Gravitation and Cosmology*, vol. 66, no. 8, Article ID 084007, 2002.

[16] K. D. Kokkotas, R. A. Konoplya, and A. Zhidenko, “Bifurcation of the quasinormal spectrum and Zero Damped Modes for rotating dilatonic black holes,” *Physical Review D: Particles, Fields, Gravitation and Cosmology*, vol. 92, no. 6, Article ID 064022, 2015.

[17] A. M. Ishkhanyan, T. A. Shahverdyan, and T. A. Ishkhanyan, “Thirty five classes of solutions of the quantum time-dependent two-state problem in terms of the general Heun functions,” *The European Physical Journal D*, vol. 69, p. 10, 2015.

[18] A. M. Ishkhanyan, T. A. Shahverdyan, and T. A. Ishkhanyan, “Schrödinger potentials solvable in terms of the general Heun functions,” *Annals of Physics*, vol. 388, pp. 456–471, 2018.

[19] H. S. Vieira and V. B. Bezerra, “Confluent Heun functions and the physics of black holes: resonant frequencies, Hawking radiation and scattering of scalar waves,” *Annals of Physics*, vol. 373, pp. 28–42, 2016.

[20] P. P. Fiziev, “Classes of exact solutions to the Teukolsky master equation,” *Classical and Quantum Gravity*, vol. 27, article 135001, 2010.

[21] A. Ashoorioon, “Non-unitary evolution in the general extended EFT of inflation & excited initial states,” *Journal of High Energy Physics*, vol. 2018, Article ID 012, 2018.

[22] E. Newman and R. Penrose, “An approach to gravitational radiation by a method of spin coefficients,” *Journal of Mathematical Physics*, vol. 3, pp. 566–578, 1962.

[23] R. A. Konoplya and A. Zhidenko, “Quasinormal modes of black holes: from astrophysics to string theory,” *Reviews of Modern Physics*, vol. 83, no. 3, pp. 793–836, 2011.

[24] X. He and J. Jing, “Late-time evolution of charged massive Dirac fields in the Kerr–Newman background,” *Nuclear Physics B*, vol. 755, no. 1–3, pp. 313–328, 2006.

[25] G. V. Kraniotis, “The massive Dirac equation in the curved spacetime of the Kerr-Newman (anti) de Sitter black hole,” 2018, https://arxiv.org/pdf/1801.03157.pdf.

[26] A. Al-Badawi, “Behavior of a spin-1/2 massive charged particle in Schwarzschild immersed in an electromagnetic universe,” *General Relativity and Gravitation*, vol. 50, p. 16, 2018.

[27] A. Al-Badawi and M. Q. Owaidat, “The Dirac equation in Schwarzschild black hole coupled to a stationary electromagnetic field,” *General Relativity and Gravitation*, vol. 49, no. 8, 2017.

[28] H. S. Vieira, V. B. Bezerra, C. R. Muniz, M. O. Tahim, and M. S. Cunha, “Garfinkle-Horowitz-Strominger dilaton black hole: resonant frequency, thermodynamics and Hawking radiation,” *General Relativity and Quantum Cosmology*, 2018.

[29] M. Wang, C. Herdeiro, and J. Jing, “Dirac perturbations on Schwarzschild–anti–de SITter spacetimes: generic boundary conditions and new quasinormal modes,” *Physical Review D: Particles, Fields, Gravitation and Cosmology*, vol. 96, no. 10, Article ID 104035, 2017.

[30] Wolfram Research, Inc., Mathematica, Version 11.3, Champaign, IL, 2018, http://support.wolfram.com/kb/472.

Hindawi
Advances in High Energy Physics
Volume 2018, Article ID 7420546, 12 pages
https://doi.org/10.1155/2018/7420546

Research Article

Models of Anisotropic Self-Gravitating Source in Einstein-Gauss-Bonnet Gravity

G. Abbas and M. Tahir

Department of Mathematics, The Islamia University of Bahawalpur, Bahawalpur-63100, Pakistan

Correspondence should be addressed to G. Abbas; abbasg91@yahoo.com

Received 1 November 2018; Accepted 13 December 2018; Published 27 December 2018

Guest Editor: Martiros Khurshudyan

Copyright © 2018 G. Abbas and M. Tahir. This is an open access article distributed under the Creative Commons Attribution License, which permits unrestricted use, distribution, and reproduction in any medium, provided the original work is properly cited.

In this paper, we have studied gravitational collapse and expansion of nonstatic anisotropic fluid in $5D$ Einstein-Gauss-Bonnet gravity. For this purpose, the field equations have been modeled and evaluated for the given source and geometry. The two metric functions have been expressed in terms of parametric form of third metric function. We have examined the range of parameter β (appearing in the form of metric functions) for which Θ, the expansion scalar, becoming positive/negative leads to expansion/collapse of the source. The trapped surface condition has been explored by using definition of Misner-Sharp mass and auxiliary solutions. The auxiliary solutions of the field equations involve a single function that generates two types of anisotropic solutions. Each solution can be represented in term of arbitrary function of time; this function has been chosen arbitrarily to fit the different astrophysical time profiles. The existing solutions forecast gravitational expansion and collapse depending on the choice of initial data. In this case, wall to wall collapse of spherical source has been investigated. The dynamics of the spherical source have been observed graphically with the effects of Gauss-Bonnet coupling term α in the case of collapse and expansion. The energy conditions are satisfied for the specific values of parameters in both solutions; this implies that the solutions are physically acceptable.

1. Introduction

In the gravitational study of more than four dimensions, the unification problem of gravity with electromagnetism and other basic connections are discussed by [1–3]. The study on supergravity by Witten [4] has strongly sported the work on unification problem of gravity. The problem of gravitational unification study is entirely based on the string theory [5, 6]. The ten-dimensional gravity that arises from string theory contains a quadratic term in its action [7, 8]; in low energy limit. Zwiebach [9] described the ghost-free nontrivial gravitational interactions for greater than 4 dimensions in the study of n-dimensional action in [7].

In recent years, the higher-order gravity included higher derivative curvature terms, which is an interesting and developing study. The most widely studied theory in the higher curvature gravities is known as Einstein-Gauss-Bonnet (EGB) theory of gravity. The EGB theory of gravity is a special case of the Lovelocks gravity. The Lagrangian of EGB gravity was obtained from the first three terms of Lagrangian of the Lovelock theory. Pedro [10] described that the 2^{nd} Euler density is the Gauss-Bonnet combination and is topological invariant in four dimensions. He also pointed out that, to make dynamical GB combination in four-dimensional theory, couple it to dynamical scalar field. The dynamical stability and adiabatic and anisotropic fluid collapse of stars in $5D$ EGB theory of gravity have been studied in [11, 12]. Gross and Sloan [13, 14] investigated that EGB theory of gravity occurs in the low energy effectual action [8] of super heterotic sting theory. The exact black hole (BH) solution in greater than or equal to five-dimensional gravitational theories is studied by [8]. Dadhich [15] examined in Newtonian theory that gravity is independent of space-time dimensions with constant density of static sphere, and this result is valid for Einstein and higher-order EGB theory of gravity. The conditions for universality of Schwarzschild interior solution describe sphere with uniform density for the dimensions greater than or equal to four. The authors in [16–20] described that the existence of EGB term in the string theory leads to singularity-free solutions in cosmology and hairy black holes. The solutions described in [8] are generalization of n-dimensional spherically symmetric BH solution determined in [21, 22]. In literatures [23–25], the authors examined the other spherical symmetric BH solutions in GB theory of gravity. Cai [26, 27] discussed the structure of topologically nontrivial black holes. The effects of GB term on the Vaidya solutions have been studied in [28–32]. Wheeler [23] discussed the spherical symmetric BH solutions and their physical properties. The GB term has no effect on the existence of local naked singularity, but the strength of the curvature is affected.

In the composition of stars, the nuclear matter is enclosed inside the stars. The stars are gravitated and attracted continuously to the direction of their center because of gravitational interaction of their matter particles; this phenomenon is known as gravitational contraction of stars, which leads to gravitational collapse. It is studied in [33] that, during the gravitational collapse, the space-time singularities are generated. When the massive stars collapse due to their own gravity, the end state of this collapse may be a neutron star, white dwarf, a BH, or a naked singularity [34]. The spherical symmetric collapse of perfect fluid is discussed in [35, 36]. The dissipative and viscous fluid gravitational collapse in GR is discussed in literatures [37–48].

Zubair et al. [49] studied a dynamical stability of cylindrical symmetric collapse of sphere filled with locally anisotropic fluid in $f(R,T)$ theory of gravity. A lot of literatures are available about the gravitational collapse and BH in GB theory of gravity [50–58]. If the $f(R,T)$ theory of gravity obeys the stress-energy tensor conservation, then unknown $f(R,T)$ function can be obtained in the closed form [59]. Abbas and Riaz [60] determined the exact solution of nonstatic anisotropic gravitational fluid in $f(R,T)$ theory of gravity, which may lead to collapse and expansion of the star. Sharif and Aisha [61] studied the models for collapse and expansion of charged self-gravitating objects in $f(R,T)$ theory of gravity.

Oppenheimer and Snyder [62] observed the gravitational contraction of inhomogeneous spherically symmetric dust collapse, and according to this end state of the gravitational collapse is BH. Markovic and Shapiro [63] studied this work for positive cosmological constant, and Lake [64] discussed this for negative as well as positive cosmological constant. Sharif and Abbas [65] studied the gravitational perfect fluid charged collapse with cosmological constant in the Friedmann universe model with weak electromagnetic field. Sharif and Ahmad [66–69] worked on the spherical symmetric gravitational collapse of perfect fluid withe positive cosmological constant. Sharif and Abbas [70] discussed the 5-dimenssional symmetric spherical gravitational collapse with positive cosmological constant in the existence of an electromagnetic field. Abbas and Zubair [71] investigated the dynamical anisotropic gravitational collapse in EGB theory of gravity. A homogeneous spherical cloud collapse with zero rotation and disappearing internal pressure leads to a singularity covered by an event horizon [72]. Jhingan and Ghosh [73] discussed the five or greater than five-dimensional gravitational inhomogeneous dust collapse in EGB theory of gravity. They investigated the exact solution in closed form. Sunil et. al [74] investigated the exact solution to the field equations for five-dimensional spherical symmetric and static distribution of the prefect fluid in EGB modified gravity. Abbas and Tahir [75] studied the exact solution of motion during gravitational collapse of prefect fluid in EGB theory of gravity. It should be observed in [73, 75–78] that coupling term α changes the structure of the singularities. Glass [79] generated the collapsing and expansion solutions of anisotropic fluid of Einstein field equations. In this paper, we extended the work of Glass [79] to model the solutions for collapse and expansion of anisotropic fluid in the EGB theory of gravity. The paper has been arranged as follows.

In Section 2, we present interior matter distribution and field equations. We discuss the generation of solutions for the gravitational collapse and expansion in Section 3. The last section presents the summary of the results of this paper.

2. Matter Distribution Inside the Star and the Field Equations

We start with the $5D$ action given as

$$S = \int d^5 x \sqrt{-g} \left[\frac{1}{2\kappa_5^2} \left(R + \alpha L_{GB} \right) \right] + S_{matter}, \qquad (1)$$

where $\kappa_5 \equiv \sqrt{8\pi G_5}$ is gravitational constant and R is a Ricci scalar in $5D$, and α is known as the coupling constant of the GB term. The GB Lagrangian is given as follows:

$$L_{GB} = R^2 - 4R_{ab}R^{ab} + R_{abcd}R^{abcd}. \qquad (2)$$

This kind of action is discussed in the low energy limit of supersting theory [13, 14]. In this paper, we consider only the case with $\alpha > 0$. The action in (1) gives the following field equations:

$$G_{ab} + \alpha H_{ab} = T_{ab}, \qquad (3)$$

where

$$G_{ab} = R_{ab} - \frac{1}{2} g_{ab} R \qquad (4)$$

is the Einstein tensor and

$$H_{ab} = 2\left(RR_{ab} - 2R_{a\alpha}R^{\alpha}_{b} - 2R^{\alpha\beta}R_{a\alpha b\beta} + R^{\alpha\beta\gamma}_{a}R_{b\alpha\beta\gamma} \right) - \frac{1}{2} g_{ab} L_{GB} \qquad (5)$$

is the Lanczos tensor. We want to find the solution for collapse and expansion of a spherical anisotropic fluid in 5D-EGB gravity.

$$ds^2 = -A(t,r)^2 dt^2 + B(t,r)^2 dr^2 + R(t,r)^2 d\Omega_3^2, \qquad (6)$$

where $d\Omega_3^2 = (d\theta^2 + \sin^2\theta(d\phi^2 + \sin^2\phi d\psi^2))$ is a metric on three spheres and $R = R(t,r) \geq 0$, $A = A(t,r)$, and $B = B(t,r)$. The energy-momentum tensor for anisotropic fluid is

$$T_{ab} = (\mu + p_{\perp}) V_a V_b + p_{\perp} g_{ab} + (p_r - p_{\perp}) \chi_a \chi_b, \qquad (7)$$

where μ, p_r, $p_\perp$, χ_a, and V_a are the energy density, radial pressure, tangential pressure, unit four vector along the radial direction, and four velocity of the fluid, respectively. For the metric in (6), V_a and χ_a are given by [60] as follows:

$$\begin{aligned} V^a &= A^{-1}\delta^a_0, \\ \chi^a &= B^{-1}\delta^a_1 \end{aligned} \tag{8}$$

which satisfy

$$\begin{aligned} V^aV_a &= -1, \\ \chi^a\chi_a &= 1, \\ \chi^aV_a &= 0. \end{aligned} \tag{9}$$

The expansion scalar is

$$\Theta = \frac{1}{A}\left(\frac{\dot{B}}{B} + \frac{3\dot{R}}{R}\right). \tag{10}$$

The dimensionless measure of anisotropy is defined as

$$\triangle a = \frac{p_r - p_\perp}{p_r}. \tag{11}$$

Equation (3) for the metric in (6) with the help of (7) is given as follows:

$$\begin{aligned} \mu = {} & \frac{12\alpha}{A^4B^5R^3}\,[\dot{R}(\dot{R}(A'^2R - B^2\dot{B}\dot{R} \\ & + A^2(BR'' - B'R'))B^2 + A^2B^2\dot{B}(R'^2 - B^2)) \\ & + 2AA'B^2R\dot{R}(\dot{B}R' - B\dot{R}') + A^4(B^2 - R'^2)(BR'' \\ & - B'R')] - \frac{3}{A^2B^3R^2}\,[B^3(A^2 + \dot{R}^2) + A^2R'(B'R \\ & - BR') + BR(B\dot{B}\dot{R} - A^2R'')], \end{aligned} \tag{12}$$

$$\begin{aligned} p_r = {} & \frac{12\alpha}{A^5B^4R^3}\,[B^2\dot{R}^2(\dot{A}\dot{R}B^2 - A(2A'^2R + B^2\ddot{R})) \\ & + A^2((A^2A'R' + B^2(\dot{A}\dot{R} - A\ddot{R}))(R'^2 - B^2) \\ & + B^2A'R'\dot{R}^2)] + \frac{3}{A^3B^2R^2}\,[A^2((A'R + AR')R' \\ & - AB^2) + B^2((\dot{A}\dot{R} - A\ddot{R})R - A\dot{R}^2)], \end{aligned} \tag{13}$$

$$\begin{aligned} p_\perp = {} & \frac{-4\alpha}{A^5B^5R^2}\,[B^3\dot{B}(3B\dot{A}\dot{R}^2 + A(A'^2\dot{R} \\ & - B(\ddot{B}\dot{R} + 2\dot{B}\ddot{R}))) + (AB)^2(\dot{R}(BA''\dot{R} \\ & + A'(4\dot{B}R' - 2B\dot{R}' - B'\dot{R})) + \dot{A}((B^2 - R'^2)\dot{B} \\ & + 2\dot{R}(B'R' - BR''))) + A^3B(\dot{B}^2R'^2 - B^3\ddot{B} \\ & + BR'(\ddot{B}R' - 2B'\ddot{R} - 2\dot{B}\dot{R}') + B^2(\dot{R}'^2 + 2\ddot{R}R'')) \\ & + A^4(A''B(B^2 - R'^2) - A'(B(BB' + 2R'R'') \\ & - 3B'R'^2))] - \frac{1}{(AB)^3R^2}\,[R^2((A\ddot{B} - \dot{A}\dot{B})B^2 \\ & + A^2(A'B' - A''B)) + 2R(AB((\dot{B}\dot{R} + B\ddot{R})B \\ & - A(A'R' + AR'')) + A^3B'R' - B^3\dot{A}\dot{R}) \\ & + AB(B^2(A^2 + \dot{R}^2) - A^2R'^2)], \end{aligned} \tag{14}$$

$$\begin{aligned} 0 = {} & \frac{-12\alpha}{A^4B^4R^3}(A'B\dot{R} - AB\dot{R}' + A\dot{B}R')(2A^2(A'B' \\ & - A''B)R^2 - B^2(AB\dot{R}^2 + 2\dot{A}\dot{B}R^2) + A^3B(R'^2 \\ & - B^2)) + \frac{3}{ABR}(A'B\dot{R} - AB\dot{R}' + A\dot{B}R') \end{aligned} \tag{15}$$

where the prime and dot denote the partial derivative with respect to r and t, respectively. The auxiliary solution of (15) is

$$\begin{aligned} A &= \frac{\dot{R}}{R^\beta}, \\ B &= R^\beta. \end{aligned} \tag{16}$$

By Using the auxiliary solution in (16) in (10), the expansion scalar becomes

$$\Theta = R^{\beta-1}(3 + \beta). \tag{17}$$

For $\beta > -3$ and $\beta < -3$, we obtained expansion and collapse regions. The matter components from (12), (13), and (14) with the help of (16) are

$$\begin{aligned} \mu = {} & \frac{12\alpha}{R^{4(1-\beta)}}\,[R^{2\beta}((((\frac{2R\dot{R}'}{\dot{R}} - \beta R')R' - R^{2\beta} - 1) \\ & \cdot R^{4\beta} - \beta R'^2) + R'^4)\beta + R^{2\beta}(1 + R^{2\beta}) - R'^2) \\ & \cdot RR'') - \frac{R^{4\beta}R^2\dot{R}'^2}{\dot{R}^2}] - \frac{3}{R^{2(1+\beta)}}\,[(\beta - 1)R'^2 - RR'' \\ & + R^{2\beta}(1 + R^{2\beta}(1 + \beta)], \\ p_r = {} & \frac{12\alpha}{R^{4(1-\beta)}}\,[R^{4\beta}(R^{2\beta}(1 - R^{2\beta}) + R'(\frac{4R\dot{R}'}{\dot{R}} \\ & + R'(\frac{1}{R^{2\beta}} + \frac{R'^2}{R^{4\beta}} - 2)))\beta + \frac{RR'\dot{R}'}{\dot{R}}((1 - R^{2\beta}) \\ & \cdot R^{2\beta} - R'^2) - 2\left(\frac{R^{2\beta}R\dot{R}'}{\dot{R}}\right)^2] + \frac{3}{R^2}\,[\frac{1}{R^{2\beta}}(R'^2 \end{aligned} \tag{18}$$

$$-R\ddot{R}-\dot{R}^{2})+\frac{1}{R^{4\beta}}\left(R\dot{R}\ddot{R}+R'\dot{R}'-\beta\dot{R}\left(\dot{R}^{2}+\dot{R}'^{2}\right)\right)-1\Bigg], \tag{19}$$

$$\begin{aligned}p_{\perp}=&\frac{4\alpha}{R^{4(1+\beta)}}\Bigg[R^{4\beta}\left(\beta\left(\left(4\beta-1\right)R^{4\beta}+R^{2\beta}\left(2\beta-1\right)\right)\right.\\&-\beta R''+R'^{2}\left(\beta^{2}-1\right)\Big)+R^{2\beta}\left(RR''\beta-R'^{2}\left(1+\beta\right.\right.\\&+\beta^{2}\big)\big)+R'^{2}\left(R'^{2}\left(1+\beta+3\beta^{2}\right)-3\beta RR''\right)\\&+\frac{R^{2\beta}R}{\dot{R}}\left(\left(\dot{R}'R'\beta-R\dot{R}''\right)\left(R^{2\beta}+1\right)\right)\\&+\frac{RR'}{\dot{R}}\left(R'\left(R\dot{R}''-5\beta\dot{R}R'\right)+2R\dot{R}'R''\right)\Bigg]\\&-\frac{1}{R^{2(1+\beta)}}\Bigg[R^{2\beta}-R'^{2}\left(\beta^{2}-3\beta+2\right)+R^{4\beta}\left(2\beta^{2}+3\beta\right.\\&+1\big)+RR''\left(\beta-2\right)+\frac{R}{\dot{R}}\left(R'\dot{R}'\left(3\beta-2\right)-R\dot{R}''\right)\Bigg].\end{aligned} \tag{20}$$

The Misner-Sharp mass function m(t,r) is given as follows:

$$\begin{aligned}m\left(t,r\right)=&\frac{\left(n-2\right)}{2k_{n}^{2}}V_{n-2}^{k}\left(R^{n-3}\left(k-g^{ab}R_{,a}R_{,b}\right)\right.\\&+\left(n-3\right)\left(n-4\right)\alpha\left(k-g^{ab}R_{,a}R_{,b}\right)^{2}\Big)\end{aligned} \tag{21}$$

where comma represents partial differentiation and the surface of $(n-2)$ dimensional unit space is represented by V_{n-2}^{k}. By using $V_{n-2}^{1}=(2\pi(n-1)/2)/\Gamma((n-1)^{2})$, $k=1$ with $n=5$, and (16) in (21), we get

$$\begin{aligned}m\left(r,t\right)=&\frac{3}{2}\left(R^{2}\left(1-\frac{R'^{2}}{R^{2\beta}}+R^{2\beta}\right)\right.\\&+2\alpha\left(1-\frac{R'^{2}}{R^{2\beta}}+R^{2\beta}\right)^{2}\Bigg).\end{aligned} \tag{22}$$

The specific values of β and $R(r,t)$ form an anisotropic configuration. When $R'=R^{2\beta}$, there exist trapped surfaces at $R=\pm\sqrt{(2/3)m-2\alpha}$, provided that $m\geq 3\alpha$. Therefore, in this case, $R'=R^{2\beta}$ is trapped surface condition.

3. Generating Solutions

For the different values of β, expansion scalar $\Theta<0$ for collapse and $\Theta>0$ for expansion solutions are discussed as follows.

4. Collapse with $\beta=-7/2$

The expansion scalar must be negative in case of the collapse, so for $\beta<-3$, from (17), we get $\Theta<0$. By assuming $\beta=-7/2$ and the trapped condition $R'=R^{2\beta}$ and then integration, we obtain

$$R_{trap}=\left(8r+z_{1}\left(t\right)\right)^{1/8}. \tag{23}$$

It is to noted that (23) is only valid for the trapped surface, and it can not be used everywhere. In order to discuss the solutions outside the trapped surface, we follow Glass [79] and take the value of $R(r,t)$ as posivite scalar $(k>1)$ multiple of R_{trap}, such that $R(r,t)>R_{trap}$. Hence the convenient form of the areal radius $R(r,t)$ for the solution outside the trapped surface is given by

$$\begin{aligned}R&=k\left(8r+z_{1}\left(t\right)\right)^{1/8},\\z_{1}\left(1\right)&=1+t^{2}.\end{aligned} \tag{24}$$

Thus (18)–(20) with (24) and $\beta=-7/2$ yield the following set of equations:

$$\begin{aligned}\mu=&\frac{-21\alpha}{k^{18}\left(8r+z_{1}\right)^{9/4}}\left[-2+k^{7}\left(\left(11-2k^{16}\right)k^{9}\right.\right.\\&\left.\left.-2\left(8r+z_{1}\right)^{7/8}\left(1-k^{25}\right)\right)\right]\\&+\frac{3}{2k^{9}\left(8r+z_{1}\right)^{9/8}}\left[5\left(k^{16}-1\right)+2k^{7}\left(8r+z_{1}\right)^{7/8}\right],\end{aligned} \tag{25}$$

$$\begin{aligned}p_{r}=&\frac{-42\alpha}{k^{18}\left(8r+z_{1}\right)^{9/4}}\left[-1+k^{7}\left(\left(9-k^{16}\right)k^{9}\right.\right.\\&\left.\left.-\left(8r+z_{1}\right)^{7/8}\left(1-k^{25}\right)\right)\right]\\&-\frac{3}{1024k^{2}\left(8r+z_{1}\right)^{5/4}}\Big[k^{9}\Big(896k^{7}\dot{z}_{1}+\left(8r+z_{1}\right)^{1/8}\\&\cdot\left(1024+96\dot{z}_{1}^{2}-k^{8}\dot{z}_{1}\left(128+7\dot{z}_{1}^{2}\right)\right)\Big)+\left(128r\right.\\&+16z_{1}\big)\left(\left(8r+z_{1}\right)^{1/8}\left(k^{8}\dot{z}_{1}-8\right)k^{9}\ddot{z}_{1}-64\right)\Big],\end{aligned} \tag{26}$$

$$\begin{aligned}p_{\perp}=&\frac{\alpha}{k^{18}\left(8r+z_{1}\right)^{9/4}}\left[210-k^{7}\left(\left(375-165k^{16}\right)k^{9}\right.\right.\\&\left.\left.-\left(8r+z_{1}\right)^{7/8}\left(112-67k^{25}\right)\right)\right]\\&+\frac{1}{4k^{9}\left(8r+z_{1}\right)^{9/8}}\left[60-k^{7}\left(315k^{9}\right.\right.\\&\left.\left.-4\left(8r+z_{1}\right)^{7/8}\right)\right].\end{aligned} \tag{27}$$

In this case, (22) is reduced to the following form:

$$\begin{aligned}m\left(r,t\right)=&\frac{3}{2}\left[k^{2}\left(8r+z_{1}\right)^{1/4}-\frac{k^{11}}{\left(8r+z_{1}\right)^{5/8}}\right.\\&+\frac{\left(8r+z_{1}\right)^{1/8}}{k^{5}}\\&\left.+2\alpha\left(1-\frac{k^{9}}{\left(8r+z_{1}\right)^{7/8}}+\frac{1}{k^{7}\left(8r+z_{1}\right)^{7/8}}\right)\right].\end{aligned} \tag{28}$$

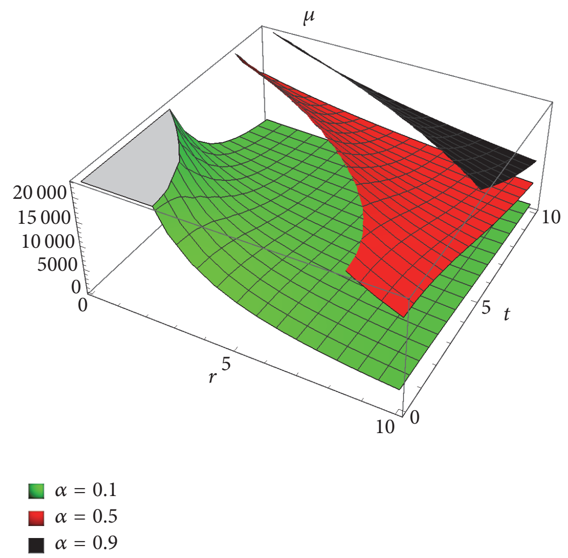

FIGURE 1: Plot of density along r and t for $k = 2.5$ and the different values of α.

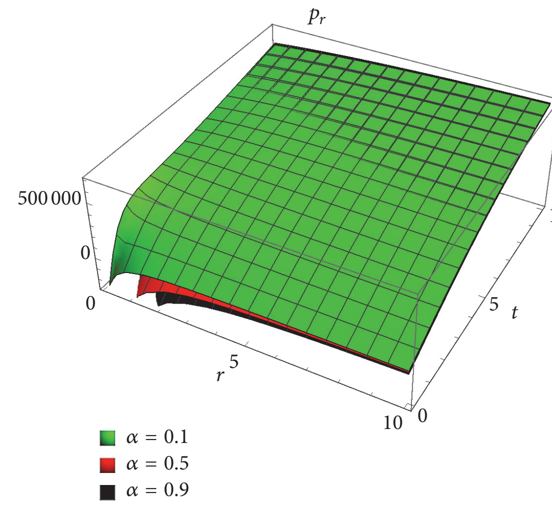

FIGURE 2: Behavior of radial pressure along r and t for $k = 2.5$ and the different values of α.

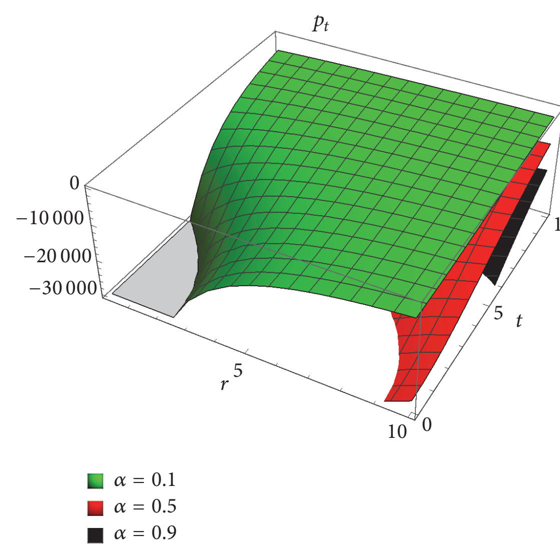

FIGURE 3: Tangential pressure along r and t for $k = 2.5$ and the different values of α.

Equation (11), with the help of (26) and (27), becomes

$$\Delta a = 1 - \frac{C_1 + C_2}{C_3 + C_4} \tag{29}$$

where $C_1 = 45\alpha/(8r + z_1)^{11/8}$, $C_2 = (1/(8r + z_1)^{1/8})[45/4(8r + z_1) + 1]$, $C_3 = -294\alpha(8r + z_1)^{-9/4}$, and $C_4 = -(3/1024)[896\dot{z}_1/(8r+z_1)^{5/4} + (1/(8r+z_1)^{9/8})(1024-128\dot{z}_1 + 96\dot{z}_1{}^2 - 7\dot{z}_1{}^3) + ((128r + 16z_1)/(8r + z_1)^{5/4})((8r + z_1)^{1/8}(\dot{z}_1 - 8)\ddot{z}_1 - 64)]$.

The energy conditions for the curvature matter coupled gravity are

(i) Null energy condition: $\mu + p_r \geq 0$; $\mu + (1/2)p_t \geq 0$

(ii) Weak energy condition: $\mu \geq 0$, $\mu + p_r \geq 0$, and $\mu + (1/2)p_t \geq 0$

(iii) Strong energy condition: $\mu + (1/4)p_r + (1/2)p_t \geq 0$

In this case, we analyzed our results for time profile $z_1 = 1 + t^2$, $k = 2.5$, and the different values of α. For $\beta = -7/2$, we obtained $\Theta < 0$; the energy density is decreasing with respect to radius r and time t and remains positive for different values of coupling constant α as shown in Figure 1. As the density is decreasing, spherical object goes to collapse outward the point. It is observed in Figure 2 that the radial pressure is increasing outward the center, and it is also noted in Figure 3 that the tangential pressure is increasing with respect to radius r and time t at various values of α. Due to this increase of radial and tangential pressure on the surface, the sphere loses the equilibrium state, which may cause the collapse of the sphere outward the center. Figure 4 shows that the mass is decreasing function of r and t during the collapse at different values of α. The anisotropy is directed outward when $p_t < p_r$; this implies that $\Delta a > 0$ and it is directed inward when $p_r < p_t$; this implies that $\Delta a < 0$. In this case $\Delta a > 0$ for increasing r and t at various values of α as shown in Figure 5. This represents that the anisotropy force allows the formation of more massive object and has attractive force for $\Delta a < 0$ near the center. In the present case, the GB coupling term α affects the anisotropy and the homogeneity of the collapsing sphere. All the energy conditions are plotted in Figure 6; these plots represent that all the energy conditions are satisfied for considered parameters in collapse solutions.

5. Expansion with β=$-5/2$

In this case, the expansion scalar Θ must be positive. When $\beta > -3$, from (17), the expansion scalar Θ is positive. We assume that

$$R = \left(r^2 + r_0^2\right)^{-1} + z_2(t), \tag{30}$$

where r_0 is constant and we take $z_2 = z_2(t) = 1 + t^2$.

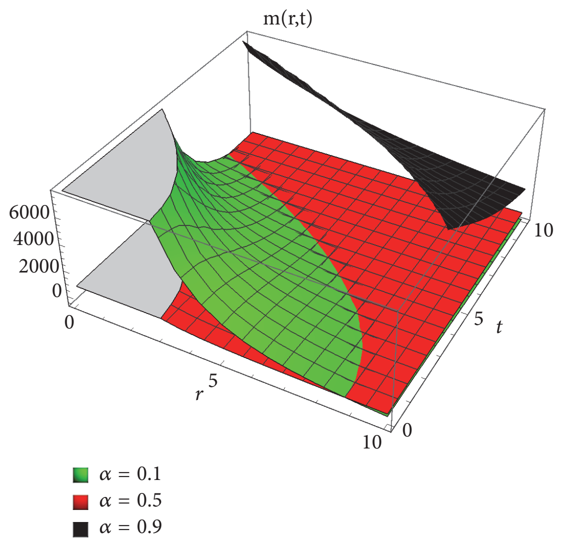

FIGURE 4: Mass plot along r and t for $k = 2.5$ and the different values of α.

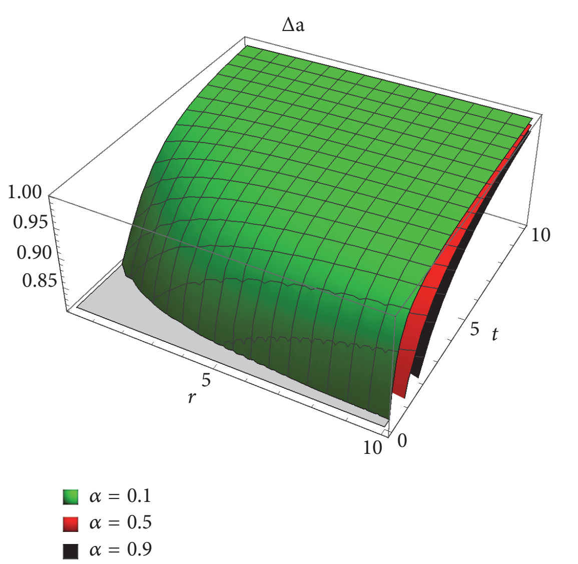

FIGURE 5: Plot of anisotropy parameter along r and t for $k = 2.5$ and the different values of α.

For $\beta = -5/2$, (18), (19), and (20) take the forms

$$\mu = \alpha\left[\frac{30}{R^9}\left(\frac{1}{R^5}+1\right)+6R\left(5R'^2+2RR''\right)\left(1-R^5R'^2\right)+\frac{1}{R^3}\left(12R''-75\frac{R'^2}{R}\right)-\frac{12\dot{R}'}{R^2\dot{R}}\left(\frac{1}{\dot{R}}+\frac{5R'}{R}\right)\right]-\frac{3}{2}\left[\frac{1}{R^2}\left(\frac{3}{R^5}-2\right)+R^3\left(7R'^2+2RR''\right)\right], \quad (31)$$

$$p_r = -6\alpha\left[\frac{2\dot{R}'}{R^2\dot{R}}\left(\frac{2\dot{R}'}{\dot{R}}+\frac{9R'}{R}\right)+RR'\left(\frac{2R\dot{R}'}{\dot{R}}+5\dot{R}^3R'\right)\left(R^5R'^2-1\right)+\frac{5\dot{R}^3}{R^{14}}\left(R^5\left(5R^5R'^2-1\right)-1\right)\right]+\frac{3}{4}\left[2R^3R'\left(\frac{2R\dot{R}'}{\dot{R}}+7R'\right)-\frac{\ddot{R}}{R^6\dot{R}^2}\left(\frac{5}{R^{7/2}}+2\right)-\frac{1}{R^2}\left(\frac{25}{R^{17/2}}+\frac{4}{R^5}+4\right)\right], \quad (32)$$

$$p_\perp = \alpha\left[\frac{1}{R^4}\left(\frac{110}{R^{10}}+\frac{60}{R^5}+21R'^2\right)+RR'^2\left(69R^5R'^2-19\right)+10R''\left(\frac{1}{R^3}+R^2\left(3R^5R'^2-1\right)\right)+\frac{2}{R^2\dot{R}}\left(\dot{R}''\left(R^5\left(R^5R'^2-1\right)-1\right)+\frac{R'\dot{R}'}{R}\left(R^5\left(4R^6R''+25R^5R'^2-15\right)-5\right)\right)\right]+\frac{1}{R^2}\left(\frac{6}{R^5}+1\right)-\frac{9}{2}R^3\left(RR''+\frac{7}{2}R'^2\right)-\frac{R^4}{\dot{R}}\left(R\dot{R}''-\frac{19}{2}R'\dot{R}'\right). \quad (33)$$

Assuming that $F(r,t) = 1 + z_2(t)(r^2 + r_0^2)$ and $R = F/(r^2 + r_0^2)$, (31), (32), and (33) in this case are

$$\mu = \alpha\left[10\left(\frac{r^2+r_0^2}{F}\right)^9\left(1+\left(\frac{r^2+r_0^2}{F}\right)^5\right)+\frac{8F^2}{\left(r^2+r_0^2\right)^5}\left(\frac{4r^2F^5}{\left(r^2+r_0^2\right)^9}-1\right)\left(F\left(5r^2+r_0^2\right)-z_2\left(r^2+r_0^2\right)\left(r_0^2-3r^2\right)\right)+4r^2\left(\frac{20F}{\left(r^2+r_0^2\right)^5}-\frac{25}{F^4}-\frac{40r^2F^6}{\left(r^2+r_0^2\right)^{14}}\right)-\frac{8\left(5r^2+r_0^2\right)}{F^2}+\frac{8z_2}{F^3}\left(r^2+r_0^2\right)\left(r_0^2-3r^2\right)\right]-\frac{3}{2}\left[\left(r^2+r_0^2\right)^2\left(\frac{3\left(r^2+r_0^2\right)^5}{F^7}-\frac{2}{F^2}\right)+\frac{4F^3}{\left(r^2+r_0^2\right)^6}\left(\left(r_0^2-3r^2\right)z_2-\frac{F^2\left(5r^2+r_0^2\right)}{\left(r^2+r_0^2\right)}+\frac{7r^2}{\left(r^2+r_0^2\right)}\right)\right], \quad (34)$$

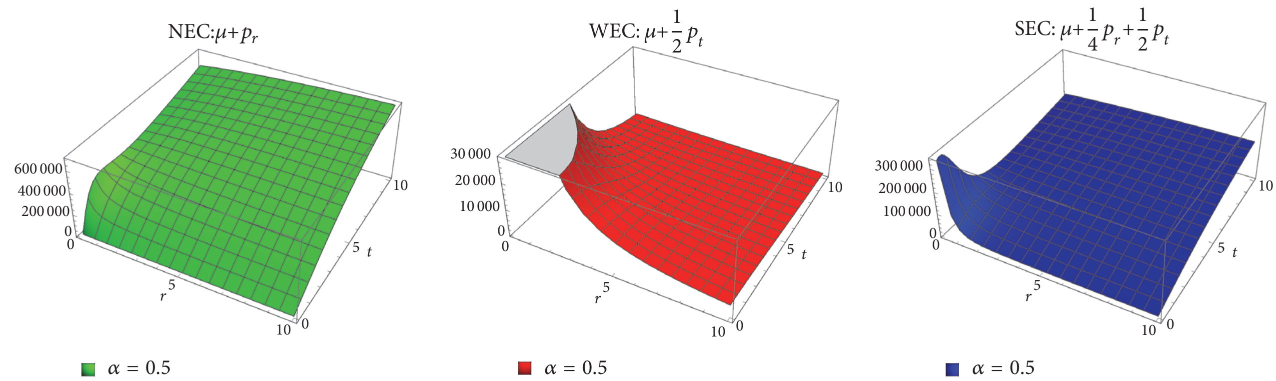

Figure 6: Plot of energy conditions along r and t for $k = 2.5$.

$$\begin{aligned}
p_r = {} & 6\alpha\left[5\left(\frac{r^2+r_0^2}{F}\right)^9\left(1+\left(\frac{r^2+r_0^2}{F}\right)^5\right)\right. \\
& \left.-4r^2\left(\frac{25}{F^4}-\frac{5F}{\left(r^2+r_0^2\right)^5}\left(1-\frac{4r^2F^5}{\left(r^2+r_0^2\right)^9}\right)\right)\right] \\
& +\frac{3}{4}\left[-2\frac{\ddot{z}_2}{\dot{z}_2}\left(\frac{r^2+r_0^2}{F}\right)^{19/2}\left(5+2\left(\frac{F}{r^2+r_0^2}\right)^{7/2}\right)\right. \\
& +\frac{56r^2F^3}{\left(r^2+r_0^2\right)^7}-25\left(\frac{r^2+r_0^2}{F}\right)^{21/2}-4\left(\frac{r^2+r_0^2}{F}\right)^7 \\
& \left.-4\left(\frac{r^2+r_0^2}{F}\right)^2\right],
\end{aligned} \tag{35}$$

$$\begin{aligned}
p_\perp = {} & \alpha\left[60\left(\frac{r^2+r_0^2}{F}\right)^9+110\frac{\left(r^2+r_0^2\right)^8}{F^{14}}\right. \\
& +\left(\frac{10F^2}{\left(r^2+r_0^2\right)^5}-\frac{10}{F^3}-\frac{60r^2F^7}{\left(r^2+r_0^2\right)^{14}}\right) \\
& \cdot\left(2F\left(5r^2+r_0^2\right)-2z_2\left(r^2+r_0^2\right)\left(r_0^2-3r^2\right)\right)+\left(69\right. \\
& \left.-16F^2\right)\left(\frac{16r^4F^6}{\left(r^2+r_0^2\right)^{14}}\right)+\frac{r^2F}{\left(r^2+r_0^2\right)^5}\left(64F^2-76\right) \\
& \left.+\frac{r^2}{F^2}\left(\frac{84}{F^2}+64\right)\right]+\left(\frac{r^2+r_0^2}{F}\right)^2+6\left(\frac{r^2+r_0^2}{F}\right)^7 \\
& +\frac{F^3}{\left(r^2+r_0^2\right)^7}\left(r^2\left(16F^2-63\right)+\frac{9F}{2}\left(2F\left(5r^2+r_0^2\right)\right.\right. \\
& \left.\left.-2z_2\left(r^2+r_0^2\right)\left(r_0^2-3r^2\right)\right)\right).
\end{aligned} \tag{36}$$

The mass function (22) in this case reduces to

$$\begin{aligned}
m(r,t) = {} & \frac{3}{2}\left[\frac{F^2}{\left(r^2+r_0^2\right)^2}\left(1\right.\right. \\
& -\left(\frac{F'}{r^2+r0^2}-\frac{2rF}{\left(r^2+r0^2\right)^2}\right)^2\left(\frac{F}{r^2+r0^2}\right)^5 \\
& \left.+\frac{\left(r^2+r0^2\right)^5}{F^5}\right)+2\alpha\left(1\right. \\
& -\left(\frac{F'}{r^2+r0^2}-\frac{2rF}{\left(r^2+r0^2\right)^2}\right)^2\left(\frac{F}{r^2+r0^2}\right)^5 \\
& \left.\left.+\frac{\left(r^2+r0^2\right)^5}{F^5}\right)^2\right].
\end{aligned} \tag{37}$$

With the help of (35) and (36), (11) takes the form

$$\Delta a = 1-\frac{E_1+E_2}{E_3+E_4} \tag{38}$$

where $E_1 = \alpha[60((r^2+r_0^2)/F)^9+110((r^2+r_0^2)^8/F^{14})+(10F^2/(r^2+r_0^2)^5-10/F^3-60r^2F^7/(r^2+r_0^2)^{14})(2F(5r^2+r_0^2)-2z_2(r^2+r_0^2)(r_0^2-3r^2))+(69-16F^2)(16r^4F^6/(r^2+r_0^2)^{14})+(r^2F/(r^2+r_0^2)^5)(64F^2-76)+(r^2/F^2)(84/F^2+64)]$, $E_2 = ((r^2+r_0^2)/F)^2+6((r^2+r_0^2)/F)^7+(F^3/(r^2+r_0^2)^7)(r^2(16F^2-63)+(9F/2)(2F(5r^2+r_0^2)-2z_2(r^2+r_0^2)(r_0^2-3r^2)))$, $E_3 = 6\alpha[5((r^2+r_0^2)/F)^9(1+((r^2+r_0^2)/F)^5)-4r^2(25/F^4-(5F/(r^2+r_0^2)^5)(1-4r^2F^5/(r^2+r_0^2)^9))]$, and $E_4 = (3/4)[-2(\ddot{z}_2/\dot{z}_2)((r^2+r_0^2)/F)^{19/2}(5+2(F/(r^2+r_0^2))^{7/2})+56r^2F^3/(r^2+r_0^2)^7-25((r^2+r_0^2)/F)^{21/2}-4((r^2+r_0^2)/F)^7-4((r^2+r_0^2)/F)^2]$.

In this case, we take $r_0 = 0.5$, $z_2 = 1+t^2$, and the various values of α and analyze our results. For $\beta = -5/2$, we obtained $\Theta > 0$; Figure 7 shows that, for the variation of α, the energy density increases for the time profile. The radial pressure is initially maximum and then decreases along t; the

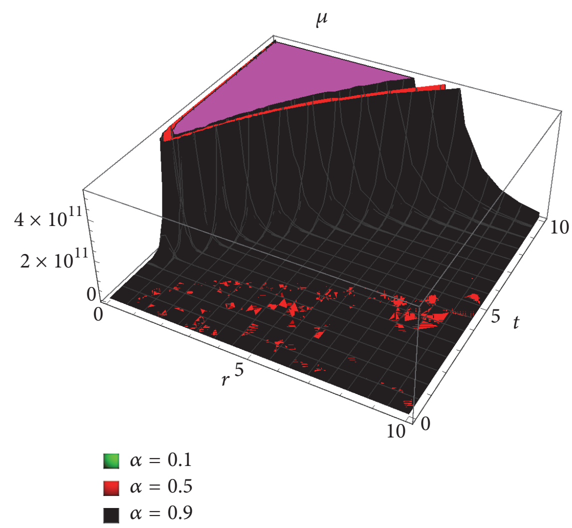

FIGURE 7: Density behavior along r and t for $r_0 = 0.5$ and the different values of α.

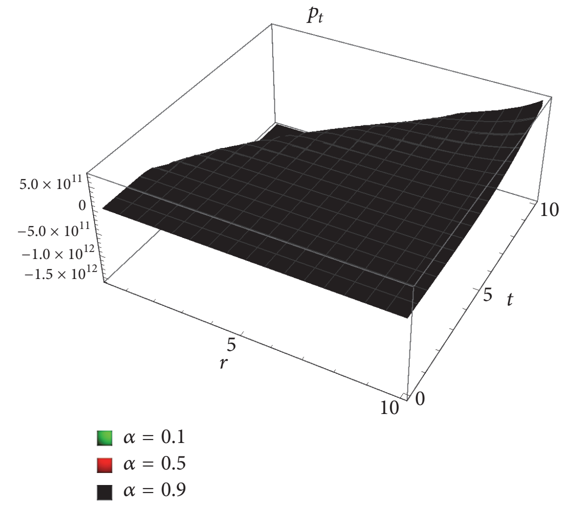

FIGURE 9: Tangential pressure behavior along r and t for $r_0 = 0.5$ and the different values of α.

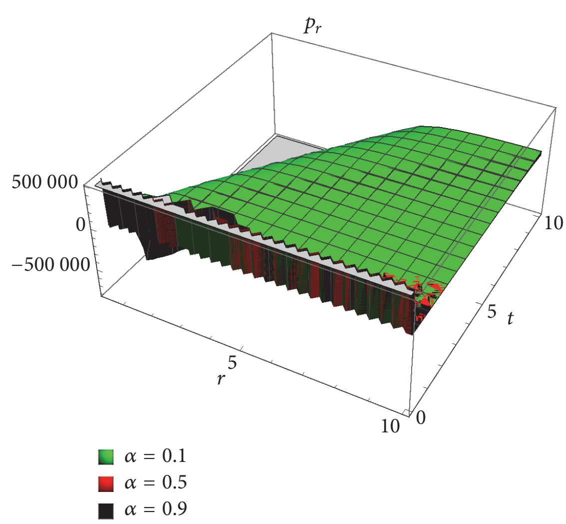

FIGURE 8: Radial pressure behavior along r and t for $r_0 = 0.5$ and the different values of α.

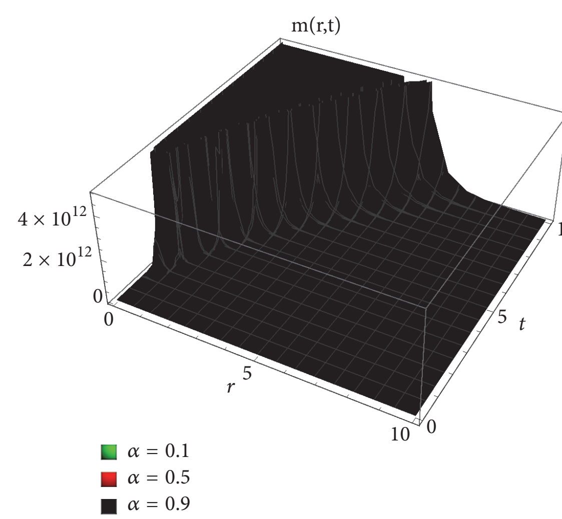

FIGURE 10: Mass behavior along r and t for $r_0 = 0.5$ and the different values of α.

tangential pressure is decreasing near the center along t at different values of α as shown in Figures 8 and 9. The mass of the sphere is increasing along t and the different values of α as shown in Figure 10. In this case, $p_t > p_r$; this implies that $\Delta a > 0$. The anisotropy parameter increases in this case for the different values of α as shown in Figure 11. It is shown that, firstly, the anisotropy decreases and then increases with radial increase of star for various values of α. The energy conditions for the expansion case are also satisfied as shown in Figure 12.

6. Summary

There has been a great interest in studying the relativistic anisotropic systems due to the existence of such systems in the astronomical objects. The exact solutions of anisotropic sphere are helpful to determine the anisotropy of the universe during any era. Barrow and Maartens [80] studied the effects of anisotropy on the late time expansion of inhomogeneous universe. Mahmood et al. [81] modeled the exact solution for the gravitational collapse and expansion of charged anisotropic cylindrical source.

The EGB gravity theory is the low energy limits of supersymmetric string theory of gravity [82]. The gravitational collapse is a highly dissipative process, in which a big amount of energy is released [37]. The dynamic of an anisotropic fluid collapse is observed in 5-dimensional Einstein-Gauss-Bonnet gravity [71]. Collin [83] modeled the inhomogeneous cosmological nonstatic expanding solutions. For the suitable values of $R(t,r)$ and β, Glass [79] observed anisotropic collapsing

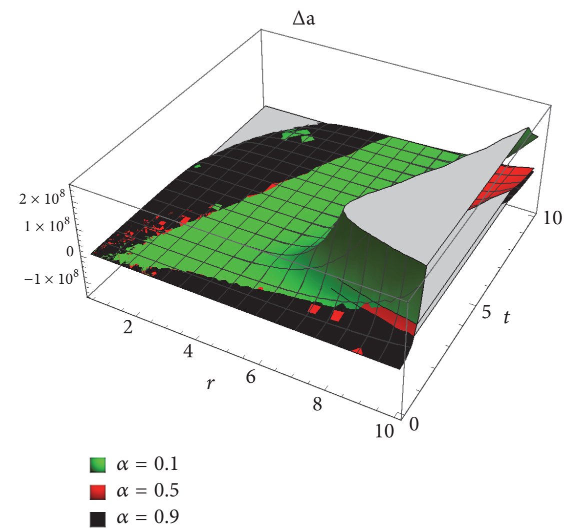

Figure 11: Anisotropy parameter behavior for $r_0 = 0.5$ and the different values of α.

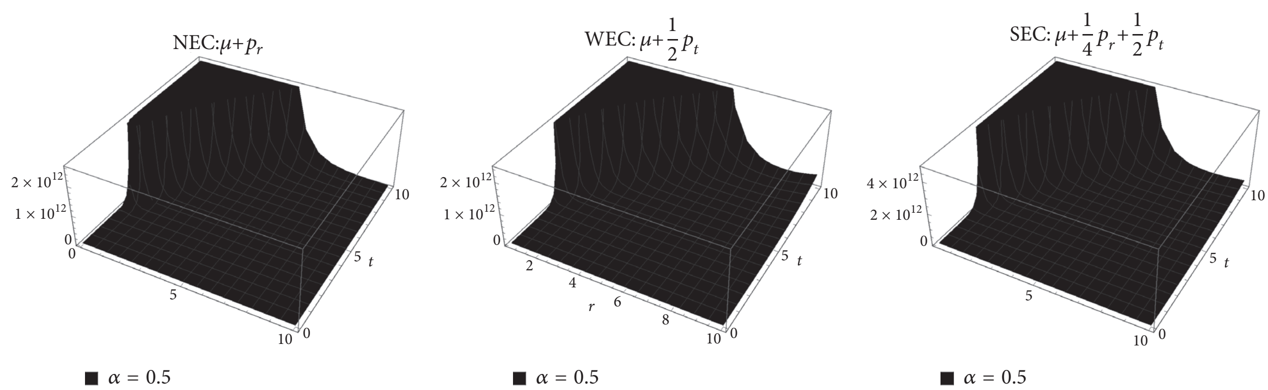

Figure 12: Plot of energy conditions along r and t for $r_0 = 0.5$ at.

and expanding of spherical object. We have modeled the field equations of anisotropic fluid in $5D$ EGB gravity.

The aim of this paper is to study the generating solutions for anisotropic spherical symmetric fluid in $5D$ EGB theory of gravity. We have used auxiliary solution of one field equation to obtain the solutions for remaining field equations. The solution for expansion scalar Θ has been depending on the range of free constant β, for which Θ being positive or negative leads to expansion and collapse of the fluid. We use the condition $\overset{\prime}{R} = R^{2\beta}$ in (22), which leads to two trapped horizons at $R = \pm\sqrt{(2/3)m - 2\alpha}$, provided that $m \geq 3\alpha$. The curvature singularity is hidden at the common center of the inner (R_+) and outer (R_-) horizon. The matter components like density, radial pressure, tangential pressure, anisotropic parameter, and mass functions have been determined in the $5D$ EGB theory of gravity. Equation (17) implies that, for $\beta = -3, \Theta = 0$, and for $\beta < -3$ the expansion scalar is negative and for $\beta > -3$ the expansion scalar is positive, which lead to bouncing, collapsing, and expanding, respectively. In other words, $\beta > 0$ and $\beta \in (-3, \infty)$; and $\beta < 0$ and $\beta \in (-\infty, -3)$. The solutions have been modeled by taking $\beta = -7/2$ and $\beta = -5/2$ for collapse and expansion of gravitating source, respectively.

We assume that the areal radius $R(r,t) = k(8r + z(t))^{1/8}$ outside the sphere for $k > 1$. It is interesting that, for $k = 1$, $R(r,t) = R_{trap}$ and it is valid only for trapped surface, so we take $k > 1$ for collapsing solutions outside the trapped surface. Further, $k < 0$ should not be considered because this leads to the solutions corresponding to the inner surface of the trapped region, which is not the case of interest in the present discussion.

The dynamics of the spherical fluid are discussed in both cases. The density of the matter is decreasing/increasing in collapse/expansion with the arbitrary choice of constant/parameter, time profile, and different values of GB term α. The radial pressure, tangential pressure, and mass have different behaviors in both cases. The anisotropy is increasing in both cases; in other words, this nonvanishing pressure anisotropy in both cases leads to collapse and expansion of the fluid. The energy conditions are satisfied for collapse and expansion; this shows that our solutions are physically acceptable.

Data Availability

The data used to support the findings of this study are available from the corresponding author upon request.

Conflicts of Interest

The authors declare that there are no conflicts of interest regarding the publication of this manuscript.

Acknowledgments

One of the authors, G. Abbas, acknowledges the financial support from HEC, Islamabad, Pakistan, under NRPU project with Grant no. 20-4059/NRPU/R&D/HEC/14/1217.

References

[1] T. Kaluza, "On the Unification Problem in Physics," Sitzungsber. Preuss. Akad. Wiss. Berlin (Math. Phys.), pp. 966–972, 1921.

[2] O. Klein, "Quantum theory and five-dimensional theory of relativity," *Zeitschrift für Physik*, vol. 37, p. 895, 1926.

[3] O. Klein, "The atomicity of electricity as a quantum theory law," *Nature*, vol. 118, no. 2971, p. 516, 1926.

[4] E. Witten, "Search for a realistic Kaluza-Klein theory," *Nuclear Physics B*, vol. 186, p. 412, 1981.

[5] M. B. Green and J. H. Schward, "Anomaly cancellations in supersymmetric D =10 gauge theory and superstring theory," *Physics Letters*, vol. 149B, p. 117, 1984.

[6] D. J. Gross, J. A. Harvey, E. Martinec, and R. Rohm, "Heterotic string," *Physical Review Letters*, vol. 54, no. 6, pp. 502–505, 1985.

[7] B. Zumino, "Gravity theories in more than four dimensions," *Physics Reports*, vol. 137, no. 1, pp. 109–114, 1986.

[8] D. G. Boulware and S. Deser, "String-generated gravity models," *Physical Review Letters*, vol. 55, p. 1039, 1985.

[9] B. Zwiebach, "Berkeley Preprint UCB.PTH-85/10".

[10] V. P. C. Pedro, A. R. H. Carlos, K. Burkhard, K. Jutta, and R. Eugen, "Shadows of Einstein–dilaton–Gauss–Bonnet black holes," *Physics Letters B*, vol. 768, pp. 373–379, 2017, arXiv: 1701.00079v2 [gr-qc].

[11] G. Abbas, A. Kanwal, and M. Zubair, "Anisotropic compact stars in $f(T)$ gravity," *Astrophysics and Space Science*, vol. 357, no. 2, article 109, 2015.

[12] G. Abbas and M. Zubair, "Dynamics of anisotropic collapsing spheres in Einstein Gauss-Bonnet gravity," *Modern Physics Letters A*, vol. 30, no. 8, 1550038, 8 pages, 2015.

[13] D. J. Gross and J. H. Sloan, "The quartic effective action for the heterotic string," *Nuclear Physics B*, vol. 291, pp. 41–89, 1987.

[14] M. C. Bento and O. Bertolami, "Maximally symmetric cosmological solutions of higher-curvature string effective theories with dilatons," *Physics Letters B*, vol. 368, p. 198, 1996.

[15] N. Dadhich, A. Molina, and A. Khugaev, "Uniform density static fluid sphere in Einstein-Gauss-Bonnet gravity and its universality," *Physical Review D: Particles, Fields, Gravitation and Cosmology*, vol. 81, no. 10, 2010.

[16] I. Antoniadis, J. Rizos, and K. Tamvakis, "Singularity-free cosmological solutions of the superstring effective action," *Nuclear Physics B*, vol. 415, p. 497, 1994.

[17] P. Kanti, J. Rizos, and K. Tamvakis, "Singularity-free cosmological solutions in quadratic gravity," *Physical Review D: Particles, Fields, Gravitation and Cosmology*, vol. 59, no. 8, Article ID 083512, 1999.

[18] P. Kanti, N. E. Mavromatos, J. Rizos, K. Tamvakis, and E. Winstanley, "Dilatonic black holes in higher curvature string gravity," *Physical Review D: Particles, Fields, Gravitation and Cosmology*, vol. 54, no. 8, pp. 5049–5058, 1996.

[19] P. Kanti, N. E. Mavromatos, J. Rizos, K. Tamvakis, and E. Winstanley, "Dilatonic black holes in higher curvature string gravity. II. Linear stability," *Physical Review D: Particles, Fields, Gravitation and Cosmology*, vol. 57, no. 10, pp. 6255–6264, 1998.

[20] T. Torii, H. Yajima, K. I. Maeda, and Phy., "Dilatonic black holes with a Gauss-Bonnet term," *Physical Review D*, vol. 55, p. 739, 1997.

[21] F. R. Tangherlini, "Schwarzschild field in n dimensions and the dimensionality of space problem," *Il Nuovo Cimento*, vol. 27, no. 3, pp. 636–651, 1963.

[22] R. C. Myers and M. J. Perry, "Black holes in higher-dimensional space-times," *Annals of Physics*, vol. 172, no. 2, pp. 304–347, 1986.

[23] J. T. Wheeler, "Symmetric solutions to the Gauss-Bonnet extended Einstein equations," *Nuclear Physics B*, vol. 268, p. 737, 1986.

[24] T. Torii and H. Maeda, "Spacetime structure of static solutions in Gauss-Bonnet gravity: Neutral case," *Physical Review D*, vol. 71, Article ID 011901, 2005.

[25] R. C. Myers and J. Z. Simon, "Black-hole thermodynamics in Lovelock gravity," *Physical Review D: Particles, Fields, Gravitation and Cosmology*, vol. 38, 1988.

[26] R. G. Cai, "Gauss-Bonnet black holes in AdS spaces," *Physical Review D: Particles, Fields, Gravitation and Cosmology*, vol. 65, 2002.

[27] R. G. Cai and Q. Guo, "Gauss-Bonnet black holes in dS spaces," *Physical Review D: Particles, Fields, Gravitation and Cosmology*, vol. 69, 2004.

[28] T. Kobayashi, "A Vaidya-type radiating solution in Einstein-Gauss-Bonnet gravity and its application to braneworld," *General Relativity and Gravitation*, vol. 37, p. 1869, 2005.

[29] H. Maeda, "Effects of Gauss-Bonnet term on the final fate of gravitational collapse," *Classical and Quantum Gravity*, vol. 23, no. 6, pp. 2155–2169, 2006.

[30] E. Ma, "Verifiable radiative seesaw mechanism of neutrino mass and dark matter," *Physical Review D: Particles, Fields, Gravitation and Cosmology*, vol. 73, Article ID 077301, 2006.

[31] A. E. Dominguez and E. Gallo, "Radiating black hole solutions in Einstein-Gauss-Bonnet gravity," *Physical Review D*, vol. 73, Article ID 064018, 2006.

[32] S. G. Ghosh and D. W. Deshkar, "Horizons of radiating black holes in Einstein-Gauss-Bonnet gravity," *Physical Review D: Particles, Fields, Gravitation and Cosmology*, vol. 77, 2008.

[33] S. W. Hawking and G. F. R. Ellis, *The Large Scale Structure of Space-Time*, Cambridge University Press, London, UK, 1979.

[34] L. Herrera, N. O. Santos, and G. Le Denmat, "Dynamical instability for non-adiabatic spherical collapse," *MNRAS*, vol. 237, p. 257, 1989.

[35] C. W. Misner and D. H. Sharp, "Relativistic equations for adiabatic, spherically symmetric gravitational collapse," *Physical Review A: Atomic, Molecular and Optical Physics*, vol. 136, no. 2, pp. B571–B576, 1964.

[36] C. W. Misner and D. Sharp, "Relativistic equations for spherical gravitational collapse with escaping neutrinos," *Physical Review Journals Archive*, vol. 137, p. 1360, 1965.

[37] L. Herrera and N. O. Santos, "Local anisotropy in self-gravitating systems," *Physics Reports*, vol. 286, no. 2, pp. 53–130, 1997.

[38] L. Herrera, A. Di Prisco, J. L. Hernandez-Pastora, and N. O. Santo, "On the role of density inhomogeneity and local anisotropy in the fate of spherical collapse," *Physics Letter A*, vol. 237, p. 113, 1998.

[39] L. Herrera and N. O. Santos, "Dynamics of dissipative gravitational collapse," *Physical Review D: Particles, Fields, Gravitation and Cosmology*, vol. 70, 2004.

[40] L. Herrera, A. Di Prisco, and J. Ospino, "Cylindrically symmetric relativistic fluids: a study based on structure scalars," *General Relativity and Gravitation*, vol. 44, no. 10, pp. 2645–2667, 2012.

[41] L. Herrera, "The inertia of heat and its role in the dynamics of dissipative collapse," *International Journal of Modern Physics D*, vol. 15, p. 1659, 2006.

[42] L. Herrera, N. O. Santos, and A. Wang, "Shearing expansion-free spherical anisotropic fluid evolution," *Physical Review D*, vol. 78, Article ID 084026, 2008.

[43] G. Abbas, "Phantom energy accretion onto a black hole in Horava Lifshitz gravity," *Science China Physics, Mechanics and Astronomy*, vol. 57, no. 4, pp. 604–607, 2014.

[44] S. M. Shah and G. Abbas, "Dynamics of charged bulk viscous collapsing cylindrical source with heat flux," *The European Physical Journal C*, vol. 77, p. 251, 2017.

[45] G. Abbas, "Collapse and expansion of anisotropic plane symmetric source," *Astrophysics and Space Science*, vol. 350, p. 307, 2014.

[46] G. Abbas, "Cardy-verlinde formula of noncommutative schwarzschild black hole," *Advances in High Energy Physics*, vol. 2014, Article ID 306256, 4 pages, 2014.

[47] G. Abbas, "Effects of electromagnetic field on the collapse and expansion of anisotropic gravitating source," *Astrophysics and Space Science*, vol. 352, p. 955, 2014.

[48] G. Abbas and U. Sabiullah, "Geodesic study of regular Hayward black hole," *Astrophysics and Space Science*, vol. 352, p. 769, 2014.

[49] M. Zubair, H. Azmat, and I. Noureen, "Dynamical analysis of cylindrically symmetric anisotropic sources in f(R, T) gravity," *The European Physical Journal C*, vol. 77, no. 3, 2017.

[50] K. Zhou, Z-Y. Yang, D.-C. Zou, and R-H. Yue, "Spherically symmetric gravitational collapse of a dust cloud in third-order lovelock gravity," *International Journal of Modern Physics D*, vol. 22, p. 2317, 2011.

[51] K. Zhou, Z. Yang, D. Zou, and R. Yue, "Spherically symmetric gravitational collapse of a dust cloud in einstein–gauss–bonnet gravity," *Modern Physics Letters A*, vol. 26, no. 28, pp. 2135–2147, 2011.

[52] R.-H. Yue, D.-C. Zou, T.-Y. Yu, and Z.-Y. Yang, "A new metric for rotating black holes in Gauss—Bonnet gravity," *Chinese Physics B*, vol. 20, 2011.

[53] K. Zhou, Z.-Y. Yang, D.-C. Zou, and R.-H. Yue, "Static spherically symmetric star in Gauss—Bonnet gravity," *Chinese Physics B*, vol. 21, 2012.

[54] D.-C. Zou, Z.-Y. Yang, R.-H. Yue, and T.-Y. Yu, "A new metric for rotating charged Gauss—Bonnet black holes in AdS space," *Chinese Physics B*, vol. 20, 2011.

[55] R. Yue, D. Zou, T. Yu, P. Li, and Z. Yang, "Slowly rotating charged black holes in anti-de Sitter third order Lovelock gravity," *General Relativity and Gravitation*, vol. 43, no. 8, pp. 2103–2114, 2011.

[56] D.-C. Zou, Z.-Y. Yang, and R.-H. Yue, "Thermodynamics of slowly rotating charged black holes in anti-de sitter Einstein—Gauss—Bonnet gravity," *Chinese Physics Letters*, vol. 28, 2011.

[57] D. Zou, Z. Yang, R. Yue, and P. Li, "Thermodynamics of gauss–bonnet–born–infeld black holes in ads space," *Modern Physics Letters A*, vol. 26, no. 07, pp. 515–529, 2011.

[58] L.-D. Gou, K. Xue, and G.-C. Wang, "Thermodynamics of third order lovelock anti-de sitter black holes revisited," *Communications in Theoretical Physics*, vol. 55, p. 499, 2011.

[59] S. Chakraborty, "An alternative f(R, T) gravity theory and the dark energy problem," *General Relativity and Gravitation*, vol. 45, p. 2039, 2013.

[60] G. Abbas and R. Ahmed, "Models of Collapsing and Expanding Anisotropic Gravitating Source in f(R,T) Theory of Gravity," *European Physical Journal C*, vol. 77, no. 441, 2017.

[61] M. Sharif and A. Siddiqa, "Study of homogeneous and isotropic universe in $f(R, T^{\varphi})$ gravity," *Advances in Higah Energy Physics*, vol. 2018, 2018.

[62] J. R. Oppenheimer and H. Snyder, "On continued gravitational contraction," *Physical Review A: Atomic, Molecular and Optical Physics*, vol. 56, no. 5, pp. 455–459, 1939.

[63] D. Markovic and S. L. Shapiro, "Gravitational collapse with a cosmological constant," *Physical Review D*, vol. 61, 2000.

[64] K. Lake, "Gravitational collapse of dust with a cosmological constant," *Physical Review D: Particles, Fields, Gravitation and Cosmology*, vol. 62, 2000.

[65] M. Sharif and G. Abbas, "Gravitational charged perfect fluid collapse in Friedmann universe models," *Astrophysics and Space Science*, vol. 327, pp. 285–291, 2010.

[66] M. Sharif and Z. Ahmad, "Gravitational perfect fluid collapse with cosmological constant," *Modern Physics Letters A*, vol. 22, no. 20, pp. 1493–1502, 2007.

[67] M. Sharif and Z. Ahmed, "Addendum: "gravitational perfect fluid collapse with cosmological constant"," *Modern Physics Letters A*, vol. 22, no. 38, pp. 2947-2948, 2007.

[68] M. Sharif and Z. Ahmad, "Five-Dimensional Perfect Fluid Collapse with the Cosmological Constant," *Journal of the Korean Physical Society*, vol. 52, no. 4, p. 980, 2008.

[69] M. Sharif and Z. Ahamd, "Higher dimensional perfect fluid collapse with cosmological constant," *Acta Physica Polonica B*, vol. 39, 2008.

[70] M. Sharif and G. Abbas, "Effects of the Electromagnetic Field on Five-dimensional Gravitational Collapse," *Journal of the Korean Physical Society*, vol. 56, p. 529, 2010.

[71] G. Abbas and M. Zubair, "Dynamics of anisotropic collapsing spheres in Einstein Gauss–Bonnet gravity," *Modern Physics Letters A*, vol. 30, 2015, Arxiv: 1504.07937v1.

[72] D. Ida and K. I. Nakao, "Isoperimetric inequality for higher-dimensional black holes," *Physical Review D: Particles, Fields, Gravitation and Cosmology*, vol. 66, 2002.

[73] S. Jhingan and S. G. Ghosh, "Inhomogeneous dust collapse in 5D Einstein-Gauss-Bonnet gravity," *Physical Review D: Particles, Fields, Gravitation and Cosmology*, vol. 81, 2010.

[74] S. D. Maharaj, B. Chilambwe, and S. Hansraj, "Exact barotropic distributions in Einstein-Gauss-Bonnet gravity," *Physical Review D: Particles, Fields, Gravitation and Cosmology*, vol. 91, no. 8, 2015.

[75] G. Abbas and M. Tahir, "Gravitational perfect fluid collapse in Gauss–Bonnet gravity," *The European Physical Journal C*, vol. 537, p. 77, 2017.

[76] A. Banerjee, A. Sil, and S. Chatterjee, "Gravitational collapse of an inhomogeneous dust sphere in higher dimensional space-time," *Astrophysical Journal*, vol. 422, pp. 681–687, 1994.

[77] S. G. Ghosh and A. Banerjee, "Non-marginally bound inhomogeneous dust collapse in higher dimensional space–time," *International Journal of Modern Physics D*, vol. 12, p. 639, 2003.

[78] S. G. Ghosh, D. W. Deshkar, and N. N. Saste, "Five-dimensional dust collapse with cosmological constant," *International Journal of Modern Physics D*, vol. 16, p. 1531, 2007.

[79] E. N. Glass, "Generating anisotropic collapse and expansion solutions of Einstein's equations," *General Relativity and Gravitation*, vol. 45, no. 12, pp. 2661–2670, 2013.

[80] J. D. Barrow and R. Maartens, "Anisotropic stresses in inhomogeneous universes," *Physical Review D: Particles, Fields, Gravitation and Cosmology*, vol. 59, Article ID 023002, 1998.

[81] T. Mahmood, S. M. Shah, and G. Abbas, "Gravitational collapse and expansion of charged anisotropic cylindrical source," *Astrophysics and Space Science*, vol. 6, p. 2234, 2015.

[82] J. J. Schwarz, "Covariant field equations of chiral $N = 2$ $D = 10$ supergravity," *Nuclear Physics B*, vol. 226, p. 269, 1983.

[83] C. B. Collins, "Global structure of the "Kantowski–Sachs" cosmological models," *Journal of Mathematical Physics*, vol. 18, no. 8, p. 2216, 1977.

Hindawi
Advances in High Energy Physics
Volume 2018, Article ID 9250786, 13 pages
https://doi.org/10.1155/2018/9250786

Research Article

Dynamics of Dissipative Viscous Cylindrical Collapse with Full Causal Approach in $f(R)$ Gravity

G. Abbas and H. Nazar

Department of Mathematics, The Islamia University of Bahawalpur, Bahawalpur, Pakistan

Correspondence should be addressed to G. Abbas; abbasg91@yahoo.com

Received 3 September 2018; Revised 28 September 2018; Accepted 2 October 2018; Published 24 October 2018

Guest Editor: Subhajit Saha

Copyright © 2018 G. Abbas and H. Nazar. This is an open access article distributed under the Creative Commons Attribution License, which permits unrestricted use, distribution, and reproduction in any medium, provided the original work is properly cited. The publication of this article was funded by SCOAP[3].

The idea of this article is to examine the effects on dynamics of dissipative gravitational collapse in nonstatic cylindrical symmetric geometry by using Misner-Sharp concept in framework of metric $f(R)$ gravity theory. In this interest, we extended our study to the dissipative dark source case in both forms of heat flow and the free radiation streaming. Moreover, the role of different quantities such as heat flux, bulk, and shear viscosity in the dynamical equation is evaluated in thorough version. The dynamical equation is then coupled with full causal transportation equations in the context of Israel-Stewart formalism. The present scheme explains the physical consequences of the gravitational collapse and that is given in the decreasing form of inertial mass density which depends on thermodynamics viscous/heat coupling factors in background of $f(R)$ theory of gravity. It is very interesting to tell us that the motives of this theory are reproduced for $f(R) = R$ into general theory of relativity that has been done earlier.

1. Introduction

A multiple work has been done in the significance of relativistic geometry of the collapsing star to the general relativity theory and higher order curvature theories. In this scenario, too many open challenges and curious issues still exist in modern physics, gravitational physics, cosmological physics, relativistic dense objects, group of galaxies, neutron star, and black holes. Currently, our aim is to discuss the gravitational collapse of the relativistic dense object in the presence of dissipative term.

In this arrangement, the formation of the dense star is highly explosive and exhaustible due to the highly inmost pull of gravity and this process is terminated with the external pressure of the interior fuel. However, once the object has wakened due to its thermodynamical fission reaction, there is no any extended thermodynamical burning and there will be an interminable gravitating collapse. The geometry of the object is made up by its explosive mass which is constantly gravitational and it is stimulating by the interior core of the object due to the gravitating interaction between their particles. Oppenheimer and Snyder [1] made an activity stride in the field of gravitating collapse and examined the nitty gritty work in regard to the gravitational collapse issues. In this order after the midway of the 20th century, a brief sensible evaluation was recognized by Misner and Sharp [2] with isotropic matter distribution for the interior of the imploding object as well as in vacuum of the outside object. Vaidya [3] explained the gravitational collapse with the radiating source.

Numerous models still exist to explain the enigmatic role of the dark energy in a system. In this inference, we use the higher order modified gravity theories such as $f(R)$, $f(G)$, and $f(R,T)$ gravity theories; it can provide the well-established framework in the significance of rushing evolution of the universe. Capozziello [4] studied the notable issues for the accelerated growth of the universe and quintessence in the Friedmann Robertson Walker (FRW) model with higher curvature gravity theories. Sharif and Yousaf [5] explored the stability of the anisotropic fluid distribution in nonstatic spherically symmetric geometry with $f(R)$ metric formalism. Mak and Harko [6] investigated the notional indications through many astrophysical estimations and found the significant natural dissimilarities in the pressure. Herrera and Santos [7] determined the impacts on imperfect fluid formation with astral spherical object for the behavior of restful rotation.

Webber [8] examined the solutions of pressure anisotropy in dense models with electromagnetic field. Chakraborty et al. [9] analyzed the gears of tangential pressure and along with radial pressure in stellar structures by quasispherical paradigms in the form of collapse. Garattini [10] evaluated the formation of exposed singularity through mass limitation in metric $f(R)$ theory of gravity. Sharif and his coresearchers [11–18] studied the various consequences of energy density inhomogeneity and Weyl tensor with gravitational collapse in dense objects with General relativity theory as well as in modified theories of gravity. Cognola et al. [19] introduced the results of spherical imploding object for the black hole in $f(R)$ context by the parameter of positive Ricci invariant R. Capozziello et al. [20] examined the modified Lan*é*-Emden equation in context of metric $f(R)$ gravity theory and studied the hydrostatic periods of astral models. Copeland et al. [21] analyzed the several concepts for the rushing growth of universe. Amendola et al. [22] discussed the feasible paradigms of metric $f(R)$ gravity in the context of both Einstein and Jordan frames.

Chandrasekhar [23] introduced the impacts on the constancy of dynamics with perfect fluid collapsing geometry. Herrera et al. [24] discussed the results of dynamical disequilibrium with spherically symmetric nonadiabatic collapse and found the heat flow out from the gravitating source in the form of radial heat flux. Abbas et al. [25] presented the results of compact star models in anisotropic fluid distribution with cylindrical symmetric static spacetime geometry. Mak and Harko [26] studied the kind of exact solutions of field equations by considering the spherical symmetric structure and also conferred the energy density along with tangential and radial pressure that are limited and increased in the core of the imperfect fluid object. Rahaman et al. [27] prolonged the Krori-Barua solution with spherical symmetric static spacetime for the investigation of charge imperfect fluid distribution. Herrera and his collaborators [28–33] did work in different directions, such as self-gravitating dens models discussed with local anisotropic matter distribution in the cracking spherical symmetric structure in context of equation of state with perturbed approach. They established the various results in gravitational collapse for the dissipative case by using Misner and Sharp approach; such gravitating source undergoes in form of free radiation streaming and diffusion approximations. They investigated the expansion free conditions for the spherically symmetric anisotropic dissipative collapsing matter. Further, Herrera and his collaborators [34–38] have evaluated the Lake algorithm in static spherically symmetric anisotropic configuration for the determination of new formalism of two functions (instead of one) to generate all possible results. They studied the results of structure scalars Y_{TF} for the charged dissipative anisotropic collapsing geometry in presence of cosmological constant. They have also done detailed work on the dynamical disequilibrium with spherically symmetric locally anisotropic fluid which collapses adiabatically under the expansion-free condition. In few investigations they have used the noncasual as well as casual approaches to discuss the dynamics of gravitating source. Nolan [39] examined the effects on gravitational collapse for counter rotating dust cloud with cylindrical paradigms and found the naked singularity. Hayward [40] produced the results of cylindrical geometry for black holes, gravitational waves, and cosmic strings.

In this paper, we analyze the self-gravitational collapse with cylindrical symmetric geometry in context of metric $f(R)$ gravity theory. The main persistence of this study is to examine the viscous dissipative collapse in the form of radial heat flow and free radiation streaming in cylindrical nonstatic spacetime with full causal approach.

The proposal of this work is as follows. In Section 2, we express the cylindrical symmetric isotropic collapsing matter distribution and its related variables in context of $f(R)$ theory of gravity. Section 3 consists of Einstein modified field equations; matching conditions are given for the interior and exterior manifolds M^- and M^+ and the dynamical equation that was accompanied with physical parameters such as heat flux, bulk, and shear viscosity. Section 4 is devoted to the transportation equations attained in frame of *Müller*-Israel-Stewart formalism [41–43]; then transportation equations are associated with dynamical equation. Finally, the conclusions of the study have been discussed in the last section.

2. Self-Gravitational Collapsing Geometry and Related Conventions

In this section, we consider a locally isotropic collapsing fluid with full causal description in context of Misner-Sharp approach, formed by cylindrically symmetric nonstatic interior and exterior geometry of the dissipative fluid which undergoes dissipation in the form of heat flow and free streaming radiation. In general relativity the Einstein-Hilbert (EH) action can be expressed as follows:

$$S_{EH} = \frac{1}{2\kappa}\int d^4x\sqrt{-g}R. \tag{1}$$

The extended formulation of the Einstein-Hilbert (EH) in $f(R)$ context is

$$S_{modif} = \frac{1}{2\kappa}\int d^4x\sqrt{-g}\left(f(R) + L_{(matter)}\right), \tag{2}$$

where $f(R)$ is arbitrary function of Ricci scalar R, κ is coupling constant, and $L_{(matter)}$ the Lagrangian matter density of the action. The following modified $f(R)$ field equations are obtained by the variation of (2) with respect to $g_{\alpha\beta}$:

$$\begin{aligned} &F(R)R_{\alpha\beta} - \frac{1}{2}f(R)g_{\alpha\beta} - \nabla_\alpha\nabla_\beta F(R) + g_{\alpha\beta}\nabla^\alpha\nabla_\alpha F(R) \\ &\quad = \kappa T_{\alpha\beta}, \end{aligned} \tag{3}$$

where $F(R) = df(R)/dR$, $\nabla^\alpha\nabla_\alpha$ is the D' Alembert operator, ∇_α denotes the covariant derivative, and $T_{\alpha\beta}$ is the isotropic energy-momentum tensor. The above equations can be expressed in Einstein tensor as given below:

$$G_{\alpha\beta} = \frac{\kappa}{F}\left(T^m_{\alpha\beta} + T^D_{\alpha\beta}\right), \tag{4}$$

where

$$T^{D}_{\alpha\beta} = \frac{1}{\kappa}\left[\frac{f(R) - RF(R)}{2}g_{\alpha\beta} + \nabla_\alpha\nabla_\beta F(R) - g_{\alpha\beta}\nabla^\alpha\nabla_\alpha F(R)\right] \quad (5)$$

represent the action energy-momentum tensor. By considering the comoving coordinates bounded by cylindrically symmetric nonstatic spacetime geometry, which contains the dissipative nature of the fluid defines by interior metric,

$$ds_{-}^{2} = -A^2dt^2 + B^2dr^2 + C^2d\phi^2 + D^2dz^2. \quad (6)$$

Here $A = A(t, r)$, $B = B(t, r)$, $C = C(t, r)$, $D = D(t, r)$ are the metric functions. We labeled the coordinates $x^0 = t$, $x^1 = r$, $x^2 = \phi$ and $x^3 = z$.

The tensor $T^{-}_{\alpha\beta}$ of the dissipative collapsing matter distribution is

$$T^{-}_{\alpha\beta} = (\mu + p + \Pi)V_\alpha V_\beta + (p + \Pi)g_{\alpha\beta} + q_\alpha V_\beta + q_\beta V_\alpha + \epsilon l_\alpha l_\beta + \pi_{\alpha\beta}, \quad (7)$$

where μ is the energy density, p is the isotropic pressure, Π the bulk viscosity, q^α the heat flux, $\pi_{\alpha\beta}$ is the shear viscosity, ϵ the radiation density, and V^α the four velocity of the fluid. Furthermore, l^α denotes radial null four vector. The above extents gratify the results as below.

$$V^\alpha V_\alpha = -1, \quad V^\alpha q_\alpha = 0, \quad l^\alpha V_\alpha = -1, \quad l^\alpha l_\alpha = 0, \quad (8)$$

$$\pi_{\mu\nu}V^\nu = 0, \quad \pi_{[\mu\nu]} = 0, \quad \pi^\alpha_\alpha = 0. \quad (9)$$

In the general nonreversible thermodynamics taken into [44, 45],

$$\pi_{\alpha\beta} = -2\eta\sigma_{\alpha\beta}, \quad \Pi = -\zeta\Theta; \quad (10)$$

wherever η is the factor of shear viscosity and ζ denotes the factor of bulk viscosity, $\sigma_{\alpha\beta}$ and Θ are the shear tensor and heat flow expansion, respectively.

The shear tensor $\sigma_{\alpha\beta}$ is defined by

$$\sigma_{\alpha\beta} = V_{(\alpha;\beta)} + a_{(\alpha V_\beta)} - \frac{1}{3}\Theta h_{\alpha\beta}, \quad (11)$$

where the acceleration a_α and the expansion Θ are recognized by

$$a_\alpha = V_{\alpha;\beta}V^\beta, \quad \Theta = V^\alpha_{;\alpha}, \quad (12)$$

and $h_{\alpha\beta} = g_{\alpha\beta} + V_\alpha V_\beta$ is the projector onto the hypersurface orthogonal to the four velocity. let us define the following quantities for the given metric:

$$V^\alpha = A^{-1}\delta^\alpha_0, \quad q^\alpha = qB^{-1}\delta^\alpha_1, \quad l^\alpha = A^{-1}\delta^\alpha_0 + B^{-1}\delta^\alpha_1, \quad (13)$$

where q depending on t and r. Also it trails from (8) so that

$$\pi_{0\alpha} = 0, \quad \pi^1_1 = -2\pi^2_2 = -2\pi^3_3. \quad (14)$$

In a more explicit formation we can write

$$\pi_{\alpha\beta} = \Omega\left(\chi_\alpha\chi_\beta - \frac{1}{3}h_{\alpha\beta}\right), \quad (15)$$

where χ^α is a unit four vector along the radial direction, fulfilling the conditions

$$\chi^\alpha\chi_\alpha = 1, \quad \chi^\alpha V_\alpha = 0, \quad \chi^\alpha = B^{-1}\delta^\alpha_1, \quad (16)$$

and $\Omega = (3/2)\pi^1_1$.

From the information of (13), we obtain the following nonnull components of shear tensor.

$$\sigma_{11} = \frac{B^2}{3A}[\Sigma_1 - \Sigma_3], \quad \sigma_{22} = \frac{C^2}{3A}[\Sigma_2 - \Sigma_1], \quad \sigma_{33} = \frac{D^2}{3A}[\Sigma_3 - \Sigma_2], \quad (17)$$

where

$$\sigma_{\alpha\beta}\sigma^{\alpha\beta} = \sigma^2 = \frac{1}{3A^2}\left[\Sigma_1^2 + \Sigma_2^2 + \Sigma_3^2\right], \quad (18)$$

where

$$\Sigma_1 = \frac{\dot{B}}{B} - \frac{\dot{C}}{C}, \quad \Sigma_2 = \frac{\dot{C}}{C} - \frac{\dot{D}}{D}, \quad \Sigma_3 = \frac{\dot{D}}{D} - \frac{\dot{B}}{B}. \quad (19)$$

Here dot denotes derivative w.r.t. t.

By using (12) and (13), we get

$$a_1 = \frac{\acute{A}}{A}, \quad \Theta = \frac{1}{A}\left(\frac{\dot{B}}{B} + \frac{\dot{C}}{C} + \frac{\dot{D}}{D}\right), \quad (20)$$

where prime represents derivative with respect to r.

3. Modified Field Equations in $f(R)$ Gravity

The modified field equation (4) for cylindrical symmetric spacetime in $f(R)$ metric formalism gives the following system of equations.

$$\begin{aligned}&\left(\frac{A}{B}\right)^2\left[-\frac{C''}{C}-\frac{D''}{D}+\frac{B'}{B}\left(\frac{C'}{C}+\frac{D'}{D}\right)-\frac{C'D'}{CD}\right]\\&\quad+\left(\frac{\dot{B}\dot{C}}{BC}+\frac{\dot{B}\dot{D}}{BD}+\frac{\dot{C}\dot{D}}{CD}\right)=\frac{\kappa}{F}\left[(\mu+\epsilon)A^2\right.\\&\quad+\frac{A^2}{\kappa}\left\{-\left(\frac{f(R)-RF(R)}{2}\right)\right.\\&\quad-\frac{\dot{F}}{A^2}\left(\frac{\dot{B}}{B}+\frac{\dot{C}}{C}+\frac{\dot{D}}{D}\right)+\frac{F''}{B^2}\\&\quad\left.\left.+\frac{F'}{B^2}\left(\frac{C'}{C}+\frac{D'}{D}-\frac{B'}{B}\right)\right\}\right],\end{aligned}\tag{21}$$

$$\begin{aligned}&-\left(\frac{\dot{C}'}{C}+\frac{\dot{D}'}{D}-\frac{\dot{B}C'}{BC}-\frac{\dot{B}D'}{BD}-\frac{\dot{C}A'}{AC}-\frac{\dot{D}A'}{AD}\right)\\&\quad=\frac{\kappa}{F}\left[-(q+\epsilon)AB+\frac{1}{\kappa}\left(\dot{F}'-\frac{A'\dot{F}}{A}-\frac{\dot{B}F'}{B}\right)\right],\end{aligned}\tag{22}$$

$$\begin{aligned}&-\left(\frac{B}{A}\right)^2\left(\frac{\ddot{C}}{C}+\frac{\ddot{D}}{D}+\frac{\dot{C}\dot{D}}{CD}-\frac{\dot{A}\dot{C}}{AC}-\frac{\dot{A}\dot{D}}{AD}\right)+\left(\frac{C'D'}{CD}\right.\\&\quad\left.+\frac{A'C'}{AC}+\frac{A'D'}{AD}\right)=\frac{\kappa}{F}\left[\left(p+\Pi+\epsilon+2\frac{\Omega}{3}\right)B^2\right.\\&\quad+\frac{B^2}{\kappa}\left\{\left(\frac{f(R)-RF(R)}{2}\right)+\frac{\ddot{F}}{A^2}\right.\\&\quad\left.\left.+\frac{\dot{F}}{A^2}\left(\frac{\dot{C}}{C}+\frac{\dot{D}}{D}-\frac{\dot{A}}{A}\right)-\frac{F'}{B^2}\left(\frac{A'}{A}+\frac{C'}{C}+\frac{D'}{D}\right)\right\}\right],\end{aligned}\tag{23}$$

$$\begin{aligned}&-\left(\frac{C}{A}\right)^2\left[\frac{\ddot{B}}{B}+\frac{\ddot{D}}{D}-\frac{\dot{A}}{A}\left(\frac{\dot{B}}{B}+\frac{\dot{D}}{D}\right)+\frac{\dot{B}\dot{D}}{BD}\right]+\left(\frac{C}{B}\right)^2\\&\quad\cdot\left[\frac{A''}{A}+\frac{D''}{D}-\frac{A'}{A}\left(\frac{B'}{B}-\frac{D'}{D}\right)-\frac{B'D'}{BD}\right]\\&\quad=\frac{\kappa}{F}\left[\left(p+\Pi-\frac{\Omega}{3}\right)C^2\right.\\&\quad-\frac{C^2}{\kappa}\left\{-\left(\frac{f(R)-RF(R)}{2}\right)-\frac{\ddot{F}}{A^2}+\frac{F''}{B^2}\right.\\&\quad+\frac{\dot{F}}{A^2}\left(\frac{\dot{A}}{A}-\frac{\dot{B}}{B}-\frac{\dot{C}}{C}-\frac{\dot{D}}{D}\right)\\&\quad\left.\left.+\frac{F'}{B^2}\left(\frac{A'}{A}-\frac{B'}{B}+\frac{C'}{C}+\frac{D'}{D}\right)\right\}\right],\end{aligned}\tag{24}$$

$$\begin{aligned}&-\left(\frac{D}{A}\right)^2\left[\frac{\ddot{B}}{B}+\frac{\ddot{C}}{C}-\frac{\dot{A}}{A}\left(\frac{\dot{B}}{B}+\frac{\dot{C}}{C}\right)+\frac{\dot{B}\dot{C}}{BC}\right]+\left(\frac{D}{B}\right)^2\\&\quad\cdot\left[\frac{A''}{A}+\frac{C''}{C}-\frac{A'}{A}\left(\frac{B'}{B}-\frac{C'}{C}\right)-\frac{B'C'}{BC}\right]\\&\quad=\frac{\kappa}{F}\left[\left(p+\Pi-\frac{\Omega}{3}\right)D^2\right.\\&\quad-\frac{D^2}{\kappa}\left\{-\left(\frac{f(R)-RF(R)}{2}\right)-\frac{\ddot{F}}{A^2}+\frac{F''}{B^2}\right.\\&\quad+\frac{\dot{F}}{A^2}\left(\frac{\dot{A}}{A}-\frac{\dot{B}}{B}-\frac{\dot{C}}{C}-\frac{\dot{D}}{D}\right)\\&\quad\left.\left.+\frac{F'}{B^2}\left(\frac{A'}{A}-\frac{B'}{B}+\frac{C'}{C}+\frac{D'}{D}\right)\right\}\right].\end{aligned}\tag{25}$$

The energy of gravitating source per specific length defined by cylindrical symmetric space-time is given by [40, 46–48].

$$E=\frac{\left(1-l^{-2}\nabla^a r\nabla_a r\right)}{8}.\tag{26}$$

For a cylindrical symmetric paradigms by killing vectors, the circumference radius ρ, and specific length l and, moreover, arial radius r are described in [40, 46–48].

$\rho^2=\xi_{(1)a}\xi^a_{(1)}$, $l^2=\xi_{(2)a}\xi^a_{(2)}$, so that $r=\rho l$.

In the whole interior region C-energy has the following form [16]:

$$\begin{aligned}m(r,t)&=El\\&=\frac{l}{8}\\&\quad+\frac{1}{8D}\left[\frac{1}{A^2}\left(C\dot{D}+\dot{C}D\right)^2-\frac{1}{B^2}\left(CD'+C'D\right)^2\right].\end{aligned}\tag{27}$$

3.1. Matching Conditions. We consider an exterior spacetime over $3D$ hypersurface Σ that describes the 4-dimensional manifold M^+ in cylindrically symmetric geometry [16, 49] is given by

$$\begin{aligned}ds_+^2&=-\left(-\frac{2\widetilde{M}(\nu)}{\widetilde{R}}\right)d\nu^2-2d\nu d\widetilde{R}\\&\quad+\widetilde{R}^2\left(d\phi^2+\gamma^2dZ^2\right),\end{aligned}\tag{28}$$

where $\widetilde{M}(\nu)$ is the total mass and ν is the usual retarded time coordinate, while γ is a constant having the dimension of 1/length. Moreover, the interior spacetime of manifold M^- over the boundary hypersurface Σ is

$$k_-(t,r)=r-r_\Sigma=0.\tag{29}$$

Here r_Σ is constant. The interior metric of M^- over bounding hypersurface becomes

$$ds_-^2\overset{\Sigma}{=\!=}-d\tau^2+C^2d\phi^2+D^2dz^2,\tag{30}$$

where

$$d\tau \overset{\Sigma}{=} Adt \tag{31}$$

indicates the time coordinate on hypersurface Σ and $\overset{\Sigma}{=}$ means the estimation is applied on Σ of both sides.

In a similar manner, we prescribed the exterior line-element M^+ on $3D$ hypersurface Σ takes the form

$$k_+\left(\nu,\widetilde{R}\right) = \widetilde{R} - \widetilde{R}_\Sigma(\nu) = 0. \tag{32}$$

Thus, the exterior spacetime manifold M^+ on hypersurface is given by

$$\begin{aligned} ds_+^2 \overset{\Sigma}{=} & -2\left(-\frac{\widetilde{M}(\nu)}{\widetilde{R}} + \frac{d\widetilde{R}_\Sigma(\nu)}{d\nu}\right)d\nu^2 \\ & + \widetilde{R}^2\left(d\phi^2 + \gamma^2 dz^2\right). \end{aligned} \tag{33}$$

The following conditions due to Darmois [50] are to be satisfied.

(i) The continuity of the first fundamental form on Σ becomes

$$ds_\Sigma^2 = \left(ds_-^2\right)_\Sigma = \left(ds_+^2\right)_\Sigma. \tag{34}$$

(ii) The continuity of the second fundamental form over boundary three-surface is as follows:

$$\left[K_{\alpha\beta}\right] = K_{\alpha\beta}^+ - K_{\alpha\beta}^- = 0, \tag{35}$$

where $K_{\alpha\beta}$ is the extrinsic curvature over the hypersurface Σ and given into

$$\begin{aligned} K_{\alpha\beta}^\pm = -n_\mu^\pm\left(\frac{\partial^2 x_\pm^\mu}{\partial\rho^\alpha\partial\rho^\beta} + \Gamma_{ab}^\mu\frac{\partial x_\pm^a\partial x_\pm^b}{\partial\rho^\alpha\partial\rho^\beta}\right), \\ (\mu,a,b = 0,1,2,3). \end{aligned} \tag{36}$$

From the above equation of the extrinsic curvature, the Christoffel symbols are calculated for the interior and exterior manifolds M^- and M^+ accordingly and we labeled $(\rho^0,\rho^2,\rho^3)=(\tau,\phi,z)$ for the intrinsic coordinates on boundary surface Σ and $n_\mu^\pm$ are the components of the outward unit normal over Σ in the coordinates $x_\pm^\mu$, thus we have

$$\begin{aligned} n_\mu^- & \overset{\Sigma}{=} (0,B,0,0), \\ n_\mu^+ & \overset{\Sigma}{=} \lambda\left(-\frac{d\widetilde{R}}{d\nu},1,0,0\right), \\ \lambda & = \frac{1}{2\left(-\widetilde{M}(\nu)/\widetilde{R} + d\widetilde{R}_\Sigma(\nu)/d\nu\right)^{1/2}}. \end{aligned} \tag{37}$$

The following expressions are taken from the continuity of the first fundamental form:

$$\begin{aligned} C\left(t,\widetilde{r}_\Sigma\right) & \overset{\Sigma}{=} \widetilde{R}_\Sigma(\nu), \\ D\left(t,\widetilde{r}_\Sigma\right) & \overset{\Sigma}{=} \gamma\widetilde{R}_\Sigma(\nu), \\ \frac{dt}{d\tau} & = \frac{1}{A}, \\ \frac{d\nu}{d\tau} & = \lambda. \end{aligned} \tag{38}$$

Hence, the nonzero components of extrinsic curvature $K_{\alpha\beta}^\pm$ are

$$K_{00}^- = \left(-\frac{A'}{AB}\right)_\Sigma, \tag{39}$$

$$K_{00}^+ = \left[\left(\frac{d\nu}{d\tau}\right)^{-1}\left(\frac{d^2\nu}{d\tau^2}\right) - \frac{\widetilde{M}}{\widetilde{R}^2}\left(\frac{d\nu}{d\tau}\right)\right]_\Sigma, \tag{40}$$

$$K_{22}^- = \left(\frac{C'C}{B}\right)_\Sigma, \tag{41}$$

$$K_{33}^- = \left(\frac{D'D}{B}\right)_\Sigma, \tag{42}$$

$$K_{22}^+ = \left[\widetilde{R}\left(\frac{d\widetilde{R}}{d\tau}\right) - 2\widetilde{M}\left(\frac{d\nu}{d\tau}\right)\right]_\Sigma = \gamma^{-2}K_{33}^+. \tag{43}$$

Thus, continuity of the extrinsic curvature is organized with (38); we obtain the following results over hypersurface Σ [16, 51]:

$$\widetilde{M}(\nu) \overset{\Sigma}{=} \frac{\widetilde{R}}{2}\left[\left(\frac{\widetilde{R}^{\cdot}}{A}\right)^2 - \left(\frac{\widetilde{R}'}{B}\right)^2\right], \tag{44}$$

$$E \overset{\Sigma}{=} \frac{l}{8} + \gamma\widetilde{M}(\nu), \tag{45}$$

$$q \overset{\Sigma}{=} \left(P + \Pi + \frac{2\Omega}{3}\right) + \frac{T_{01}^D}{AB} + \frac{T_{11}^D}{B^2}. \tag{46}$$

Here T_{01}^D and T_{11}^D are the dark source components given in Appendices (A.1) and (A.2), respectively.

Therefore, (44) shows the total mass of the interior boundary surface Σ, whereas (45) gives the smooth association between the C energy for the cylindrical symmetric geometry and the active mass on hypersurface Σ. Moreover, (46) describes the linear association among the fluid quantities (P,Π,Ω,q) over the boundary three-surface Σ. Thus effective pressure is in usual nonvanishing over Σ due to dissipative nature of the dark source and this dissipation through viscosity parameters in the form of heat flow and undergoes free radiation streaming on the boundary surface. The extra components on the right hand side defines the dark source and appeared due to higher curvature of the geometry. It should be very interesting to mention that if the fluid has no dark source components then effective pressure and heat flux are equal on the boundary surface Σ.

Furthermore, other important results of the collapsing fluid are performed on the bounding three-surface Σ for the matching conditions of the Ricci invariant R and its normal derivative. The detailed description of matching conditions in $f(R)$ gravity theory has been given in [50, 52–56]. We require the matching conditions for the continuity of both spacetimes M^{-} and M^{+} over the hypersurface Σ; the following matching conditions $f(R)$ theory are given by

$$\begin{gathered} R|^{\pm} = 0, \\ f_{,RR}\left[\partial_{\gamma} R\right|^{\pm} = 0, \\ f_{,RR} \neq 0. \end{gathered} \tag{47}$$

The above expressions are required for the continuity of Ricci invariant R over the boundary surface Σ in the cylindrical collapsing fluid.

3.2. Dynamical Equations. The proper time and radial derivatives are given; we use Misner and Sharp technique [2].

$$\begin{aligned} D_T &= \frac{1}{A}\frac{\partial}{\partial t}, \\ D_C &= \frac{1}{C'}\frac{\partial}{\partial r}, \end{aligned} \tag{48}$$

where C is the areal radius of a spherical surface inside the limit. The velocity of the collapsing matter is described by the proper time derivative of C and D [17]; i.e.,

$$\begin{aligned} U &= D_T C = \frac{\dot{C}}{A}, \\ V &= D_T D = \frac{\dot{D}}{A}, \end{aligned} \tag{49}$$

which is always negative. Applying these results and (27), it turns out into

$$\begin{aligned} \tilde{E} &\equiv \frac{C'}{B} \\ &= \left[\left(\frac{VC+UD}{D}\right)^2 - \frac{8}{D}\left(m(r,t) - \frac{l}{8}\right)\right]^{1/2} - \frac{CD'}{BD}. \end{aligned} \tag{50}$$

The rate of change of mass is w.r.t. proper time in (27); we use (21), (22), and (23)-(25) as follows:

$$\begin{aligned} D_T m(r,t) = \frac{CD}{F}\Bigg[&-4\pi\bigg\{\left(\mu + 2\epsilon - p - \Pi + \frac{4\Omega}{3}\right)U \\ &+ \tilde{E}(q+\epsilon)\bigg\} \\ &- U\bigg\{\frac{\tilde{E}^2}{C'^2}\left(\frac{F'C'}{C} + \frac{F'D'}{D} - \frac{3\tilde{E}F'D_C B}{2}\right) \\ &+ \frac{\tilde{E}^2}{2}\left(\frac{D_C A D_T F}{\dot{C}} + \frac{3F''}{C'^2}\right) \\ &+ \frac{\tilde{E}^2 F}{D}\left(D_{CC}D + \frac{(D_C D)^2}{4D} + \frac{D_C D}{4C}\right) \\ &+ \frac{\tilde{E}^2 F D_{CC} C}{C} - \frac{\tilde{E}^3 F D_C B}{C'}\left(\frac{1}{C} + \frac{D_C D}{D}\right) \\ &- \frac{F}{B}\left(\frac{V D_T B}{D} + D_{TT}B\right) - \frac{F}{4}\left(\frac{D_{TT}C}{C} + \frac{D_{TT}D}{D}\right) \\ &+ \frac{RF(R)}{2} - \frac{f(R)}{2}\bigg\} - U^3\bigg\{\frac{\dot{F}}{\dot{C}}\left(\frac{D_T A}{2\dot{C}} - \frac{1}{C}\right) \\ &- \frac{\ddot{F}}{2\dot{C}^2} + \frac{F D_T A}{4C\dot{C}}\bigg\} \\ &+ U^2\bigg\{\frac{\tilde{E}^2}{\dot{C}}\left(\frac{3\dot{F}D_T B}{2\tilde{E}C'} - \frac{F'D_C A}{2C'}\right) + \frac{V\dot{F}}{\dot{C}D} \\ &+ \frac{F D_T B}{B}\left(\frac{1}{C} - \frac{D_T A}{\dot{C}}\right) \\ &- \frac{\tilde{E}^2 F}{\dot{C}}\left(D_{CC}A - \frac{\tilde{E}D_C A D_C B}{C'} + \frac{D_C A}{2C}\right) \\ &+ \frac{VF}{2D}\left(\frac{3}{4C} - \frac{D_T A}{\dot{C}}\right)\bigg\} - \frac{V^2 F}{2D}\left(\frac{\tilde{E}^2 D_C A}{\dot{D}} - \frac{U}{2D}\right) \\ &- \frac{V^3 F}{4D^2}\left(\frac{C}{D} + \frac{C D_T A}{\dot{D}}\right) + \frac{VF}{4D}\bigg\{\frac{C D_{TT} D}{D} + D_{TT}C \\ &+ \tilde{E}^2\left(\frac{C(D_C D)^2}{2D^2} - \frac{1}{2C}\right)\bigg\} \\ &- \frac{\tilde{E}^2}{2C'}\bigg\{\tilde{E}D_T B\left(D_C F + \frac{F}{2C} - \frac{C(D_C D)^2 F}{2D^2}\right) \\ &- F\left(\frac{D_T C'}{2C} + \frac{D_T D'}{2D}\right) \\ &+ \frac{F D_C D}{2D}\left(\frac{C D_T D'}{D} + D_T C'\right) - D_T F'\bigg\}\Bigg]. \end{aligned} \tag{51}$$

The overhead result leads to telling us that the variation rate of the total energy interior of the cylinder of radius C and the R.H.S of (51), $(\mu + 2\epsilon - p - \Pi + 4\Omega/3)U$ reflects that the energy is increasing in the interior surface of radius C (in case of collapsing situation ($U < 0$)) through the rate of work being done by the active radial pressure, the energy density μ, and the radiation pressure ϵ. The usual thermodynamical result is $\pi_{\alpha\beta} = -2\eta\sigma_{\alpha\beta}$ used in the relaxation phase. The second value $\tilde{E}(q+\epsilon)$ of the right-hand side illustrates the matter energy of the fluid, which is leaving the cylindrical surface. Moreover, all other extra terms play the natural role of the dark energy dissipative source under the formation of modified theory of gravity and decreasing the pressure in the core of the star due to continuous collapsing phase of the dark energy. Similarly, we can calculate

$$D_C m(r,t) = \frac{CD}{2F}\left[\kappa\left\{\mu + 2\epsilon + p + \Pi + \frac{2\Omega}{3} + \frac{U}{\widetilde{E}}(q + \epsilon)\right\} + \frac{U^3 F D_C A}{2C\dot{C}} + U^2\left\{\frac{D_T F D_C A}{\dot{C}} + \frac{F}{C}\left(\frac{D_C D}{4D} - \frac{D_T A}{\dot{C}}\right)\right\} - U\left\{\widetilde{E} D_C F\left(\frac{\widetilde{E} D_C A}{\dot{C}} - \frac{D_T B}{C'}\right) + \frac{D_T F D_T A}{\dot{C}} + F\left(\frac{1}{C'}\left(\frac{D_T C'}{2C} + \frac{D_T D'}{2D} - \frac{\widetilde{E} D_T B D_C D}{D}\right) + \frac{\widetilde{E}^2}{\dot{C}}\left(\frac{D_C A}{C} + \frac{D_C A D_C D}{D}\right)\right)\right\} - \frac{V^2 F}{2D^2}\left\{C\left(\frac{U D_C A}{\dot{C}} + \frac{D_C D}{2D}\right) - 1\right\} + \frac{VF}{2C'D}\left(\frac{C D_T D'}{D} + D_T C'\right) + \frac{UVF}{D}\left(\frac{1}{2C} - \frac{D_T A}{\dot{C}}\right) - \widetilde{E}^2 F\left\{\frac{D_C D}{2D^2}\left(C D_{CC} D + D_C D - \frac{C(D_C D)^2}{2D} - \frac{\widetilde{E} C D_C B D_C D}{C'}\right) - \frac{1}{2C}\left(D_{CC} C - \frac{3 D_C D}{2D} - \frac{\widetilde{E} D_C B}{C'}\right) + \frac{1}{2D}\left(D_C D D_{CC} C - D_{CC} D\right)\right\} - \frac{\widetilde{E}}{C'}\left(D_T F D_T B + \widetilde{E}^2 D_C F D_C B + \frac{F D_T B D_T D}{D}\right) + D_{TT} F + \frac{F'' \widetilde{E}^2}{C'^2} - \frac{U D_T F'}{C'} + \frac{F D_{TT} C}{C} + \frac{F D_{TT} D}{D}\right]. \tag{52}$$

This solution of (52) explains how variational quantities affect the matter distribution between the neighboring exteriors in the object of radius C. The picture of the first two quantities on the R.H.S of (52) is $\mu + 2\epsilon$ related with energy density of the fluid and plus the addiction of the null fluid conferring dissipation in the outgoing streaming approximation. The last factor $(U/\widetilde{E})(q + \epsilon)$ plays negative role in the collapsing situation and estimates the dissipation in terms of heat flow and radiation streaming. The extra values signify the input of the dark energy (DE) due to its higher order of the curvature matter. We Apply integration on (52) with C; we get

$$m(r,t) = \frac{1}{2}\int_0^C \frac{CD}{2F}\left[\kappa\left\{\mu + 2\epsilon + p + \Pi + \frac{2\Omega}{3} + \frac{U}{\widetilde{E}}(q + \epsilon)\right\} + \frac{U^3 F D_C A}{2C\dot{C}} + U^2\left\{\frac{D_T F D_C A}{\dot{C}} + \frac{F}{C}\left(\frac{D_C D}{4D} - \frac{D_T A}{\dot{C}}\right)\right\} - U\left\{\widetilde{E} D_C F\left(\frac{\widetilde{E} D_C A}{\dot{C}} - \frac{D_T B}{C'}\right) + \frac{D_T F D_T A}{\dot{C}} + F\left(\frac{1}{C'}\left(\frac{D_T C'}{2C} + \frac{D_T D'}{2D} - \frac{\widetilde{E} D_T B D_C D}{D}\right) + \frac{\widetilde{E}^2}{\dot{C}}\left(\frac{D_C A}{C} + \frac{D_C A D_C D}{D}\right)\right)\right\} - \frac{V^2 F}{2D^2}\left\{C\left(\frac{U D_C A}{\dot{C}} + \frac{D_C D}{2D}\right) - 1\right\} + \frac{VF}{2C'D}\left(\frac{C D_T D'}{D} + D_T C'\right) + \frac{UVF}{D}\left(\frac{1}{2C} - \frac{D_T A}{\dot{C}}\right) - \widetilde{E}^2 F\left\{\frac{D_C D}{2D^2}\left(C D_{CC} D + D_C D - \frac{C(D_C D)^2}{2D} - \frac{\widetilde{E} C D_C B D_C D}{C'}\right) - \frac{1}{2C}\left(D_{CC} C - \frac{3 D_C D}{2D} - \frac{\widetilde{E} D_C B}{C'}\right) + \frac{1}{2D}\left(D_C D D_{CC} C - D_{CC} D\right)\right\} - \frac{\widetilde{E}}{C'}\left(D_T F D_T B + \widetilde{E}^2 D_C F D_C B + \frac{F D_T B D_T D}{D}\right) + D_{TT} F + \frac{F'' \widetilde{E}^2}{C'^2} - \frac{U D_T F'}{C'} + \frac{F D_{TT} C}{C} + \frac{F D_{TT} D}{D}\right] dC. \tag{53}$$

The above equation gives the total mass in terms of C-energy inside the cylinder with the contribution of $f(R)$ dark source term. To observe the dynamical equation by assuming Misner and Sharp approach[2, 57], the contracted Bianchi identities take the form,

$$\begin{aligned}&\left(T^{(m)}_{\alpha\beta}+T^{(D)}_{\alpha\beta}\right)_{;\beta}V_{\alpha}=0,\\&\left(T^{(m)}_{\alpha\beta}+T^{(D)}_{\alpha\beta}\right)_{;\beta}\chi_{\alpha}=0,\end{aligned}\tag{54}$$

which produce

$$\begin{aligned}&\frac{1}{A}\left[(\dot{\mu+\epsilon})+\left(\mu+p+\Pi+2\epsilon+\frac{2\Omega}{3}\right)\frac{\dot{B}}{B}\right.\\&\quad\left.+\left(\mu+p+\Pi+\epsilon-\frac{\Omega}{3}\right)\left(\frac{\dot{C}}{C}+\frac{\dot{D}}{D}\right)\right]\\&\quad+\frac{1}{B}\left[(q+\epsilon)'+(q+\epsilon)\left(\frac{2A'}{A}+\frac{(CD)'}{CD}\right)\right]-D_1\\&\quad=0,\end{aligned}\tag{55}$$

$$\begin{aligned}&\frac{1}{A}\left[(\dot{q+\epsilon})+(q+\epsilon)\left(2\frac{\dot{B}}{B}+\frac{\dot{C}}{C}+\frac{\dot{D}}{D}\right)\right]\\&\quad+\frac{1}{B}\left[\left(p+\Pi+\epsilon+\frac{2\Omega}{3}\right)'\right.\\&\quad\left.+\left(\mu+p+\Pi+2\epsilon+\frac{2\Omega}{3}\right)\frac{A'}{A}+(\epsilon+\Omega)\frac{(CD)'}{CD}\right]\\&\quad+D_2=0.\end{aligned}\tag{56}$$

Here D_1 and D_2 are the dark source components shown in Appendix (A.3) and (A.4), respectively.

From (23) and (48)-(50), it follows that

$$\begin{aligned}&D_T(\mu+\epsilon)+\frac{1}{3}(3\mu+3p+3\Pi+4\epsilon)\Theta\\&\quad+\frac{1}{3}(\epsilon+\Omega)\left(\frac{2\dot{B}}{AB}-\frac{U}{C}-\frac{V}{D}\right)+\tilde{E}D_C(q+\epsilon)\\&\quad+(q+\epsilon)\left(2\frac{a_1}{B}+\frac{\tilde{E}}{C}+\frac{D'}{BD}\right)-D_1=0.\end{aligned}\tag{57}$$

$$\begin{aligned}&D_T(q+\epsilon)+(q+\epsilon)\left(\Theta+\frac{D_TB}{B}\right)\\&\quad+\tilde{E}D_C\left(p+\Pi+\epsilon+\frac{2\Omega}{3}\right)\\&\quad+\left(\mu+p+\Pi+2\epsilon+\frac{2\Omega}{3}\right)\frac{a_1}{B}+(\epsilon+\Omega)\frac{(CD)'}{BCD}\\&\quad+D_2=0.\end{aligned}\tag{58}$$

The acceleration D_TU of the dissipative viscous collapsing source is attained by using (23) and (48)-(50); it becomes

$$\begin{aligned}D_TU=&-\frac{m(r,t)}{CD}+\frac{l}{8CD}-\frac{4\pi C}{F}\left(p+\Pi+\epsilon+\frac{2\Omega}{3}\right)\\&+\left(\frac{\tilde{E}}{2}+\frac{D'C}{2BD}\right)\frac{a_1}{B}-\frac{C}{F}\left[\frac{D_{TT}F}{2}\right.\\&+\frac{UD_TF}{2}\left(\frac{1}{C}-\frac{D_TA}{\dot{C}}\right)+\frac{VD_TF}{2D}-\frac{\tilde{E}D'D_CF}{2BD}\\&\left.-\frac{\tilde{E}^2D_CF}{2}\left(\frac{UD_CA}{\dot{C}}+\frac{1}{C}\right)\right]+\frac{D_{TT}C}{2}-\frac{CD_{TT}D}{2D}\\&-\frac{D_TA}{2A}\left(U-\frac{CV}{D}\right)-\frac{1}{4D}\left(UV-\frac{\tilde{E}D'}{B}\right)\\&+\frac{1}{8D^2}\left(CV^2-\frac{CD'^2}{B^2}\right)+\frac{1}{8C}\left(U^2-\tilde{E}^2\right)\\&-\frac{C\left(f(R)-RF(R)\right)}{4F}.\end{aligned}\tag{59}$$

After, inserting a_1/B from (59) into (58), we get

$$\begin{aligned}&\left(\mu+p+\Pi+2\epsilon+\frac{2\Omega}{3}\right)D_TU=-\left(\mu+p+\Pi+2\epsilon\right.\\&\quad\left.+\frac{2\Omega}{3}\right)\left[\frac{m(r,t)}{CD}-\frac{l}{8CD}\right.\\&\quad+\frac{4\pi C}{F}\left(p+\Pi+\epsilon+\frac{2\Omega}{3}\right)+\frac{C\left(f(R)-RF(R)\right)}{4F}\\&\quad+\frac{CD_{TT}F}{2F}+\left(\frac{1}{C}-\frac{D_TA}{\dot{C}}\right)\frac{UCD_TF}{2F}+\frac{VCD_TF}{2DF}\\&\quad-\frac{\tilde{E}CD'D_CF}{2BDF}-\frac{\tilde{E}^2CD_CF}{2F}\left(\frac{1}{C}+\frac{UD_CA}{\dot{C}}\right)\\&\quad-\frac{D_{TT}C}{2}+\frac{CD_{TT}D}{2D}+\frac{D_TA}{2A}\left(U-\frac{VC}{D}\right)\\&\quad+\frac{1}{4D}\left(UV-\frac{\tilde{E}D'}{B}\right)-\frac{1}{8D^2}\left(V^2C-\frac{CD'^2}{B^2}\right)\\&\quad\left.-\frac{1}{8C}\left(U^2-\tilde{E}^2\right)\right]-\left(\frac{\tilde{E}}{2}+\frac{D'C}{2BD}\right)\\&\quad\cdot\left[\tilde{E}D_C\left(p+\Pi+\epsilon+\frac{2\Omega}{3}\right)+\frac{\tilde{E}}{C}(\epsilon+\Omega)\right.\\&\quad\left.+\frac{D'}{BD}(\epsilon+\Omega)\right]-\left(\frac{\tilde{E}}{2}+\frac{D'C}{2BD}\right)\left[D_T(q+\epsilon)\right.\\&\quad\left.+(q+\epsilon)\left(\Theta+\frac{D_TB}{B}\right)+D_2\right].\end{aligned}\tag{60}$$

In this interpretation, to analyze the factor $(\mu+p+\Pi+2\epsilon+2\Omega/3)$, that comes on the L.H.S and on the R.H.S, this is effective inertial mass and defines through equivalence principle. It can also be recognized as passive gravitational mass. On the R.H.S, the first term of square bracket illustrates the impacts of the collapsing variables on the active gravitational mass for the cylindrical collapsing object with the dissipative dark source in f(R) metric theory; this datum was early pointed by Herrera et al. [35] in the context of GR. Moreover, in the second square bracket there is the gradient of the whole active pressure which is influenced by collapsing variables and radiating density. The final bracket includes unalike quantities that define the collapsing nature of the source. The second value of this bracket $(q+\epsilon)$ is positive concluding that dissipation is continuous in the form of heat flow and free streaming radiation and finally decreases the total energy of the system, which reduces the degree of collapse. The last term of this bracket expresses the dark energy source of the dissipative gravitating collapse.

4. Transport Equations

The purpose of this profile is to discuss the full causal technique for the viscous dissipative gravitating collapse in self-gravitating system accompanied by heat transference. This study tells us that all collapsing variables should satisfy the transportation equations attained from causal thermodynamics. Therefore, we take the transportation equations for heat, bulk, and shear viscosity from *Müller*-Israel-Stewart formalism [41–43] for dissipative source. Herrera et al. [35] discussed transportation equations for heat, bulk, and shear viscosity. The entropy flux is given by

$$S^{\mu} = SnV^{\mu} + \frac{q^{\mu}}{T} - \left(\beta_0\Pi^2 + \beta_1 q_{\nu}q^{\nu} + \beta_2\pi_{\nu\kappa}\pi^{\nu\kappa}\right)\frac{V^{\mu}}{2T} + \frac{\alpha_0\Pi q^{\mu}}{T} + \frac{\alpha_1\pi^{\mu\nu}q_{\nu}}{T}, \tag{61}$$

where β_1 and β_2 are thermodynamic factors for unalike additions to entropy density, α_0 and α_1 are thermodynamics heat coupling factors, and T is temperature.

Furthermore, from the Gibbs equation and Bianchi identities, it follows that

$$\begin{aligned} TS^{\alpha}_{;\alpha} &= -\Pi\left[V^{\alpha}_{;\alpha} - \alpha_0 q^{\alpha}_{;\alpha} + \beta_0\Pi_{;\alpha}V^{\alpha} + \frac{T}{2}\left(\frac{\beta_0}{T}V^{\alpha}\right)_{;\alpha}\Pi\right] - q^{\alpha}\left[h^{\mu}_{\alpha}(\ln T)_{,\mu}(1+\alpha_0\Pi)\right. \\ &\quad + V_{\alpha;\mu}V^{\mu} - \alpha_0\Pi_{;\alpha} - \alpha_1\pi^{\mu}_{\alpha;\mu} + \alpha_1\pi^{\mu}_{\alpha}h^{\beta}_{\mu}(\ln T)_{,\beta} \\ &\quad \left. + \beta_1 q_{\alpha;\mu}V^{\mu} + \frac{T}{2}\left(\frac{\beta_1}{T}V^{\mu}\right)_{;\mu}q_{\alpha}\right] - \pi^{\alpha\mu}\left[\sigma_{\alpha\mu}\right. \\ &\quad \left. - \alpha_1 q_{\mu;\alpha} + \beta_2\pi_{\alpha\mu;\nu}V^{\nu} + \frac{T}{2}\left(\frac{\beta_2}{T}V^{\nu}\right)_{;\nu}\pi_{\alpha\mu}\right]. \end{aligned} \tag{62}$$

Finally, by the standard procedure, the constitutive transport equations follow from the requirement $S^{\alpha}_{;\alpha} \geq 0$:

$$\tau_0\Pi_{,\alpha}V^{\alpha} + \Pi = -\zeta\theta + \alpha_0\zeta q^{\alpha}_{;\alpha} - \frac{1}{2}\zeta T\left(\frac{\tau_0}{\zeta T}V^{\alpha}\right)_{;\alpha}\Pi. \tag{63}$$

$$\begin{aligned} \tau_1 h^{\beta}_{\alpha}q_{\beta;\mu}V^{\mu} + q_{\alpha} &= -\kappa\left[h^{\beta}_{\alpha}T_{,\beta}(1+\alpha_0\Pi) + \alpha_1\pi^{\mu}_{\alpha}h^{\beta}_{\mu}T_{,\beta}\right. \\ &\quad \left. + T\left(a_{\alpha} - \alpha_0\Pi_{;\alpha} - \alpha_1\pi^{\mu}_{\alpha;\mu}\right)\right] - \frac{1}{2}\kappa T^2\left(\frac{\tau_1}{\kappa T^2}V^{\beta}\right)_{;\beta} \\ &\quad \cdot q_{\alpha} \end{aligned} \tag{64}$$

$$\begin{aligned} \tau_2 h^{\mu}_{\alpha}h^{\nu}_{\beta}\pi_{\mu\nu;\rho}V^{\rho} + \pi_{\alpha\beta} &= -2\eta\sigma_{\alpha\beta} + 2\eta\alpha_1 q_{\langle\beta;\alpha\rangle} \\ &\quad - \eta T\left(\frac{\tau_2}{2\eta T}V^{\nu}\right)_{;\nu}\pi_{\alpha\beta}, \end{aligned} \tag{65}$$

with

$$q_{\langle\beta;\alpha\rangle} = h^{\mu}_{\beta}h^{\nu}_{\alpha}\left(\frac{1}{2}\left(q_{\mu;\nu} + q_{\nu;\mu}\right) - \frac{1}{3}q_{\sigma;\kappa}h^{\sigma\kappa}h_{\mu\nu}\right), \tag{66}$$

and where the relaxational times are given by

$$\begin{aligned} \tau_0 &= \zeta\beta_0, \\ \tau_1 &= \kappa T\beta_1, \\ \tau_2 &= 2\eta\beta_2, \end{aligned} \tag{67}$$

where ζ and η are the factors of bulk and shear viscosity. We use the interior metric of the cylindrical structure from (63)-(65), to get the following set of equations:

$$\begin{aligned} \tau_0\dot{\Pi} &= -\left(\zeta + \frac{\tau_0}{2}\Pi\right)A\Theta + \frac{A}{B}\alpha_0\zeta\left[q' + q\left(\frac{A'}{A} + \frac{C'}{C}\right.\right. \\ &\quad \left.\left. + \frac{D'}{D}\right)\right] - \Pi\left[\frac{\zeta T}{2}\dot{\left(\frac{\tau_0}{\zeta T}\right)} + A\right], \end{aligned} \tag{68}$$

$$\begin{aligned} \tau_1\dot{q} &= -\frac{A}{B}\kappa\left\{T'\left(1 + \alpha_0\Pi + \frac{2}{3}\alpha_1\Omega\right) + T\left[\frac{A'}{A} - \alpha_0\Pi'\right.\right. \\ &\quad \left.\left. - \frac{2}{3}\alpha_1\left(\Omega' + \frac{A'}{A}\Omega + \frac{3}{2}\left(\frac{C'}{C} + \frac{D'}{D}\right)\Omega\right)\right]\right\} \\ &\quad - q\left[\frac{\kappa T^2}{2}\dot{\left(\frac{\tau_1}{\kappa T^2}\right)} + \frac{\tau_1}{2}A\Theta + A\right], \end{aligned} \tag{69}$$

$$\begin{aligned} \tau_2\dot{\Omega} &= -\eta\left(\frac{2\dot{B}}{B} - \frac{\dot{C}}{C} - \frac{\dot{D}}{D}\right) + 2\eta\alpha_1\frac{A}{B}q' \\ &\quad - \Omega\left[\eta T\dot{\left(\frac{\tau_2}{2\eta T}\right)} + \frac{\tau_2}{2}A\Theta + A\right], \end{aligned} \tag{70}$$

where we have to analyze the effect on several dissipative variables for the cylindrical interior surface. For this persistence, we use (69) and (60) and get

$$\begin{aligned}
&\left(\mu + p + \Pi + 2\epsilon + \frac{2}{3}\Omega\right)(1-\Lambda) D_T U = (1-\Lambda) F_{grav} \\
&\quad + F_{hyd} + \widetilde{E}\left(\frac{\widetilde{E}}{2} + \frac{D'C}{2BD}\right) \\
&\quad \cdot \frac{\kappa}{\tau_1}\left\{D_C T\left(1 + \alpha_0\Pi + \frac{2}{3}\alpha_1\Omega\right)\right. \\
&\quad \left. - T\left[\alpha_0 D_C \Pi + \frac{2}{3}\alpha_1\left(D_C\Omega + \frac{3(CD)'}{2CDC'}\Omega\right)\right]\right\} \\
&\quad + \left(\frac{\widetilde{E}}{2} + \frac{D'C}{2BD}\right)\left[\frac{\kappa T^2 q}{2\tau_1} D_T\left(\frac{\tau_1}{\kappa T^2}\right) - D_T\epsilon\right] - \left(\frac{\widetilde{E}}{2}\right. \\
&\quad \left. + \frac{D'C}{2BD}\right)\left[\left(\frac{q}{2} + 2\epsilon\right)\Theta - \frac{q}{\tau_1} + (q+\epsilon)\frac{D_T B}{B} + D_2\right].
\end{aligned} \tag{71}$$

Here F_{grav} and F_{hyd} are introduced into the form

$$\begin{aligned}
F_{grav} &= -\left(\mu + p + \Pi + 2\epsilon + \frac{2\Omega}{3}\right)\left[m(r,t) - \frac{l}{8}\right. \\
&\quad + 4\pi\left(p + \Pi + \epsilon + \frac{2\Omega}{3}\right)\frac{C^2 D}{F} \\
&\quad + \frac{C^2 D\left(f(R) - RF(R)\right)}{4F} + \frac{C^2 D D_{TT} F}{2F} \\
&\quad + \frac{UC^2 D D_T F}{2F}\left(\frac{1}{C} - \frac{D_T A}{\dot{C}}\right) + \frac{VC^2 D_T F}{2F} \\
&\quad - \frac{\widetilde{E}C^2 D' D_C F}{2BF} - \frac{\widetilde{E}^2 C^2 D D_C F}{2F}\left(\frac{1}{C} + \frac{UD_C A}{\dot{C}}\right) \\
&\quad - \frac{CDD_{TT}C}{2} + \frac{C^2 D_{TT} D}{2} + \frac{CDD_T A}{2A}\left(U - \frac{VC}{D}\right) \\
&\quad + \frac{C}{4}\left(UV - \frac{\widetilde{E}D'}{B}\right) - \frac{C}{8D}\left(V^2 C - \frac{CD'^2}{B^2}\right) \\
&\quad \left. + -\frac{D}{8}\left(U^2 - \widetilde{E}^2\right)\right]\frac{1}{CD}, \\
F_{hyd} &= -\left(\frac{\widetilde{E}}{2} + \frac{D'C}{2BD}\right)\left[\widetilde{E}D_C\left(p + \Pi + \epsilon + \frac{2\Omega}{3}\right)\right. \\
&\quad \left. + \frac{\widetilde{E}}{C}(\epsilon + \Omega) + \frac{D'}{BD}(\epsilon + \Omega)\right],
\end{aligned} \tag{72}$$

and Λ is defined as

$$\Lambda = \frac{\kappa T}{\tau_1}\left(\mu + p + \Pi + 2\epsilon + \frac{2}{3}\Omega\right)^{-1}\left(1 - \frac{2}{3}\alpha_1\Omega\right). \tag{73}$$

From (68) and (71) subsequently it becomes

$$\begin{aligned}
&\left(\mu + p + \Pi + 2\epsilon + \frac{2}{3}\Omega\right)(1 - \Lambda + \Delta) D_T U = (1 - \Lambda \\
&\quad + \Delta) F_{grav} + F_{hyd} + \frac{\widetilde{E}\kappa}{\tau_1}\left(\frac{\widetilde{E}}{2} + \frac{D'C}{2BD}\right) \\
&\quad \cdot \left\{D_C T\left(1 + \alpha_0\Pi + \frac{2}{3}\alpha_1\Omega\right)\right. \\
&\quad \left. - T\left[\alpha_0 D_C\Pi + \frac{2}{3}\alpha_1\left(D_C\Omega + \frac{3(CD)'}{2CDC'}\Omega\right)\right]\right\} \\
&\quad - \widetilde{E}\left(\frac{\widetilde{E}}{2} + \frac{D'C}{2BD}\right)\left(\mu + p + \Pi + 2\epsilon + \frac{2}{3}\Omega\right) \\
&\quad \cdot \Delta\left(\frac{D_C q}{q} + \frac{(CD)'}{CDC'}\right) + \left(\frac{\widetilde{E}}{2} + \frac{D'C}{2BD}\right) \\
&\quad \cdot \left[\frac{\kappa T^2 q}{2\tau_1} D_T\left(\frac{\tau_1}{\kappa T^2}\right) - D_T\epsilon\right] + \left(\frac{\widetilde{E}}{2} + \frac{D'C}{2BD}\right)\left[\frac{q}{\tau_1}\right. \\
&\quad \left. - (q+\epsilon)\frac{D_T B}{B} - D_2\right] + \left(\frac{\widetilde{E}}{2} + \frac{D'C}{2BD}\right)\frac{\Delta}{\alpha_0\zeta q}\left(\mu\right. \\
&\quad \left. + p + \Pi + 2\epsilon + \frac{2}{3}\Omega\right)\left\{\left[1 + \frac{\zeta T}{2} D_T\left(\frac{\tau_0}{\zeta T}\right)\right]\Pi \right. \\
&\quad \left. + \tau_0 D_T \Pi\right\},
\end{aligned} \tag{74}$$

where Δ is recognized as

$$\Delta = \alpha_0\zeta q\left(\mu + p + \Pi + 2\epsilon + \frac{2}{3}\Omega\right)^{-1}\left(\frac{q + 2\epsilon}{2\zeta + \tau_0\Pi}\right). \tag{75}$$

In this account, once we have made the interpretation of the causal transportation equations and then, coupled with the dynamical equation, we found the factor $1 - \Lambda + \Delta$; the roll of this factor reduced the inertial energy density and effective gravitational mass density that appears in the system. This consequence agrees with the findings of Herrera et al. [35].

5. Conclusions

The beginning of the 20th century, after presenting general theory of relativity Weyl [58] and Levi-Civita [59] discussed the current issues with static cylindrical symmetric structures. In the starting scenario astrophysicists were focused to find the self-gravitating models that are axially symmetric. The relativistic fluids having dissipative nature are very useful in the formulation of stellar models. Therefore, one can not disagree with the effects of dissipation during the self-gravitational collapse.

In this format, we have arranged the dynamical equation which plays the meaningful role in progressive stages of the viscous dissipative gravitational collapse. We notice the impacts of $f(R)$ terms in the dynamical progression for the dissipative case; this dissipation is undergone in the form of heat flow and free streaming approximation. We have considered the convenient formation of the collapsing variables involved in the transportation equations in terms of heat flux, bulk, and shear viscosity ensuing from causal thermodynamical approach. Moreover, the dynamical equation is coupled with full causal transportation equations for getting the meaningful results that appear in the form of heat dissipation, bulk, and shear viscosity. In extensive point of view, the main debate of the general thermodynamical approach is to notice the relaxation phase whose direction either less than or equal to radiating time. It is interesting to mention that the hyperbolic concept of the collapse is much consistent and having rare problems than parabolic concept [60–62].

A full causal technique has been implemented in [35], to evaluate the impacts on collapsing variables with spherically symmetric collapse geometry: this study gives the expressive and momentous contribution in relativistic physics. The application of this work is obtained by some astral objects and relativistic structures. These massive systems have possessive nature in dissipative collapsing situation in which dissipation is undergone in the form of heat flow and radiation streaming. The system was weakened due to leaving the energy from the system and continues collapse. Furthermore, in this connection it is worth mentioning that thermodynamical viscous/heat coupling factors have nonterminating possibility due to dissipative gravitational collapse; this framework gives the momentous foundation in the modeling of relativistic structures. In this respect we see another previous work given by [63]; a partial technique is used to discuss the impacts of bulk dissipative gravitating collapse in cylindrical surface of the star with leaving the thermodynamical heat radiating coupling factors in the transport equations.

Finally, in this evaluation we analyze the full causal technique with viscous dissipative gravitational collapse and get the dynamical equation (74), which explain how passive gravitational mass and heat coupling factors influence the gravitational collapse of radiating source. The passive gravitational mass density is affected by bulk and shear viscosity and these factors are responsible for decreasing the internal radial pressure of the collapsing source. These factors also decrease the force of gravity in a system, this lessening due to huge dissipation in the form of thermal conduction of the gravitational collapse. Consequently, the outflow of heat reduces the total energy of the collapsing cylindrical object. Herrera et al. [64] investigated the bouncing action predicted in mathematical framework for the current arithmetic calculation. The present work is reproduced in future with other modified theories such as Gauss-Bonnet and $f(R,T)$ gravity theories. This work has been done for spherical symmetry with and without electromagnetic field [65].

Appendix

$$T_{01}^{D} = \frac{1}{\kappa}\left(\dot{F}' - \frac{A'\dot{F}}{A} - \frac{\dot{B}F'}{B}\right), \tag{A.1}$$

$$\begin{aligned} T_{11}^{D} = \frac{B^2}{\kappa}\Bigg\{&\left(\frac{f(R) - RF(R)}{2}\right) + \frac{\ddot{F}}{A^2} + \frac{\dot{F}}{A^2}\left(\frac{\dot{C}}{C} + \frac{\dot{D}}{D}\right. \\ &\left. - \frac{\dot{A}}{A}\right) - \frac{F'}{B^2}\left(\frac{A'}{A} + \frac{C'}{C} + \frac{D'}{D}\right)\Bigg\}, \end{aligned} \tag{A.2}$$

$$\begin{aligned} D_1 = \frac{A}{\kappa}\Bigg[&\left\{\frac{1}{A^2B^2}\left(\dot{F}' - \frac{A'\dot{F}}{A} - \frac{\dot{B}F'}{B}\right)\right\}_{,1} \\ &+ \left\{\frac{f(R) - RF(R)}{2A^2} - \frac{F''}{A^2B^2}\right. \\ &+ \frac{\dot{F}}{A^4}\left(\frac{\dot{B}}{B} + \frac{\dot{C}}{C} + \frac{\dot{D}}{D}\right) \\ &\left. - \frac{F'}{A^2B^2}\left(\frac{C'}{C} + \frac{D'}{D} - \frac{B'}{B}\right)\right\}_{,0} \\ &+ \frac{2\dot{A}}{A^3}\left\{\frac{f(R) - RF(R)}{2} - \frac{F''}{B^2}\right. \\ &\left. + \frac{\dot{F}}{A^2}\left(\frac{\dot{B}}{B} + \frac{\dot{C}}{C} + \frac{\dot{D}}{D}\right) - \frac{F'}{B^2}\left(\frac{C'}{C} + \frac{D'}{D} - \frac{B'}{B}\right)\right\} \\ &+ \frac{\dot{B}}{A^2B}\left\{-\frac{\ddot{F}}{A^2} - \frac{F''}{B^2} + \frac{\dot{F}}{A^2}\left(\frac{\dot{A}}{A} + \frac{\dot{B}}{B}\right)\right. \\ &\left. + \frac{F'}{B^2}\left(\frac{A'}{A} + \frac{B'}{B}\right)\right\} + \frac{\dot{C}}{A^2C}\left\{-\frac{\ddot{F}}{A^2} + \frac{\dot{F}}{A^2}\frac{\dot{A}}{A}\right. \\ &\left. + \frac{F'}{B^2}\frac{A'}{A}\right\} + \frac{\dot{D}}{A^2D}\left\{-\frac{\ddot{F}}{A^2} + \frac{\dot{F}}{A^2}\frac{\dot{A}}{A} + \frac{F'}{B^2}\frac{A'}{A}\right\} \\ &+ \frac{1}{A^2B^2}\left(\dot{F}' - \frac{A'\dot{F}}{A} - \frac{\dot{B}F'}{B}\right)\left(\frac{3A'}{A} + \frac{B'}{B} + \frac{C'}{C}\right. \\ &\left. + \frac{D'}{D}\right)\Bigg], \end{aligned} \tag{A.3}$$

$$\begin{aligned} D_2 = \frac{B}{\kappa}\Bigg[&-\left\{\frac{1}{A^2B^2}\left(\dot{F}' - \frac{A'\dot{F}}{A} - \frac{\dot{B}F'}{B}\right)\right\}_{,0} \\ &+ \left\{\frac{f(R) - RF(R)}{2B^2} + \frac{\ddot{F}}{A^2B^2}\right. \\ &+ \frac{\dot{F}}{A^2B^2}\left(\frac{\dot{C}}{C} + \frac{\dot{D}}{D} - \frac{\dot{A}}{A}\right) \\ &\left. - \frac{F'}{B^4}\left(\frac{A'}{A} + \frac{C'}{C} + \frac{D'}{D}\right)\right\}_{,1} + \frac{A'}{AB^2}\left\{\frac{\ddot{F}}{A^2} + \frac{F''}{B^2}\right. \\ &\left. - \frac{\dot{F}}{A^2}\left(\frac{\dot{A}}{A} + \frac{\dot{B}}{B}\right) - \frac{F'}{B^2}\left(\frac{A'}{A} + \frac{B'}{B}\right)\right\} \\ &+ \frac{2B'}{B^3}\left\{\frac{f(R) - RF(R)}{2} + \frac{\ddot{F}}{A^2}\right. \\ &\left. + \frac{\dot{F}}{A^2}\left(\frac{\dot{C}}{C} + \frac{\dot{D}}{D} - \frac{\dot{A}}{A}\right) - \frac{F'}{B^2}\left(\frac{A'}{A} + \frac{C'}{C} + \frac{D'}{D}\right)\right\} \\ &+ \frac{C'}{B^2C}\left\{\frac{F''}{B^2} - \frac{\dot{F}}{A^2}\frac{\dot{B}}{B} - \frac{F'}{B^2}\frac{B'}{B}\right\} + \frac{D'}{B^2D}\left\{\frac{F''}{B^2}\right. \\ &\left. - \frac{\dot{F}}{A^2}\frac{\dot{B}}{B} - \frac{F'}{B^2}\frac{B'}{B}\right\} - \frac{1}{A^2B^2}\left(\frac{\dot{A}}{A} + \frac{3\dot{B}}{B} + \frac{\dot{C}}{C} + \frac{\dot{D}}{D}\right) \\ &\cdot\left(\dot{F}' - \frac{A'\dot{F}}{A} - \frac{\dot{B}F'}{B}\right)\Bigg]. \end{aligned} \tag{A.4}$$

Data Availability

The data used to support the findings of this study are available from the corresponding author upon request.

Conflicts of Interest

The authors declare that they have no conflicts of interest.

Acknowledgments

One of the authors, G. Abbas, appreciates the financial support from HEC, Islamabad, Pakistan, under NRPU project with Grant no. 20-4059/NRPU/R & D/HEC/14/1217.

References

[1] J. R. Oppenheimer and H. Snyder, "On continued gravitational contraction," *Physical Review A: Atomic, Molecular and Optical Physics*, vol. 56, no. 5, pp. 455–459, 1939.

[2] C. W. Misner and D. H. Sharp, "Relativistic equations for adiabatic, spherically symmetric gravitational collapse," *Physical Review A: Atomic, Molecular and Optical Physics*, vol. 136, no. 2, pp. B571–B576, 1964.

[3] P. C. Vaidya, "The gravitational field of a radiating star," *Proceedings of the Indian Academy of Science*, vol. A33, p. 264, 1951.

[4] S. Capozziello, "Curvature quintessence," *International Journal of Modern Physics D*, vol. 11, pp. 483–492, 2002.

[5] M. Sharif and Z. Yousaf, "Stability of a Class of Non-Static Axial Self-Gravitating Systems in *f(R)* Gravity," *Astrophysics and Space Science*, vol. 352, p. 943, 2014.

[6] M. K. Mak, T. Harko, and R. Soc, "Anisotropic Stars in General Relativity," *Proceedings of the Royal Society*, vol. A459, p. 393, 2003.

[7] L. Herrera and N. O. Santos, "Jeans mass for anisotropic matter," *The Astrophysical Journal*, vol. 438, p. 308, 1995.

[8] F. Weber, *Pulsars as Astrophysical Laboratories for Nuclear and Particle Physics*, vol. BS1, Bristol, UK, Institute of Physics Publishing, Dirac House, Temple Back, 1999.

[9] S. Chakraborty, S. Chakraborty, and U. Debnath, "Role of Pressure in Quasi-Spherical Gravitational Collapse," *International Journal of Modern Physics*, vol. D14, p. 1707, 2005.

[10] R. Garattini, "Naked Singularity in a Modified Gravity Theory," *Journal of Physics: Conference Series*, Article ID 012066, 2009.

[11] M. Sharif and M. Zaeem Ul Haq Bhatti, "Structure scalars for charged cylindrically symmetric relativistic fluids," *General Relativity and Gravitation*, vol. 44, no. 11, pp. 2811–2823, 2012.

[12] M. Sharif and M. Z. Bhatti, "Structure scalars in charged plane symmetry," *Modern Physics Letters A*, vol. 27, no. 27, p. 1250141, 2012.

[13] M. Sharif and Z. Yousaf, "Evolution of expansion-free self-gravitating fluids and plane symmetry," *International Journal of Modern Physics*, vol. D21, Article ID 1250095, 2012.

[14] M. Sharif and Z. Yousaf, "Expansion-free Cylindrically Symmetric Models," *Canadian Journal of Physics*, vol. 90, p. 865, 2012.

[15] M. Sharif and H. R. Kausar, "Effects of *f(R)* model on the dynamical instability of expansionfree gravitational collapse," *Journal of Cosmology and Astroparticle Physics*, vol. 7, p. 022, 2011.

[16] M. Sharif and M. Azam, "Effects of Electromagnetic Field on the Dynamical Instability of Cylindrical Collapse," *Journal of Cosmology and Astroparticle Physics*, vol. 02, p. 043, 2012.

[17] M. Sharif and S. Fatima, "Charged cylindrical collapse of anisotropic fluid," *General Relativity and Gravitation*, vol. 43, no. 1, pp. 127–142, 2011.

[18] M. Sharif and G. Abbas, "Dynamics of Non-adiabatic Charged Cylindrical Gravitational Collapse," *Astrophysics and Space Science*, vol. 335, p. 515, 2011.

[19] G. Cognola, E. Elizalde, S. Nojiri, S. D. Odintsov, and S. Zerbini, "One-loop f(R) gravity in de Sitter universe," *Journal of Cosmology and Astroparticle Physics*, vol. 02, Article ID 010, p. 010, 2005.

[20] S. Capozziello and M. de Laurentis, "Extended Theories of Gravity," *Physics Reports*, vol. 509, no. 4-5, pp. 167–321, 2011.

[21] E. J. Copeland, M. Sami, and S. Tsujikawa, "Dynamics of dark energy," *International Journal of Modern Physics D*, vol. 15, no. 11, pp. 1753–1936, 2006.

[22] L. Amendola, R. Gannouji, D. Polarski, and S. Tsujikawa, "Conditions for the cosmological viability of $f(R)$ dark energy models," *Physical Review D: Particles, Fields, Gravitation and Cosmology*, vol. 75, no. 8, Article ID 083504, 2007.

[23] S. Chandrasekhar, "The dynamical instability of gaseous masses approaching the Schwarzschild limit in general relativity," *The Astrophysical Journal*, vol. 140, pp. 417–433, 1964.

[24] L. Herrera, G. le Denmat, and N. O. Santos, "Dynamical instability for nonadiabatic spherical collapse," *Royal Astronomical Society. Monthly Notices*, vol. 237, no. 2, pp. 257–268, 1989.

[25] G. Abbas, S. Nazeer, and M. A. Meraj, "Cylindrically symmetric models of anisotropic compact stars," *Astrophysics and Space Science*, vol. 354, p. 449, 2014.

[26] M. K. Mak and T. Harko, "Quark stars admitting a one-parameter group of conformal motions," *International Journal of Modern Physics*, vol. D13, p. 149, 2004.

[27] F. Rahaman, R. Sharma, S. Ray, R. Maulick, and I. Karar, "Strange stars in Krori-Barua space-time," *The European Physical Journal C*, vol. 72, p. 2071, 2012.

[28] L. Herrera, "Cracking of self-gravitating compact objects," *Physics Letters A*, vol. 165, no. 3, pp. 206–210, 1992.

[29] L. Herrera, D. Prisco, and A. Ibanez, "On the Role of Electric Charge and Cosmological Constant in Structure Scalars," *Physical Review A*, vol. D84, p. 107501, 2011.

[30] L. Herrera, J. Ospino, and A. D. Prisco, "All static spherically symmetric anisotropic solutions of Einstein's equations," *Physical Review*, vol. D77, p. 027502, 2008.

[31] L. Herrera, N. O. Santos, and A. Wang, "Shearing Expansion-free Spherical Anisotropic Fluid Evolution," *Physical Review*, p. D78, 2008.

[32] L. Herrera and N. O. Santos, "Dynamics of dissipative gravitational collapse," *Physical Review*, vol. D70, p. 084004, 2004.

[33] L. Herrera, G. Le Denmat, and N. O. Santos, "Dynamical instability and the expansion-free condition," *General Relativity and Gravitation*, vol. 44, no. 5, pp. 1143–1162, 2012.

[34] A. D. Prisco, L. Herrera, J. Ospino, N. O. Santos, and V. M. Vina-Cervantes, "Expansion-Free Cavity Evolution: Some exact Analytical Models," *International Journal of Modern Physics*, vol. D20, p. D20, 2011.

[35] L. Herrera, A. D. Prisco, E. Fuenmayor, and O. Troconis, "Dynamics of viscous dissipative gravitational collapse: A full causal approach," *International Journal of Modern Physics*, vol. D18, p. 129, 2009.

[36] A. Di Prisco, L. Herrera, G. Le Denmat, M. A. H. MacCallum, and N. O. Santos, “Nonadiabatic charged spherical gravitational collapse,” *Physical Review D: Particles, Fields, Gravitation and Cosmology*, vol. 76, Article ID 064017, 2007.

[37] L. Herrera, M. A. H. Maccallum, and N. O. Santos, “On the Matching Conditions for the Collapsing Cylinder,” *Classical and Quantum Gravity*, vol. 24, p. 1033, 2007.

[38] A. Di Prisco, L. Herrera, M. A. MacCallum, and N. O. Santos, “Shearfree cylindrical gravitational collapse,” *Physical Review D: Particles, Fields, Gravitation and Cosmology*, vol. 80, no. 6, Article ID 064031, 10 pages, 2009.

[39] B. C. Nolan, “Naked singularities in cylindrical collapse of counterrotating dust shells,” *Physical Review*, vol. D65, p. 104006, 2002.

[40] S. A. Hayward, “Gravitational waves, black holes and cosmic strings in cylindrical symmetry,” *Classical and Quantum Gravity*, vol. 17, p. 1749, 2000.

[41] I. Müller, “Zum Paradoxon der Wärmeleitungstheorie,” *Zeitschrift für Physik*, vol. 198, no. 4, pp. 329–344, 1967.

[42] W. Israel, “Nonstationary irreversible thermodynamics: a causal relativistic theory,” *Annals of Physics*, vol. 100, no. 1-2, pp. 310–331, 1976.

[43] W. Israel and J. M. Stewart, “Transient relativistic thermodynamics and kinetic theory,” *Annals of Physics*, vol. 118, no. 2, pp. 341–372, 1979.

[44] R. Maartens, “Causal Thermodynamics in Relativity,” *Astrophysics*, Article ID 9609119.

[45] R. Chan, “Radiating gravitational collapse with shear viscosity,” *Monthly Notices of the Royal Astronomical Society*, vol. 316, p. 588, 2000.

[46] K. S. Thorne, “Energy of infinitely long, cylindrically symmetric systems in general relativity,” *Physical Review B: Condensed Matter and Materials Physics*, vol. 138, p. B251, 1965.

[47] S. M. Shah and G. Abbas, “Dynamics of charged viscous dissipative cylindrical collapse with full causal approach,” *European Physical Journal*, vol. A53, p. 53, 2017.

[48] T. Chiba, “Cylindrical dust collapse in general relativity: toward higher dimensional collapse,” *Progress of Theoretical and Experimental Physics*, vol. 95, no. 2, pp. 321–338, 1996.

[49] H. Chao-Guang, “Charged static cylindrical black hole,” *Acta Physica Sinica*, vol. 4, no. 8, pp. 617–630, 1995.

[50] G. Darmois, *Memorial des Sciences Mathematiques*, vol. 25, Gautheir-Viuars, Paris, France, 1927.

[51] S. Guha and R. Banerji, “Dissipative cylindrical collapse of charged anisotropic fluid,” *International Journal of Theoretical Physics*, vol. 53, no. 7, pp. 2332–2348, 2014.

[52] J. M. M. Senovilla, “Junction conditions for *F(R)*-gravity and their consequences,” *Physical Review*, vol. 88, p. 064015, 2013.

[53] T. Clifton, P. K. S. Dunsby, R. Goswami, and A. M. Nzioki, “On the absence of the usual weak-field limit, and the impossibility of embedding some known solutions for isolated masses in cosmologies with *f(R)* dark energy,” *Physical Review*, vol. D87, p. 063517, 2013.

[54] N. Deruelle, M. Sasaki, and Y. Sendouda, “Junction Conditions in *f(R)* Theories of Gravity,” *Progress of Theoretical and Experimental Physics*, vol. 119, p. 237, 2008.

[55] A. Ganguly, R. Gannouji, R. Goswami, and S. Ray, “Neutron stars in the Starobinsky model,” *Physical Review D: Particles, Fields, Gravitation and Cosmology*, vol. 89, no. 6, 2014.

[56] R. Goswami, A. M. Nzioki, S. D. Maharaj, and S. G. Ghosh, “Collapsing spherical stars in *f(R)* gravity,” *Physical Review D*, vol. 90, no. 8, 2014.

[57] C. W. Misner and D. Sharp, “Relativistic equations for spherical gravitational collapse with escaping neutrinos,” *Physical Review*, vol. B137, p. 1360, 1965.

[58] H. Weyl, “On the Theory of Gravitation,” *Annalen der Physik (Leipzig)*, vol. 54, p. 117, 1917.

[59] T. Levi-Civita, “d2 einsteiniani in campi newtoniani. IX. L’analogo del potenziale logaritmico,” *Atti Della Reale Accademia Dei Lincei. Rendiconti*, vol. 28, p. 101, 1919.

[60] C. Cattaneo, “Sulla conduzione del calore,” *Atti del Seminario Matematico e Fisico dell’ Universita di Modena e Reggio Emilia*, vol. 3, p. 3, 1948.

[61] A. Anile, D. Pavon, and V. Romano, “The Case for Hyperbolic Theories of Dissipation in Relativistic Fluids,” https://arxiv.org/abs/gr-qc/9810014.

[62] L. Herrera and D. Pavon, “Hyperbolic theories of dissipation: Why and when do we need them?” *Physica*, vol. A307, p. 121, 2002.

[63] S. M. Shah and G. Abbas, “Dynamics of charged bulk viscous collapsing cylindrical source with heat flux,” *Journal of Physics*, vol. C77, p. 251, 2017.

[64] L. Herrera, A. Di Prisco, and W. Barreto, “Thermoinertial bouncing of a relativistic collapsing sphere: A numerical model,” *Physical Review D: Particles, Fields, Gravitation and Cosmology*, vol. 73, no. 2, 2006.

[65] G. Abbas and H. Nazar, *Dissipative and Viscous Gravitational Collapse in* f(R) *Gravity With Full Causal Approach (submitted for publication 2018)*.